

DISSERTATION

COMPLEX REGULATION OF BpeEF-OprC MEDIATED DRUG EFFLUX IN

*Burkholderia pseudomallei*

Submitted by

Katherine Rhodes

Department of Microbiology, Immunology and Pathology

In partial fulfillment of the requirements

For the Degree of Doctor of Philosophy

Colorado State University

Fort Collins, Colorado

Spring 2016

Doctoral Committee:

Advisor: John Belisle

Co-Advisor: Herbert Schweizer

Steven Dow

Laurie Stargell

Copyright by Katherine Rhodes 2016

All Rights Reserved

## ABSTRACT

### COMPLEX REGULATION OF BpeEF-OprC MEDIATED DRUG EFFLUX IN *Burkholderia pseudomallei*

*Burkholderia pseudomallei* (*Bp*) is a Gram-negative bacillus and the etiologic agent of melioidosis, a multifaceted syndrome causing high mortality in tropical regions of the world. The bacteria is classified as a Tier-1 Select Agent due to the seriousness of infection, low infectious dose, lack of effective vaccine, and difficulty of treatment. *Bp*'s many acquired and intrinsic antimicrobial resistance determinants make the study of these factors vital to improving the efficacy of bi-phasic treatment currently used to treat melioidosis. This study examines one factor in particular: the BpeEF-OprC efflux pump, a member of the resistance-nodulation and cell division family of efflux proteins, and capable of extruding both trimethoprim and sulfamethoxazole. A combination of these compounds (co-trimoxazole) is the first line of eradication phase therapy, making BpeEF-OprC the most clinically important efflux pump encoded by *Bp*. In spite of this, little is understood of the regulation of *bpeEF-oprC*, other than it is controlled in part by two LysR family proteins, BpeS, and BpeT. We hypothesized that these regulatory proteins 1) exert their action(s) by interacting with *bpeEF-oprC* at a specific site within the *bpeT-llpE-bpeEF-oprC* intergenic region, 2) are capable of influencing transcription of additional operons, and 3) that mutations to these proteins altered ability to form multimers, thereby influencing their function as observed by increased co-trimoxazole resistance and *bpeF* transcript levels.

In Aim I of the study, we identified the *cis* regulatory regions by which these proteins interact within the *bpeT-llpE-bpeE* intergenic region using a combination of 5' deletion assays,

S1 nuclease protection, fluorescent-linked oligo extension and electrophoretic mobility assays. With this information we were able to locate *bpeT* transcriptional start sites and promoter regions as well as binding sites for both BpeT and BpeS.

In Aim II, we examined the function of BpeT and BpeS as *trans* regulatory factors of BpeEF-OprC through mutation and deletion of both genes in part I, and as global regulatory factors in part II. Through overexpression and qRT-PCR or MIC analysis of wild type and mutant forms of both genes, we observed that while BpeT is a direct transcriptional activator of *bpeEF-oprC*, BpeS is not. Additionally, mutation position in BpeS seems to play a role in the expression phenotype of *bpeEF-oprC*. However, these mutations do not influence the ability of BpeS or BpeT to form multimers, as we observed no change between wild type and mutant protein oligomer formation through low-pressure gel chromatography and native gel electrophoresis. These same mutations also appeared to have no deleterious effect on the ability of the protein to bind their consensus region within the IR. Additionally, the loss of both genes did not interrupt the ability of *bpeEF-oprC* to be induced by substrates of BpeEF-OprC, suggesting an additional regulatory factor is at play.

In Part II, RNA sequencing analysis and confirmation of select transcriptionally altered operons by RT-qPCR revealed that BpeS might influence expression of the Bsa Type 3 Secretion System (T3SS), while BpeT seems only to target *bpeEF-oprC*. This may have implication in the pathogenesis of *Bp*, and must be confirmed in *in-vivo* cell models using Select Agent excluded strain Bp82 in order to solidify the link between efflux and T3SS during infection. Ultimately, more work is needed to identify the missing regulatory factors in play during expression of *bpeEF-oprC*, understand how mutations to BpeT and BpeS alter their function, and confirm the relevance of a putative link between co-regulation of efflux and of virulence during *Bp* infection.

## ACKNOWLEDGEMENTS

First and foremost, I'd like to thank Dr. Schweizer for the opportunity to work in his lab. The experience I've gained while working on this project has been invaluable and I am grateful for the lessons I've learned as your student. I'd also like to thank the members of my committee for their support and valuable input throughout this process. And, to Dr. RoxAnn, thank you for your wise words and unwavering support. Thank you to all current and former members of the Schweizer lab, especially Nicole Podnecky, Linnell Randall, and Erin Breland, as well as Amber Rico, and Bryna Fitzgerald, for your input, friendship, and willingness to listen to my nonsense. Finally I'd like to thank my family and friends; without you, I couldn't have made it this far.

## DEDICATION

*To my parents: without you, I would have been a (more) neurotic mess during my tenure as a graduate student. I owe everything to you.*

## TABLE OF CONTENTS

ABSTRACT.....	ii
ACKNOWLEDGEMENTS.....	iv
DEDICATION.....	v
LIST OF TABLES.....	x
LIST OF FIGURES.....	xi
Chapter 1: Melioidosis.....	1
1.1 <i>Burkholderia pseudomallei</i> and the genus <i>Burkholderia</i> .....	1
1.2 History of melioidosis.....	2
1.3 The <i>Burkholderia</i> genus.....	3
1.4 Genetics of <i>Burkholderia pseudomallei</i> .....	4
1.5 Global distribution of melioidosis.....	5
1.6 Virulence factors and pathogenesis of <i>Burkholderia pseudomallei</i> .....	6
1.6.1 Extracellular motility.....	7
1.6.2 Cell adhesion and invasion.....	7
1.6.3 Type III secretion.....	8
1.6.4 Type VI secretion.....	9
1.6.5 Toxin production.....	11
1.6.6 Intracellular motility.....	11
1.6.7 Multinucleated giant cell formation.....	12
1.6.8 LPS structure and function.....	12
1.7 Melioidosis.....	13
1.7.1 Recurrent melioidosis.....	15
1.7.2 Neurological melioidosis.....	16
1.7.3 Zoonotic melioidosis.....	17
1.8 Routes of exposure to <i>Burkholderia pseudomallei</i> .....	18
1.9 Melioidosis risk factors.....	19
1.9.1 Melioidosis and diabetes.....	19
1.9.2 Renal disease.....	20
1.9.3 Thalassemia.....	21
1.9.4 Drug use and melioidosis.....	22
1.9.5 Occupational and environmental risk factors.....	23
1.10 Melioidosis diagnosis.....	24
1.11 Current efforts in vaccine development.....	25
1.12 Treatment of melioidosis.....	26
Chapter 1 References.....	28

Chapter 2: Antimicrobial resistance.....	50
2.1 The post-antibiotic era .....	50
2.2 Antibiotics.....	53
2.2.1 Treatment of <i>Burkholderia pseudomallei</i> .....	55
2.3 Drug resistance mechanisms.....	55
2.3.1 Enzymatic inactivation.....	56
2.3.2 Metabolic bypass and target duplication.....	56
2.3.3 Exclusion and sequestration of antimicrobial compounds.....	57
2.3.4 Target modification.....	58
2.3.5 Antibiotic tolerance.....	59
2.3.6 Efflux .....	59
2.4 Families of efflux systems .....	60
2.4.1 Major facilitator (MF) systems .....	60
2.4.2 Small multidrug resistance (SMR) family .....	60
2.4.3 ABC transporters .....	61
2.4.4 Multidrug and toxic compound exclusion (MATE) family.....	61
2.4.5 Resistance nodulation cell division (RND) family .....	62
2.5 RND transporters in <i>Burkholderia pseudomallei</i> .....	63
2.6 Efflux linked resistance trends in <i>Burkholderia pseudomallei</i> .....	63
2.6.1 Previous data and research rationale.....	64
2.7 Summary of aims .....	68
Chapter 2 References .....	70
Chapter 3: Genetic characterization of the <i>bpeEF-oprC</i> operon .....	80
Summary.....	80
Introduction.....	80
3.1 Materials and methods .....	82
3.1.1. General DNA methodology .....	82
3.1.2 Plasmids and bacterial strains .....	84
3.1.3 Gene deletion .....	87
3.1.4 Marker removal using the Flp- <i>FRT</i> system .....	91
3.1.5 Construction of pUC18-mini-Tn <sup>7</sup> - <i>lacZ</i> reporter fusion plasmids.....	92
3.1.6 $\beta$ -galactosidase transcriptional activity assay for start site analysis .....	93
3.1.7 RNA extraction .....	93
3.1.8 Fluorescent primer extension.....	94
3.1.9 S1 Nuclease protection assay.....	94
3.1.10 Protein expression and purification .....	95
3.1.11 Electrophoretic mobility shift assays .....	98

3.2 Results and Discussion .....	99
3.2.1 The <i>bpeT-llpeE</i> intergenic region contains the promoter regions necessary for transcription of <i>llpeE-bpeEF-oprC</i> and <i>bpeT</i> .....	99
3.2.2 Transcriptional start sites for both <i>bpeT</i> and <i>llpeE-bpeEF-oprC</i> are located within promoter regions of the IR identified by $\beta$ -galactosidase assays. ....	102
3.2.3 S1 Nuclease assays pinpoint 5' transcriptional start sites within the <i>bpeT-llpeE-bpeEF-oprC</i> intergenic region. ....	104
3.2.4 BpeT and BpeS bind to the intergenic region between <i>bpeT</i> and <i>llpeE-bpeEF-oprC</i> . ....	106
3.2.5 BpeT and BpeS interact with the intergenic region at sites closely associated with promoter region and transcriptional start sites of <i>bpeT</i> and <i>llpeE-bpeEF-oprC</i> . ....	107
3.2.7 Mutations to BpeS and BpeT do not impede their ability to interact with the intergenic region. ....	109
3.3 Conclusions.....	110
Chapter 3 References .....	114
Chapter 4: Regulatory functions of BpeS and BpeT .....	117
Summary .....	117
Introduction.....	117
4.1 Materials and methods .....	118
4.1.1 General DNA methodology .....	118
4.1.2 Plasmids and bacterial strains .....	120
4.1.3 Construction of Bp82 strains .....	123
4.1.4 Gene complementation and single copy insertions using the mini-Tn7 system .....	124
4.1.5 Construction of strains expressing <i>bpeS</i> and <i>bpeT</i> from the P1 promoter. ....	124
4.1.6 Antibiotic susceptibility assays.....	126
4.1.7 RNA extraction .....	127
4.1.8 qRT-PCR.....	127
4.1.9 Drug dose dependent induction of <i>bpeEF-oprC</i> .....	128
4.1.10 RNA sequencing and analysis .....	128
4.1.11 Protein purification .....	130
4.1.12 Native gel electrophoresis.....	130
4.1.13 Size exclusion chromatography .....	131
4.2 Results and discussion .....	132
4.2.1 BpeT is a transcriptional activator of the <i>bpeEF-oprC</i> efflux pump operon .....	132

4.2.2 BpeS is not a transcriptional activator of the <i>bpeEF-oprC</i> operon under wild-type <i>in-vitro</i> conditions.....	134
4.2.3 <i>bpeS</i> mutations, not changes to <i>bpeS</i> expression level, cause BpeEF-OprC dependent resistance to co- trimoxazole.....	137
4.2.4 Mutation position in BpeS alters expression phenotypes of BpeF. ....	140
4.2.5 BpeT and BpeS are not required for pump substrate induction of <i>bpeEF-oprC</i> expression. ....	142
4.2.6 BpeS and BpeT form multimers. ....	146
4.2.7 Mutations causing elevated pump expression do not influence multimer formation of BpeT or BpeS.....	148
4.2.8 Mutations to BpeT and BpeS alter global gene expression of <i>B. pseudomallei</i> .....	150
4.3 Conclusions.....	156
Chapter 4 References .....	159
Chapter 5.....	164
Conclusions and future directions.....	164
Chapter 5 References .....	171
APPENDIX.....	174
ABBREVIATIONS AND DEFINITIONS.....	192

## LIST OF TABLES

Table 2.1 Antibiotic classes,targets, and resistance mechanisms .....	54
Table 3.1.A Cloning primers .....	82
Table 3.1.B Detection primers .....	83
Table 3.1.C. Plasmids .....	84
Table 3.1.D <i>Escherichia coli</i> strains utilized in this study .....	87
Table 3.1.E <i>Burkholderia pseudomallei</i> Strains Utilized in This Study.....	89
Table 4.1.A Cloning primers .....	119
Table 4.1.B Primers for gene deletion and mini-Tn7 insertion identification .....	119
Table 4.1.C Primers utilized for qRT-PCR.....	119
Table 4.1.D Plasmids .....	120
Table 4.1.E <i>E. coli</i> strains utilized in this study.....	122
Table 4.1.F <i>B. pseudomallei</i> strains utilized in this study .....	122
Table 4.2.1 MIC testing in Bp82 <i>bpeT</i> overexpression strains.....	133
Table 4.2.2. BpeS is not a direct transcriptional regulator of <i>bpeEF-opC</i> .....	135
Table 4.2.3. Antibiotic susceptibility of strains expressing BpeS <sub>P28S</sub> or BpeS <sub>K267T</sub> variants lacking native <i>bpeS</i> or <i>bpeS</i> and <i>bpeT</i> . .....	137
Table A 1. Mapping statistics of RNAseq analysis .....	174
Table A2. RNAseq gene expression in Bp82 <i>bpeS</i> <sub>K267T</sub> vs. Bp82 .....	176
Table A3. RNA-seq gene expression in <i>bpeS</i> <sub>P28S</sub> vs. Bp82 .....	177
Table A4. RNAseq gene expression in Bp82 <i>bpeT</i> <sub>S280P</sub> vs. Bp82 .....	182
Table A.5 RNAseq KEGG pathway analysis .....	185

## LIST OF FIGURES

Figure 1.1. Global distribution of melioidosis. Areas highlighted where disease is highly endemic, endemic or sporadic and possibly endemic .....	6
Figure 1.2. Melioidosis is a multifaceted disease. ....	14
Figure 2.1. Timeline of the identification of antibiotic resistance. ....	52
Figure 2.2. The <i>bpeEF-oprC</i> operon and currently identified regulatory factors.....	67
Figure 3.2.2. Identification of promoter regions within the <i>bpeT-llpE</i> intergenic region. ....	100
Figure 3.2.1. Summary of 5' deletion constructs created for analysis of the <i>bpeT-llpE-bpeEF-oprC</i> intergenic region. ....	100
Figure 3.2.3. Analysis mutant BpeS effects on <i>bpeT</i> transcription. ....	101
Figure 3.2.4. Fluorescent linked oligo extension identifies a putative transcriptional start site within the <i>bpeT-llpE</i> intergenic region. ....	103
Figure 3.2.5. Fluorescent linked oligo extension identifies a putative transcriptional start site within the <i>bpeT-llpE</i> intergenic region. ....	103
Figure 3.2.5. S1 nuclease protection assay extends the 5' transcript end of <i>bpeT</i> to bp 88 of the intergenic region. ....	104
Figure 3.2.6. S1 Nuclease protection assay identifies a putative 5' transcript end within the <i>bpeT-llpE</i> intergenic region.....	105
Figure 3.2.7. Both BpeT and BpeS can bind the IR. ....	106
Figure. 3.2.9 BpeT and BpeS share binding sequence located within the promoter regions of the intergenic sequence.....	108

Figure 3.2.8. BpeT and BpeS utilize the same or closely associated binding sites within the IR. .....	108
Figure 3.2.10. Mutant BpeT and BpeS retain the ability to interact with the intergenic region of <i>bpeEF-oprC</i> . .....	110
Figure 3.2.11. Final summary of <i>cis</i> regulatory elements located within the <i>bpeT-llpE-bpeEF- oprC</i> intergenic sequence.....	111
Figure 4.2.1. BpeT is a transcriptional activator of the <i>bpeEF-oprC</i> operon. ....	133
Figure 4.2.2. Transcription from the <i>PI</i> promoter causes overexpression of wild-type <i>bpeS</i> ....	135
Figure 4.2.3. The <i>bpeS</i> <sub>P28S</sub> mutation causes high level expression of <i>bpeF</i> .....	138
Figure 4.2.4. The <i>bpeS</i> <sub>K267T</sub> mutation causes high level expression of <i>bpeF</i> . ....	139
Figure 4.2.5. Position of mutations in <i>bpeS</i> has an effect on expression of <i>bpeF</i> . ....	141
Figure 4.2.6. <i>bpeT</i> is dispensable for efflux pump substrate mediated induction of <i>bpeF</i> expression. ....	143
Figure 4.2.7. <i>bpeS</i> is dispensable for efflux pump substrate mediated induction of <i>bpeF</i> expression. ....	144
Figure 4.2.8. Molecular weight characterization of BpeS and BpeT by size exclusion chromatography shows both proteins form multimers. ....	147
Figure 4.2.9. BpeT forms high molecular weight complexes under native conditions. ....	148
Figure 4.2.10. BpeS and BpeS mutants form high molecular weight complexes under native conditions.....	149
Figure 4.2.11. The distribution of global gene expression in <i>bpeS</i> <sub>K267T</sub> , <i>bpeS</i> <sub>P28S</sub> and <i>bpeT</i> <sub>S280P</sub> mutants.....	151
Figure 4.2.12. <i>bpeT</i> and <i>bpeS</i> mutants show significantly altered global gene expression.....	152

Figure 4.2.13. *bpeS* mutations cause upregulation of the *Bsa* Type III secretion system of *Bp*. 153

Figure 4.2.14. Virulence related gene expression depends on the presence of BpeS..... 155

Figure 5.1. The BpeT BpeS regulatory cascade. .... 167

Figure A.1. Kyoto encyclopedia of genes and genomes (KEGG) functional pathway associations  
of transcriptionally altered genes identified by RNAseq..... 184

## Chapter 1: Melioidosis

### 1.1 *Burkholderia pseudomallei* and the genus *Burkholderia*

*Burkholderia pseudomallei* (*Bp*) is a Gram-negative bacillus found primarily in surface water and soil.<sup>1</sup> The organism is a motile, non-sporulating aerobe and the etiologic agent of melioidosis. *Bp* has a wide environmental distribution roughly restricted between the Tropic of Cancer and the Tropic of Capricorn.<sup>1,2</sup> To date, hyper-endemic regions have been identified within Northeastern Thailand and Northern Australia, but as diagnostic accuracy improves, it is likely that a more widespread incidence of infection with *Bp* will be described.<sup>3-8</sup>

Even with treatment, melioidosis has a mortality rate of up to 40% in Thailand and 14% in Australian cases.<sup>8</sup> In certain regions of Southeast Asia, the disease is now recognized as one of the most commonly fatal infections after HIV and Tuberculosis and incidence of disease is as high as 12.7 per 100,000 individuals.<sup>2,9</sup> Because of the seriousness of the syndrome caused by *Bp*, the lack of an effective vaccine, low infectious dose, difficulty of treatment and possibility of weaponization to create mass panic, *Bp* has been classified by the CDC as a Tier-1 Select Agent (SA).<sup>10</sup> Because of this classification, research into all aspects of the physiology and pathogenesis of *Bp* is tightly regulated.

*Bp* is an especially hardy organism, with evidence of prolonged survival in otherwise unfavorable environments, e.g. distilled water 16 years post inoculation, reported.<sup>11,12</sup> Several studies have suggested this ability to persist in austere conditions may play a role in *Bp*'s contamination of bore-well water, a common outbreak source in the Northern territory of Australia.<sup>13-16</sup> Unsurprisingly, *Bp* is routinely isolated from soil samples in endemic regions. The bacteria is also very capable of persisting for long periods within a mammalian host. This is

best illustrated by a case report of reactivation of disease in a former WWII P.O.W. 60 years after his initial exposure during an interment in a labor camp in the Thai peninsula.<sup>17</sup> However, despite multiple instances of long incubation and latency, the phenomenon is still not well understood in *Burkholderia* infection.

## 1.2 History of melioidosis

Melioidosis was first described in Rangoon (now Yangon, Myanmar) during the early 20<sup>th</sup> century by A. Whitmore as part of his duties as a pathologist for the British Medical Service.<sup>18</sup> The first clinical cases were described among morphine addicts who presented with generalized fever and sepsis. Upon autopsy, Whitmore and Krishnaswami identified caseous consolidation of the lungs in most cases, along with enlarged abscessed spleens. Occasionally, abscessed pockets of tissue around puncture wounds associated with morphia (morphine) use suggested that this would be the route of inoculation.<sup>18,19</sup> This led to an important observation in the distinction the scientists made between melioidosis and glanders (a known disease of solipeds); the first patient studied had no known contact with potentially infected horses or donkeys due to a recent stay in jail. The track marks found on the body indicated a viable route of entry and the living conditions of the patient predisposed him to probable contraction of disease. After several more similar cases, all lacking interaction with an ungulate carrier of glanders, and pathological investigations into the etiologic agent, Whitmore and Krishnaswami were able to definitively describe a new species, later called Whitmore's bacillus.<sup>19</sup>

In the years following its discovery in Burma, new cases were occasionally reported to western medical journals, usually as a result of contact with colonial physicians and with varying patient outcomes.<sup>20-23</sup> Although only 83 cases had been reported to western medical journals by 1932, the mortality rate in these studies was a staggering 98 percent.<sup>24,25</sup> It wasn't until the early

1940s that clinicians began to truly investigate all forms of disease, including those cases that were self-limiting, or experiment with newly developed antimicrobials as treatment.<sup>24,26</sup> Heavy fighting in the Southeast Asian region during both WWII and the Vietnam conflict further increased western awareness of the disease as a potential cause of infection in soldiers in the area.<sup>26-30</sup> Its classification as a potential bioterror agent and subsequent increased research importance continue to drive our inquiries of its distribution, pathogenesis and treatment.

### 1.3 The *Burkholderia* genus

*Bp* has undergone several name changes as scientists tried to classify the bacteria into existing genera. It was proposed as a member of *Malleomyces*, *Pfeifferella* and *Pseudomonas* until the creation of the genus *Burkholderia* in 1992.<sup>31,32</sup> At this point, comparisons in 16s rRNA and physical characteristics were used to develop a group of closely related organisms pulled from other genera. These include what we now know as *Bp*, *mallei*, *cepacia*, *gladioli* and *vietnamensis*. To date, the taxon is comprised of more than 70 different species, most of which lead a saprophytic lifestyle and are opportunistic pathogens of both plants and animals.<sup>33-35</sup>

The exception to this observation is found in the obligate parasite *B. mallei* (*Bm*), which is thought to be a clone of *Bp* that has undergone extensive genome reduction during colonization of domesticated and wild ungulates.<sup>1,34</sup> Melioidosis, the term coined by Stanton and Fletcher in the early 20<sup>th</sup> century, is so reminiscent of *Bm* infection (glanders) that it translates to “similar to the distemper of asses”—a direct reference to the historically acknowledged syndrome.<sup>36</sup> Unlike *Bp*, *Bm* infection was a recognized disease early in human history and was described in Greece as early as the 3<sup>rd</sup> century BC.<sup>37</sup> Interestingly, *Bm* is the only member of the genus known to have been weaponized, not just investigated for potential efficacy in such a capacity. It was widely used during WWI by German operatives to infect livestock of potential

enemy trading partners, by the Japanese during the Manchurian campaign prior to the start of the Pacific theater of WWII, and by the Soviet Union in Afghanistan as the late 1980's.<sup>37-42</sup>

The next most closely related species is *B. thailandensis* (*Bt*), which was moved into its own species after careful delineation in 1998.<sup>43</sup> This organism is closely related to *Bp* and occupies the same environmental niche, but can be differentiated by its inability to efficiently infect a mammalian host, and ability to utilize L-arabinose.<sup>44,45</sup> *Bt* is commonly used as a *Bp* model because of the similarities between the two organisms and its exclusion from SA regulation due to relative avirulence in comparison to *Bp* or *Bm*.

Like *Bp* and *Bm*, *B. cepacia* complex organisms are capable of infecting plants and humans. This group consists of nine genomovars all grouped by phenotypic similarity, and with much wider geographic distribution than their more pathogenic relatives.<sup>46,47</sup> All are opportunistic pathogens that share the ability of *B. pseudomallei* to infect the upper respiratory tract, but lack the full virulence arsenal. Even so, this group of organisms are a commonly found colonizing the lungs of patients with cystic fibrosis and retain the innate antimicrobial resistance factors common to the genus, making them of serious concern to clinicians.<sup>46,48</sup> Interestingly, some members of this classification are capable of unusual metabolic adaptation and commensalism with plants that could have ramifications in bioremediation research.<sup>49-51</sup>

#### **1.4 Genetics of *Burkholderia pseudomallei***

*Bp* contains two large circular chromosomes, totaling ~7.2 million base pairs with core and accessory regions typically distributed on chromosome 1 and chromosome 2, respectively.<sup>52</sup> The genome of *Bp* displays a high level of recombinant plasticity, with “hotspots” of recombination identified in accessory genome regions associated with environmental persistence and adaptation.<sup>53</sup> The bacterium is cited as having one of the most complex genomes sequenced

to date.<sup>2</sup> This characteristic may be the result of *Bp*'s evolution in a soil environment that is inherently poly-microbial, leading to accidental uptake of foreign DNA illustrated by differences in GC content of newly acquired regions in comparison to the core genome. The average GC content of regions thought to be more highly conserved is 68% while accessory regions more recently recombined or taken up by the species hover around 59%.<sup>53</sup> Even within the same environmental sampling region, high levels of sequence diversity are commonly seen, again pointing to the highly recombinant nature of the bacteria.<sup>54</sup> Sequencing of successive patient isolates commonly show sequence divergence over relatively short periods, again reinforcing the highly mutable nature of the species' genome, and leading to improved adaptation within the host. Deletions or inversions of large sections of the chromosome have been reported in successive clinical isolates, on two reported occasions leading to decreased antimicrobial susceptibility as a direct result of these alterations.<sup>55,56</sup>

### **1.5 Global distribution of melioidosis**

Since the first report of melioidosis in the early 20<sup>th</sup> century by Whitmore and Krishnaswami, *Bp* infection was thought to be mostly localized to South East Asia (SEA) and Oceania. As diagnostic methods improve, it is becoming more apparent that *Bp*'s global distribution is more widespread than previously thought. Cases of melioidosis have now been reported from South and Central America, the Caribbean, and Africa in addition to sporadic suspected incidents within North America and Europe as a result of travel.<sup>57-69</sup> The apparent increased incidence of disease raises important questions about the true cause of this trend: is the bacteria emerging in new areas due to colonization of ecological niches or are we simply better able to detect its presence? Several authors suggest the emergence of disease is directly linked to the latter, and caused by increased awareness by diagnostic microbiological labs in regions

where the bacteria is already endemic.<sup>2,69</sup> The former idea suggests that changing environmental factors could allow for a continuous spread of the bacteria into new regions e.g. climate change. This concept is of great concern, as the potential for inadvertent introduction of *Bp* into new territory is possible because of increasingly globalized trade and travel. The current distribution of *Bp* is depicted in **Fig. 1.1** below.

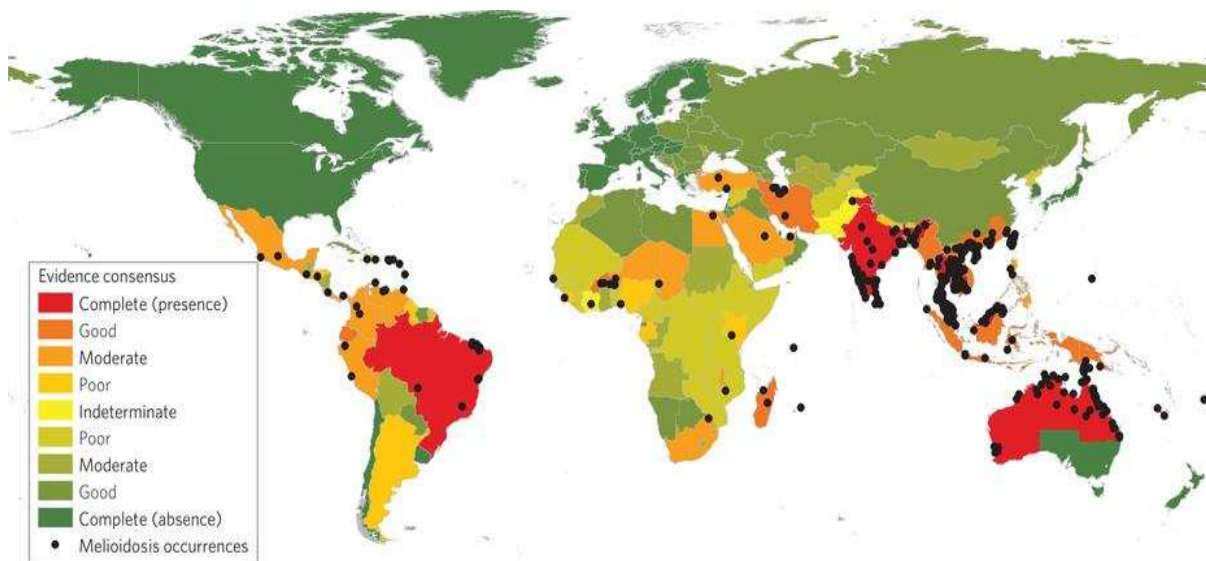


**Figure 1.1. Global distribution of melioidosis.** Areas highlighted where disease is highly endemic, endemic or sporadic and possibly endemic. This figure is based on current information and is likely to change with time. Black dots represent confirmed cases while color scale indicates the probability of presence of *Bp* based on clinical and diagnostic evidence. Taken from Limmathurotsakul et al., 2016<sup>69</sup>

### 1.6 Virulence factors and pathogenesis of *Burkholderia pseudomallei*

*Bp* relies on intracellular persistence to evade the immune system. The bacteria display tropism for macrophages and possess multiple methods of both depressing the action of innate immunity within the cell and preventing a sterilizing adaptive response. This section will discuss effectors utilized by *Bp* to manipulate host cell function leading to phagolysosome escape, actin based motility and intracellular spread.

### 1.6.1 Extracellular motility

*Bp* is a motile organism able to utilize a flagella regulated by a highly conserved chemotaxis response operon for extracellular movement.<sup>36,70</sup> The change from a planktonic to sessile lifestyle is tightly regulated by signaling networks linking motility, quorum sensing and biofilm formation through molecules such as cyclic-di-GMP, and may play a role in host colonization.<sup>70,71</sup> However, deletion of the flagellar synthesis operon only produces slight decreases in virulence during infection of non-phagocytic cells and may suggest other virulence factors are more important.<sup>72</sup> Interestingly, the flagellar hook protein FlgK is one of few immunogenic proteins produced by *Bp* that is detectable in convalescent serum, making it an interesting target for vaccine study.<sup>73</sup>

### 1.6.2 Cell adhesion and invasion

The attachment of the bacteria to the host is a vital step in pathogenesis after exposure to *Bp*. To this end, the bacteria has multiple methods of adhering to both phagocytic and non-phagocytic targets.<sup>74</sup> *Bp* possesses eight operons thought to encode different pilin proteins, however, few have been functionally characterized.<sup>75</sup> The *pilA* gene is thus far the only type A pilin loci to be investigated for its role in infection. Pilin proteins, or fimbriae are necessary for the formation of loose attachments between one bacterial cell and another, or between bacterial cells and eukaryotic targets.<sup>36</sup> While originally believed to be indispensable for the invasion process, *pilA* is now thought to mainly allow for the formation of micro colonies in a temperature dependent manner as opposed to direct attachment to the host.<sup>75-77</sup> These micro colonies then allow for interaction with the host at higher numbers, greatly increasing the probability that a strong attachment mediated by an adhesin will occur. However, the function and temporal regulation of the gene varies greatly, most likely due to inter-strain heterogeneity found in both

clinical and environmental isolates.<sup>76</sup> Additionally, no studies have investigated the possibility of utilization of *pilA* with the other pilin loci in combination or with environmental cues other than temperature.

The bacteria also encodes several putative adhesins important for the infectious process, but again, little work has currently been published on their exact function or mechanism of action. To date, only *boaA*, *boaB* and *bcaA* encoded adhesins have been characterized. Bioinformatic analysis shows that these proteins are trimeric autotransporters who share significant homology to an adhesion domain of the *yadA* gene product produced by *Yersinia enterocolitica*, and are conserved in both *Bp* and *Bm*.<sup>126–128</sup> In this species, the protein is necessary for binding to collagen during infection. In *Bp* these genes play a similar role by mediating adherence to lung epithelial cells in vitro. Loss of any of these genes causes reduction in both adherence, and invasion but it does not completely abrogate these functions.<sup>78–80</sup> This suggests that there are probably more proteins involved in the adherence to host cells, most likely both temporally and environmentally regulated. Again, inter-strain variation may play a large role in differences noted between different studies investigating the same genes.

### 1.6.3 Type III secretion

*Bp* encodes three Type III secretion systems (T3SS). These operons are necessary for persistence in the environment, infection of plants and survival within animal hosts.<sup>36,81</sup> T3SS-3 or the *Bsa* system, is most important for animal infection. This system is homologous to the *inv/spa/prg* system of *Salmonella typhimurium* and the *ipa/mxi/spa* system of *Shigella flexneri*.<sup>82</sup> The operon plays a significant role in bacterial invasion of host cells, vacuolar escape intracellular motility and replication, evasion of autophagy and potential spread to neighboring host cells.<sup>83–87</sup> To date, only a few effector proteins are known to be secreted by the *Bsa* T3SS,

but deletion analysis shows that loss of many of the known structural, regulatory, or effector proteins associated with this operon lead to drastically altered or reduced pathogenicity in vitro. The loss of ATPase *bsaS* leads to almost a completely avirulent phenotype, severely impaired vacuolar escape and inability to detect known secreted effectors in cell culture supernatants.<sup>88</sup> Loss of *bopE* produces mutants incapable of vacuolar escape of before changes in the pH of the compartment lead to cell destruction.<sup>89</sup> Loss of *bopA* may decrease the ability of the bacteria to evade the autophagy process, again leading to decreased intracellular persistence.<sup>85</sup> Conversely, deletion of *bprD*, a gene encoding a hypothetical protein located within the Bsa T3SS leads to a heightened inflammatory response in target tissues but markedly increased cell replication and increased pathology scores suggesting that it may act as either an immune suppressor or regulate an additional virulence factor.<sup>90</sup> Studies have now shown that the regulatory network controlling T3SS-3 may also extend to control of Type 6 secretion and a two component regulatory system which in turn regulates an additional type 6 operon.<sup>91,92</sup> However, not all genes encoded on the operon have been assigned functions, and even less is known about T3SS-1 and 2. Together this suggests that these systems are tightly linked during infection and may act in a complexly coordinated manner to combat the host immune system and promote bacterial survival.<sup>91</sup>

#### **1.6.4 Type VI secretion**

*Bp* encodes six type VI secretion systems, more than any known microbe to date. The characterization of these operons began shortly after the discovery of the system in *Vibrio cholerae* in 2006, but little is yet known about the full function of these systems.<sup>93,94</sup> What is known is that they play an important role in both host-bacterial and bacterial-bacterial interaction by secretion of effectors capable of subverting immune cell or competing bacterial cell function.

In *Burkholderia* species these operons are relatively conserved, with five being present in *Bt* and three in *Bm*.<sup>95</sup> Interestingly, only one of these operons is encoded on chromosome 1 in *Bp*, while the rest make up almost 3 percent of chromosome 2's total coding capacity.<sup>96</sup> Variations in the GC content of these gene islands suggest that two clusters have been acquired through horizontal gene transfer while others may be the result of gene duplication.<sup>96</sup> Of these operons, it appears that only T6SS-1 is active during host cell infection, and plays a role in the formation of multi nucleated giant cells (MNGC).<sup>97,98</sup> The two-component regulatory system VirAG is now known to be a positive regulator of T6SS-1 and may modulate expression of the secretion system by sensing divalent metals in the environment, specifically iron and zinc, which were found to suppress activation.<sup>99</sup>

In the absence of this regulatory system induction of T6SS-1 is abrogated as measured by production of Hcp-1, a known effector associated with T6SS in many species. In the absence of Hcp1 through repression or deletion of the *hcp1* gene, drastic changes can be seen in host cell infection by *Bp*.<sup>98</sup> Not only is mononuclear giant cell (MNGC) formation abolished, but intracellular replication is reduced early in infection and cytotoxicity is decreased. The Hcp protein is also thought to be a secreted protein necessary for formation of the secretion tube and may bind to antigen presenting cells *in-vivo*, promoting interaction between host and bacteria.<sup>100</sup> This may also account for the high immunogenicity of the Hcp-1 protein, which has been detected in convalescent serum. Because of this, attempts at production of a conjugate vaccine have been attempted utilizing each secretion cluster's cognate Hcp protein, but only those associated with clusters 1 and 2 provided any immunity to infection with *Bp*. Unfortunately, bacteria were found to have colonized the spleen, proving that sterilizing immunity was not achieved.<sup>98</sup>

### 1.6.5 Toxin production

To date, only one toxin has been identified during *Bp* infection. This protein is a potent inhibitor of elongation factor eIF4A, a host cell protein necessary for the elongation phase of protein synthesis.<sup>101</sup> The protein, termed BLF1 or *Burkholderia* lethal factor 1, is found in the supernatant and thought to be directly secreted upon contact with host cells. By acting as a glutamine deamidase, the toxin directly inhibits nascent protein synthesis by interfering with the helicase activity of eIF4A. This leads to apoptotic cell death and/or cytotoxicity.<sup>101</sup>

### 1.6.6 Intracellular motility

While inside the animal host, *Bp* utilizes polymerization of actin to move within the cytosol and potentially invade neighboring cells.<sup>36,102,103</sup> This adaptation allows for movement towards nutrient sources throughout the cell, in addition to evasion of external immune surveillance. The polymerization of host actin also aids in creation of MNGCs and cell membrane fusions seen during *Bp* infection.<sup>36,70</sup> This is accomplished through the use of the *bim* gene cluster located on chromosome two.<sup>103,104</sup> *BimA* encodes an auto-transporter protein that allows for nucleation of actin filaments similar to the process seen in *Listeria* pathogenesis.<sup>103</sup> Interestingly, although an ortholog for this gene is found in both *Bp* near neighbor species, *Bt* and *Bm*, the proteins encoded by these genes act in different ways.

Both *Bm* and *Bp* utilize a *bimA* ortholog similar to the host Ena/VASP system that is capable of polymerization of more than one filament at a time and produces long unbranched, bundled tails.<sup>105</sup> In contrast, *Bt* encodes a Arp2/3-like protein that produces densely branched chains of actin leading to curved tail formation and less efficient movement.<sup>106</sup> While both orthologs mimic host proteins, the Arp2/3 complex found in *Bt* is commonly utilized across multiple bacterial species, while there are currently no other examples of an Ena/VASP system

utilized by an intracellular pathogen.<sup>105</sup> This system is more commonly associated with eukaryotic organisms, and may point to the adaptability of *Bp* species.

### **1.6.7 Multinucleated giant cell formation**

Similar to other known intracellular pathogens e.g. *Mycobacterium tuberculosis*, *Bp* is capable of causing the coalescence of macrophages into multinucleated giant cells.<sup>36,107,108</sup> The purpose of this action is still not well understood, but by causing membrane fusion of host cells the bacteria no longer need to enter the comparatively inhospitable extracellular environment to spread from cell to cell; this could in turn lead to increased bacterial survival.<sup>109</sup> Additionally, MNGC's have lost the ability to act as functional leukocytes meaning that *Bp* retained within the MNGC is protected from internal defense mechanisms as well as external surveillance. During infection with *Bp*, the process of MNGC formation is thought to be controlled in part by the expression of several Type 3 and 6 secretion systems effectors, lipases and environmental sensing proteins, but much research is needed before the process is well characterized.<sup>84,86,110–113</sup>

### **1.6.8 LPS structure and function**

The *Bp* lipopolysaccharide is an important virulence factor during infection but is still relatively uncharacterized. Within the species, LPS can be divided into 3 sub-types based on the different sugars making up the O-polysaccharide unit and modifications to its side chains.<sup>114,115</sup> Interestingly, the prevalence of subtype is linked to geographic location.<sup>114</sup> Type A LPS is primarily found in South East Asian strains while Type B and B2 LPS are found primarily in strains discovered in Australia and Papua New Guinea.<sup>114</sup> The unifying factor between the types of *Bp* LPS is thought to be their relative lack of pyrogenicity in comparison to the same molecule from other Gram-negative species, such as that of *E.coli* or *S. typhi*.<sup>70,116</sup> Although still capable of stimulating cytokine production in the host and causing septic shock at high concentrations,

some studies show a significantly slower activation of TNF- $\alpha$  and iNOS.<sup>116</sup> When the O-polysaccharide synthesis cluster is deleted, pro-inflammatory cytokine levels increase and bacterial survival declines.<sup>117</sup> However, the role of LPS is contested as in-vivo LPS driven cytokine production may differ based on the host species; recent evidence shows human cell lines and patient sera are more reactive than murine models, casting doubt on previous estimations of LPS's immunogenicity.<sup>118,119</sup>

Additionally, the unique structure of *Bp*'s LPS adds to its intrinsic antimicrobial resistance; although polymyxin B is a drug of last resort in many MDR Gram-negative infections, *Bp* is polymyxin resistant due to modification of the lipid A. This is thought to be caused by unique arabinose and O-acetyl modifications of the O-polysaccharide blocking interaction between the drug and LPS. When O-polysaccharide synthesis is interrupted, *Bp* becomes sensitive to polymyxin B.<sup>120</sup>

## 1.7 Melioidosis

The large number of virulence factors encoded by *Bp* allows the bacterium to gain a firm foothold in human hosts and the disease it causes takes on so many clinical manifestations that it has earned the epithet “the great mimicker”. Clinical case reports of disease have included pneumonia and pleural effusion (the typical presentation), and in chronic cases, have sometimes been mistaken for tuberculosis infection based on chest radiographs displaying consolidation or even cavitation in the lungs, low grade fever and cachexia.<sup>121–123</sup> During acute infection, bacteremic spread of the bacillus can lead to fulminant sepsis and fever, solid organ and tissue abscess, brain stem and cerebral infection, necrotizing fasciitis and infection of the prostate in men.<sup>8,34,67,124–126</sup> Osteomyelitis and septic arthritis has also been reported as a result of both chronic and acute infection.<sup>123,127–130</sup> In Thai cases, especially in children, suppurative parotid

abscess is a common symptom of disease found in almost 1/3 of patients as compared to only 2% of Australian cases identified in a prospectus study.<sup>34,131</sup>

With cutaneous inoculation, the disease may manifest as a self-limiting abscess in an otherwise healthy patient. Sinusoidal abscess or septicemic melioidosis secondary to near drowning has been reported.<sup>132,132-135</sup> **Figure 1.2** gives a summary of the common manifestations of disease caused by *Bp* infection, as well as routes of inoculation. In many other cases however, an initial abscess at the site of inoculation may not be identifiable. In those with

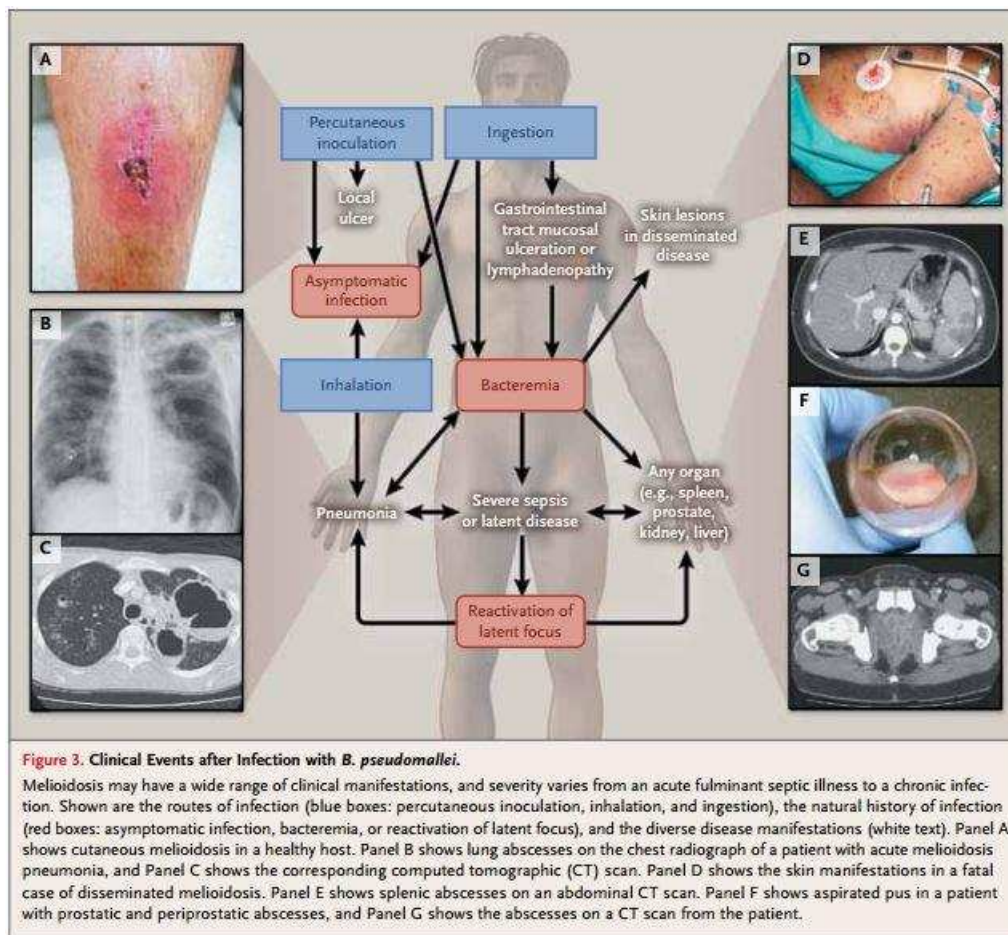


**Figure 1.2. Melioidosis is a multifaceted disease.** Taken from Wiersinga et al. 2012.<sup>2</sup> The diagram depicts common routes of exposure and inoculation to melioidosis (blue boxes: percutaneous inoculation, inhalation and ingestion) as well as radiological and gross clinical findings of associated with different forms of infection (red boxes, white text, and side panels)

underlying predispositions, the outcome of infection can turn from a relatively minor skin or upper respiratory infection to a systemic potentially life-threatening disease in a short period. Depending on route of inoculation, strain variability, dose and host status, disease presentation ranges a full spectrum of symptoms with variable outcomes leading in many cases to misdiagnosis and subsequent treatment failure.

Melioidosis is very commonly mistaken for tuberculosis based on the similarities between chronic presentation of disease and active TB, both in radiologic findings and overall patient presentation.<sup>121,122</sup> However, more extreme misdiagnosis is occasionally seen as a result of the wide diversity of clinical presentations. A recent case reported from Bangladesh described an infection displaying symptoms identical to *Pseudomyxoma peritonei*, a form of peritoneal neoplasm often discovered by accident in patients who have recently undergone abdominal surgery.<sup>136</sup> Another describes an Ohio man who was misdiagnosed with a *Bacillus anthracis* infection, despite correct lab diagnostics indicating melioidosis, and later succumbed to disease.<sup>137</sup> Whether this is the fault of the treatment team or because of the unexpected presentation of disease is unknown, but it underscores the unpredictability sometimes associated with a bacteria that can infect many different ways.

### **1.7.1 Recurrent melioidosis**

Even with seemingly successful treatment, relapses of infection can occur. Most incidents of relapsing melioidosis occur within seven months of the initial infection and are more common in complicated cases in which multiple foci of infection are observed and in patients with a shortened duration of either therapy phase.<sup>138-141</sup> Previous rates of relapse have been recorded as high as 9% in Thailand prior to standardized intensive phase therapy and now range from 1-6%, and up to 5% in Northern Australia.<sup>138,141,142</sup> However, it is interesting to note that

previously observed relapse rates may have included a high number of reinfections. In a Thai study investigating the true rates of recrudescence over a ten year period in Ubon Ratchatani, an estimated 25% of the 125 cases of recurrent melioidosis studied were found to be reinfection with a molecularly distinct strain.<sup>143</sup> This is interesting because it highlights two factors: the importance of risk factors, both physiological and occupational, that lead to re-exposure, and the inability of the adaptive immune system to mount a sterilizing humoral response against *Bp*.

### **1.7.2 Neurological melioidosis**

In a small percentage of clinical cases, infection of the central nervous system is observed. Interestingly, the presentation of neurological melioidosis tends to occur more often in Australian isolates than in SEA strains. An estimated of 4% of all melioidosis patients in one Australian prospectus study of 540 cases developed neurological complications as compared to only 1% of Thai cases.<sup>8,144</sup> Additionally, the pathological focus of infection appears to vary by region as well; in Southeast Asia CNS-melioidosis, macroscopic cortical abscesses are observed, suggesting hematogenous spread of the bacteria from other inoculation points in the body.<sup>145</sup> In Australian cases, CNS involvement was observed even in cases where bacteremia was not, suggesting that the bacteria were able to enter the brain without first causing systemic infection.<sup>125,145,146</sup> This was later confirmed experimentally by intranasal inoculation of a mouse with a capsule negative mutant, unable to survive within the blood stream.<sup>147</sup> The capsule mutant, though unable to spread to distal foci within the body as typically seen during infection, was still isolated from the brain tissues of infected animals. Later experiments suggest that the bacteria is able to travel along the olfactory bulb to the brain where it can cause encephalitis or utilize a “Trojan horse strategy” and enter the brain by being trafficked by infected immune cells.<sup>147,148</sup>

Aiding in the suggestion that these strains may directly infect the brain as opposed to random CNS colonization as a result of systemic infection is the absence of typical bacterial meningitis symptoms during *Bp* infection leading to neurological melioidosis.<sup>146,149</sup> Additionally, in these cases, *Bp* is typically only isolated from the brain stem as opposed to the cortical regions of the brain as expected in cases of systemic melioidosis.<sup>147,148</sup> This observation is contentious, however, as one recent Australian study maintains that neurologic isolates are simply more virulent in general and the perceived tropism for brain infection is a result of more invasive spread as opposed to targeted infection after both intranasal and subcutaneous inoculation.<sup>150</sup> Genetic analysis of strains isolated from cases of primary neurological melioidosis identified additional clues into the progression of this form of disease. The *bimA* gene, encoding the protein BimA necessary for actin utilization during intracellular motility, was found to have a high degree of similarity to that of *bimA* in *Bm* in some strains isolated from patients with neurological melioidosis.<sup>102</sup> Further examination showed that these strains were 14 times more likely to result in brain infection.<sup>102,151</sup> This fact, combined with the observation that this isoform of the protein has only been isolated in Australian variants associated with brain-stem encephalopathy suggests a potential role for BimA in CNS infection.<sup>133,152</sup>

Despite regional variation between infecting strains, the outcome of CNS involvement remains unchanged. Progression to or contraction of this form of disease results in increased mortality in a majority of cases, and a high incidence of lingering CNS dysfunction in survivors.

### **1.7.3 Zoonotic melioidosis**

*Bp* is capable of infecting both plants and animals. While human cases are the main focus of most research of disease caused by *Bp*, it is also recognized as a serious veterinary concern. In Australia, melioidosis was diagnosed in sheep a year before the first official human case was

reported in 1950.<sup>153,154</sup> Since that time, the disease has been established as a pathogen of horses, mules, sheep, goats, pigs and camels with sporadic cases identified in cattle, cats and dogs.<sup>155,156</sup> Melioidosis is also an especially concerning issue in zoos and aquariums where primates and marine mammals are particularly susceptible. Many cases have been described in several species of monkeys including macaques and orangutans either in captive breeding colonies or in zoos.<sup>156</sup> Reports of melioidosis from an aquarium in Hong Kong have described infection of captive populations of multiple species of dolphins, small whales, and fur bearing seals. In a pathologic prospectus of 25 subjects from 1982-1992, soil sample analysis and MLST typing of isolates collectively suggest that these cases resulted from oral infection of the animals after their tanks became contaminated with soil during heavy rains.<sup>157-159</sup> Interestingly, a small proportion were thought to be chronic cases, as some animals showed signs of low level illness for months before succumbing to disease.

### **1.8 Routes of exposure to *Burkholderia pseudomallei***

As *Bp* is a soil saprophyte, most infections are thought to begin through cutaneous inoculation of small cuts in the skin, or through inhalation of aerosolized soil and surface water during heavy rain.<sup>160-162</sup> Contamination of municipal and private water sources also represents a common route of transmission and typically results in clusters of cases after ingestion or inhalation.<sup>13,15,16</sup> Near drowning events, either during otherwise routine outdoor activity or survival of a severe weather event such as a hurricane or tsunami are also known to be important routes of infection with *Bp*.<sup>133,152</sup>

Anecdotal reports of iatrogenic and person-to-person transmission have also been recorded. In patients with prostatic abscess, sexual transmission is possible, although rarely seen. *Bp* infection can also be passed vertically, during parturition or through breast milk in mothers

with breast abscesses or mastitis.<sup>34,163</sup> As the disease also infects a number of livestock species, creating the potential for passage of disease to veterinarians or animal handlers. Skin infections in farmers can occur after milking infected animals, or during the birthing process.<sup>164</sup> Cases of transplacental transmission have been observed in animals, but as of yet no vertical transmission by this route has been identified in humans.<sup>164</sup>

## **1.9 Melioidosis risk factors**

While infection with *Bp* can lead to acute infection in otherwise healthy individuals, mortality in this cohort is a relatively rare occurrence. Patients with underlying health conditions before contact with *Bp* are both more likely to become infected, and for that infection to have a potentially serious outcome. With the improvement of diagnostic capabilities in highly endemic areas, and increased awareness in potentially endemic areas, there is hope that early detection of infection may counteract the effects of these risk factors. However, a majority of fatalities from melioidosis still occur in patients with these confounding health issues.

### **1.9.1 Melioidosis and diabetes**

The number one melioidosis risk factor is diabetes mellitus (DM). Up to 76% of patients admitted for treatment of melioidosis have a new or preexisting diagnosis of type I or II DM.<sup>8,165,166</sup> This is especially concerning given the fact that in areas where melioidosis is highly endemic, cases of type II DM are rapidly increasing in number. WHO estimates of DM prevalence within the ASEAN group project over 100-200 million new cases by 2030.<sup>167</sup> This is of additional concern as global rates of type II DM have reached epidemic proportions and are projected to increase to almost 600 million by that same year.<sup>168</sup> Combining this fact with increasing reports of melioidosis from areas where the disease was previously undetected could lead to infection with *Bp* becoming a more and more prevalent issue worldwide.

To date, little is known about the exact cause of increased melioidosis susceptibility in patients with DM. It is understood however, that DM substantially dysregulates immune function.<sup>165,169,170</sup> Studies into the association of DM and the immune response during melioidosis have noted decreased uptake of live bacteria in both macrophages and neutrophils as well as inability to properly destroy phagocytosed cells, delayed antigen presentation, and vastly altered cytokine profiles skewed towards unregulated inflammation.<sup>165,168,171,172</sup> All these effects together lead to increased bacterial burdens and faster progression of disease

Investigations into the co-administration of glyburide during treatment of melioidosis attempt to curb the impact of DM as a co-factor of disease. The drug is commonly prescribed to DM patients to mediate the effects of insulin insufficiency by regulating sugar metabolism. Glyburide treatment has shown mixed success in managing sepsis in these patients, but it has been demonstrated that good control of blood glucose levels during infection correlates to improved patient outcome.<sup>17,173</sup> This fact underscores the direct correlation of DM and impaired immune function to progression of melioidosis.

### **1.9.2 Renal disease**

Renal disease refers to any dysfunction of the kidney resulting in loss of its ability to filter toxins from the blood. Interestingly, it is commonly associated with a diagnosis of diabetes, but chronic stages of renal disease are their own independent risk factor. In the Top End of Australia, one study of dialysis patients found that the risk of melioidosis increased from 24/100,000 patient years, to 988/100,000 patient years within a cohort of patients undergoing dialysis from 1989-2012.<sup>174</sup> Of the almost 800 cases of melioidosis during this time period, 3.4% of patients had end-stage renal disease.<sup>174</sup> It is important to note however, that patients undergoing treatment for renal disease have a higher co-occurrence of other risk factors,

including diabetes.<sup>174</sup> Some 60% of dialysis patients in this prospectus were receiving treatment as a direct result of diabetic neuropathy.

### 1.9.3 Thalassemia

Thalassemia is a disease similar to Sickle cell anemia and is commonly found in areas where malaria is endemic.<sup>175</sup> Heterozygosity for the mutation causing disease is thought to protect against infection with *Plasmodium falciparum*, but full-fledged thalassemia can lead to severe anemia, liver failure and increased susceptibility to infection. As a result many patients with more serious forms of disease require complete transfusion from infancy.<sup>176</sup> Beta-thalassemia, the most common form, results from inheritance of an autosomal recessive mutation to the beta-globin chain of hemoglobin leading to defects or in some cases complete absence of the functional protein.<sup>175,176</sup> Multiple types of this form of the disease exist, and can result from one of over 200 known mutations. In areas endemic to *Bp*, E- $\beta$ -thalassemia is the most common phenotype of disease and is diagnosed in about 3,000 births in Thailand alone, each year.<sup>176,177</sup> Dysregulated immune function is a common side effect of the disease and therefore many patients are more prone to blood-borne disease, certain forms of cancer, and infection in general. Both the innate and adaptive response are affected.

The inability of the body to fight infection as a result of thalassemia is closely linked to iron metabolism. Destruction of defective erythrocytic precursors leads to both a counterintuitive increase in free iron, and chronic anemia, compensated by increased iron absorption in the gut. This cycle causes severe iron overload in serious cases that can be compounded by transfusions with blood from healthy donors.<sup>176</sup> Additionally, a chronic inflammatory state caused by perpetual activation of monocytes targeting defective or dying erythrocytes for destruction may lead to immune depletion.<sup>178</sup> Taken together this may result in the propensity for *Bp* infection.

#### 1.9.4 Drug use and melioidosis

While the direct relationship between melioidosis and drug use has not been well studied, both behaviors are known risk factors for contracting the disease. Mounting evidence suggests that prolonged or chronic use of either alcohol or kava may have a profound effect on the immune system. Kava, or *Piper methysticum*, is a shrub cultivated in the western pacific. Preparations of its stems and roots possess mild psychotropic qualities and are used both recreationally and in traditional ceremonies in Oceania to this day. In the 1980's the drug was introduced into the northern territory of Australia as a surrogate for alcohol, as it possesses the same calming effect in small amounts.<sup>179</sup> Overconsumption of kava has emerged as an independent risk factor for infection with *Bp* and a link has been observed between over use and generalized predisposition to infection.<sup>5</sup> A recent study by Kwon et al, demonstrated the ability of flavokawain A, one of the chalcone compounds found in Kava, to attenuate the in-vitro cytokine response of macrophages to LPS through a putative block in Nfkb/Ap-1 signaling.<sup>180</sup> The observed reduction in TNF- $\alpha$ , IL-6, IL-12 and iNOS may be to blame for the increased susceptibility of kava drinkers to infection with *Bp*.<sup>180</sup> While certain bioactive compounds in kava are being investigated for their anti-carcinogenic properties, overuse could lead to predisposition to chronic infections through an immunosuppressive mechanism.

Alcoholism may increase the risk of infection through a similar general mechanisms centered in the lung. Chronic alcohol consumption is known to increase the risk of acute respiratory distress syndrome, or ARDS, especially in cases of sepsis.<sup>181</sup> Recent studies suggest this may be influenced by gross immune dysregulation promoted by both changes in fatty acid metabolism in the alveolar air space leading to more free fatty acid and increased production of reactive oxygen species.<sup>182,183</sup> In response to this change, alveolar macrophages display increased

levels of TGF- $\beta$  and IL-13 and enter into an alternative activation mode necessary for tissue repair and angiogenesis as opposed to pathogen clearance, with decreased pro-inflammatory cytokine production and phagocytosis.<sup>182,184</sup> As the macrophage response becomes polarized to a more adaptive state through the alternative pathway, the air space now becomes more prone to colonization by pathogenic microbes, as the macrophages are unable to either secrete pro-inflammatory cytokines or chemokines or phagocytose and clear the invading bacteria.<sup>183</sup>

### **1.9.5 Occupational and environmental risk factors**

Based in its environmental niche as a soil saprophyte, it is unsurprising that a high association exists between exposure to contaminated soil or water and *Bp* infection. This is best illustrated by the high incidence of melioidosis among rice farmers in south East Asia. In several studies examining risk factors of disease, up to 85% of patients listed their occupation as rice farmer. In a matched pair case control study of risk factors associated with *Bp* infection, activities requiring prolonged contact with soil and water were directly related to disease, rice farming being one of these.<sup>6,139,185</sup> A comparison of practices within this occupation found that increased depth of soil or water submergence during tasks associated with rice cultivation increased the risk of melioidosis.<sup>185</sup> Conversely, the use of long pants and rubber boots greatly diminished this risk. This fact also reinforced the need for public awareness and modification of farming practices as a way to curb incidence of disease in endemic regions where rice farming occurs.

Environmental exposure is also intrinsically linked to weather events and highlights the need for evaluation of infection control in emergency response plans formed in areas endemic to *Bp*. In fact, cluster cases following serious weather events including hurricanes, typhoons and tsunamis are responsible for the confirmation of *Bp* endemicity in previously undocumented

regions.<sup>152</sup> Additionally, coinfection of emergency response personnel as a result of rescue operations during these weather events has been documented on underscoring the need for increased awareness of the signs and symptoms of disease during emergency management.<sup>133,152,186</sup>

Serious weather events are not the sole determining factor however, as seasonal rainfall within the limits of normal monsoon seasons have been directly correlated to spikes in the number of melioidosis cases reported.<sup>2</sup> From 80-85% of cases reported in Thailand occur during or immediately after the rainy season.<sup>187</sup> A similar pattern is seen in Northern Australia, with spikes in cases directly related to seasonal rainfall. This is hypothesized to be the result of heavy rain both aerosolizing contaminating soil, and introducing newly mixed soil into poorly maintained drinking water systems.

### **1.10 Melioidosis diagnosis**

Rapid, accurate identification of *Bp* remains vital to effective treatment of infection in cases of melioidosis. To accomplish this many methods are currently in use, with varying degrees of success. The gold standard for identification of *Bp* is culture of the organism on selective media (typically Ashdown's agar), but a combination of gene-specific PCR, differential microbiological techniques and indirect hemagglutination assays have also been developed.<sup>188-191</sup> While these are effective in combination for a majority of *Bp* strains, such methods rely on both the ability to culture the bacteria as well a considerable amount of time. The potential for delayed diagnosis greatly disadvantages patients with more advanced disease. Attempts to shorten the time to accurate identification have been bolstered by *Bp*'s classification as a potential biothreat agent. This has resulted in investigations of MALDI-TOF analysis, lateral flow assays utilizing monoclonal CPS and LPS antibodies and multiplex PCR identification assays targeting 16S

RNA, elements of the Type III secretion system and *groEL*.<sup>190,192,193</sup> While some of these tests still require the ability to culture a pure population of bacteria, they produce rapid results once initiated. However, some newer methods, specifically those requiring specialized equipment, may not be available in endemic regions where the disease is highly prevalent but well equipped laboratories are not. Methods that do not rely on the presence of bacteria, specifically the lateral flow assay and IHA, are especially promising in these more remote areas. Unfortunately, development efforts have been hampered by cross reactivity between near neighbor species, and in the case of the IHA, lack of standardization between preparations which could decrease the accuracy of the test.<sup>190</sup> Even so, these assays may be vital to improving the survival rate in suspected endemic regions where the disease has been previously undiagnosed simply because of a lack of diagnostic capability.

Commercial assays have also been developed for identification of *Bp* in clinical labs equipped with molecular biotypers, or staff capable of interpreting the API 2One test, but these remain only about 80% accurate according to a study by Lau et al.<sup>190,194</sup> In fact, misdiagnosis is a commonly reported event in *Bp* infection and may play a role in both under reporting in potentially endemic regions as well as mortality.<sup>188,195,196</sup> Unfortunately, the ability to accurately identify the bacteria is no guarantee that a correct diagnosis will be made, especially in areas where the disease is not endemic.

### **1.11 Current efforts in vaccine development**

To date, there is no effective vaccine capable of providing reliable protection against infection with *Bp*.<sup>197</sup> While many studies are in progress to identify potential candidates for vaccine developments, none have been tested in a non-human primate model. Current strategies address this issue from many perspectives; investigations into live attenuated strain production,

carrier molecules, epitope discovery and subunit vaccines have all been attempted but with little success to date because in most cases, sterilizing immunity is not achieved.<sup>73,198–201</sup> However, advances are being made: a recent report from Moustafa et al. describes a *S. typhi* strain engineered to express *Bm* LPS that effectively protects against infection with a lethal dose of *Bt.* In this study, no bacteria were recovered from the organs of intranasally-vaccinated mice and a robust T<sub>H</sub>2 cytokine response was observed, both indicating the production of protective immunity.<sup>202</sup> Further investigation is still needed to determine if this is predictive of the post-vaccination response to infection with *Bp* or *Bm*.

### 1.12 Treatment of melioidosis

*Bp* infections remain very difficult to treat. Until the late 1980's and the incorporation of ceftazidime into treatment regimens, mortality rates in Thai cases hovered around 85 percent. Prior to this, clinicians typically administered a drug cocktail of trimethoprim, sulfamethoxazole, chloramphenicol, doxycycline or carbenicillin, but these treatment efforts were met with high rates of treatment failure and resistance.<sup>203</sup>

With intravenous ceftazidime monotherapy over a period of at least 2 weeks during the acute phase of infection, mortality rates were cut in half.<sup>204</sup> This became the standard for intensive phase therapy, with administration of carbapenem or co-amoxiclav administered in complicated or contraindicated cases.<sup>2,140,161</sup> The four drug combo therapy became the new standard for oral eradication phase until worries of patient non-compliance and drug toxicity lead to examinations of the efficacy of using all four drugs simultaneously.<sup>140</sup> Chloramphenicol displayed no additive effect to treatment in randomized studies, and was eventually contraindicated due to high toxicity rates.<sup>140,205</sup> Doxycycline is still administered with trimethoprim + sulfamethoxazole (co-trimoxazole) during the eradication phase in some areas,

but recent investigations have found it adds no benefit and could in fact lead to seriously increased resistance to itself and other compounds.<sup>142,206</sup>

During the eradication phase of disease, patients are administered oral co-trimoxazole for up to six months in an effort to completely clear the infection. Strict compliance to the minimum recommended 12 weeks may be necessary, as one Thai study observed a five-fold increased risk of death or relapse in patients who underwent a shortened eradication phase.<sup>205</sup> However, similar investigations into relapse risk factors in Australia found that increasing the intensive phase of therapy based on the disease focus reduced the rate of relapse to less than 1%, even with only 50% compliance to the recommended eradication phase. It may be that clearance of distal infection foci during an extended intensive phase could drastically improve the efficacy of the eradication phase, or remove the need for it entirely in uncomplicated cases.<sup>141</sup>

Even with antimicrobial therapy, the mortality rates for disease range from 6 to almost 40 percent depending on the region. However, it is important to note that the majority of these mortalities occur in patients with an underlying risk factor, especially if that risk factor is previously undiagnosed. Resistance mechanisms complicating the already laborious treatment of melioidosis relying on a few efficacious antibiotics will be reviewed in the next chapter. *Bp* is a fascinating organism that poses a severe burden on the community health in endemic regions. Continued investigation of all aspects of disease prevention, treatment and pathogenesis is necessary to prevent this burden from increasing.

## Chapter 1 References

1. Cheng, A. C. & Currie, B. J. Melioidosis: epidemiology, pathophysiology, and management. *Clin. Microbiol. Rev.* **18**, 383–416 (2005).
2. Wiersinga, W. J., Currie, B. J. & Peacock, S. J. Melioidosis. *N. Engl. J. Med.* **367**, 1035–1044 (2012).
3. Leelarasamee, A. Epidemiology of melioidosis. *J. Infect. Dis. Antimicrob. Agents* **3**, 84–93 (1989).
4. McRobb, E. *et al.* Distribution of *Burkholderia pseudomallei* in Northern Australia, a land of diversity. *Appl. Environ. Microbiol.* **80**, 3463–3468 (2014).
5. Currie, B. J. *et al.* Endemic melioidosis in tropical Northern Australia: A 10- year prospective study and review of the literature. *Clin. Infect. Dis.* **31**, 981–986 (2000).
6. Hassan, M. R. *et al.* Incidence, risk factors and clinical epidemiology of melioidosis: a complex socio-ecological emerging infectious disease in the Alor Setar region of Kedah, Malaysia. *BMC Infect. Dis.* **10**, 302 (2010).
7. Le Hello, S. *et al.* Melioidosis in New Caledonia. *Emerg. Infect. Dis.* **11**, 1607–1609 (2005).
8. Currie, B. J., Ward, L. & Cheng, A. C. The epidemiology and clinical spectrum of melioidosis: 540 cases from the 20 year darwin prospective study. *PLoS Negl. Trop. Dis.* **4**, e900 (2010).
9. Limmathurotsakul, D. *et al.* Increasing incidence of human melioidosis in Northeast Thailand. *Am. J. Trop. Med. Hyg.* **82**, 1113–1117 (2010).
10. *Public Health Security and Bioterrorism Preparedness and Response Act. Title 42 Chapter*

**1 Subsection F**, (2012).

11. Pumpuang, A. *et al.* Survival of *Burkholderia pseudomallei* in distilled water for 16 years. *Trans. R. Soc. Trop. Med. Hyg.* **105**, 598–600 (2011).
12. Wuthiekanun, V., Smith, M. D. & White, N. J. Survival of *Burkholderia pseudomallei* in the absence of nutrients. *Trans. R. Soc. Trop. Med. Hyg.* **89**, 491 (1995).
13. McRobb, E. *et al.* Melioidosis from contaminated bore water and successful uv sterilization. *Am. J. Trop. Med. Hyg.* **89**, 367–368 (2013).
14. Robertson, J., Levy, A., Sagripanti, J.-L. & Inglis, T. J. J. The survival of *Burkholderia pseudomallei* in liquid media. *Am. J. Trop. Med. Hyg.* **82**, 88–94 (2010).
15. Draper, A. D. K. *et al.* Association of the melioidosis agent *Burkholderia pseudomallei* with water parameters in rural water supplies in Northern Australia. *Appl. Environ. Microbiol.* **76**, 5305–5307 (2010).
16. Currie, B. J. *et al.* A cluster of melioidosis cases from an endemic region is clonal and is linked to the water supply using molecular typing of *Burkholderia pseudomallei* isolates. *Am. J. Trop. Med. Hyg.* **65**, 177–179 (2001).
17. Ngauy, V., Lemeshev, Y., Sadkowski, L. & Crawford, G. Cutaneous melioidosis in a man who was taken as a prisoner of war by the Japanese during World War II *J. Clin. Microbiol.* **43**, 970–972 (2005).
18. Whitmore, A. An Account of a glanders-like disease occurring in Rangoon. *J. Hygiene* **13**, 34 (1913).
19. Whitmore, A. & Krishnaswami, C. S. An account of the discovery of a hitherto underscribed infective disease occurring among the population of Rangoon. *Indian Med. Gaz.* 262–267 (1912).

20. Stanton, A. T., Fletcher, W. & Kanagarayer, K. Two cases of melioidosis. *J. Hyg. (Lond.)* **23**, 268–276.7 (1924).
21. Stanton, A. T., Fletcher, W. & Symonds, S. L. Melioidosis in a horse. *J. Hyg. (Lond.)* **26**, 33–35 (1927).
22. Stanton, A. T. & Fletcher, W. Melioidosis: notes on a culture of *B. whitmori* from Saigon. *J. Hyg. (Lond.)* **26**, 31–32 (1927).
23. Pons, R. & Advier, M. Melioidosis in Cochin China. *J. Hyg. (Lond.)* **26**, 28–30 (1927).
24. Green, R. & Mankikar, D. S. Afebrile cases of melioidosis. *Br. Med. J.* **1**, 308–311 (1949).
25. Stanton, A. & Fletcher, W. *Studies from the Institute for Medical Research, Federated Malay States.* 1–97 (1932).
26. Harries, E. J. & Lewis, A. a. G. Melioidosis treated with sulphonamides and penicillin. *Lancet Lond. Engl.* **1**, 363–366 (1948).
27. Thin, R. N. Melioidosis antibodies in Commonwealth soldiers. *Lancet* **1**, 31–33 (1976).
28. Paton, J. P. J., Peck, C. R. & Van De Schaff, A. Report on a case of melioidosis from Siam. *Br. Med. J.* **1**, 336 (1947).
29. Cox, C. D. & Arbogast, J. L. Melioidosis. *Am. J. Clin. Pathol.* **15**, 567–570 (1945).
30. Kishimoto, R., Brown, G., Blair, E. & Wenkheimer, D. Melioidosis: Serologic studies on us army personnel returning from Southeast Asia. *Mil. Med.* **136**, 694–698 (1971).
31. Yabuuchi, E. *et al.* Proposal of *Burkholderia gen. nov.* and transfer of seven species of the genus *Pseudomonas* homology group II to the new genus, with the type species *Burkholderia cepacia* (Palleroni and Holmes 1981) *comb. nov.* *Microbiol. Immunol.* **36**, 1251–1275 (1992).
32. Woods, D. E. & Sokol, P. A. in *The Prokaryotes* (eds. Dworkin, M., Falkow, S., Rosenberg, E., Schleifer, K.-H. & Stackebrandt, E.) 848–860 (Springer New York, 2006). at

<[http://link.springer.com/10.1007/0-387-30745-1\\_40](http://link.springer.com/10.1007/0-387-30745-1_40)>

33. Sawana, A., Adeolu, M. & Gupta, R. S. Molecular signatures and phylogenomic analysis of the genus *Burkholderia*: proposal for division of this genus into the emended genus *Burkholderia* containing pathogenic organisms and a new genus *Paraburkholderia* gen. nov. harboring environmental species. *Front. Genet.* **5**, (2014).
34. White, N. Melioidosis. *The Lancet* **361**, 1715–1722 (2003).
35. Coenye, T. & Vandamme, P. Diversity and significance of *Burkholderia* species occupying diverse ecological niches. *Environ. Microbiol.* **5**, 719–729 (2003).
36. Galyov, E. E., Brett, P. J. & DeShazer, D. Molecular insights into *Burkholderia pseudomallei* and *Burkholderia mallei* pathogenesis. *Annu. Rev. Microbiol.* **64**, 495–517 (2010).
37. Van Zandt, K. E., Greer, M. T. & Gelhaus, H. Glanders: an overview of infection in humans. *Orphanet J. Rare Dis.* **8**, 131 (2013).
38. Wheelis, M. First shots fired in biological warfare. *Nature* **395**, 213 (1998).
39. Alibek, K. & Handelman, S. *Biohazard: the chilling true story of the largest covert biological weapons program in the world, told from the inside by the man who ran it.* (Random House, 1999).
40. Harris, S. Japanese biological warfare research on humans: a case study of microbiology and ethics. *Ann. N. Y. Acad. Sci.* **666**, 21–52 (1992).
41. Frischknecht, F. The history of biological warfare. *EMBO Rep.* **4**, S47–S52 (2003).
42. Ciottone, G. *et al.* *Ciottone's Disaster Medicine.* (2016).
43. Brett, P. J., DeShazer, D. & Woods, D. E. *Burkholderia thailandensis* sp. nov., a *Burkholderia pseudomallei*-like species. *Int. J. Syst. Bacteriol.* **48 Pt 1**, 317–320 (1998).

44. Chaiyaroj, S. C. *et al.* Differences in genomic macrorestriction patterns of arabinose-positive (*Burkholderia thailandensis*) and arabinose-negative *Burkholderia pseudomallei*. *Microbiol. Immunol.* **43**, 625–630 (1999).
45. Wuthiekanun, V., Anuntagool, N., White, N. J. & Sirisinha, S. Short report: a rapid method for the differentiation of *Burkholderia pseudomallei* and *Burkholderia thailandensis*. *Am. J. Trop. Med. Hyg.* **66**, 759–761 (2002).
46. Mahenthiralingam, E., Urban, T. A. & Goldberg, J. B. The multifarious, multireplicon *Burkholderia cepacia* complex. *Nat. Rev. Microbiol.* **3**, 144–156 (2005).
47. Hall, C. M. *et al.* Diverse *Burkholderia* species isolated from soils in the Southern United States with no evidence of *B. pseudomallei*. *PloS One* **10**, e0143254 (2015).
48. Leitão, J. H. *et al.* Pathogenicity, virulence factors, and strategies to fight against *Burkholderia cepacia* complex pathogens and related species. *Appl. Microbiol. Biotechnol.* **87**, 31–40 (2010).
49. Jin, Z. M., Sha, W., Zhang, Y. F., Zhao, J. & Ji, H. Isolation of *Burkholderia cepacia* JB12 from lead- and cadmium-contaminated soil and its potential in promoting phytoremediation with tall fescue and red clover. *Can. J. Microbiol.* **59**, 449–455 (2013).
50. Laocharoen, S., Plangklang, P. & Reungsang, A. Selection of support materials for immobilization of *Burkholderia cepacia* PCL3 in treatment of carbofuran-contaminated water. *Environ. Technol.* **34**, 2587–2597 (2013).
51. Vidal-Quist, J. C. *et al.* *Arabidopsis thaliana* and *Pisum sativum* models demonstrate that root colonization is an intrinsic trait of *Burkholderia cepacia* complex bacteria. *Microbiol. Read. Engl.* **160**, 373–384 (2014).
52. Sim, S. H. *et al.* The core and accessory genomes of *Burkholderia pseudomallei*:

- Implications for human melioidosis. *PLoS Pathog.* **4**, e1000178 (2008).
53. Nandi, T. *et al.* *Burkholderia pseudomallei* sequencing identifies genomic clades with distinct recombination, accessory, and epigenetic profiles. *Genome Res.* **25**, 129–141 (2015).
54. Chantratita, N. *et al.* Genetic diversity and microevolution of *Burkholderia pseudomallei* in the environment. *PLoS Negl. Trop. Dis.* **2**, e182 (2008).
55. Chantratita, N. *et al.* Antimicrobial resistance to ceftazidime involving loss of penicillin-binding protein 3 in *Burkholderia pseudomallei*. *Proc. Natl. Acad. Sci.* **108**, 17165–17170 (2011).
56. Hayden, H. S. *et al.* Evolution of *Burkholderia pseudomallei* in recurrent melioidosis. *PLoS ONE* **7**, e36507 (2012).
57. Katangwe, T. *et al.* Human melioidosis, Malawi, 2011. *Emerg. Infect. Dis.* **19**, 981–984 (2013).
58. Garin, B. *et al.* Autochthonous melioidosis in humans, Madagascar, 2012 and 2013. *Emerg. Infect. Dis.* **20**, 1739–1741 (2014).
59. Gétaz, L. *et al.* Fatal acute melioidosis in a tourist returning from Martinique Island, November 2010. *Euro Surveill. Bull. Eur. Sur Mal. Transm. Eur. Commun. Dis. Bull.* **16**, (2011).
60. Meckenstock, R. *et al.* Cutaneous melioidosis in adolescent returning from Guadeloupe. *Emerg. Infect. Dis.* **18**, 359–360 (2012).
61. Dorman, S. E., Gill, V. J., Gallin, J. I. & Holland, S. M. *Burkholderia pseudomallei* infection in a Puerto Rican patient with chronic granulomatous disease: case report and review of occurrences in the Americas. *Clin. Infect. Dis. Off. Publ. Infect. Dis. Soc. Am.* **26**, 889–894 (1998).
62. Dance, D. A. B. Editorial commentary: melioidosis in Puerto Rico: the iceberg slowly

- emerges. *Clin. Infect. Dis. Off. Publ. Infect. Dis. Soc. Am.* **60**, 251–253 (2015).
63. Barth, A. L. *et al.* Cystic fibrosis patient with *Burkholderia pseudomallei* infection acquired in Brazil. *J. Clin. Microbiol.* **45**, 4077–4080 (2007).
64. Brilhante, R. S. N. *et al.* Clinical-epidemiological features of 13 cases of melioidosis in Brazil. *J. Clin. Microbiol.* **50**, 3349–3352 (2012).
65. Rolim, D. B. *et al.* *Burkholderia pseudomallei* antibodies in individuals living in endemic regions in Northeastern Brazil. *Am. J. Trop. Med. Hyg.* **84**, 302–305 (2011).
66. Montúfar, F. E. *et al.* Melioidosis in Antioquia, Colombia. An emerging or endemic disease: a cases series. *Int. J. Infect. Dis. IJID Off. Publ. Int. Soc. Infect. Dis.* (2015).  
doi:10.1016/j.ijid.2015.05.023
67. Sood, S., Khedar, R. S., Joad, S. H. & Gupta, R. Septicaemic melioidosis: case report from a non-endemic area. *J. Clin. Diagn. Res. JCDR* **8**, DD01–02 (2014).
68. Diefenbach-Elstob, T. R., Graves, P. M., Burgess, G. W., Pelowa, D. B. & Warner, J. M. Seroepidemiology of melioidosis in children from a remote region of Papua New Guinea. *Int. Health* (2014). doi:10.1093/inthealth/ihu088
69. Limmathurotsakul, D. *et al.* Predicted global distribution of *Burkholderia pseudomallei* and burden of melioidosis. *Nat. Microbiol.* **1**, 15008 (2016).
70. Wiersinga, W. J., van der Poll, T., White, N. J., Day, N. P. & Peacock, S. J. Melioidosis: insights into the pathogenicity of *Burkholderia pseudomallei*. *Nat. Rev. Microbiol.* **4**, 272–282 (2006).
71. Lee, H. S., Gu, F., Ching, S. M., Lam, Y. & Chua, K. L. CdpA is a *Burkholderia pseudomallei* cyclic di-GMP phosphodiesterase involved in autoaggregation, flagellum synthesis, motility, biofilm formation, cell invasion, and cytotoxicity. *Infect. Immun.* **78**, 1832–

1840 (2010).

72. Chuaygud, T., Tungpradabkul, S., Sirisinha, S., Chua, K. L. & Utaisincharoen, P. A role of *Burkholderia pseudomallei* flagella as a virulent factor. *Trans. R. Soc. Trop. Med. Hyg.* **102**, S140–S144 (2008).

73. Gourlay, L. J. *et al.* From crystal structure to *in silico* epitope discovery in the *Burkholderia pseudomallei* flagellar hook-associated protein FlgK. *FEBS J.* **282**, 1319–1333 (2015).

74. Allwood, E. M., Devenish, R. J., Prescott, M., Adler, B. & Boyce, J. D. Strategies for intracellular survival of *Burkholderia pseudomallei*. *Front. Microbiol.* **2**, (2011).

75. Essex-Lopresti, A. E. *et al.* A Type IV Pilin, PilA, contributes to adherence of *Burkholderia pseudomallei* and virulence in vivo. *Infect. Immun.* **73**, 1260–1264 (2005).

76. Boddey, J. A., Flegg, C. P., Day, C. J., Beacham, I. R. & Peak, I. R. Temperature-regulated microcolony formation by *Burkholderia pseudomallei* requires *pilA* and enhances association with cultured human cells. *Infect. Immun.* **74**, 5374–5381 (2006).

77. Brown, N. F. Adherence of *Burkholderia pseudomallei* cells to cultured human epithelial cell lines is regulated by growth temperature. *Infect. Immun.* **70**, 974–980 (2002).

78. Campos, C. G., Borst, L. & Cotter, P. A. Characterization of BcaA, a putative classical autotransporter protein in *Burkholderia pseudomallei*. *Infect. Immun.* **81**, 1121–1128 (2013).

79. Balder, R. *et al.* Identification of *Burkholderia mallei* and *Burkholderia pseudomallei* adhesins for human respiratory cells. *BMC Microbiol.* **10**, 19 (2010).

80. Lafontaine, E. R., Balder, R., Michel, F. & Hogan, R. J. Characterization of an autotransporter adhesin protein shared by *Burkholderia mallei* and *Burkholderia pseudomallei*. *BMC Microbiol.* **14**, 92 (2014).

81. Stevens, M. P. & Galyov, E. E. Exploitation of host cells by *Burkholderia pseudomallei*.

*Int. J. Med. Microbiol.* **293**, 549–555 (2004).

82. Stevens, M. P. *et al.* An Inv/Mxi-Spa-like type III protein secretion system in *Burkholderia pseudomallei* modulates intracellular behaviour of the pathogen: Role of a TTSS in *B.*

*pseudomallei*-host cell interactions. *Mol. Microbiol.* **46**, 649–659 (2002).

83. Burtnick, M. N. *et al.* *Burkholderia pseudomallei* type III secretion system mutants exhibit delayed vacuolar escape phenotypes in RAW 264.7 murine macrophages. *Infect. Immun.* **76**, 2991–3000 (2008).

84. Suparak, S. *et al.* Multinucleated giant cell formation and apoptosis in infected host cells is mediated by *Burkholderia pseudomallei* Type III Secretion protein BipB. *J. Bacteriol.* **187**, 6556–6560 (2005).

85. Gong, L. *et al.* The burkholderia pseudomallei Type III Secretion System and BopA Are required for evasion of LC3-associated phagocytosis. *PLoS ONE* **6**, e17852 (2011).

86. French, C. T. *et al.* Dissection of the *Burkholderia* intracellular life cycle using a photothermal nanoblade. *Proc. Natl. Acad. Sci.* **108**, 12095–12100 (2011).

87. Teh, B. *et al.* Type three secretion system-mediated escape of *Burkholderia pseudomallei* into the host cytosol is critical for the activation of NF $\kappa$ B. *BMC Microbiol.* **14**, 115 (2014).

88. Gong, L. *et al.* *Burkholderia pseudomallei* Type III Secretion System Cluster 3 ATPase BsaS, a Chemotherapeutic Target for Small-Molecule ATPase Inhibitors. *Infect. Immun.* **83**, 1276–1285 (2015).

89. Treerat, P. *et al.* The *Burkholderia pseudomallei* Proteins BapA and BapC are secreted TTSS3 effectors and BapB levels modulate expression of BopE. *PLOS ONE* **10**, e0143916 (2015).

90. Chirakul, S. *et al.* Characterization of *BPSSI521* (*bprD*), a regulator of *Burkholderia*

- pseudomallei* virulence gene expression in the mouse model. *PLoS ONE* **9**, e104313 (2014).
91. Sun, G. W. *et al.* Identification of a regulatory cascade controlling Type III Secretion System 3 gene expression in *Burkholderia pseudomallei*. *Mol. Microbiol.* **76**, 677–689 (2010).
  92. Sun, G. W. & Gan, Y.-H. Unraveling type III secretion systems in the highly versatile *Burkholderia pseudomallei*. *Trends Microbiol.* **18**, 561–568 (2010).
  93. Pukatzki, S. *et al.* Identification of a conserved bacterial protein secretion system in *Vibrio cholerae* using the *Dictyostelium* host model system. *Proc. Natl. Acad. Sci.* **103**, 1528–1533 (2006).
  94. Russell, A. B., Peterson, S. B. & Mougous, J. D. Type VI secretion system effectors: poisons with a purpose. *Nat. Rev. Microbiol.* **12**, 137–148 (2014).
  95. Schell, M. A. *et al.* Type VI secretion is a major virulence determinant in *Burkholderia mallei*. *Mol. Microbiol.* **64**, 1466–1485 (2007).
  96. Shalom, G., Shaw, J. G. & Thomas, M. S. In vivo expression technology identifies a type VI secretion system locus in *Burkholderia pseudomallei* that is induced upon invasion of macrophages. *Microbiology* **153**, 2689–2699 (2007).
  97. Schwarz, S. *et al.* *Burkholderia* Type VI Secretion Systems have distinct roles in eukaryotic and bacterial cell interactions. *PLoS Pathog.* **6**, e1001068 (2010).
  98. Burtnick, M. N. *et al.* The Cluster 1 Type VI Secretion System is a major virulence determinant in *Burkholderia pseudomallei*. *Infect. Immun.* **79**, 1512–1525 (2011).
  99. Burtnick, M. N. & Brett, P. J. *Burkholderia mallei* and *Burkholderia pseudomallei* cluster 1 type VI secretion system gene expression is negatively regulated by iron and zinc. *PloS One* **8**, e76767 (2013).
  100. Lim, Y. T. *et al.* Extended loop region of Hcp1 is critical for the assembly and function of

- type VI secretion system in *Burkholderia pseudomallei*. *Sci. Rep.* **5**, 8235 (2015).
101. Cruz-Migoni, A. *et al.* A *Burkholderia pseudomallei* toxin inhibits helicase activity of translation factor eIF4A. *Science* **334**, 821–824 (2011).
102. Sitthidet, C. *et al.* Prevalence and sequence diversity of a factor required for actin-based motility in natural populations of *Burkholderia* Species. *J. Clin. Microbiol.* **46**, 2418–2422 (2008).
103. Lu, Q., Xu, Y., Yao, Q., Niu, M. & Shao, F. A polar-localized iron-binding protein determines the polar targeting of *Burkholderia* BimA autotransporter and actin tail formation. *Cell. Microbiol.* (2014). doi:10.1111/cmi.12376
104. Stevens, M. P. *et al.* Identification of a bacterial factor required for actin-based motility of *Burkholderia pseudomallei*. *Mol. Microbiol.* **56**, 40–53 (2005).
105. Benanti, E. L., Nguyen, C. M. & Welch, M. D. Virulent *Burkholderia* species mimic host actin polymerases to drive actin-based motility. *Cell* **161**, 348–360 (2015).
106. Sitthidet, C. *et al.* Actin-based motility of *Burkholderia thailandensis* requires a central acidic domain of BimA that recruits and activates the cellular Arp2/3 complex. *J. Bacteriol.* **192**, 5249–5252 (2010).
107. Pegoraro, G. *et al.* A high-content imaging assay for the quantification of the *Burkholderia pseudomallei* induced multinucleated giant cell (MNGC) phenotype in murine macrophages. *BMC Microbiol.* **14**, 98 (2014).
108. Lazar Adler, N. R. *et al.* The molecular and cellular basis of pathogenesis in melioidosis: how does *Burkholderia pseudomallei* cause disease? *FEMS Microbiol. Rev.* **33**, 1079–1099 (2009).
109. Kespichayawattana, W., Rattanachetkul, S., Wanun, T., Utaisincharoen, P. & Sirisinha, S.

- Burkholderia pseudomallei* induces cell fusion and actin-associated membrane protrusion: a possible mechanism for cell-to-cell spreading. *Infect. Immun.* **68**, 5377–5384 (2000).
110. Boddey, J. A. *et al.* The bacterial gene *lfpA* influences the potent induction of calcitonin receptor and osteoclast-related genes in *Burkholderia pseudomallei*-induced TRAP-positive multinucleated giant cells. *Cell. Microbiol.* **9**, 514–531 (2007).
111. Utaisincharoen, P., Arjcharoen, S., Limposuwan, K., Tungradabkul, S. & Sirisinha, S. *Burkholderia pseudomallei* RpoS regulates multinucleated giant cell formation and inducible nitric oxide synthase expression in mouse macrophage cell line (RAW 264.7). *Microb. Pathog.* **40**, 184–189 (2006).
112. Toesca, I. J., French, C. T. & Miller, J. F. The Type VI secretion system spike protein VgrG5 mediates membrane fusion during intercellular spread by pseudomallei group *Burkholderia* species. *Infect. Immun.* **82**, 1436–1444 (2014).
113. Schwarz, S. *et al.* VgrG-5 Is a *Burkholderia* Type VI secretion system-exported protein required for multinucleated giant cell formation and virulence. *Infect. Immun.* **82**, 1445–1452 (2014).
114. Tuanyok, A. *et al.* The Genetic and Molecular Basis of O-Antigenic Diversity in *Burkholderia pseudomallei* Lipopolysaccharide. *PLoS Negl. Trop. Dis.* **6**, e1453 (2012).
115. DeShazer, D., Brett, P. J. & Woods, D. E. The type II O-antigenic polysaccharide moiety of *Burkholderia pseudomallei* lipopolysaccharide is required for serum resistance and virulence. *Mol. Microbiol.* **30**, 1081–1100 (1998).
116. Utaisincharoen, P. *et al.* Kinetic studies of the production of nitric oxide (NO) and tumour necrosis factor-alpha (TNF-alpha) in macrophages stimulated with *Burkholderia pseudomallei* endotoxin. *Clin. Exp. Immunol.* **122**, 324–329 (2000).

117. Arjcharoen, S. *et al.* Fate of a *Burkholderia pseudomallei* lipopolysaccharide mutant in the mouse macrophage cell line RAW 264.7: possible role for the O-antigenic polysaccharide moiety of lipopolysaccharide in internalization and intracellular survival. *Infect. Immun.* **75**, 4298–4304 (2007).
118. Chantratita, N. *et al.* Survey of Innate Immune Responses to *Burkholderia pseudomallei* in Human Blood Identifies a Central Role for Lipopolysaccharide. *PLoS ONE* **8**, e81617 (2013).
119. Weehuizen, T. A. F. *et al.* Differential Toll-Like Receptor-signalling of *Burkholderia pseudomallei* lipopolysaccharide in murine and human models. *PLOS ONE* **10**, e0145397 (2015).
120. Burtnick, M. N. & Woods, D. E. Isolation of polymyxin B-susceptible mutants of *Burkholderia pseudomallei* and molecular characterization of genetic loci involved in polymyxin B resistance. *Antimicrob. Agents Chemother.* **43**, 2648–2656 (1999).
121. Vidyalakshmi, K. *et al.* Tuberculosis mimicked by melioidosis. *Int. J. Tuberc. Lung Dis. Off. J. Int. Union Tuberc. Lung Dis.* **12**, 1209–1215 (2008).
122. Vishnu Prasad, N. R., Balasubramaniam, G., Karthikeyan, V. S., Ramesh, C. K. & Srinivasan, K. Melioidosis of chest wall masquerading as a tubercular cold abscess. *J. Surg. Tech. Case Rep.* **4**, 115–117 (2012).
123. AlShati, M. H. & Joshi, R. M. A 42-year-old farmer from Bangladesh with respiratory failure, septic arthritis, and multiple cavitating consolidations. *Chest* **146**, e56–59 (2014).
124. Wang, Y.-S., Wong, C.-H. & Kurup, A. Cutaneous melioidosis and necrotizing fasciitis caused by *burkholderia pseudomallei*. *Emerg. Infect. Dis.* **9**, 1484–1485 (2003).
125. Woods, M. L. *et al.* Neurological melioidosis: seven cases from the Northern Territory of Australia. *Clin. Infect. Dis.* **15**, 163–169 (1992).

126. Kung, C.-T., Li, C.-J., Ko, S.-F. & Lee, C.-H. A melioidosis patient presenting with brainstem signs in the emergency department. *J. Emerg. Med.* **44**, e9–12 (2013).
127. Jane, L., Crowe, A., Daffy, J. & Gock, H. *Burkholderia pseudomallei* osteomyelitis: An unusual cause of fever in a returned traveller. *Australas. Med. J.* **5**, 141–143 (2012).
128. Morse, L. P. *et al.* Osteomyelitis and septic arthritis from infection with *Burkholderia pseudomallei*: A 20-year prospective melioidosis study from northern Australia. *J. Orthop.* **10**, 86–91 (2013).
129. Caldera, A. S., Kumanan, T. & Corea, E. A rare cause of septic arthritis: melioidosis. *Trop. Doct.* **43**, 164–166 (2013).
130. Thomas, J., Jayachandran, N. V., Shenoy Chandrasekhara, P. K., Lakshmi, V. & Narsimulu, G. Melioidosis--an unusual cause of septic arthritis. *Clin. Rheumatol.* **27 Suppl 2**, S59–61 (2008).
131. McLeod, C. *et al.* Clinical presentation and medical management of Melioidosis in children: a 24-year prospective study in the Northern Territory of Australia and review of the literature. *Clin. Infect. Dis.* **60**, 21–26 (2015).
132. Pruekprasert, P. & Jitsurong, S. Case report: septicemic melioidosis following near drowning. *Southeast Asian J. Trop. Med. Public Health* **22**, 276–278 (1991).
133. Chierakul, W. *et al.* Melioidosis in 6 tsunami survivors in southern Thailand. *Clin. Infect. Dis. Off. Publ. Infect. Dis. Soc. Am.* **41**, 982–990 (2005).
134. Lim, R. S. M., Flatman, S. & Dahm, M. C. Sinonasal melioidosis in a returned traveller presenting with nasal cellulitis and sinusitis. *Case Rep. Otolaryngol.* **2013**, 920352 (2013).
135. Lee, N., Wu, J. L., Lee, C. H. & Tsai, W. C. *Pseudomonas pseudomallei* infection from drowning: the first reported case in Taiwan. *J. Clin. Microbiol.* **22**, 352–354 (1985).

136. Sugi Subramaniam, R. V. *et al.* Melioidosis presenting as pseudomyxoma peritonei: yet another pretense of the great mimicker: an unreported entity. *Surg. Infect.* **14**, 415–417 (2013).
137. Doker, T. J. *et al.* Fatal *Burkholderia pseudomallei* infection initially reported as a bacillus species, Ohio, 2013. *Am. J. Trop. Med. Hyg.* **91**, 743–746 (2014).
138. Sarovich, D. S. *et al.* Recurrent melioidosis in the darwin prospective melioidosis study: improving therapies mean that relapse cases are now rare. *J. Clin. Microbiol.* **52**, 650–653 (2014).
139. Limmathurotsakul, D. *et al.* Risk factors for recurrent melioidosis in Northeast Thailand. *Clin. Infect. Dis.* **43**, 979–986 (2006).
140. Dance, D. Treatment and prophylaxis of melioidosis. *Int. J. Antimicrob. Agents* **43**, 310–318 (2014).
141. Pitman, M. C. *et al.* Intravenous therapy duration and outcomes in melioidosis: a new treatment paradigm. *PLoS Negl. Trop. Dis.* **9**, e0003586 (2015).
142. Chetchotisakd, P. *et al.* Trimethoprim-sulfamethoxazole versus trimethoprim-sulfamethoxazole plus doxycycline as oral eradication treatment for melioidosis (MERTH): a multicentre, double-blind, non-inferiority, randomised controlled trial. *Lancet* **383**, 807–814 (2014).
143. Maharjan, B. *et al.* Recurrent melioidosis in patients in northeast Thailand is frequently due to reinfection rather than relapse. *J. Clin. Microbiol.* **43**, 6032–6034 (2005).
144. Dando, S. J. *et al.* Pathogens penetrating the central nervous system: infection pathways and the cellular and molecular mechanisms of invasion. *Clin. Microbiol. Rev.* **27**, 691–726 (2014).
145. Chadwick, D. R., Ang, B., Sitoh, Y. Y. & Lee, C. C. Cerebral melioidosis in Singapore: a

- review of five cases. *Trans. R. Soc. Trop. Med. Hyg.* **96**, 72–76 (2002).
146. Currie, B. J., Fisher, D. A., Howard, D. M. & Burrow, J. N. . Neurological melioidosis. *Acta Trop.* **74**, 145–151 (2000).
147. Owen, S. J. *et al.* Nasal-associated lymphoid tissue and olfactory epithelium as portals of entry for *Burkholderia pseudomallei* in murine melioidosis. *J. Infect. Dis.* **199**, 1761–1770 (2009).
148. St. John, J. A. *et al.* *Burkholderia pseudomallei* penetrates the brain via destruction of the olfactory and trigeminal nerves: implications for the pathogenesis of neurological melioidosis. *mBio* **5**, e00025–14–e00025–14 (2014).
149. Liu, P.-J. *et al.* Induction of mouse melioidosis with meningitis by CD11b+ phagocytic cells harboring intracellular *B. pseudomallei* as a Trojan Horse. *PLoS Negl. Trop. Dis.* **7**, e2363 (2013).
150. Morris, J. *et al.* Neurotropic Threat Characterization of *Burkholderia pseudomallei* Strains. *Emerg. Infect. Dis.* **21**, 58–63 (2015).
151. Sarovich, D. S. *et al.* Variable virulence factors in *Burkholderia pseudomallei* (Melioidosis) Associated with Human Disease. *PLoS ONE* **9**, e91682 (2014).
152. Ko, W.-C. *et al.* Melioidosis outbreak after typhoon, Southern Taiwan. *Emerg. Infect. Dis.* **13**, 896–898 (2007).
153. Cottew, G. S., Sutherland, A. K. & Meehan, J. F. Melioidosis in sheep in queensland: description of an Outbreak. *Aust. Vet. J.* **28**, 113–123 (1952).
154. Rimington, R. A. Melioidosis in north Queensland. *Med. J. Aust.* **49**(1), 50–53 (1962).
155. Warawa, J. M. Evaluation of surrogate animal models of melioidosis. *Front. Microbiol.* **1**, (2010).

156. Sprague, L. D. & Neubauer, H. Melioidosis in animals: a review on epizootiology, Diagnosis and Clinical Presentation. *J. Vet. Med. Ser. B* **51**, 305–320 (2004).
157. Hicks, C. L., Kinoshita, R. & Ladds, P. W. Pathology of melioidosis in captive marine mammals. *Aust. Vet. J.* **78**, 193–195 (2000).
158. Lau, S. K. *et al.* *Burkholderia pseudomallei* in soil samples from an oceanarium in Hong Kong detected using a sensitive PCR assay. *Emerg. Microbes Infect.* **3**, e69 (2014).
159. Godoy, D. *et al.* Multilocus sequence typing and evolutionary relationships among the causative agents of melioidosis and glanders, *burkholderia pseudomallei* and *Burkholderia mallei*. *J. Clin. Microbiol.* **41**, 2068–2079 (2003).
160. Peacock, S. J. Melioidosis: *Curr. Opin. Infect. Dis.* **19**, 421–428 (2006).
161. Limmathurotsakul, D. & Peacock, S. J. Melioidosis: a clinical overview. *Br. Med. Bull.* **99**, 125–139 (2011).
162. Lim, C., Peacock, S. J. & Limmathurotsakul, D. Association between activities related to routes of infection and clinical manifestations of melioidosis. *Clin. Microbiol. Infect.* **22**, 79.e1–79.e3 (2016).
163. Abbink, F. C., Orendi, J. M. & de Beaufort, A. J. Mother-to-child transmission of *Burkholderia pseudomallei*. *N. Engl. J. Med.* **344**, 1171–1172 (2001).
164. Choy, J. L., Mayo, M., Janmaat, A. & Currie, B. J. Animal melioidosis in Australia. *Acta Trop.* **74**, 153–158 (2000).
165. Hodgson, K. *et al.* Immunological mechanisms contributing to the double burden of diabetes and intracellular bacterial infections. *Immunology* n/a–n/a (2014).  
doi:10.1111/imm.12394
166. Vidyalakshmi, K., Lipika, S., Vishal, S., Damodar, S. & Chakrapani, M. Emerging clinico-

- epidemiological trends in melioidosis: analysis of 95 cases from western coastal India. *Int. J. Infect. Dis.* **16**, e491–e497 (2012).
167. Suparee, N., McGee, P., Khan, S. & Pinyopasakul, W. Life-long battle: Perceptions of Type 2 diabetes in Thailand. *Chronic Illn.* (2014). doi:10.1177/1742395314526761
168. Hodgson, K. A., Morris, J. L., Feterl, M. L., Govan, B. L. & Ketheesan, N. Altered macrophage function is associated with severe *Burkholderia pseudomallei* infection in a murine model of type 2 diabetes. *Microbes Infect.* **13**, 1177–1184 (2011).
169. Roep, B. O. & Tree, T. I. M. Immune modulation in humans: implications for type 1 diabetes mellitus. *Nat. Rev. Endocrinol.* **10**, 229–242 (2014).
170. Khanna, S. *et al.* Macrophage dysfunction impairs resolution of inflammation in the wounds of diabetic mice. *PLoS ONE* **5**, e9539 (2010).
171. de Jong, H. K. *et al.* Diabetes-independent increase of factor VII-activating protease activation in patients with Gram-negative sepsis (melioidosis). *J. Thromb. Haemost.* n/a–n/a (2014). doi:10.1111/jth.12776
172. Morris, J. *et al.* *Burkholderia pseudomallei* triggers altered inflammatory profiles in a whole-blood model of type 2 diabetes-melioidosis comorbidity. *Infect. Immun.* **80**, 2089–2099 (2012).
173. Koh, G. C. K. W. *et al.* Glyburide reduces bacterial dissemination in a mouse model of melioidosis. *PLoS Negl. Trop. Dis.* **7**, e2500 (2013).
174. Chalmers, R. M. S. *et al.* Melioidosis and end-stage renal disease in tropical northern Australia. *Kidney Int.* **86**, 867–870 (2014).
175. Farmakis, D., Giakoumis, A., Polymeropoulos, E. & Aessopos, A. Pathogenetic aspects of immune deficiency associated with beta-thalassemia. *Med. Sci. Monit. Int. Med. J. Exp. Clin.*

*Res.* **9**, RA19–22 (2003).

176. Olivieri, N. F. The  $\beta$ -Thalasseмии. *N. Engl. J. Med.* **341**, 99–109 (1999).

177. Olivieri, N. F., Pakbaz, Z. & Vichinsky, E. Hb E/beta-thalassaemia: a common & clinically diverse disorder. *Indian J. Med. Res.* **134**, 522–531 (2011).

178. Wanachiwanawin, W. *et al.* Activation of monocytes for the immune clearance of red cells in beta zero-thalassaemia/HbE. *Br. J. Haematol.* **85**, 773–777 (1993).

179. Rychetnik, L. & Madronio, C. M. The health and social effects of drinking water-based infusions of kava: A review of the evidence: Health and social effects of drinking kava. *Drug Alcohol Rev.* **30**, 74–83 (2011).

180. Kwon, D.-J., Ju, S. M., Youn, G. S., Choi, S. Y. & Park, J. Suppression of iNOS and COX-2 expression by flavokawain A via blockade of NF- $\kappa$ B and AP-1 activation in RAW 264.7 macrophages. *Food Chem. Toxicol.* **58**, 479–486 (2013).

181. Holguin, F., Moss, I., Brown, L. A. & Guidot, D. M. Chronic ethanol ingestion impairs alveolar type II cell glutathione homeostasis and function and predisposes to endotoxin-mediated acute edematous lung injury in rats. *J. Clin. Invest.* **101**, 761–768 (1998).

182. Brown, S. D. & Brown, L. A. S. Ethanol (EtOH)-Induced TGF- $\beta$ <sub>1</sub> and reactive oxygen species production are necessary for EtOH-induced alveolar macrophage dysfunction and induction of alternative activation. *Alcohol. Clin. Exp. Res.* **36**, 1952–1962 (2012).

183. Romero, F. *et al.* Chronic alcohol ingestion in rats alters lung metabolism, promotes lipid accumulation, and impairs alveolar macrophage functions. *Am. J. Respir. Cell Mol. Biol.* **51**, 840–849 (2014).

184. Standiford, T. J. & Danforth, J. M. Ethanol feeding inhibits proinflammatory cytokine expression from murine alveolar macrophages ex vivo. *Alcohol. Clin. Exp. Res.* **21**, 1212–1217

(1997).

185. Limmathurotsakul, D. *et al.* Activities of daily living associated with acquisition of melioidosis in Northeast Thailand: a matched case-control study. *PLoS Negl. Trop. Dis.* **7**, e2072 (2013).

186. Sopian, M. *et al.* Outbreak of melioidosis and leptospirosis co-infection following a rescue operation. *Med. J. Malaysia* **67**, 293–297 (2012).

187. Currie, B. J. & Jacups, S. P. Intensity of rainfall and severity of melioidosis, Australia. *Emerg. Infect. Dis.* **9**, 1538–1542 (2003).

188. Hoffmaster, A. R. *et al.* Melioidosis Diagnostic Workshop, 2013. *Emerg. Infect. Dis.* **21**, (2015).

189. Wuthiekanun, V. *et al.* The use of selective media for the isolation of *Pseudomonas pseudomallei* in clinical practice. *J. Med. Microbiol.* **33**, 121–126 (1990).

190. Lau, S. K. *et al.* Laboratory diagnosis of melioidosis: Past, present and future. *Exp. Biol. Med.* (2015). doi:10.1177/1535370215583801

191. Peacock, S. J. *et al.* Comparison of Ashdown's Medium, *Burkholderia cepacia* Medium, and *Burkholderia pseudomallei* selective agar for clinical isolation of *Burkholderia pseudomallei*. *J. Clin. Microbiol.* **43**, 5359–5361 (2005).

192. Lasch, P. *et al.* Identification of highly pathogenic microorganisms using MALDI-TOF mass spectrometry – results of an inter-laboratory ring trial. *J. Clin. Microbiol.* JCM.00813–15 (2015). doi:10.1128/JCM.00813-15

193. Suttisunhakul, V. *et al.* Evaluation of polysaccharide-based latex agglutination assays for the rapid detection of antibodies to *Burkholderia pseudomallei*. *Am. J. Trop. Med. Hyg.* **93**, 542–546 (2015).

194. Dance, D. A., Wuthiekanun, V., Naigowit, P. & White, N. J. Identification of *Pseudomonas pseudomallei* in clinical practice: use of simple screening tests and API 20NE. *J. Clin. Pathol.* **42**, 645–648 (1989).
195. Inglis, T. J., Chiang, D., Lee, G. S. & Chor-Kiang, L. Potential misidentification of *Burkholderia pseudomallei* by API 20NE. *Pathology (Phila.)* **30**, 62–64 (1998).
196. Zong, Z., Wang, X., Deng, Y. & Zhou, T. Misidentification of *Burkholderia pseudomallei* as *Burkholderia cepacia* by the VITEK 2 system. *J. Med. Microbiol.* **61**, 1483–1484 (2012).
197. Limmathurotsakul, D. *et al.* Consensus on the development of vaccines against naturally acquired melioidosis. *Emerg. Infect. Dis.* **21**, (2015).
198. Nieves, W. *et al.* A naturally derived outer-membrane vesicle vaccine protects against lethal pulmonary *Burkholderia pseudomallei* infection. *Vaccine* **29**, 8381–8389 (2011).
199. Schully, K. L. *et al.* Evaluation of a biodegradable microparticulate polymer as a carrier for *Burkholderia pseudomallei* subunit vaccines in a mouse model of melioidosis. *Int. J. Pharm.* **495**, 849–861 (2015).
200. Levine, H. B. & Maurer, R. L. Immunization with an induced avirulent auxotrophic mutant of *Pseudomonas pseudomallei*. *J. Immunol. Baltim. Md 1950* **81**, 433–438 (1958).
201. Peacock, S. J. *et al.* Melioidosis vaccines: a systematic review and appraisal of the potential to exploit biodefense vaccines for public health purposes. *PLoS Negl. Trop. Dis.* **6**, e1488 (2012).
202. Moustafa, D. A. *et al.* Recombinant salmonella expressing *Burkholderia mallei* LPS O antigen provides protection in a murine model of melioidosis and glanders. *PloS One* **10**, e0132032 (2015).
203. Dance, D. A., Wuthiekanun, V., Chaowagul, W. & White, N. J. The antimicrobial susceptibility of *Pseudomonas pseudomallei*. Emergence of resistance in vitro and during

treatment. *J. Antimicrob. Chemother.* **24**, 295–309 (1989).

204. White, N. . Halving of mortality of severe melioidosis by ceftazidime. *The Lancet* 697–701 (1989).

205. Chaowagul, W. *et al.* Open-label randomized trial of oral trimethoprim-sulfamethoxazole, doxycycline, and chloramphenicol compared with trimethoprim-sulfamethoxazole and doxycycline for maintenance therapy of melioidosis. *Antimicrob. Agents Chemother.* **49**, 4020–4025 (2005).

206. Dance, D. A. B. *et al.* Trimethoprim/sulfamethoxazole resistance in *Burkholderia pseudomallei*. *Int. J. Antimicrob. Agents* **44**, 368–369 (2014).

## Chapter 2: Antimicrobial resistance

This chapter will discuss recent advances in the understanding of antimicrobial resistance caused by resistance nodulation cell division (RND) efflux pumps. As these tripartite pumps are only one of many methods utilized by bacteria to survive antimicrobial pressure, a brief overview of bacterial resistance mechanisms will be presented. The different classes of antimicrobials used in the treatment of melioidosis will be reviewed, followed by observations of efflux related resistance in *B. pseudomallei* (*Bp*), and a summary of previous findings and research aims.

### 2.1 The post-antibiotic era

The invention of the microscope in the 17<sup>th</sup> century opened the door for study of the microscopic world. Unfortunately, it wasn't until the conception of "germ theory", Koch's postulates and the implementation of standardized public sanitation that rates of infection by bacterial agents gradually started to decrease. However, while these concepts slowed transmission of disease they did little to fight active infection. Tuberculosis and syphilis were endemic, while cholera, typhus, typhoid, diphtheria, and undifferentiated enteric disease routinely swept through urban centers despite efforts to control their spread.<sup>1,2</sup> Additionally, many deaths from viral disease are now thought to be linked to secondary bacterial infections, e.g. the 1918 influenza pandemic and bacterial pneumonia.<sup>3</sup> Surgical procedures we now consider routine were a dangerous proposition due to less than sterile conditions, as was childbirth, and childhood mortality rates due to now treatable or preventable infections were as high as 200/1000 live births. In some urban areas only 1 in 5 were predicted to make it to adulthood.<sup>1,2</sup> For those immunized by childhood illness, injuries sustained from combat or

accident were prime entry portals for environmental pathogens capable of causing massive systemic infections.<sup>1,4,3</sup>

For a vast majority of patients with serious bacterial infection, palliative or supportive care was the only medical recourse and as a result, mortality rates remained high well into the 20<sup>th</sup> century and past the advent of the modern medical era. It is not surprising then, that the three leading causes of death at the turn of the 20<sup>th</sup> century remained tuberculosis, pneumonia and diarrheal disease.<sup>1</sup>

The implementation of the progenitor sulfadruq prontosil in 1936 almost immediately began reducing the number of deaths caused by bacterial infection.<sup>5</sup> Soon, the discovery and deployment of penicillin was heralded as one of the most significant medical advances of the 20<sup>th</sup> century, and similarly improved the life expectancies of millions of people.<sup>5,6</sup>

However, with the administration of these new treatments came new challenges: specifically, resistance (**Fig. 2.1**). The early  $\beta$ -lactams provide striking examples of rapid resistance development. Isolates resistant to penicillin were observed three years before its widespread deployment in civilian medicine in 1943. Methicillin was even worse, with resistance observed two years after its introduction to general use. The same trend is seen repeatedly, with resistance to a drug closely following its appearance in the treatment arsenal.<sup>6,7</sup> It is important to remember that while these mechanisms existed long before the implementation of antibiotic compounds, use and misuse of antimicrobials in the modern era has rapidly accelerated the rate at which resistance occurs.<sup>8-10</sup> Because of our attempts at intervention either in human health or in agricultural use, and the selective pressure placed on bacterial populations by these interventions, antimicrobial resistance is positioned as a looming obstacle that threatens our current health standards.<sup>6,8,11</sup> Both the WHO and the CDC have issued global warnings of the

dangers posed by failure to address the issue of wide scale resistance. The CDC estimates that in the United States alone, 2 million people are infected with antibiotic resistant bacteria resulting in 23,000 deaths every year.<sup>7</sup> Worldwide estimates of deaths caused by antimicrobial resistance (including in malaria and HIV) place this number at 700,000 according to the *Review on Antimicrobial Resistance* published in 2014.<sup>12</sup> Many of these deaths will occur from infection with bacterial agents that are resistant to every known antibiotic.

Without any changes to global stewardship, it is predicted that antimicrobial resistance will account for 10 million yearly deaths worldwide by 2050, and a corresponding global cost of 100 trillion U.S. dollars in gross domestic product. For developing countries with poor health care infrastructure this could equate to a loss of up to 25% of the total population in a single twelve-month period.<sup>12</sup> The bulk

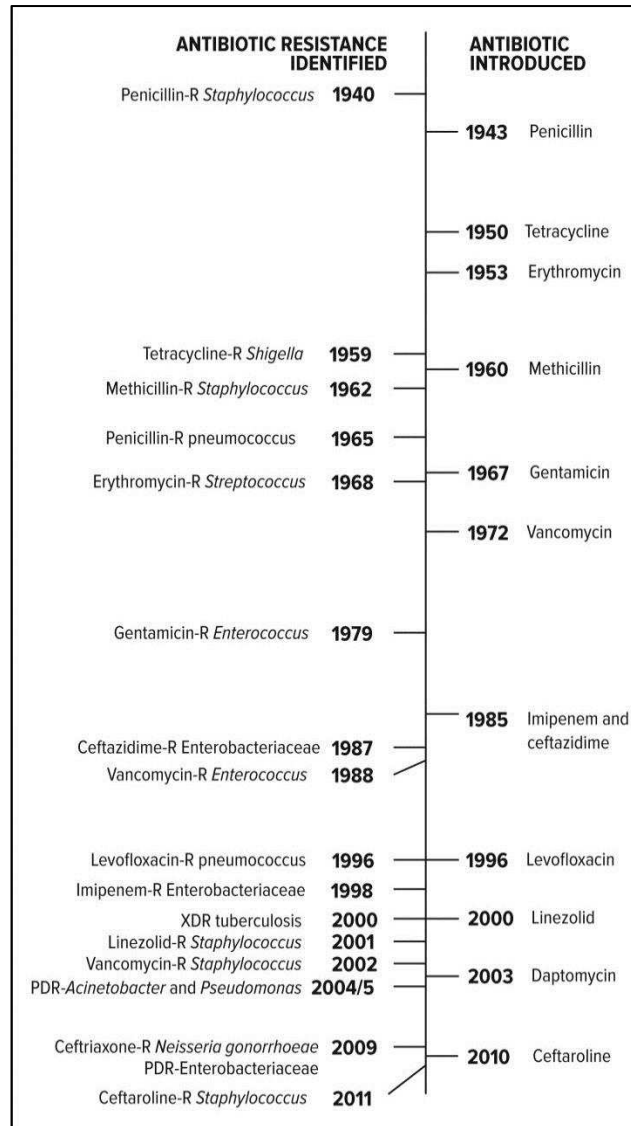


**Figure 2.1. Timeline of the identification of antibiotic resistance.**

Detection of antibiotic resistant isolates often rapidly follows a compounds introduction to clinical use. Left and right sides of figure represent identification of resistance isolates, and introduction of compound for medical use, respectively. PDR= pan drug resistant, XDR= extensively drug resistant. All dates listed are representative of first published reports of resistance. Taken from the CDC's report *Antibiotic resistance threats in the United States, 2013*<sup>7</sup>.

of this increase may be due to bacterial infections, both primary or secondary to viral disease. It is very possible that without significant advances in our ability to produce new compounds or find alternative therapies that are effective against bacterial infection, we will essentially be returned to a pre-antibiotic era, and all the hardships that entails. An understanding of these resistance mechanisms, how they occur and how they are inherited is vital to retaining what little chemotherapeutic arsenal remains.

Treatment methods used for eradication of *Bp* infections are not excluded from this trend. While the disease may not have the current reach of other infections, e.g. those commonly acquired in hospital settings, it shares many of the same resistance mechanisms found in these Gram negative organisms. Its inherent resistance to these drugs, highly virulent etiology, increasing susceptible population, and widening geographic range, make it essential that we understand how these mechanisms combine to impede treatment in an effort to prevent increased mortality.

## **2.2 Antibiotics**

The development of prontosil and penicillin in the early part of the 20<sup>th</sup> century sparked years of scientific research into the discovery of new antimicrobial compounds. Unfortunately, soon after the discovery of these classes of compounds came the discovery of resistance mechanisms capable of rendering them inactive. Increasingly effective compounds are needed, but are difficult to identify or expensive to synthesize and as a result their development has slowed; from 2000-2014 only 13 new drugs were approved by the FDA in comparison to 41 from 1980-1994.<sup>6,8,11</sup> In the United States, regulations concerning minimum acceptable safety limits may prevent otherwise effective compounds from proceeding to clinical trials, further reducing the number of new drugs available for physician use.<sup>6,11,13</sup> These issues combined to

produce a shrinking profit margin for pharmaceutical companies making antibiotic development a riskier proposition, highly dependent on both academic and government funded research efforts.<sup>7,13</sup> To date, the compounds that have been successfully developed for human treatment target bacterial processes ranging from central metabolism to cell wall synthesis. **Table 2.1** summarizes these currently utilized antibiotic classes, their targets, and potential modes of resistance described in bacteria.

**Table 2.1 Antibiotic classes, targets, and resistance mechanisms**

Antibiotic Class	Example(s)	Target	Mode(s) of Resistance
β-Lactams	Penicillins, cephalosporins, penems, monobactams	Peptidoglycan biosynthesis	Hydrolysis, efflux, altered target
Aminoglycosides	Gentamicin, streptomycin, spectinomycin	Translation	Phosphorylation, acetylation, nucleotidylation, efflux, altered target
Glycopeptides	Vancomycin, teicoplanin	Peptidoglycan biosynthesis	Monooxygenation, efflux, altered target
Tetracyclines	Minocycline, tigecycline	Translation	Monooxygenation, efflux, altered target
Macrolides	Erythromycin, azithromycin	Translation	Hydrolysis, glycosylation, phosphorylation, efflux, altered target
Licosamides	Clindamycin	Translation	Nucleotidylation, efflux, altered target
Streptogramins	Synercid	Translation	C-O lyase (type B streptogramins), acetylation (type a streptogramins), efflux, altered target
Oxazolidinones*	Linezolid	Translation	Efflux, altered target
Phenicols	Chloramphenicol	Translation	Acetylation, efflux, altered target
Quinolones	Ciprofloxacin	DNA replication	Acetylation, efflux, altered target
Pyrimidines	Trimethoprim	C1 metabolism	Efflux, altered target
Sulfonamides*	Sulfamethoxazole	C1 metabolism	Efflux, altered target
Rifamycins	Rifampin	Transcription	ADP-ribozylation, efflux, altered target
Lipopeptides	Daptomycin	Cell membrane	Altered target
Cationic peptides	Colistin	Cell membrane	Altered target, efflux

Adapted from Davies and Davies, 2010.<sup>19</sup> \* Denotes synthetic antimicrobial.

### **2.2.1 Treatment of *Burkholderia pseudomallei***

Because of the bacteria's intrinsic antimicrobial resistance, treatment of *Bp* infection is complex and split into two phases. The first phase consists of intravenous administration of ceftazidime or a carbapenem for 10 days to 2 weeks before transition to the eradication phase.<sup>14,15</sup> In cases where side effects are of concern, amoxicillin-clavulanate can be substituted for the other  $\beta$ -lactams. Additionally, in complicated or severe infection this treatment phase may be extended or combined with trimethoprim-sulfamethoxazole (co-trimoxazole).<sup>14,15</sup>

The eradication phase of treatment uses oral administration of co-trimoxazole for up to 20 weeks in an effort to prevent relapse and control development of resistance.<sup>14,16</sup> Though both components of this drug combo are bacteriostatic, they exhibit high efficacy as they target two concurrent enzymes needed for production of tetrahydrofolate for nucleotide synthesis; dihydropteroate synthase by sulfamethoxazole, and dihydrofolate reductase, by trimethoprim.<sup>17,18</sup> The mechanisms causing resistance to both phases of treatment will be discussed in greater detail later in this chapter.

### **2.3 Drug resistance mechanisms**

Resistance mechanisms found bacteria are a combination of acquired and intrinsic traits. These mechanisms are usually not utilized alone, but combine to render some classes of antibiotic completely ineffective against a given species. The generation of these factors is partially rooted in the fact that many antimicrobials are products of a hostile environment and their production is not restricted solely to the pharmaceutical lab.<sup>11,19</sup> In fact, many microorganisms naturally found in polymicrobial environments use these compounds to increase their odds of survival in a hostile niche, either through use in communication, cell-cell competition or even subsistence.<sup>19,20</sup> With the production of such secondary metabolites may

have come the evolution of mechanisms capable of inactivating these compounds in order to prevent self-harm, as well as in response to the selective pressure caused by other species' compounds.<sup>21</sup> As a result, a multitude of proteins and evasion strategies now exist that can be classified into one of seven categories: enzymatic inactivation, target modification, compound exclusion, target overproduction, and efflux, sequestration and metabolic bypass. When combined together, these methods can lead to levels of resistance that make the odds of survival much higher on a population level.

### **2.3.1 Enzymatic inactivation**

This category of drug resistance mechanism is characterized by alteration of the chemical structure of the antimicrobial compound through enzymatic cleavage. Perhaps the best known example of this mechanism are the  $\beta$ -lactamases. These proteins specifically hydrolyze the lactam ring within  $\beta$ -lactam compounds rendering it incapable of acetylation of penicillin binding proteins during cell wall synthesis.<sup>22</sup> In *Bp*, the best-characterized and clinically most significant  $\beta$ -lactamase is a TAT secreted Class A  $\beta$ -lactamase called PenA<sup>23-25</sup>. Mutations causing PenA amino acid substitutions are known to cause decreased susceptibility to ceftazidime and amoxicillin+clavulanic acid, and are associated with poor treatment efficacy in clinical cases.<sup>26,27</sup>

### **2.3.2 Metabolic bypass and target duplication**

Both of these drug resistance mechanisms rely on redundancy, and are exemplified in resistance to folate inhibitors. Trimethoprim and sulfamethoxazole target different genes within the same pathway necessary for production of tetrahydrofolic acid.<sup>18</sup> In some species, the reliance on the tetrahydrofolate synthesis pathway can be replaced with thymidine auxotrophy in host tissues, bypassing the metabolic reactions that could be inhibited by sulfamethoxazole

through uptake of the preformed nucleoside.<sup>18,28</sup> Alternatively, overproduction of dihydrofolate reductase (DHFR), the target of trimethoprim (which competes with dihydrofolate for modification by DHFR) causes increased resistance in *E. coli*. This is predicted to be based on simple changes in stoichiometry through the production of more copies of active enzyme than could be bound by the drug.<sup>29</sup>

### **2.3.3 Exclusion and sequestration of antimicrobial compounds**

By preventing the drug from ever entering the cell, it is *de facto* rendered inactive. In *Bp*, an example of this mechanism can be seen in its resistance to polymyxin B. This cationic antimicrobial normally intercalates into the outer membrane of the cell and takes the place of ion bridges that stabilize LPS, causing massive changes in membrane permeability and leading to cell death.<sup>30</sup> The structure of LPS in *Burkholderia* species is unique from other Gram negative species based on both o-acetyl and 4-amino-4-deoxy-l-arabinose modifications that can occur on both the lipid A and O antigen.<sup>31</sup> These intrinsic modifications prevent the interaction of polymyxin B with the outer membrane, preventing the peptide from changing membrane permeability and killing the target.<sup>24,31,32</sup> This is especially concerning in *Bp*, as polymyxin B is considered a drug of last resort in other Gram negative infections.

Another example of drug exclusion can be seen in the expression of porin proteins. Most antimicrobials are too large to enter the cell through diffusion and must rely on facilitated transport to cross the outer membrane.<sup>33</sup> By reducing the number of porin proteins capable of moving these compounds, bacteria decrease their permeability and increase resistance to antimicrobial compounds that require the use of these proteins to enter the cell.<sup>34</sup> This process is tightly regulated as it can affect the import of vital nutrients as well, but can be initiated by the presence of antibiotic compounds like tetracycline, as seen in studies of *E. coli* outer membrane

proteins.<sup>34–36</sup> This mechanism can synergize with active efflux to greatly decrease susceptibility to a wide range of antimicrobial substrates, and is of great concern in Gram-negatives.<sup>34</sup>

Antimicrobial sequestration also causes resistance by preventing drug contact with its target, but through a different mechanism, e.g. biofilm production. This can cause bacterial populations to become highly resistant to antimicrobials without traditional inactivation of the drug compound. In *P. aeruginosa*, the formation of such biofilms also induces *ndvB* dependent synthesis of periplasmic cyclic-glucans.<sup>37,38</sup> In the absence of *ndvB*, susceptibility to aminoglycosides and fluoroquinolones was increased despite no other changes to biofilm formation.<sup>39</sup> In planktonic cultures, susceptibilities returned to wild-type levels, suggesting that the effect on resistance was lifestyle dependent. The authors proposed the glucans produced by biofilm dependent expression of *ndvB* were capable of sequestering antimicrobials within the periplasm, preventing them from entering the cytoplasmic space where they could interact with the ribosome or prevent DNA replication.<sup>37,39</sup>

#### **2.3.4 Target modification**

Target modification is a common mechanism of resistance that relies on chemical modification, mutation, or deletion of a target in order to prevent interaction with an antimicrobial compound.<sup>24</sup> A drastic example of this is observed in *Bp*, after exposure to ceftazidime. The drug normally binds to a specific penicillin binding protein 3 (PBP3) and by doing so interferes with cell wall synthesis. Clinical isolates were discovered containing large chromosomal deletions including the PBP3 gene after primary exposure to ceftazidime, causing severe growth defects, but resistance to ceftazidime, because of the loss of the drug target.<sup>40</sup> A more classical example of target modification can be seen in vancomycin resistance in both *Enterococcus faecium* and *Staphylococcus aureus* carrying transposon Tn1546.<sup>41–43</sup> In these

isolates, the transposon promotes terminal modification of the peptidoglycan peptide bridge from D-alanine-D-alanine to D-alanine-D-lactate, greatly reducing the affinity of vancomycin binding to the dipeptide and allowing peptidoglycan crosslinking to still occur.<sup>41</sup>

### **2.3.5 Antibiotic tolerance**

Bacterial populations are also able to evade the effects of antibiotics without the activation or acquisition of traditional resistance determinants. The presence of an environmental stressor, e.g. an antibiotic, may trigger wholesale changes to the metabolism of the cell leading to greatly reduced susceptibility to that stressor.<sup>88</sup> Through tight regulation of metabolic activity using mechanisms such as toxin-antitoxin loci, subgroups of bacterial cells within a population enter a dormant state, effectively rendering them resistant to antimicrobials that require active transport or metabolic activity to manifest their antimicrobial function.<sup>88-90</sup> These “persister cells” are able to remain in such a state until the stressor diffuses away from the population, at which time they reactivate, and resume growth. This mechanism allows resistance to many forms of antibiotics without necessitating the production of active resistance factors or selection of mutants with altered antimicrobial targets.<sup>90</sup> Such populations commonly arise in a biofilm setting, which already display heightened resistance to certain antimicrobial compounds.<sup>88,89</sup> The combination of these two lifestyle adaptations produces highly recalcitrant populations that may prevent clearance of chronic infection without complementary therapy using non-traditional compounds to reactivate dormant cells.<sup>91</sup>

### **2.3.6 Efflux**

Efflux is a method of facilitated transport carried out by protein complexes that fall into one of six currently identified classes based on their protein structure.<sup>44</sup> These complexes are commonly able to recognize more than one substrate, making them a major cause of multidrug

resistance, especially in Gram-negative organisms.<sup>45</sup> As many of these proteins are not expressed constitutively, it may be hard to predict the effect these complexes have on in-vivo treatment; many are tightly regulated to maintain cell homeostasis, and alterations to the control of these systems can cause drastic changes in resistance. The genes encoding efflux proteins can be both chromosomal and harbored on plasmids, making it possible for horizontal transmission from one species to another very easily. As a result, it is possible for one organism to encode multiple efflux systems, each with different substrate specificity ranges making it highly resistant to many different classes of antimicrobials.

## **2.4 Families of efflux systems**

### **2.4.1 Major facilitator (MF) systems**

The major facilitator family of efflux pump is the largest known to date, and consists of monomeric protein complexes that use the proton gradient for transport of substrates.<sup>46,47</sup> These proteins are characterized by 12-14 membrane spanning loops that form a central pore, allowing export from the cytoplasm to the periplasm or, in Gram-positive bacteria, extracellular milieu.<sup>47</sup> In Gram-negative organisms, these complexes can work in conjunction with outer membrane channels and fusion proteins associated with the resistance nodulation cell division family (RND), and thus form efflux systems that span the entire cell envelope.<sup>44,46</sup> Proteins in this family may have the widest substrate range and are associated with export and import of sugars, metabolites, drugs, dyes, inorganic and organic ions and other biochemical precursors.<sup>47</sup>

### **2.4.2 Small multidrug resistance (SMR) family**

Efflux transporters of the SMR protein family are integral membrane proteins that utilize the proton gradient for efflux of substrates from the cytoplasm to the periplasmic space.<sup>46</sup> Currently identified substrates include dyes, quaternary amides, lipophilic cations,  $\beta$ -lactams,

cephalosporins and aminoglycosides, but the pumps are also implicated in transport of compounds needed for chaperon protein regulation.<sup>46,48</sup> These proteins are widely distributed and found in both Gram-positive and negative bacteria, and crystallographic studies show that they may act as dimers.<sup>44</sup> Interestingly, SMR protein EmrE was found to be a major resistance factor in *E. coli* despite only transporting compounds as far as the periplasm, from where they were extruded from the cell by transporters involving TolC.<sup>44,49</sup> This illustrates the ability of different protein families to act synergistically during the efflux process and may be a common phenomenon in Gram-negative bacteria.<sup>44,49</sup>

### **2.4.3 ABC transporters**

The ATP binding cassette (ABC) superfamily of efflux pumps uses ATP hydrolysis for transport energization and typically consists of two cytoplasmic domains for ATP binding, and two intermembrane regions needed for substrate interaction and export.<sup>50</sup> The family is the only ATP-dependent class of efflux pumps known to date and is found in all kingdoms of life, although relatively few examples are found among bacteria.<sup>51</sup> In Gram-negatives, the best described examples of this family are involved in LPS synthesis and macrolide export.<sup>50,51</sup>

### **2.4.4 Multidrug and toxic compound exclusion (MATE) family**

The MATE family transporter proteins are H<sup>+</sup>/Na<sup>+</sup> ion antiporters first described in *Vibrio parahaemolyticus*.<sup>52,53</sup> While the substrate specificity is thought to be narrower than that of other families of efflux proteins, the MATE family is known to be able to extrude a wide range of structurally dissimilar compounds including fluoroquinolones, aminoglycosides and some synthetic dyes.<sup>50,52</sup> MATE operons have wide phylogenetic diversity and are found in both Gram-positive and negative organisms as well as eukaryotes. Recent investigations have described two human MATE pumps expressed in the liver and kidneys, *hMATE-1* and *2*, thought

to be necessary for removing toxic substances from the body.<sup>54,55</sup> The membrane transport protein structure of this protein family is characterized by several transmembrane loops that form a hydrophobic binding pocket that extends partway across the cell membrane. Binding to the transport ion (either Na<sup>+</sup> or H<sup>+</sup>) at an adjacent region causes this pocket to collapse and release the bound substrate into the periplasm, while release of the ion into the cytoplasm allows interaction with the next molecule of export substrate.<sup>56</sup>

#### **2.4.5 Resistance nodulation cell division (RND) family**

The RND family of efflux pumps were first described in *E. coli*.<sup>57</sup> Subsequent study of these protein complexes over the past two decades has identified a class-specific tripartite nature consisting of cytoplasmic membrane transporter, a membrane fusion protein and an outer membrane protein channel.<sup>57-59</sup> This allows the protein complex to span the cell envelope and provides an efficient system, in conjunction with other transport proteins, to move noxious compounds into the periplasm from the cytosol.<sup>49,59-61</sup> The extrusion of substrate through the efflux complex is thought to be driven by the proton gradient in a “peristaltic” fashion.<sup>46,58,60,62,63</sup>

RND efflux systems are highly conserved across the Gram-negative clade, and are identified as a vital environmental survival mechanism capable of interacting with a multitude of noxious compounds in order to maintain cell homeostasis.<sup>58</sup> This includes substrates as varied as antimicrobial compounds, excess products of metabolism, heavy metals and salts.

It has also become apparent in recent years that these pumps may also affect interaction and persistence within a host organism.<sup>64-67</sup> A study investigating the effects of overexpression of an RND efflux operon in *Listeria* reported massive increases in the amount of Type II interferon in mutant-infected host cells, indicative of an altered response to infection.<sup>64</sup> Additionally, regulatory networks controlling the *mexEF-oprN* operon in *P. aeruginosa* are

known to be tightly linked to control of genes necessary for Type 3 secretion, quorum sensing and biofilm formation suggesting a potential connection between these processes.<sup>66,68,69</sup>

## **2.5 RND transporters in *Burkholderia pseudomallei***

*Bp* is a highly adaptable soil saprophyte and the etiologic agent of melioidosis. As described in the previous chapter, *Bp* infections are difficult to treat and highly virulent, making the study of the organism imperative from both a public health and biodefense standpoint. The highly complex and plastic genome also makes the organism an interesting case study in adaptability. *Bp* contains as many as 10 putative RND efflux operons, with seven located on chromosome 1 and the remaining three found on chromosome 2.<sup>70</sup> Of these operons, only three, *bpeAB-oprA*, *bpeEF-oprC* and *amrAB-oprA* have been characterized for their impact on clinical treatment.<sup>71-73</sup> There has been relatively little investigation into the diverse cell processes suggested by homology comparisons of these *Bp* operons to other species, including efflux of environmental metals and secondary metabolites. However, mounting evidence suggests that these complexes play a large role in development of MDR phenotypes and may influence the signaling molecules needed for quorum sensing and virulence in certain strains.<sup>70,74-76</sup>

## **2.6 Efflux linked resistance trends in *Burkholderia pseudomallei***

In multiple studies, resistance to co-trimoxazole, aminoglycosides, fluoroquinolones macrolides, tetracycline and phenicols have been directly linked to the expression of the three characterized efflux pumps, *bpeEF-oprC*, *amrAB-oprA*, and *bpeAB-oprB*.<sup>70,75,77-79</sup> However, not all these classes of antimicrobials are utilized during treatment, specifically because of efflux-mediated resistance phenotypes rendering whole classes of drugs ineffective. For instance, *Bp* is naturally resistant to aminoglycosides and macrolides due efflux by *AmrAB-OprA* and *BpeAB-OprB*.<sup>71,72,79</sup> Co-trimoxazole, a combination of trimethoprim and sulfamethoxazole, remains the

first-line, eradication phase treatment for melioidosis despite the ability for BpeEF-OprC to extrude it from the cell at low levels. This makes this system the most important efflux determinant from a clinical standpoint.<sup>14,24,74</sup> Doxycycline and chloramphenicol are similarly effluxed by BpeEF-OprC and evidence exists that they may induce increased expression of the pump, thereby further decreasing susceptibility to all other substrates of BpeEF-OprC.<sup>80</sup>

This may have been first documented in studies showing development of cross resistance and antagonism in patients administered a multidrug therapy (known as the conventional or combined regimen) consisting of chloramphenicol, doxycycline and co-trimoxazole with high rates of treatment failure.<sup>14,80,81</sup> In one study, incidence of side effects caused by this regimen resulted in almost 40% of participants switching to an alternate method, and it was noted that non-compliance (possibly due to these side effects) causing treatment duration less than the recommended 12 weeks caused a five fold increase in relapse.<sup>82</sup> As a result, calls for the removal of both chloramphenicol in 2005, and doxycycline in 2014, as potential therapeutics were published in an effort to better inform the medical communities of endemic regions.<sup>16,81,82</sup> These observations have subsequently been reinforced by molecular data showing the ability of both these drugs to induce expression of BpeEF-OprC in *Bt*, as well as our own studies in *Bp*.<sup>83,84</sup> Taken together, the reliance on BpeEF-OprC substrates for eradication phase therapy, and subsequent acquired resistance to those substrates, underlines the need for increased understanding of the pump.

### **2.6.1 Previous data and research rationale**

Previous investigations into BpeEF-OprC are closely linked to the genetic context of the operon. The *bpeEF-oprC* operon is located on chromosome 2 of *Bp* strain 1026b and is bordered by a divergently transcribed regulatory gene BP1026b\_IIRS20165 encoding a LysR type

transcriptional regulator, also known as BpeT. Between *bpeT* and the structural pump elements (BP1026b\_IIRS20175 encoding the membrane fusion protein BpeE, BP1026b\_IIRS20180 encoding the RND transporter BpeF, and BP1026B\_IIRS20185 encoding the outer membrane channel protein OprC), is a 188 base pair intergenic region and an additional gene *llpE* (BP1026B\_IIRS20170).

The current function of LlpE is unknown but homology comparisons describe it as a putative lipase/carboxyl esterase enzyme. While the *llpE* gene is in the same transcriptional unit as *bpeE*, *bpeF* and *oprC*, LlpE is not required for BpeEF-OprC function. It may be possible that this gene encodes a protein necessary for modification of substrates of the efflux pump, or modification of co-inducer molecules which activate the LysR regulatory proteins needed for control of the efflux operon. The LysR type regulator encoding gene *bpeT* provides some clues as to the regulation of the pump. This family of protein is wide spread throughout the bacterial kingdom, and can act as both transcriptional activators and repressors by recruiting RNA polymerase to the transcriptional start site where the LysR family protein is bound.<sup>85</sup> The family is characterized by an N-terminal helix-turn-helix DNA binding domain and a C-terminal co-inducer and oligomerization domain. This region of the protein serves two functions necessary for the activity of the complex as a whole: interaction with a stimulatory molecule to activate or repress transcription of its target operon, and coalescence into active multimers with other LysR-family binding partners.<sup>86</sup> When this domain is altered, drastic changes in expression of the target operon can be observed.

Our first experience with *bpeEF-oprC* expression caused by mutations to BpeT came through experimentation in *Bp* 1026b. A mutant strain lacking both *amrAB-oprA* and *bpeAB-oprB* was exposed to ciprofloxacin in an effort to study *bpeEF-oprC*. Decreased susceptibility to

substrates of BpeEF-OprC were observed in several isolates over time, and qRT-PCR analysis showed elevated expression of the *bpeEF-oprC* operon. Later sequencing of *bpeT* revealed an amino acid substitution at position 280, changing a serine to a proline, and subsequent introduction of this mutation into Select Agent excluded strain Bp82 confirmed that the mutation was responsible for constitutive expression of the pump. Other groups besides our own have observed this trend in naturally occurring isolates as well: whole genome sequencing of paired isolates during recurrent melioidosis identified a large inversion on chromosome 2 that deleted the 24 C-terminal amino acids of BpeT and lead to increased MIC values for BpeEF-OprC substrates.<sup>87</sup> This highlights the importance of BpeT in control of MDR phenotypes in a clinical setting. However, despite the apparent ability of BpeT to induce *bpeEF-oprC* transcription, loss of the gene did not abrogate operon expression in the presence of sub-inhibitory concentrations of pump substrates. This suggests an additional regulatory factor could be in play. To test this, a Bp82 strain lacking *bpeT* was selected on co-trimoxazole until isolates able to overexpress *bpeEF-oprC* were identified through a combination of MIC analysis and qRT-PCR. Whole genome sequencing of these isolates located mutations to an additional LysR regulator encoding gene BP1026b\_RS13955, located on chromosome 1. BLAST analyses of BpeT and BP1026B\_RS13955 revealed that they share very similar sequences. Overall, the proteins shared 66% identity. The N-termini of the proteins containing the DNA binding domains, are 90% identical over the first 60 amino acids, indicating that these proteins likely bind to similar regulatory sequences. Based on the extensive similarity of the two proteins BP1026b\_RS13955 was named BpeS. A full summary of the currently identified elements of the *bpeEF-oprC* operon is shown in **Fig. 2.2**. BpeS in the BpeEF-OprC overexpressing mutants was found to contain two mutations, P28S or K267T. When these mutations were introduced into wild type

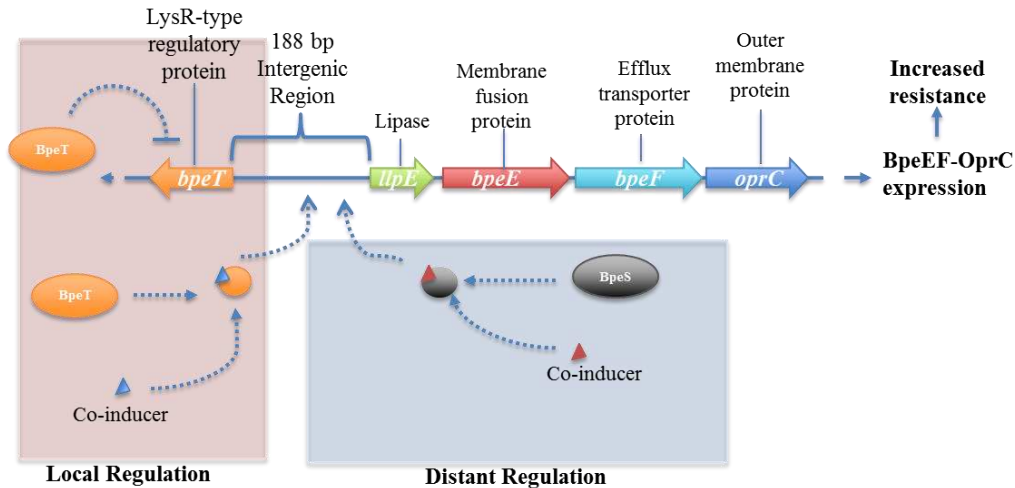


**Figure 2.2. The *bpeEF-oprC* operon and currently identified regulatory factors**

The arrangement of BP1026B\_IIRS20165; *bpeT*, BP1026B\_IIRS20170; *llpE*, BP1026B\_IIRS20175; *bpeE*, BP1026B\_IIRS20180; *bpeF*, and BP1026B\_IIRS20185; *oprC*, is depicted by block letters. The 188 bp intergenic region (IR) between *bpeT* and *llpE* is marked with a bracket. Local regulation (red box) is thought to be driven by the BpeT protein (orange ovals). Distant regulation (blue box) is thought to be driven by the BpeS protein (black ovals). Theorized interactions (dashed arrows) between both proteins and their respective co-inducers are believed necessary for these proteins to interact with a putative binding sequence within the IR. This process promotes expression of *bpeEF-oprC* leading to increased BpeEF-OprC efflux and decreased susceptibility to pump substrate antibiotics.

Bp82, mutants overexpressing BpeEF-OprC were observed, as assessed by qRT-PCR and MIC analysis of pump substrates. Not only was trimethoprim able to be extruded by the efflux pump, but sulfamethoxazole susceptibility was greatly reduced, causing resistance to co-trimoxazole. When these mutations were repaired to wild type, the expression of the pump returned to basal levels, and the MIC for trimethoprim, sulfamethoxazole and co-trimoxazole reverted to susceptible concentrations. Perhaps most significantly, a survey of co-trimoxazole resistant clinical isolates identified similar mutations within BpeS. The knowledge that mutations to both BpeS and BpeT are naturally occurring, cause clinical resistance, and complicate treatment underlines the importance of understanding the role of BpeEF-OprC in *Bp* antibiotic resistance to clinically significant melioidosis therapeutics.

While the connection between BpeT, BpeS and BpeEF-OprC clearly exists, little is understood of the interaction between these elements. Regulatory regions necessary for the

expression of the pump could be a vital link between the LysR type regulatory proteins and expression of the efflux pump components, but have yet to be identified. The mechanism by which mutations to either gene alters their structure to promote pump overexpression remains to be established. There has been no investigation into the cooperativity or interference of BpeT and BpeS in the context of efflux pump regulation, let alone any connection to the global transcriptional response of *Bp*. It is also unknown if there are any additional regulatory factors that influence transcription of the *bpeEF-oprC* operon in concert with currently identified regulatory genes.

In an effort to control resistance to eradication phase therapy in melioidosis, the main mechanism of resistance to co-trimoxazole must first be understood. The ability to predict the phenotypic outcome of mutations to the BpeEF-OprC pump, or correlate existing resistance profiles to overexpression of this pump, could allow clinicians to rapidly modify treatment methods in an effort to reduce patient morbidity and mortality. Two Study Aims are proposed in an effort to elucidate the answers to these questions and contribute to this future goal, and are described in the following section.

## **2.7 Summary of aims**

### **Aim I Chapter 3**

To identify the *cis* regulatory elements required for expression of the BpeEF-OprC efflux pump.

#### **Hypothesis:**

The *cis* regulatory elements control of *bpeEF-oprC* transcription, including BpeT and BpeS binding sites and promoters for both structural and local regulatory elements are located with the 188 nucleotide *bpeT-llpE-bpeEF-oprC* intergenic region.

## **Aim II Chapter 4**

**Part I:** To characterize the role of BpeT and BpeS in control of *bpeEF-oprC* operon expression.

### **Hypothesis:**

Expression of the operon is under the control of BpeT, BpeS and perhaps additional unidentified factor(s). Mutations in the genes coding for these proteins affect their multimerization, co-effector binding capability and interaction with DNA binding sites, all leading to changes in *bpeEF-oprC* expression and causing resistance to critical antibiotics used in eradication phase therapy.

**Part II:** To probe the BpeT and BpeS regulon(s) using Next Generation sequencing methods

### **Hypothesis:**

BpeS is a global regulatory protein affecting transcription of operons besides *bpeEF-oprC*. BpeT is a local regulatory protein only affecting transcription of *bpeEF-oprC*.

It is our hope that the data presented in the next two chapters will provide insights into the complex interplay of *cis* and *trans* regulatory factors controlling drug efflux in *Bp*, ultimately leading to improvements in antimicrobial administration and stewardship during melioidosis treatment.

## Chapter 2 References

1. Centers for Disease Control and Prevention (CDC). Control of infectious diseases. *MMWR Morb. Mortal. Wkly. Rep.* **48**, 621–629 (1999).
2. Shulman, S. T. The history of pediatric infectious diseases. *Pediatr. Res.* **55**, 163–176 (2004).
3. Shanks, G. D. How World War 1 changed global attitudes to war and infectious diseases. *The Lancet* **384**, 1699–1707 (2014).
4. Murray, C. K., Hinkle, M. K. & Yun, H. C. History of infections associated with combat-related injuries: *J. Trauma Inj. Infect. Crit. Care* **64**, S221–S231 (2008).
5. Aminov, R. I. A Brief history of the antibiotic era: lessons learned and challenges for the future. *Front. Microbiol.* **1**, (2010).
6. Ventola, C. L. The antibiotic resistance crisis: part 1: causes and threats. *P T Peer-Rev. J. Formul. Manag.* **40**, 277–283 (2015).
7. *Antibiotic Resistance Threats in the United States, 2013*. 114 (Centers for Disease Control and Prevention, 2013).
8. Piddock, L. J. The crisis of no new antibiotics—what is the way forward? *Lancet Infect. Dis.* **12**, 249–253 (2012).
9. Bhullar, K. *et al.* Antibiotic resistance is prevalent in an isolated cave microbiome. *PLoS ONE* **7**, e34953 (2012).
10. D’Costa, V. M. *et al.* Antibiotic resistance is ancient. *Nature* **477**, 457–461 (2011).
11. Brown, E. D. & Wright, G. D. Antibacterial drug discovery in the resistance era. *Nature* **529**, 336–343 (2016).
12. *Antimicrobial Resistance: Tackling a crisis for the health and wealth of nations*. 2014 (The

Review on Antimicrobial Resistance, 2014).

13. Christoffersen, R. E. Antibiotics—an investment worth making? *Nat. Biotechnol.* **24**, 1512–1514 (2006).

14. Dance, D. Treatment and prophylaxis of melioidosis. *Int. J. Antimicrob. Agents* **43**, 310–318 (2014).

15. White, N. Melioidosis. *The Lancet* **361**, 1715–1722 (2003).

16. Chetchotisakd, P. *et al.* Trimethoprim-sulfamethoxazole versus trimethoprim-sulfamethoxazole plus doxycycline as oral eradication treatment for melioidosis (MERTH): a multicentre, double-blind, non-inferiority, randomised controlled trial. *Lancet* **383**, 807–814 (2014).

17. Gleckman, R., Blagg, N. & Joubert, D. W. Trimethoprim: mechanisms of action, antimicrobial activity, bacterial resistance, pharmacokinetics, adverse reactions, and therapeutic indications. *Pharmacotherapy* **1**, 14–20 (1981).

18. Dax, S. L. *Antibacterial Chemotherapeutic Agents*. (Springer Netherlands, 1996). at <<http://dx.doi.org/10.1007/978-94-009-0097-4>>

19. Davies, J. & Davies, D. Origins and evolution of antibiotic resistance. *Microbiol. Mol. Biol. Rev.* **74**, 417–433 (2010).

20. Dantas, G., Sommer, M. O. A., Oluwasegun, R. D. & Church, G. M. Bacteria subsisting on antibiotics. *Science* **320**, 100–103 (2008).

21. Forsberg, K. J. *et al.* The shared antibiotic resistome of soil bacteria and human pathogens. *Science* **337**, 1107–1111 (2012).

22. Zeng, X. & Lin, J. Beta-lactamase induction and cell wall metabolism in Gram-negative bacteria. *Front. Microbiol.* **4**, (2013).

23. Randall, L. B., Dobos, K., Papp-Wallace, K. M., Bonomo, R. A. & Schweizer, H. P. membrane bound PenA  $\beta$ -lactamase of *Burkholderia pseudomallei*. *Antimicrob. Agents Chemother.* **60**, 1509-1514. (2015). doi:10.1128/AAC.02444-15
24. Schweizer, H. P. Mechanisms of antibiotic resistance in *Burkholderia pseudomallei* : implications for treatment of melioidosis. *Future Microbiol.* **7**, 1389–1399 (2012).
25. Rhol, D. A. *et al.* Molecular investigations of PenA-mediated  $\beta$ -lactam resistance in *Burkholderia pseudomallei*. *Front. Microbiol.* **2**, 139 (2011).
26. Tribuddharat, C., Moore, R. A., Baker, P. & Woods, D. E. *Burkholderia pseudomallei* Class A  $\beta$ -Lactamase mutations that confer selective resistance against ceftazidime or clavulanic acid inhibition. *Antimicrob. Agents Chemother.* **47**, 2082–2087 (2003).
27. Sarovich, D. S. *et al.* Development of ceftazidime resistance in an acute *Burkholderia pseudomallei* infection. *Infect. Drug Resist.* **5**, 129–132 (2012).
28. Goldstein, E. J. C. & Proctor, R. A. Role of folate antagonists in the treatment of methicillin-resistant *Staphylococcus aureus* Infection. *Clin. Infect. Dis.* **46**, 584–593 (2008).
29. Palmer, A. C. & Kishony, R. Opposing effects of target overexpression reveal drug mechanisms. *Nat. Commun.* **5**, (2014).
30. Zavascki, A. P., Goldani, L. Z., Li, J. & Nation, R. L. Polymyxin B for the treatment of multidrug-resistant pathogens: a critical review. *J. Antimicrob. Chemother.* **60**, 1206–1215 (2007).
31. Loutet, S. A. & Valvano, M. A. Extreme antimicrobial peptide and polymyxin B resistance in the genus *Burkholderia*. *Front. Microbiol.* **2**, (2011).
32. Burtnick, M. N. & Woods, D. E. Isolation of polymyxin B-susceptible mutants of *Burkholderia pseudomallei* and molecular characterization of genetic loci involved in polymyxin

- B resistance. *Antimicrob. Agents Chemother.* **43**, 2648–2656 (1999).
33. Nikaido, H. & Pagès, J.-M. Broad-specificity efflux pumps and their role in multidrug resistance of Gram-negative bacteria. *FEMS Microbiol. Rev.* **36**, 340–363 (2012).
34. Fernandez, L. & Hancock, R. E. W. Adaptive and mutational resistance: role of porins and efflux pumps in drug resistance. *Clin. Microbiol. Rev.* **25**, 661–681 (2012).
35. Lin, X.-M., Yang, J.-N., Peng, X.-X. & Li, H. A Novel negative regulation mechanism of bacterial outer membrane proteins in response to antibiotic resistance. *J. Proteome Res.* **9**, 5952–5959 (2010).
36. Zhang, D., Jiang, B., Xiang, Z. & Wang, S. Functional characterisation of altered outer membrane proteins for tetracycline resistance in *Escherichia coli*. *Int. J. Antimicrob. Agents* **32**, 315–319 (2008).
37. Mah, T.-F. *et al.* A genetic basis for *Pseudomonas aeruginosa* biofilm antibiotic resistance. *Nature* **426**, 306–310 (2003).
38. Beaudoin, T., Zhang, L., Hinz, A. J., Parr, C. J. & Mah, T.-F. The biofilm-specific antibiotic resistance gene *ndvB* is important for expression of ethanol oxidation genes in *Pseudomonas aeruginosa* biofilms. *J. Bacteriol.* **194**, 3128–3136 (2012).
39. Sadovskaya, I. *et al.* High-level antibiotic resistance in *Pseudomonas aeruginosa* biofilm: the *ndvB* gene is involved in the production of highly glycerol-phosphorylated  $\alpha$ -D-glucans, which bind aminoglycosides. *Glycobiology* **20**, 895–904 (2010).
40. Chantratita, N. *et al.* Antimicrobial resistance to ceftazidime involving loss of penicillin-binding protein 3 in *Burkholderia pseudomallei*. *Proc. Natl. Acad. Sci.* **108**, 17165–17170 (2011).
41. Gardete, S. & Tomasz, A. Mechanisms of vancomycin resistance in *Staphylococcus aureus*.

*J. Clin. Invest.* **124**, 2836–2840 (2014).

42. Handwerger, S. & Skoble, J. Identification of chromosomal mobile element conferring high-level vancomycin resistance in *Enterococcus faecium*. *Antimicrob. Agents Chemother.* **39**, 2446–2453 (1995).

43. Arthur, M. & Courvalin, P. Genetics and mechanisms of glycopeptide resistance in enterococci. *Antimicrob. Agents Chemother.* **37**, 1563–1571 (1993).

44. Li, X.-Z. & Nikaido, H. Efflux-mediated drug resistance in bacteria. *Drugs* **69**, 1555–1623 (2009).

45. Poole, K. Efflux pumps as antimicrobial resistance mechanisms. *Ann. Med.* **39**, 162–176 (2007).

46. Du, D., van Veen, H. W., Murakami, S., Pos, K. M. & Luisi, B. F. Structure, mechanism and cooperation of bacterial multidrug transporters. *Curr. Opin. Struct. Biol.* **33**, 76–91 (2015).

47. Pao, S. S., Paulsen, I. T. & Saier, M. H. Major facilitator superfamily. *Microbiol. Mol. Biol. Rev. MMBR* **62**, 1–34 (1998).

48. Bay, D. C., Rommens, K. L. & Turner, R. J. Small multidrug resistance proteins: a multidrug transporter family that continues to grow. *Biochim. Biophys. Acta* **1778**, 1814–1838 (2008).

49. Tal, N. & Schuldiner, S. A coordinated network of transporters with overlapping specificities provides a robust survival strategy. *Proc. Natl. Acad. Sci.* **106**, 9051–9056 (2009).

50. Wong, K., Ma, J., Rothnie, A., Biggin, P. C. & Kerr, I. D. Towards understanding promiscuity in multidrug efflux pumps. *Trends Biochem. Sci.* **39**, 8–16 (2014).

51. Li, X.-Z., Plésiat, P. & Nikaido, H. The challenge of efflux-mediated antibiotic resistance in Gram-negative bacteria. *Clin. Microbiol. Rev.* **28**, 337–418 (2015).

52. Kuroda, T. & Tsuchiya, T. Multidrug efflux transporters in the MATE family. *Biochim.*

- Biophys. Acta BBA - Proteins Proteomics* **1794**, 763–768 (2009).
53. Morita, Y. *et al.* NorM, a putative multidrug efflux protein, of *Vibrio parahaemolyticus* and its homolog in *Escherichia coli*. *Antimicrob. Agents Chemother.* **42**, 1778–1782 (1998).
54. Masuda, S. identification and functional characterization of a new human kidney-specific h<sup>+</sup>/organic cation antiporter, kidney-specific multidrug and toxin extrusion 2. *J. Am. Soc. Nephrol.* **17**, 2127–2135 (2006).
55. Otsuka, M. *et al.* A human transporter protein that mediates the final excretion step for toxic organic cations. *Proc. Natl. Acad. Sci.* **102**, 17923–17928 (2005).
56. Lu, M. *et al.* Structures of a Na<sup>+</sup>-coupled, substrate-bound MATE multidrug transporter. *Proc. Natl. Acad. Sci.* **110**, 2099–2104 (2013).
57. Venter, H., Mowla, R., Ohene-Agyei, T. & Ma, S. RND-type drug efflux pumps from Gram-negative bacteria: molecular mechanism and inhibition. *Front. Microbiol.* **06**, (2015).
58. Nikaido, H. & Takatsuka, Y. Mechanisms of RND multidrug efflux pumps. *Biochim. Biophys. Acta BBA - Proteins Proteomics* **1794**, 769–781 (2009).
59. Blair, J. M. & Piddock, L. J. Structure, function and inhibition of RND efflux pumps in Gram-negative bacteria: an update. *Curr. Opin. Microbiol.* **12**, 512–519 (2009).
60. Anes, J., McCusker, M. P., Fanning, S., & Martins, M. The ins and outs of RND efflux pumps in *Escherichia coli*. *Front. Microbiol.* **6**, (2015).
61. Godoy, P., Molina-Henares, A. J., de la Torre, J., Duque, E. & Ramos, J. L. Characterization of the RND family of multidrug efflux pumps: in silico to in vivo confirmation of four functionally distinct subgroups. *Microb. Biotechnol.* **3**, 691–700 (2010).
62. Murakami, S., Nakashima, R., Yamashita, E., Matsumoto, T. & Yamaguchi, A. Crystal structures of a multidrug transporter reveal a functionally rotating mechanism. *Nature* **443**, 173–

179 (2006).

63. Seeger, M. A., *et al.* Structural asymmetry of AcrB trimer suggests a peristaltic pump mechanism. *Science* **313**, 1295–1298 (2006).

64. Schwartz, K. T. *et al.* Hyper-induction of host Interferon  $\gamma$  by a *Listeria monocytogenes* strain naturally over-expressing the multi-drug efflux pump MdrT. *Infect. Immun.* (2012).

doi:10.1128/IAI.06286-11

65. Blair, J. M. A. *et al.* Expression of homologous RND efflux pump genes is dependent upon AcrB expression: implications for efflux and virulence inhibitor design. *J. Antimicrob. Chemother.* **70**, 424–431 (2015).

66. Lamarche, M. G. & Déziel, E. MexEF-OprN efflux pump exports the *Pseudomonas* quinolone signal (PQS) precursor HHQ (4-hydroxy-2-heptylquinoline). *PLoS One* **6**, e24310 (2011).

67. Olivares, J. *et al.* Overproduction of the multidrug efflux pump MexEF-OprN does not impair *Pseudomonas aeruginosa* fitness in competition tests, but produces specific changes in bacterial regulatory networks. *Environ. Microbiol.* 1968–1981 (2012). doi:10.1111/j.1462-2920.2012.02727.x

68. Hideaki Maseda, Maki Uwate & Taiji Nakae. Transcriptional regulation of the *mexEF-oprN* multidrug efflux pump operon by MexT and an unidentified repressor in nfxC-type mutant of *Pseudomonas aeruginosa*. *FEMS Microbiol. Lett.* **311**, 36–43 (2010).

69. Tian, Z.-X. *et al.* MexT modulates virulence determinants in *Pseudomonas aeruginosa* independent of the MexEF-OprN efflux pump. *Microb. Pathog.* **47**, 237–241 (2009).

70. Kumar, A. *et al.* Expression of resistance-nodulation-cell-division efflux pumps in commonly used *Burkholderia pseudomallei* strains and clinical isolates from northern Australia.

*Trans. R. Soc. Trop. Med. Hyg.* **102 Suppl 1**, S145–151 (2008).

71. Moore, R. A., DeShazer, D., Reckseidler, S., Weissman, A. & Woods, D. E. Efflux-mediated aminoglycoside and macrolide resistance in *Burkholderia pseudomallei*. *Antimicrob. Agents Chemother.* **43**, 465–470 (1999).

72. Chan, Y. Y., Tan, T. M. C., Ong, Y. M. & Chua, K. L. BpeAB-OprB, a multidrug efflux pump in *Burkholderia pseudomallei*. *Antimicrob. Agents Chemother.* **48**, 1128–1135 (2004).

73. Kumar, A., Chua, K.-L. & Schweizer, H. P. Method for regulated expression of single-copy efflux pump genes in a surrogate *Pseudomonas aeruginosa* Strain: Identification of the BpeEF-OprC chloramphenicol and trimethoprim efflux pump of *Burkholderia pseudomallei* 1026b. *Antimicrob. Agents Chemother.* **50**, 3460–3463 (2006).

74. Podnecky, N. L., Wuthiekanun, V., Peacock, S. J. & Schweizer, H. P. The BpeEF-OprC efflux pump is responsible for widespread trimethoprim resistance in clinical and environmental *Burkholderia pseudomallei* isolates. *Antimicrob. Agents Chemother.* **57**, 4381–4386 (2013).

75. Mima, T. & Schweizer, H. P. The BpeAB-OprB efflux pump of *Burkholderia pseudomallei* 1026b does not play a role in quorum sensing, virulence factor production, or extrusion of aminoglycosides but is a broad-spectrum drug efflux system. *Antimicrob. Agents Chemother.* **54**, 3113–3120 (2010).

76. Chan, Y. Y. *et al.* Control of quorum sensing by a *Burkholderia pseudomallei* multidrug efflux pump. *J. Bacteriol.* **189**, 4320–4324 (2007).

77. Podnecky, N. L., Rhodes, K. A. & Schweizer, H. P. Efflux pump-mediated drug resistance in *Burkholderia*. *Front. Microbiol.* **06**, 305 (2015).

78. Mima, T., Schweizer, H. P. & Xu, Z.-Q. In vitro activity of cethromycin against *Burkholderia pseudomallei* and investigation of mechanism of resistance. *J. Antimicrob.*

*Chemother.* **66**, 73–78 (2010).

79. Trunck, L. A. *et al.* Molecular basis of rare aminoglycoside susceptibility and pathogenesis of *Burkholderia pseudomallei* clinical isolates from Thailand. *PLoS Negl. Trop. Dis.* **3**, e519 (2009).

80. Dance, D. A., Wuthiekanun, V., Chaowagul, W. & White, N. J. The antimicrobial susceptibility of *Pseudomonas pseudomallei*. Emergence of resistance in vitro and during treatment. *J. Antimicrob. Chemother.* **24**, 295–309 (1989).

81. Saraya, S., Soontornpas, C., Chindavijak, B. & Mootsikapun, P. In vitro interactions between cotrimoxazole and doxycycline in *Burkholderia pseudomallei*: how important is this combination in maintenance therapy of melioidosis? *Indian J. Med. Microbiol.* **27**, 88–89 (2009).

82. Chaowagul, W. *et al.* Open-label randomized trial of oral trimethoprim-sulfamethoxazole, doxycycline, and chloramphenicol compared with trimethoprim-sulfamethoxazole and doxycycline for maintenance therapy of melioidosis. *Antimicrob. Agents Chemother.* **49**, 4020–4025 (2005).

83. Biot, F. V. *et al.* Involvement of the efflux pumps in chloramphenicol selected strains of *Burkholderia thailandensis*: proteomic and mechanistic evidence. *PLoS ONE* **6**, e16892 (2011).

84. Biot, F. V. *et al.* Interplay between three RND efflux pumps in doxycycline-selected strains of *Burkholderia thailandensis*. *PLoS ONE* **8**, e84068 (2013).

85. Maddocks, S. E. & Oyston, P. C. F. Structure and function of the LysR-type transcriptional regulator (LTTR) family proteins. *Microbiology* **154**, 3609–3623 (2008).

86. Ruangprasert, A., Craven, S. H., Neidle, E. L. & Momany, C. Full-Length Structures of BenM and two variants reveal different oligomerization schemes for LysR-Type transcriptional Regulators. *J. Mol. Biol.* **404**, 568–586 (2010).

87. Hayden, H. S. *et al.* Evolution of *Burkholderia pseudomallei* in Recurrent Melioidosis. *PLoS ONE* **7**, e36507 (2012).
88. Wood, T. K.. Combating bacterial persister cells. *Biotechnology and Bioengineering* **113**, 476-483 (2016).
89. Lewis, K. Multidrug tolerance of persister cells. *Current Top. in Immun. and Micro.***322**, 107-131 (2008).
90. Kwan, B.W. *et al.* The MqsR/MqsA toxin-antitoxin system protects *Escherichia coli* during bile acid stress: MqsR/MqsA increases growth with bile acid.*Environmental Micro.***17**, 3168-3181 (2015).
91. Kwan, B.W. *et al.* Combatting bacterial infections by killing persister cells with mitomycin C: eradication of persisters with mitomycin C. *Environmental Micro.* **17**, 4406-4414 (2015).

## Chapter 3: Genetic characterization of the *bpeEF-oprC* operon

### Summary

The first aim of this study was to identify the *cis* regulatory elements we hypothesized to exist within the 188 base pair *bpeT-llpE* intergenic region located between *bpeT* and the *llpE-bpeEF-oprC* operon. We proposed that these sites govern expression of the BpeEF-OprC efflux pump through their interaction with BpeT and BpeS. Through a combination of successive 5' deletion analysis of the intergenic region, fluorescent primer extension and S1 nuclease protection assays, the putative promoter regions and transcriptional start sites for both *bpeT* and *llpE-bpeEF-oprC* were identified within closely associated regions in the center of the intergenic region. Binding sites for both BpeT and BpeS were identified at an overlapping region located between the putative promoter regions, confirming shared regulation of the pump by these proteins

### Introduction

BpeEF-OprC is the only RND efflux pump encoded by *Bp* currently known to have clinical significance because it extrudes antibiotics that have been or are currently used for melioidosis therapy.<sup>1</sup> The substrates extruded by the efflux pump include fluoroquinolones, tetracyclines, folate biosynthesis inhibitors, and chloramphenicol. Two folate biosynthesis inhibitors targeted by BpeEF-OprC, trimethoprim and sulfamethoxazole (or co-trimoxazole), are currently used in eradication phase therapy of melioidosis.<sup>2</sup> Expression of this protein complex in response to antimicrobial stimuli has been documented on several occasions by our laboratory, and may have played a role in the high rates of treatment failure seen in studies evaluating the so-called “combined regimen”. This therapy consisted of co-trimoxazole, chloramphenicol and

doxycycline, and was previously used in eradication phase therapy of melioidosis.<sup>3-7</sup> Mutations to known regulatory factors in control of BpeEF-OprC are capable of causing high level expression of the *bpeEF-oprC* efflux operon, subsequently causing decreased susceptibility to the folate inhibitor cocktail co-trimoxazole (Podnecky and Rhodes, unpublished).

Our original investigations of BpeEF-OprC showed that this pump was not capable of exporting sulfamethoxazole at basal levels of expression. However, with the overexpression caused by mutations to one regulatory protein in particular, BpeS, efflux of both trimethoprim and sulfamethoxazole is observed: the substrate specificity of the pump is effectively broadened without structural changes to the export channel. This is of great importance based on the fact that these mutations, although first observed through laboratory manipulation, were also found in subsets of co-trimoxazole resistant clinical isolates. This proves that these regulatory changes are naturally occurring and could potentially hinder treatment of melioidosis if not identified in time. However, these regulatory elements are not well understood.

A complete characterization of the factors governing expression of *bpeEF-oprC*, both *cis* and *trans*, is necessary to understand how mutations to these factors alter resistance phenotypes of *Bp*, and thereby impede clinical intervention in cases of melioidosis.

We hypothesize that the 188 base pair *bpeT-llpE* intergenic region contains many, if not all, of the necessary regulatory regions needed for DNA-protein interaction and gene expression. To that effect, the aims of this study were to identify transcriptional start sites, promoters and regulatory protein binding regions through molecular methods to assess how mutations to these factors might influence efflux pump expression.

### 3.1 Materials and methods

#### 3.1.1. General DNA methodology

All genomic DNA extractions were performed using the Qiagen Tissue core kit A following the manufacturers instructions for Gram-negative bacteria. All plasmid DNA was extracted using the Sigma (St. Louis, MO) GeneJet Mini-prep kit according to the supplied protocol for Gram negative bacteria. PCR and cloning techniques were performed using previously described molecular methods.<sup>5,8,9</sup> All primers utilized in this study are noted in **Tables 3.1.A** and **3.1.B**.

**Table 3.1.A Cloning primers**

Name	Target	Sequence (5'>3')
2384	bpeE fusion rev	GCTCGTCG GAGCGTTCG
2446	2394HindIII_for	<u>AAGCTT</u> CCACTTACTCTACCTCCGCGATATTGGC
2447	1934Nco1_rev	CCATGGAATCGGTGATCGTCTTCGAC
2483	HindIII_1	<u>AAGCTT</u> TGAATTGTGTTGCCGGATT
2484	HindIII_2	<u>AAGCTT</u> CTGCCGGACCCAGAAT
2485	HindIII_3	<u>AAGCTT</u> CATTTATCCCGATG
2486	HindIII_4	<u>AAGCTT</u> TGCGATCCATCTCGC
2605	HindIII_6llpE	<u>AAGCTT</u> ATGGACGCATTCGATTTCGG
2606	HindIII_5llpE	<u>AAGCTT</u> GCCGCGCAACACA
2624	HindIII_7	<u>AAGCTT</u> TGAAGGCGACGCAGC
2625	HindIII_8	<u>AAGCTT</u> GATATTGGCACCCCGAAC
2626	KpnI_bpeErev	GGTACCAATCGGTGATCGTCTTCGAC
2651	bpeTHindIII_6	<u>AAGCTT</u> ATGGACCGGCTGCAAGCCAT
2652	bpeTHindIII_5	<u>AAGCTT</u> CGTCGGCTGCGTGCCTTC
2653	bpeTHindIII_4	<u>AAGCTT</u> GCCAATATCGCGGAGGTAGAGTAATG
2654	bpeTHindIII_3	<u>AAGCTT</u> CGGAAATCGAATGCGTCCAT
2655	bpeTHindIII_2	<u>AAGCTT</u> ATTCTGGGTCCGGCAG
2656	bpeTHindIII_1	<u>AAGCTT</u> AATCCGGCAACACAATTCACG
2657	bpeT_KpnIrev	GGTACCGTAGCGTGAGTGGAAATTCGC
2536	NdeIbpeT_pet21b	CGGAGGTAGAc <u>atATGGACCGGCTGCAAGC</u>
2537	HindIII_pet21bbpeT	CTGCGCGACTAAaagcttATACGCCACCCACTC
2849	pET21b_bpeS_EcoR1	gaattcCGCGCCACCTGCC
2850	pET21b_bpeS_Nde1	<u>catATGGACCGCATT</u> CAGGCAATGG
2871	bpes for	ATGGACCGCATT <u>CAGGCAATGGAAGTCTTC</u>

<sup>1</sup>Restriction enzyme cleavage sites are underlined, mutagenized bases indicated by lower case letters.

**Table 3.1.B Detection primers**

<b>Name</b>	<b>Target</b>	<b>Sequence 5'&gt; 3'</b>
<b>Oligonucleotides for detecting Mini-Tn7 insertions</b>		
479	TN7L	ATTAGCTTACGACGCTACACCC
1509	BPGLMS1	GAGGAGTGGGCGTCGATCAAC
1510	BPGLMS2	ACACGACGCAAGAGCGGAATC
1511	BPGLMS3	CGGACAGGTTCGCGCCATGC
<b>pEX system associated primers</b>		
2213	FK.chk.rev	AGCGCTCTGAAGTTCCTATACTTTCT
536	oriT-UP	TCCGCTGCATAACCCTGCTTC
537	oriT-DN	CAGCCTCGCAGAGCAGGATTC
1790	<i>dbpeT</i> for	ATGGACCGGCTGCAAGCCAT
1791	<i>dbpeT</i> rev	CGACGCATCGCGATGGAAAC
1726	<i>oprB</i> -Rev	CTCTGGATCGCCTTCTCGTA
1729	<i>bpeA</i> -For	GTACGAGCGCCTATCTGGTC
<b>Oligonucleotides used for promoter and binding site mapping</b>		
2474	6FAM_llpErev	/6FAM/GTAGCCGCCGATCACGACGT
2475	6FAM_bpeTrev 2142	/6FAM/TCTGAATGATCGTCGTCACC
2394	ingn 2F	TCCATTACTCTACCTCCGCGATATTGGC
2476	<i>llpErev</i> _S1	GTAGCCGCCGATCACGACGT
2956	2394_hex	/5HEX/ TCCATTACTCTACCTCCGCGATAT TGGC
2627	<i>llpePE2</i> _rev	/6FAM/CGCCGCCGTGGAAATAAAG
2923	IR_rev	CATTGCGAGATGGATCGCATTCTGG
2928	2483 no HindIII	TGAATTGTGTTGCCGGATT
2929	2484 no HindIII	CTGCCGGACCCAGAAT
2930	2485 no HindIII	CATTTATCCCGATGTCTGCC
2931	2486 no HindIII	TGCGATCCATCTCGC
2932	2605 no HindIII	ATGGACGCATTCGATTTCCG
2933	2606 No HindIII	GCCGCGCAACACACGT
2934	2625 no HindIII	TGAAGGCGACGCAGC
2935	2626 no HindIII	GATATTGGCACCCCGAAC
2936	2651 no HindIII	ATGGACCGGCTGCAAGCCAT
2937	2652 no HindIII	CGTCGGCTGCGTCGCCTTC
2938	2653 no HindIII	GCCAATATCGCGGAGGTAGAGTAATG
2939	2654 no HindIII	CGGAAATCGAATGCGTCCAT
2940	2655 no HindIII	ATTCTGGGTCCGGCAG
2941	2656 no HindIII	AATCCGGCAACACAATTCACG
2942	2657 no kpn1	GTAGCGTGAGTGGAATTCGC

\*/6FAM/ indicates 5' linkage to Fluorescein, /5HEX/ indicates 5' linkage to hexachlorofluorescein

### 3.1.2 Plasmids and bacterial strains

*E. coli* and *B. pseudomallei* strains were grown in Lennox- LB broth or agar supplemented with the appropriate antibiotic for plasmid maintenance at 37°C unless otherwise stated. *E. coli* RHO3 strains used for conjugation were grown in media containing 400 µg/ml diaminopimelic acid (DAP) unless undergoing counter selection. All *B. pseudomallei* Bp82 derivatives were grown in Lennox LB media containing the appropriate antibiotic and supplemented with adenine to a final concentration of 80 µg/ml. Liquid cultures were shaken at 250 RPM. All plasmids constructed in this study are listed in **Table 3.1.C**. All *E.coli* strains used or in the study are listed in **Table 3.1.D**. *E. coli* strains carrying plasmids were selected with 100 µg/ml ampicillin, 35 µg/ml kanamycin, 15 µg/ml gentamicin or 25 µg/ml zeocin. For *B. pseudomallei*, AmrA<sup>+</sup> B<sup>+</sup>-OprA<sup>+</sup> strains were grown in media containing 1000 µg/ml kanamycin, 500 µg/ml gentamicin or 2000 µg/ml zeocin. Strains lacking *amrAB-oprA* were cultivated in 35 µg/ml kanamycin, 15 µg/ml gentamicin, or 35 µg/ml zeocin. Methods used to perform gene deletions or complementation described in later sections of this chapter. All procedures with virulent *B. pseudomallei* strains were performed in select agent approved biosafety level 3 (BSL-3) facilities at Colorado State University, or the University of Florida using approved select-agent-compliant procedures and protocols. Experiments with select agent excluded strain Bp82 and its derivatives were performed at BSL-2 with Institutional Biosafety Committee approval.

**Table 3.1.C. Plasmids**

Name	Relevant properties	Source
pPS2234	pTNS3, transposition helper plasmid expressing <i>tnsABCD</i> from <i>P<sub>I</sub></i> and <i>P<sub>lac</sub></i>	8
pFLPe3	<i>rhaB-rhaS-rhaR-FLPe-Km-rep(Ts)-oriT</i> , plasmid encoding <i>flp</i> recombinase, temperature sensitive, Km <sup>r</sup>	8
pFLPe2	<i>rhaB-rhaS-rhaR-FLPe-Km-rep(Ts)-oriT</i> , plasmid encoding <i>flp</i> recombinase, temperature sensitive, Zeo <sup>r</sup> ;	8
pPS2594	pEXGM5, dual counter-selectable allelic exchange suicide	B. Kvitko,

	vector, Gm <sup>r</sup>	unpublished
pPS2412	pGEM-T Easy with $\Delta(bpeAB-oprB)::FRT-nptII$ - <i>FRT</i> recombinant DNA fragment	25
pPS2899	pEXKm5- $\Delta(bpeAB-oprB)::FRT$ Km, pPS2594 with EcoRI fragment from pPS2412 Km <sup>r</sup>	This study
pPS2833	pEXKm5- $\Delta(amrAB-oprA)$	8
pPS2571	pEXKm5: $\Delta bpeT::FRT-ble-FRT$ ,	T. Mima, unpublished
pPS3189	pEXKm5 <i>bpeS</i> <sub>P28S</sub>	N. Podnecky unpublished
pPS3190	pEXKm5 <i>bpeS</i> <sub>K267T</sub>	N. Podnecky unpublished
pGEM-TEasy	Ap <sup>r</sup> , TA cloning vector	Promega, Madison WI
pPS3011	pGEM-TEasy with <i>bpeE'</i> IR 5' deletion fragment amplified with primers 2483 and 2447, $\Delta 88$	This study
pPS3012	pGEM-TEasy with <i>bpeE'</i> IR 5' deletion fragment amplified with primers 2484 and 2447, $\Delta 126$	This Study
pPS3013	pGEM-TEasy with <i>bpeE'</i> IR 5' deletion fragment amplified with primers 2485 and 2447, $\Delta 112$	This Study
pPS3014	pGEM-TEasy with <i>bpeE'</i> IR 5' deletion fragment amplified with primers 2486 and 2447, $\Delta 142$	This Study
pPS3116	pGEM-TEasy with <i>bpeE'</i> IR 5' deletion fragment amplified with primers 2605 and 2626, $\Delta 188$	This Study
pPS3119	pGEM-TEasy with <i>bpeE'</i> IR 5' deletion fragment amplified with primers 2625 and 2626, $\Delta 15$	This Study
pPS3120	pGEM-TEasy with <i>bpeE'</i> IR deletion fragment amplified with primers 2484 and 2626, $\Delta 126$	This Study
pPS3131	pGEM-TEasy with <i>bpeT'</i> IR 5' deletion fragment amplified with primers 2651 and 2657, $\Delta 188$	This Study
pPS3132	pGEM-TEasy with <i>bpeT'</i> IR 5' deletion fragment amplified with primers 2652 and 2657, $\Delta 115$	This Study
pPS3133	pGEM-TEasy with <i>bpeT'</i> IR 5' deletion fragment amplified with primers 2653 and 2657, $\Delta 165$	This Study
pPS3134	pGEM-TEasy with <i>bpeT'</i> IR 5' fragment amplified with primers 2654 and 2657, +19	This Study
pPS3136	pGEM-TEasy with <i>bpeT'</i> IR 5' deletion fragment amplified with primers 2656 and 2657, $\Delta 82$	This Study
pTZ120	Medium copy transcriptional fusion vector with promoter-less <i>lacZ</i> , Cb <sup>r</sup>	10
pPS2963	pTZ120 with full length 1300 bp IR- <i>bpeE'</i> fusion,	This Study
pPS3035	pTZ120 with <i>HindIII/NcoI</i> IR- <i>llpE/bpeE'</i> fragment from pPS3011, $\Delta 88$	This Study
pPS3036	pTZ120 with <i>HindIII/NcoI</i> IR- <i>llpE/bpeE'</i> fragment from	This Study

	pPS3012 , $\Delta$ 126	
pPS3037	pTZ120 with <i>Hind</i> III/ <i>Nco</i> I IR- <i>llpE/bpeE'</i> fragment from pPS3013, $\Delta$ 112	This Study
pPS3079	pTZ120 with <i>Hind</i> III/ <i>Nco</i> I IR- <i>llpE/bpeE'</i> fragment from pPS3014, $\Delta$ 142	This Study
pPS1453	pUC18-mini-Tn7T-Gm-lacZ, miniTn7 transposon with promoter-lacZ MCS transcriptional fusion, Gm <sup>r</sup>	11
pPS2976	pPS1453 with full length <i>bpeT-llpE-bpe'</i> IR fragment amplified with primers 2446 and 2447, (mini-Tn7T-Gm- <i>bpe'</i> -lacZ entire IR)	This study
pPS3070	pPS1453 with <i>Hind</i> III/ <i>Dra</i> III IR fragment from pPS3036, (mini-Tn7T-Gm- <i>bpeE'</i> -lacZ IR 5' $\Delta$ 126)	This Study
pPS3081	pPS1453 with <i>Hind</i> III/ <i>Dra</i> III IR fragment from pPS3035, (mini-Tn7T-Gm- <i>bpeE'</i> -lacZ IR 5' $\Delta$ 88)	This Study
pPS3082	pPS1453 with <i>Hind</i> III/ <i>Dra</i> III IR fragment from pPS3037, (mini-Tn7T-Gm- <i>bpeE'</i> -lacZ IR 5', $\Delta$ 112)	This Study
pPS3083	pPS1453 with <i>Hind</i> III/ <i>Dra</i> III IR fragment of pPS3079, (mini-Tn7T-Gm- <i>bpeE'</i> -lacZ IR 5' $\Delta$ 142)	This Study
pPS3121	pPS1453 with <i>Hind</i> III/ <i>Kpn</i> I IR fragment from pPS3120 (mini-Tn7T-Gm- <i>bpeE'</i> -lacZ IR 5' $\Delta$ 126)	This Study
pPS3122	pPS1453 with <i>Hind</i> III/ <i>Kpn</i> I IR fragment from pPS3116 (mini-Tn7T-Gm- <i>bpeE'</i> -lacZ IR 5' $\Delta$ 188)	This Study
pPS3138	pPS1453 with <i>Hind</i> III/ <i>Kpn</i> I IR fragment amplified with primers 2626 and 2624, (mini-Tn7T-Gm- <i>bpeE'</i> -lacZ IR 5' $\Delta$ 53)	This Study
pPS3139	pPS1453 with <i>Hind</i> III/ <i>Kpn</i> I IR fragment from pPS3119, (mini-Tn7T-Gm- <i>bpeE'</i> -lacZ IR 5' $\Delta$ 15)	This Study
pPS3146	pPS1453 with <i>Hind</i> III/ <i>Kpn</i> I IR fragment from pPS3131, (mini-Tn7T-Gm- <i>bpeT'</i> -lacZ IR 5' $\Delta$ 188)	This Study
pPS3147	pPS1453 with <i>Hind</i> III/ <i>Kpn</i> I IR fragment from pPS3132, (mini-Tn7T-Gm- <i>bpeT'</i> -lacZ IR 5' $\Delta$ 115)	This Study
pPS3148	pPS1453 with <i>Hind</i> III/ <i>Kpn</i> I IR fragment from from pPS3133, (mini-Tn7T-Gm- <i>bpeT'</i> -lacZ IR 5' $\Delta$ 165)	This Study
pPS3149	pPS1453 with <i>Hind</i> III/ <i>Kpn</i> I IR fragment from pPS3134, (mini-Tn7T-Gm- <i>bpeT'</i> -lacZ IR 5' $\Delta$ +19)	This Study
pPS3150	pPS1453 with <i>Hind</i> III/ <i>Kpn</i> I IR fragment from pPS3136, (mini-Tn7T-Gm- <i>bpeT'</i> -lacZ IR 5' $\Delta$ 82)	This Study
pPS3258	pGEM-TEasy with <i>bpeS</i> <sub>P28S</sub> amplified from pPS3189 with primers 2849 and 2850	This Study
pPS3259	pGEM-TEasy with <i>bpeS</i> amplified with primers 2849 and 2850	This Study
pPS3260	pGEM-TEasy with <i>bpeS</i> <sub>K267T</sub> amplified from pPS3190 with primers 2849 and 2850.	This Study
pET-21b	C-Terminal Hexahistidine fusion vector, IPTG inducible T7 promoter system, Ap <sup>r</sup>	Millipore
pPS3069	pET-21b- <i>bpeT</i> , pET-21b with <i>bpeT</i> amplified with primers 2536 and 2537	This study
pPS3253	pET-21b <i>bpeT</i> <sub>S280P</sub> , pET21b with <i>bpeT</i> amplified from Bp82.270	This Study

	using primers 2536 and 2537,	
pPS3265	pET-21b <i>bpeS</i> , pET-21b with <i>NdeI/EcoRI</i> wild-type <i>bpeS</i> fragment from pPS3259	This Study
pPS3266	pET-21b <i>bpeS</i> <sub>K267T</sub> , pET21-b with <i>NdeI/EcoRI</i> <i>bpeS</i> <sub>K267T</sub> fragment from pPS3260	This Study
pPS3276	pET-21b with <i>NdeI/EcoRI</i> <i>bpeS</i> <sub>P28S</sub> fragment from pPS3258	This Study

**Table 3.1.D *Escherichia coli* strains utilized in this study**

Strain	Genotype/Description	Source
DH5 $\alpha$	Subcloning strain, genotype: F <sup>-</sup> $\Phi$ 80 <i>lacZ</i> $\Delta$ M15 $\Delta$ ( <i>lacZYA-argF</i> ) U169 <i>recA1 endA1 hsdR17</i> (r <sub>k</sub> <sup>-</sup> , m <sub>k</sub> <sup>+</sup> ) <i>phoA</i> <i>supE44 thi-1 gyrA96 relA1 <math>\lambda</math></i>	12
NEB5 $\alpha$	Subcloning strain, K12 derivative, genotype: <i>fhuA2 <math>\Delta</math>(argF-lacZ)U169 phoA glnV44 <math>\Phi</math>80 <math>\Delta</math>(lacZ)M15 gyrA96 recA1 relA1 endA1 thi-1 hsdR17</i>	New England Biolabs, Ipswich MA
BL21(DE3)	<i>E. coli</i> T7 lysogen lacking <i>Lon</i> and <i>Omp</i> proteases, protein expression strain. Genotype: <i>fhuA2 [lon] ompT gal (<math>\lambda</math> DE3) [dcm] <math>\Delta</math>hsdS <math>\lambda</math> DE3 = <math>\lambda</math> sBamHIo <math>\Delta</math>EcoRI-B int:lacI::PlacUV5::T7 gene1) i21 <math>\Delta</math>nin5</i>	New England Biolabs, Ipswich MA
B121(DE3)-RP (codonplus)	BL21(DE3) harboring Cm <sup>r</sup> tRNA codon plasmids for <i>argU</i> (AGA AGG) and <i>proC</i> (CCC)	Agilent, inc.
RHO3	Conjugation donor strain, SM10 $\Delta$ <i>asd</i> :: <i>FRT-<math>\Delta</math>aphA::FRT</i> , diaminopimelic acid auxotroph	9

### 3.1.3 Gene deletion

All chromosomal gene deletions were performed using the pEX allelic exchange system designed by previous members of the Schweizer laboratory.<sup>8</sup> Suicide vectors were transformed into RHO3 cells and selected on LB media containing 400  $\mu$ g/ml Diaminopimelic acid (DAP). Recipient and donor parent strains were cultured overnight, then centrifuged and washed with either 10 mM MgSO<sub>4</sub> or cold water. 50  $\mu$ l each of parent were mixed together in an Eppendorf tube before the whole volume was spotted onto LB agar containing 400  $\mu$ g/ml DAP and 80  $\mu$ g/ml adenine as well as the appropriate antibiotic. 50  $\mu$ l of each parent strain were spotted as

controls and then incubated 24 h at 37° C. Cells were harvested and washed in fresh media before being plated on LB agar with 80 µg/ml adenine and 50 µg/ml X-gluc (5-bromo-4-chloro-3-indolyl-β-D-glucuronic acid) with appropriate antibiotics, but lacking DAP. This allowed for counter-selection against RHO3, and selection of exconjugant *B. pseudomallei* colonies. Plates were incubated again at 37°C until blue merodiploids colonies became visible. Merodiploids were patched onto the same media and allowed 24h of growth at 37°C before being struck for isolation on Yeast-tryptone media containing 15% sucrose and the appropriate antibiotic. Plates were incubated at 37°C until white colonies were visible. These were patched for further testing by phenotypic analysis and PCR confirmation.

In instances where the deletion was more difficult to obtain, the I-*Sce* homing endonuclease functions of the pEX system were utilized.<sup>9</sup> Briefly, the pEX allelic exchange procedure was followed to up to the isolation of merodiploid cells. At this point, individual merodiploids were cultivated overnight in LB containing the appropriate antibiotic. One ml of culture was pelleted, and cells were washed with 300 mM sucrose before being electroporated with 100 ng of pBAD*Sce*. Cells were recovered in LB containing 80 µg/ml adenine and plated on YT+ sucrose + 80 µg/ml adenine + 0.1% arabinose and the appropriate antibiotic. Plates were incubated for 24-72 h at 30°C until white clones were visible. Individual colonies were struck for isolation on YT Suc Ade 80 and incubated at 42°C to cure pBAD*Sce*. Clones were patched on the same media and allowed to grow at 37°C for 24 h before boiling lysis was used to isolate crude DNA samples for PCR screening. Following these procedures, all strains lacking *bpeT* were created by conjugation of RHO3 containing the pEXKM5  $\Delta bpeT$ ( pPS2571) (**Table 3.1.C**) construct into various Bp82 strains (**Table 3.1.E**). Loss of *bpeT* was confirmed by PCR in comparison to merodiploid and wild type controls with primers 1790 and 1791 (**Table 3.1.B**) and

amplicon sequencing. Strains lacking *bpeAB-oprB* were constructed in the same manner using pPS2899 and primers 1726, 1729, and 2213. Removal of antibiotic markers is described in the next section.

**Table 3.1.E *Burkholderia pseudomallei* Strains Utilized in This Study**

<b>Parent Strains</b>		
<b>Number</b>	<b>Description</b>	<b>Source</b>
1026b	<i>Burkholderia pseudomallei</i> clinical strain, isolated from blood sample of infected Thai patient in 1993	NCBI Biosample
Bp282	1026b $\Delta(amrAB-oprA)$ $\Delta(bpeAB-oprB)$ <i>bpeT</i> <sub>S280P</sub> , constitutively expresses BpeEF-OprC	T. Mima, unpublished
Bp82	Bp1026b $\Delta purM$ select agent excluded strain	9
Bp82.27	Bp82 $\Delta(amrAB-oprA)$	B. Kvitko, unpublished
Bp82.57	Bp82.27 $\Delta(bpeAB-oprB)$	This study
<b>Bp82 <i>bpeS bpeT</i> Mutant Strains</b>		
Bp82.87	Bp82.57 $\Delta bpeT$	This study
Bp82.253	Bp82 $\Delta bpeT$	N. Podnecky, unpublished
Bp82.264	Bp82 $\Delta bpeS$	N. Podnecky, unpublished
Bp82.270	Bp82 <i>bpeT</i> <sub>S280P</sub>	N. Podnecky, unpublished
Bp82.284	Bp82 <i>bpeS</i> <sub>P28S</sub>	N. Podnecky, unpublished
Bp82.285	Bp82 <i>bpeS</i> <sub>K267T</sub>	N. Podnecky, unpublished
Bp82.286	Bp82.264 $\Delta bpeT$	This study
Bp82.292	Bp82.284 $\Delta bpeT$	This Study
Bp82.317	Bp82.285 $\Delta bpeT$	This Study
<b>Bp1026b Expression Strains</b>		
Bp769	Bp282::pPS1453 (mini-Tn7T-Gm- <i>lacZ</i> )	This Study
Bp770	Bp282::pPS2976 (mini-Tn7T-Gm- <i>bpeE'</i> - <i>lacZ</i> entire IR)	This Study
Bp771	Bp282::pPS3081 (mini-Tn7T-Gm- <i>bpeE'</i> - <i>lacZ</i> IR 5' $\Delta$ 88)	This Study

Bp772	Bp282::pPS3070 (mini-Tn7T-Gm- <i>bpeE'</i> - <i>lacZ</i> IR 5' Δ126)	This Study
Bp773	Bp282::pPS3082(mini-Tn7T-Gm- <i>bpeE'</i> - <i>lacZ</i> IR 5'Δ112)	This Study
Bp774	Bp282::pPS3083(mini-Tn7T-Gm- <i>bpeE'</i> - <i>lacZ</i> IR 5'Δ142)	This Study
Bp816	Bp282::pPS3122 (mini-Tn7T-Gm- <i>bpeE'</i> - <i>lacZ</i> IR 5'Δ188)	This Study
Bp817	Bp282::pPS3121 (mini-Tn7T-Gm- <i>bpeE'</i> - <i>lacZ</i> IR 5'Δ126)	This Study
Bp825	Bp282::pPS3138 (mini-Tn7T-Gm- <i>bpeE'</i> - <i>lacZ</i> IR 5'Δ53)	This Study
Bp826	Bp282::pPS3139 (mini-Tn7T-Gm- <i>bpeE'</i> - <i>lacZ</i> IR 5'Δ15)	This Study
Bp831	Bp282::pPS3147 ( mini-Tn7T-Gm- <i>bpeT'</i> - <i>lacZ</i> IR 5'Δ115)	This Study
Bp832	Bp282::pPS3148 (mini-Tn7T-Gm- <i>bpeT'</i> - <i>lacZ</i> IR 5'Δ165)	This Study
Bp833	Bp282::pPS3149 (mini-Tn7T-Gm- <i>bpeT'</i> - <i>lacZ</i> IR 5'Δ +19)	This Study
Bp834	Bp282::pPS3150 (mini-Tn7T-Gm- <i>bpeT'</i> - <i>lacZ</i> IR 5'Δ82)	This Study
Bp836	Bp282::pPS3146 (mini-Tn7T-Gm- <i>bpeT'</i> - <i>lacZ</i> IR 5'Δ188)	This Study
Bp82.329	82.284::pPS1453 (mini-Tn7T-Gm- <i>lacZ</i> empty)	This Study
<b>Bp82 Expression Strains</b>		
Bp82.330	82.284::pPS2976(mini-Tn7T-Gm- <i>bpeE'</i> - <i>lacZ</i> entire IR)	This Study
Bp82.331	82.284::pPS3081(mini-Tn7T-Gm- <i>bpeE'</i> - <i>lacZ</i> IR 5' Δ88)	This Study
Bp82.332	82.284::pPS3083(mini-Tn7T-Gm- <i>bpeE'</i> - <i>lacZ</i> IR 5'Δ142)	This Study
Bp82.333	82.284::pPS3121(mini-Tn7T-Gm- <i>bpeE'</i> - <i>lacZ</i> IR 5' Δ126)	This Study
Bp82.334	82.284::pPS3122 (mini-Tn7T-Gm- <i>bpeE'</i> - <i>lacZ</i> IR 5'Δ188)	This Study
Bp82.335	82.284::pPS3146 (mini-Tn7T-Gm- <i>bpeT'</i> - <i>lacZ</i> IR 5'Δ188)	This study
Bp82.336	82.284::pPS3147( mini-Tn7T-Gm- <i>bpeT'</i> - <i>lacZ</i> IR 5'Δ115)	This Study
Bp82.337	82.284::pPS3148 (mini-Tn7T-Gm- <i>bpeT'</i> - <i>lacZ</i> IR 5'Δ165)	This Study
Bp82.338	82.284::pPS3149 (mini-Tn7T-Gm- <i>bpeT'</i> - <i>lacZ</i> IR 5' +19)	This Study
Bp82.339	Bp82.285::pPS1453(mini-Tn7T-Gm- <i>lacZ</i> )	This Study

Bp82.340	Bp82.285::pPS2976(mini-Tn7T-Gm- <i>bpeE'</i> - <i>lacZ</i> entire IR)	This Study
Bp82.341	Bp82.285::pPS3081(mini-Tn7T-Gm- <i>bpeE'</i> - <i>lacZ</i> IR 5'Δ88)	This Study
Bp82.342	Bp82.285::pPS3082(mini-Tn7T-Gm- <i>bpeE'</i> - <i>lacZ</i> Δ112)	This Study
Bp82.343	Bp82.285::pPS3083(mini-Tn7T-Gm- <i>bpeE'</i> - <i>lacZ</i> IR 5'Δ142)	This Study
Bp82.344	Bp82.285::pPS3121(mini-Tn7T-Gm- <i>bpeE'</i> - <i>lacZ</i> IR 5' Δ126)	This Study
Bp82.345	Bp82.285::pPS3122 (mini-Tn7T-Gm- <i>bpeE'</i> - <i>lacZ</i> IR 5'Δ188)	This Study
Bp82.346	Bp82.285::pPS3146 (mini-Tn7T-Gm- <i>bpeT'</i> - <i>lacZ</i> IR 5'Δ188)	This Study
Bp82.347	Bp82.285::pPS3147( mini-Tn7T-Gm- <i>bpeT'</i> - <i>lacZ</i> IR 5'Δ115)	This Study
Bp82.348	Bp82.285::pPS3148 (mini-Tn7T-Gm- <i>bpeT'</i> - <i>lacZ</i> IR 5'Δ165)	This Study
Bp82.349	Bp82.285::pPS3149 (mini-Tn7T-Gm- <i>bpeT'</i> - <i>lacZ</i> IR 5'Δ+19)	This Study
Bp82.350	Bp82.285::pPS3150 (mini-Tn7T-Gm- <i>bpeT'</i> - <i>lacZ</i> IR 5'Δ82)	This Study
Bp82.351	Bp82.284::pPS3082 (mini-Tn7T-Gm- <i>bpeE'</i> - <i>lacZ</i> IR 5' Δ112)	This Study

### 3.1.4 Marker removal using the Flp-*FRT* system

Flp recombinase target (*FRT*) flanked antibiotic resistance genes were removed from the chromosome using the pFLP system developed by previous members of the Schweizer lab.<sup>8</sup> One ml of overnight cultures was prepared for electroporation by washing with 300 mM sucrose. To remove zeocin markers, 100 ng of pFLPe3 (**Table 3.1.C**) was added to 100 μl of resuspended cells and electroporation was performed as previously described. The cells were recovered for 1 h in LB broth with 80 μg/ml adenine before being plated on LB + adenine agar with 35 or 1000 μg/ml kanamycin, and 0.2% rhamnose to induce Flp recombinase gene expression, then incubated at 37°C. Colonies were later struck for isolation on media lacking rhamnose, and incubated at 42°C for 72 h. The resulting colonies were patched on media containing no antibiotic, kanamycin at the selective concentration for the respective strain, or only the selective

concentration of zeocin. Clones that did not grow on either antibiotic were considered markerless, and were frozen at -80°C in LB medium containing 20% glycerol for further analysis. An similar scheme utilizing zeocin selection was executed using pFLPe2 (**Table 3.1.C**) to remove *FRT* flanked kanamycin genes.

### **3.1.5 Construction of pUC18-mini-Tn7T-*lacZ* reporter fusion plasmids**

Fragments of varying sizes of the *bpeT-llpE* intergenic region were amplified by PCR using primers listed in **Table 3.1.A**. These amplicons were TA cloned into pGEM-TEasy and sequenced. The inserts were excised by *Hind*III and *Kpn*I digestion and ligated into either pTZ120 or pUC18T-mini-Tn7T-Gm-*lacZ* (**Table 3.1.C**) digested with the same enzymes. pTZ120 vectors were then digested with *Dra*III and *Hind*III and the resulting fragments were ligated between the *Dra*III and *Hind*III sites of pUC18T-mini-Tn7T-Gm-*lacZ*. After confirming the presence of the correct sequences, the mini-Tn7-*lacZ* vectors containing either the 5' deletion fragments, or the wild-type intergenic region (WT-IR) and the mini-Tn7-*lacZ* empty vector control were introduced into either virulent Bp282, or excluded strains Bp82<sub>P28S</sub> or Bp82<sub>K267T</sub> by electroporation along with helper plasmid pTNS3. Transformants were selected on LB-Lennox with or without 80 µg/ml adenine and 15 µg/ml (efflux deficient) or 500 µg/ml Gm (efflux proficient), and 50 µg/ml of X-Gal. Transformants that appeared gentamicin resistant and blue contained the mini-Tn7-*lacZ* element inserted at one of three *glmS* associated *att*Tn7 sites. Insertion at these sites was verified by PCR with primers 479, 1509, 1510 and 1511 as described previously.<sup>11</sup> Only isolates with a single *glmS* insertion were utilized in further studies (**Table 3.1.E**).

### 3.1.6 $\beta$ -galactosidase transcriptional activity assay for start site analysis

The use of  $\beta$ -galactosidase to identify promoter regions was first described by Miller and was adapted for use with *Bp*.<sup>13,14</sup> 1026b or Bp82 cells harboring the mini-Tn7-*lacZ* fused to a 5' segment of the the *llpE-bpeEF-oprC* operon or an empty vector control were cultured overnight. These cultures were then diluted 1:100 in fresh LB with or without adenine to an OD<sub>600</sub> of 0.6-0.8. Fifty-100  $\mu$ l of cells were then pelleted and resuspended in Z buffer (60 mM Na<sub>2</sub>HPO<sub>4</sub> • 7H<sub>2</sub>O, 40 mM NaHPO<sub>4</sub> • H<sub>2</sub>O, 10 mM KCl, 1 mM MgSO<sub>4</sub> • 7H<sub>2</sub>O) and 0.3%  $\beta$ -mercaptoethanol. Cells were lysed by the addition of chloroform and SDS to a final concentration of 2% and 0.2%, respectively, and vortexed for 30 s. 200  $\mu$ l of 4 mg/ml *o*-nitrophenyl- $\beta$ -D-galactopyranoside (ONPG) was added at time zero. The reaction was allowed to continue until a uniform yellow color was observed, then was stopped by the addition of 250  $\mu$ l of 1 M Na<sub>2</sub>CO<sub>3</sub> and the time was recorded. The absorbance at 470 nm was then measured for each sample.  $\beta$ -galactosidase activity in Miller units was determined using the formula:  $1000 \times \frac{A_{420 \text{ nm}}}{T \times V \times A_{600 \text{ nm}}}$ , where T= time and V= volume of cell culture assayed. The transcriptional activity of each sample was normalized to the baseline activity produced by both the background strain and again by the  $\beta$ -galactosidase activity produced by the strain harboring an empty mini-Tn7-*lacZ* element. One-way ANOVA with Dunnet's post test were performed for each sample against the full length control using GraphPad Prism V6 to identify significant loss of transcriptional activity.

### 3.1.7 RNA extraction

Overnight cultures of the strains of interest were used to subculture fresh media at a dilution of 1:100. Cultures were incubated at 37°C with shaking at 250 RPM until they reached an OD<sub>600nm</sub> =0.6-0.8. RNA extraction was carried out using the RNeasy RNA protect mini kit

(Qiagen, Germantown, MD) following manufacturers guidelines, with the addition of a 10 min room temperature incubation with 3 mg/ml lysozyme and vortexing. Samples were recovered in 30  $\mu$ l of sterile, RNase-free water, quantified and stored at -80°C until further use.

### **3.1.8 Fluorescent primer extension**

The procedure for fluorescently linked oligo extension was adapted from Hirakawa et al, in studies of *Rhodopseudomonas palustris*.<sup>15,16</sup> Briefly, total RNA was extracted from 1 ml of log phase cells using the RNeasy RNA protect mini kit as described above. Up to 10  $\mu$ g of RNA was treated with DNaseI (Invitrogen, Carlsbad, CA) following the manufacturer's protocol. An HPLC purified 6-FAM labeled reverse primer (2627, 2475 or 2744, **Table 3.1.B**) was added to a final concentration of 10 pg, and the mixture was hybridized at 58°C for 20 min. cDNA was generated from the hybridized mixture by Superscript III (Invitrogen, Carlsbad, CA) omitting random hexamers, followed by RNase H (Invitrogen, Carlsbad, CA) treatment to remove RNA/rRNA. Samples were purified on a PCR clean up column (Zymo Research, Irvine, CA), and concentrations were assessed via absorption at 260 nm on a Nano-drop (Thermo Scientific, Waltham, MA). Sample analysis was conducted at the Colorado State University proteomics and metabolomics facility on an ABI-3130xl genetic analyzer by capillary gel electrophoresis using a Liz-120 sizing standard (ABI, Waltham, MA). Later replicates were completed at the University of Florida ICBR genotyping core, on an ABI 3730Xl against a Liz600 standard. Peak analysis was performed using ABI Peakscanner software V.2.0 (ABI, Waltham, MA).

### **3.1.9 S1 Nuclease protection assay**

S1 nuclease protection assays were adapted from protocols found in Hirakawa's investigations of *Rhodopseudomonas* species.<sup>15,16</sup> To identify putative transcript start sites for both *bpeT* and the *llpe-bpeEF-oprC* operon, three probes were PCR amplified with a

fluorescently tagged oligo in the 5' sense (**Table 3.1.B**). Oligos 2474, 2475, 2627 and 2656 were designed to bind within either *llpE* or *bpeT*, and used in combination with an untagged forward primer binding 200-400 base pairs upstream (primers 2394 or 2476). The size of the probe was confirmed by gel electrophoresis, and amplicons were purified using the Zymo Clean and Concentrate kit (Irvine, CA). The purified probes were then diluted to a working concentration of 0.02 picomoles per  $\mu$ l. Five to 10  $\mu$ g of total RNA from Bp82 mutants expressing either BpeT<sub>S280P</sub>, or BpeS<sub>K267T/P28S</sub> was warmed to 55°C with 2x RNA hybridization buffer (38mM HEPES-pH 7.4, 300mM NaCl, 1mM EDTA, 0.01% Triton X-100) in a total volume of 45 $\mu$ l. A total of 100 nMoles of fluorescent probe was denatured at 95°C for 10 min before being quenched on ice, and then added to the pre-warmed total RNA hybridization buffer sample. This mixture was incubated at 55°C for 16-20 h before the addition of 10x S1 nuclease buffer, 100 units of S1 nuclease (Thermo Scientific, Waltham, MA) and water to a total volume of 400  $\mu$ l. The S1 nuclease digestion was incubated at 37 °C for an additional 30 min before the samples were purified by PCR purification column (Zymo Research, Irvine, CA), and eluted in 12  $\mu$ l of TE buffer. All incubation steps occurred in the dark to preserve probe fluorescence. Samples were submitted to the University of Florida genotyping core for fragment analysis on an ABI 3137 xl Biotyper in comparison to a LIZ or ROX 600 standard. Subsequent electropherograms were analyzed with ABI Peak Scanner software V.2.0 to identify changes in fragment size.

### 3.1.10 Protein expression and purification

The *bpeT* or *bpeS* coding sequences were PCR amplified from genomic DNA of Bp82, Bp82.270 or plasmids pPS3189 or 3190 using primer pairs 2536 and 2537 or 2849 and 2850 listed in **Table 4.1.A**. The 3' primers were designed to remove the stop codon of each gene and form in-frame hexahistidine fusions of *bpeT* or *bpeS* when cloned into pET-21b. Amplicons

consisting of the ~1 kb *bpeT* or *bpeS* region were purified from a 1% agarose gel using a GenElute kit (Sigma Aldrich, St. Louis, MO) and later TA cloned into pGEM-TEasy (Promega, Madison, WI) following the manufacturers protocol. The *bpeT* constructs were immediately confirmed by DNA sequencing, then ligated with T4 DNA ligase (Invitrogen, Waltham, MA) into dephosphorylated pET-21b digested with *HindIII+NdeI* to create plasmids pPS3069 and pPS3253 (**Table 4.1.D**). The *bpeS* fragments were sub-cloned into pGEM-TEasy to create plasmids pPS3258-pPS3250. Insertions were confirmed by *EcoRI* and *HindIII+NdeI* digestion and DNA sequencing to confirm the mutation of the stop codon. The ~1kb *bpeS* fragment was excised from pGEM-TEasy by *EcoRI+NdeI* digest and ligated with T4 DNA ligase into the dephosphorylated *NdeI+EcoRI* digested pET21b fragment. Ligation reactions were incubated at 14°C overnight, then transformed into chemically competent DH5 $\alpha$  or NEB5 $\alpha$  cells. After transformant recovery and confirmation by DNA sequencing, correct constructs were transformed into strain BL21(DE3) or BL21(DE3)-RP cells to identify high expression clones.

Briefly, freshly transformed clones were picked from LB + 100  $\mu$ g/ml amp plates and inoculated into 5 ml of LB broth with 100  $\mu$ g/ml ampicillin or 100  $\mu$ g/ml amp + 34  $\mu$ g/ml chloramphenicol for BL21(DE3) or BL21(DE3)-RP expression strains, respectively. Cultures were incubated to OD<sub>600 nm</sub> = 0.6 before being split into two tubes. Isopropyl- $\beta$ -D-galactopyranoside (IPTG) was added to a final concentration of 1 mM to one sample of each pair, and all were replaced in the 37°C shaking incubator. Cells were incubated for a further 1-2 h before being pelleted and re-suspended in 10  $\mu$ l of sterile water. 2x Laemmli buffer (4% SDS, 20% glycerol, 120 mM Tris-HCL pH6.8, 0.02% bromophenol blue) with 0.5% beta-mercaptoethanol was added to 1x final concentration. Each sample was boiled for 10 min before 8  $\mu$  samples were loaded onto a 1% SDS-PAGE gel, and run for approximately 1h at 120-130V.

Clones that produced the highest levels of the 35-37 kD BpeT or BpeS proteins in induced samples were grown for storage as protein expression clones.

Protein purification was scaled to 150-500 ml cultures using these isolates. All samples were induced by the addition of 1 mM to 5 mM IPTG starting at  $OD_{600nm}=0.8-1.0$  for up to 4 h or an OD of 1.5-2.0. Cells were harvested and proteins were extracted using an adapted protocol first developed elsewhere.<sup>17</sup> Cell pellets underwent one freeze-thaw before being resuspended in PCL buffer (8 mM  $Na_2HPO_4$ , 286 mM NaCl, 1.4 mM  $KH_2PO_4$ , 2.6 mM KCl, 1% SDS and 0.1% Sarkosyl) and incubated at RT for 30 min. Lysates were then sonicated at 30% amplitude with 1-2 second pulses at RT with care to prevent foaming. Sonication-cleared lysates were then either placed at 4°C overnight, or chilled in an ice bath for 1-2 h to “cold-crash” the SDS present in buffer PCL. The lysates were then re-pelleted, and the cleared lysate was applied to a column packed with Ni NTA (ThermoFisher, Waltham, MA) slurry and equilibrated with 10 bed volumes of buffer PCW (PCL without SDS). Flow-through was collected and the column was washed with 10-15 bed volumes of PCW with 10 mM imidazole. BpeS or BpeT was eluted off the column in fractions of PCW + 40-100 mM imidazole. These fractions were analyzed by SDS-PAGE. Fractions with the highest concentrations of the proteins of interest were combined, and dialyzed against 175 mM Tris-HCL pH 7.2 or PBS (137 mM NaCl, 2.7 mM KCl, 8 mM  $Na_2HPO_4$  and 2 mM  $KH_2PO_4$  pH 7.4) overnight at 4°C with multiple buffer changes. Protein sample concentrations were measured using a BCA assay Kit (Thermo-Pierce, Rockford, IL) and averaged a concentration of 1-2 mg/ml. Glycerol was added to samples to a final concentration of 20% and samples were stored at -80°C until further use.

### 3.1.11 Electrophoretic mobility shift assays

Electrophoretic mobility shift assay (EMSA) was used to assess binding of BpeT and BpeS to sites within the *bpeT-llpE* intergenic region. In an effort to avoid the use of radioactivity for probe visualization, a fluorescent staining method was utilized. Probe segments of the intergenic region were PCR amplified, both full length or from varying regions within the putative promoter sequences (primers 2394, 2476, 2923-2942, **Table 3.1.A**). These were excised and purified from a 1% agarose gel using a Gen-Elute kit (Sigma-Aldrich, St. Louis, MO) following the manufacturers protocol.

2x binding buffer (375 mM KCl, 100 mM Tris pH 8.5, 10 mM DTT, 10 mM MgCl<sub>2</sub>, 2 mM EDTA, 10 % glycerol) was mixed with 10-100 ng of probe DNA, 30 µg/µl BSA and 1.25 ng/µl of poly(dI:dC) (ThermoFisher, Waltham, MA). Varying amounts of protein and water were added to a final volume of 20 µl. Reactions were incubated at RT for 20 min. An empty 5% TBE PAGE gel (Bio-Rad, Hercules, CA) was run at 100V in 1X TBE for 1 hour prior to the start of incubation after having its wells rinsed with TBE buffer. Samples were loaded onto the gel, with a lane reserved for 10 µl of 1X DNA loading dye (30% glycerol, 0.25% bromophenol blue) alone. The gel was run at 120-130V for approximately 1.5 h and stained with SYBR Gold (Molecular Probes, Eugene, OR) before visualization on a Bio-Rad Chemidoc (Hercules, CA). The procedure was repeated after determining the concentration of recombinant protein to produce a shift in comparison to the control reaction lacking protein (from 20-100 µM). Probes of varying sequences were interrogated using the same protocol to identify a binding site.

## 3.2 Results and Discussion

### 3.2.1 The *bpeT-llpeE* intergenic region contains the promoter regions necessary for transcription of *llpeE-bpeEF-oprC* and *bpeT*

Successive 5' deletions of the intergenic region with constant 3' ends in the *bpeE* gene for *llpe-bpeE'-lacZ* fusions, or in *bpeT* for *bpeT'-lacZ* fusions were constructed and fused to a promoter-less *lacZ* gene harbored on a mini-Tn7 vector. **Fig. 3.2.1** summarizes the regions of DNA deleted from the individual *bpeE'-lacZ* and *bpeT'-lacZ* constructs. The resulting fusion constructs were integrated into the chromosome of Bp282 at a single *glmS2* associated *attTn7* site. Bp282 is a Bp 1026b derivative which contains a serine to proline change at amino acid 280 causing constitutive overexpression of the *llpe-bpeEF-oprC* operon. The strains containing the chromosomally integrated *lacZ* fusions (**Fig. 3.2.1**) were tested by  $\beta$ -galactosidase assays to assess the relative levels of transcription of either *bpeT* or the *llpe-bpeEF-oprC* operon in the presence or absence of different portions of intergenic sequence (**Fig. 3.2.2**). When analyzing *bpeE'-lacZ* fusions, complete loss of activity was observed for constructs lacking base pairs after nucleotide 53 of the IR using the first base after the start codon of *bpeT* as position 1.

Comparisons to the full length control showed that all deletions lacking more than the first 53 base pairs had transcriptional activity indistinguishable from the strain carrying none of the IR. This would suggest the promoter region for the *llpe-bpeEF-oprC* transcription unit is located within the sequence spanning IR basepairs 54-88, 5'. However, investigations to pinpoint the promoter for *bpeT* were less successful. There was no significant loss of activity in any strain except the complete IR deletion. This may be complicated by the presence of a secondary regulator and the fact that BpeT, as a LysR family protein, is regulating its own expression (Mima and Schweizer, unpublished observations).

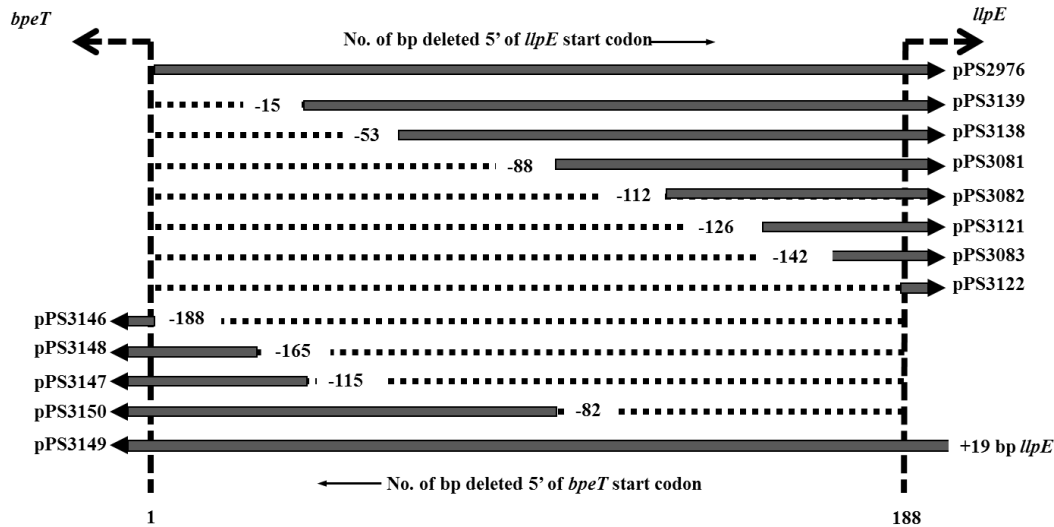


**Figure 3.2.1. Summary of 5' deletion constructs created for analysis of the *bpeT-llpE-bpeEF-oprC* intergenic region.** Black bars represent remaining sequences in *bpeE'-lacZ* fusions (upper part of figure) and *bpeT'-lacZ*, while the numbers immediately preceding each bar dictate the total nucleotides deleted from the 5' end of each IR fragment. Arrows indicate translational start codons preceding position 1 and 188 of the IR sequence. pPS numbers indicate plasmid designations, and all constructs are listed in more detail in **Table 4.1.C**.

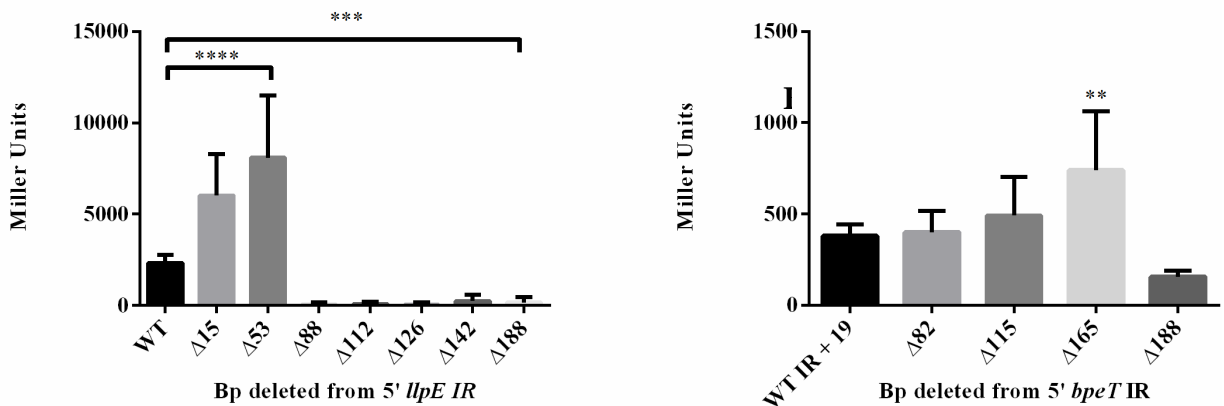


**Figure 3.2.2. Identification of promoter regions within the *bpeT-llpE* intergenic region.** Expression in all strains was normalized to an empty vector *lacZ* reporter integrant strain, and compared to a wild-type control consisting of the full 188 bp IR fused to *lacZ* to identify either *bpeT* or *llpE-bpeEF-oprC* promoter regions. Data is shown as means of two biological replicates in technical triplicate, with error bars representing one standard deviation. Statistical analysis was performed by One way ANOVA with Tukey's multiple comparison test to compare all samples to each other.

**A. Strains with *bpeE'-lacZ* fusions.** Strains with inserts lacking base pairs 54-188 of the IR show no expression, while expression is retained in strains with possessing base pairs 15 to 53.

**B. Strains with *bpeT'-lacZ* fusions.** Only the construct lacking 165 base pairs 5' of the *bpeT* start codon expresses significant levels of  $\beta$ -galactosidase activity in comparison to the other *bpeT'-lacZ* fusion strains. \*\*\*\* =  $p < 0.0001$ , \*\*\* =  $p < 0.001$  \*\* =  $p < 0.01$ .

The tests were conducted in Bp282, to produce a detectable  $\beta$ -galactosidase signal, as this was not observed at basal levels of *bpeEF-oprC* expression. Bp282 BpeT<sub>S280P</sub> promotes constitutive overexpression of BpeEF-OprC without affecting the transcription of itself. Therefore, the chosen background strain, though necessary for study of the structural elements of the operon, may be ill suited for identifying regulatory mechanisms in control of itself.

To overcome this, the assay was repeated in select agent excluded strain Bp82 and its derivatives (**Fig. 3.2.3**). Previous observations noted that select BpeS mutation lead to a constitutive overexpression phenotype similar to that found in BpeT<sub>S280P</sub>. This occurs despite the fact that in one strain, the mutation affecting BpeS causes an amino acid change in the N-terminus of the protein. Using these mutant isolates, significant differences in  $\beta$ -galactosidase activity were observed between the construct containing the entire *bpeT-llpE* IR and strains

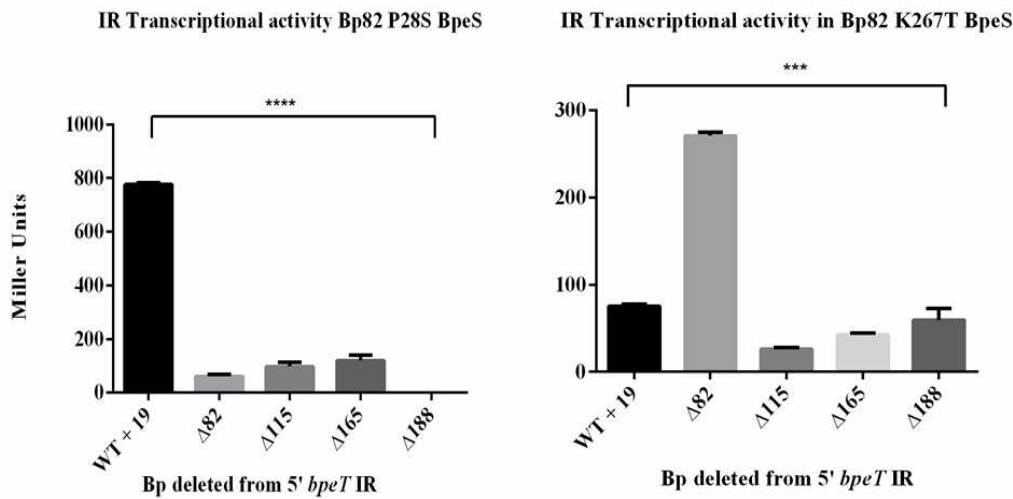


**Figure 3.2.3. Analysis mutant BpeS effects on *bpeT* transcription.**  $\beta$ -galactosidase expression was assessed in Bp82 strains expressing BpeS<sub>P28S</sub> (A) and BpeS<sub>K267T</sub> (B) and the indicated *bpeT-lacZ* fusion constructs. Activities in all strains were normalized to an empty vector *lacZ* reporter strain and compared to the WT control consisting of the full 188 bp intergenic region fused to *lacZ*. Data is shown as means of two biological replicates in technical triplicate, with error bars representing one standard deviation. Statistical analysis was performed by One Way ANOVA with Tukey's multiple comparison test to compare all samples. \*\*\*\*=  $p < .00001$ , \*\*\*=  $p < .001$

containing constructs with successive 5' IR deletions. In *bpeS*<sub>P28S</sub> derivatives, no strains except those containing the entire IR fusion expressed  $\beta$ -galactosidase, suggesting that the entire IR is necessary for transcription of the gene. But, in strains expressing BpeS<sub>K267T</sub>, an increase of  $\beta$ -galactosidase expression above that observed in the full length IR control isolate, and other 5' deletions, is observed after deletion of the 5' 82 base pairs. This may be caused by an artifact in the experimental method due to inherently altered transcription levels, and as such cannot be used to support a conclusive identification of a *bpeT* promoter region without further testing.

### **3.2.2 Transcriptional start sites for both *bpeT* and *llpE-bpeEF-oprC* are located within promoter regions of the IR identified by $\beta$ -galactosidase assays.**

Primer extension analysis with 5'6-FAM linked oligos was performed on cDNA (**Fig. 3.2.4**). A primer approximately 150 bp upstream of the translational start site of *bpeT* was used for detection of the *bpeT* transcript end. An oligo designed approximately 200 bp upstream of the *llpE* start codon was used for identification of the transcriptional start site of the *llpE-bpeEF-oprC* operon. Fragment sizing was performed through capillary electro-phoresis against either a Liz120 or Liz600 standard, with the lowest standard peak intensity used as a cut off for all experimental samples. Analysis of the resultant electropherograms of *bpeT* returned a peak at approximately 160 bp, correlating to position 45 of the intergenic region using the base immediately preceding the start codon of BpeT as base 1 (**Figs. 3.2.4 and 3.2.5**).

For analysis of the *llpE-bpeEF-oprC* region, peaks at approximately 50 bp were obtained (data not shown). This correlated to a position still within the coding region of *llpE*. Previous studies had shown that *llpE* is co-transcribed with the rest of the structural operon elements. This would suggest that the transcriptional start site for the *llpE* gene must be located within the IR, and that it is not a pseudogene containing regulatory sequence for the *bpeEF-oprC* alleles.





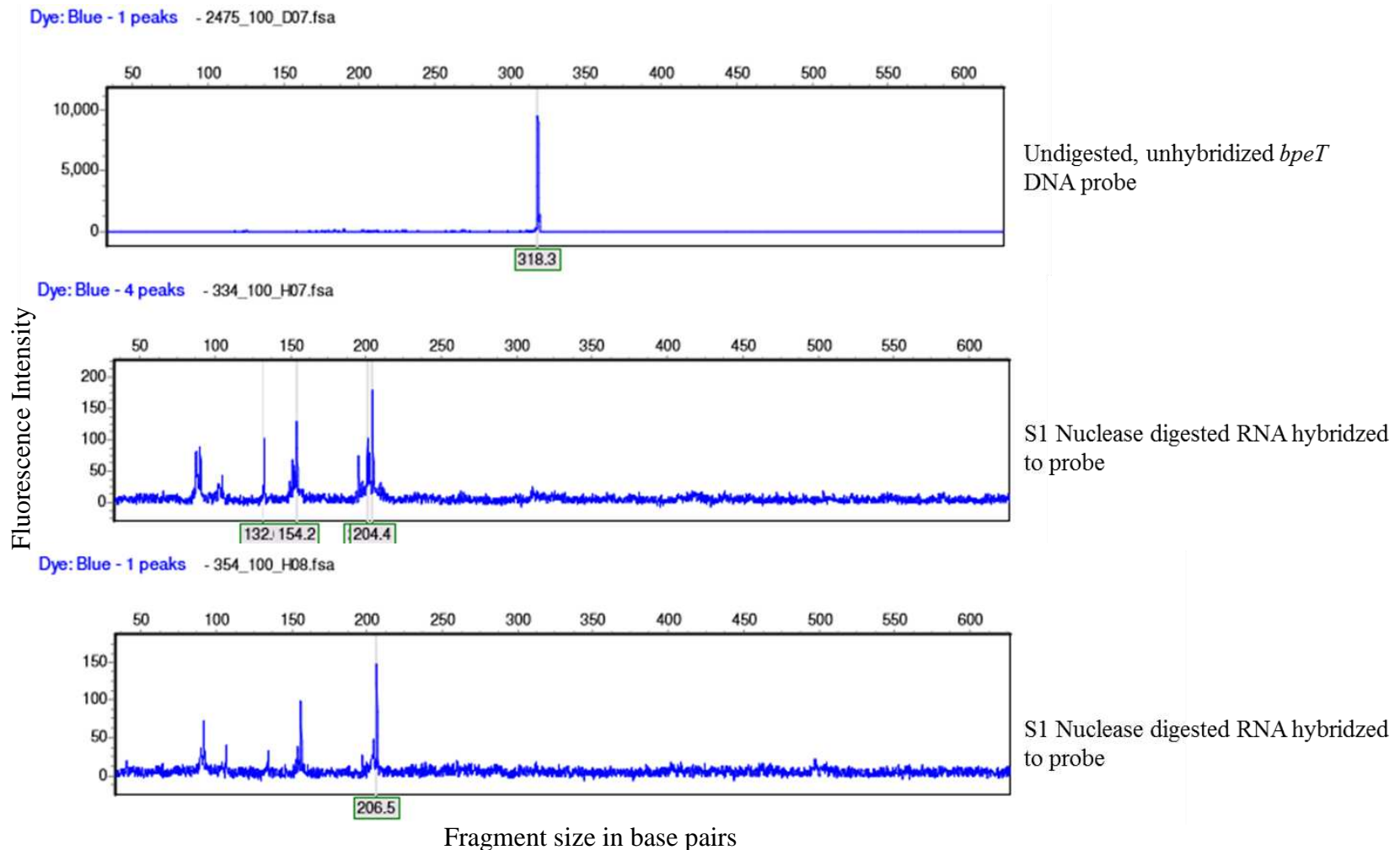


**Figure 3.2.6. S1 Nuclease protection assay identifies a putative 5' transcript end within the *bpeT-llpE* intergenic region**

Two replicates of the S1 nuclease assay returned a “protected” or RNA-DNA duplex fragments of approximately 204, 205 and 206 base pairs, ~113 base pairs shorter than the undigested control probe. This correlates to a 5' transcript end occurring anywhere from base pair 89-91 5' of the *bpeT* start codon.

Additional peaks seen in digested samples may represent RNA-DNA hybrid complexes that formed between partially decayed transcripts bound to full length probe. This would leave single stranded DNA “tails” that could later be digested by S1 nuclease to result in smaller detectable fragments. All attempts to investigate the *llpE* transcriptional start site were unsuccessful, as only peaks corresponding to the full length probe were obtained, suggesting that the hybridization process may not have occurred in these samples (data not shown).

### 3.2.4 BpeT and BpeS bind to the intergenic region between *bpeT* and *llpE-bpeEF-oprC*.

To locate binding sites of both BpeS and BpeT, DNA band shifts using the entire 188 base pair IR were performed using recombinant, wild type BpeT or BpeS. Experimental reactions with up to 40  $\mu$ M recombinant protein were compared to control reactions consisting of only binding buffer and a full length IR DNA probe. In comparison to the negative control, both BpeT and BpeS were able to retard DNA probe gel migration (band shift). This indicates the formation of a DNA- protein complex under similar conditions (Fig. 3.2.7). This observation was expected, as the two LysR family regulators share N-terminal homology suggesting that they

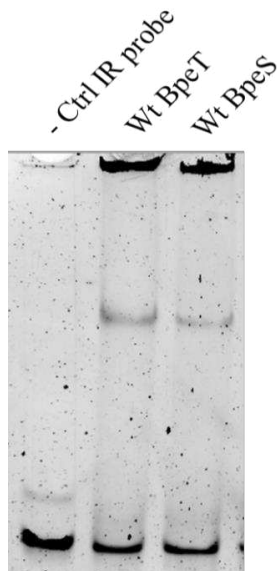


**Figure 3.2.7. Both BpeT and BpeS can bind the IR.**

A DNA probe containing the entire 188 bp IR sequence was incubated with purified recombinant BpeT or BpeS at a final concentration of approximately 40  $\mu$ M. A control sample was prepared with only probe DNA, and samples were stained with SYBR gold after electrophoresis. In both BpeT and BpeS reactions, a clear shift can be seen indicating that protein was capable of binding to the intergenic region.

may interact with a similar binding site. It is also not surprising that the reaction conditions were identical for both proteins. Extensive optimization was required for identification of the in-vitro binding conditions of BpeT, the first identified regulatory protein. It is possible that the high level of identity between BpeS and BpeT allowed both proteins to interact with their cognate binding region under identical in-vitro conditions.

### **3.2.5 BpeT and BpeS interact with the intergenic region at sites closely associated with promoter region and transcriptional start sites of *bpeT* and *llpE-bpeEF-oprC*.**

To locate exact binding regions for BpeT and BpeS, the same assay was repeated using DNA probes consisting of different segments of the IR. These were designed to correlate to 5' deletion sequences used to locate promoter regions of *bpeT* and *llpE-bpeEF-oprC*. BpeS or BpeT bound to full length IR probe was used as a positive control. In reactions containing BpeT (**Fig. 3.2.8, panel A**), the absence of a shift was observed in all probes lacking bp 74-88 of the IR despite a shifted positive control. This suggests BpeT preferentially binds to the 14 base pair sequence from bp 74-88. Interestingly, when the experiment was repeated using BpeS (**Fig. 3.2.8, panel B**), the same trend was observed. Taken together this suggests that not only do the proteins interact directly with the IR, but they bind in the same site located within the promoter region of both *bpeT* and *llpE-bpeEF-oprC* identified by 5' deletion assays. This site is flanked on either side by putative transcriptional start sites for the *bpeT* gene as identified by primer extension and S1 nuclease protection assays (**Fig. 3.2.9**).

To attempt to confirm these results by an alternate method, DNase1 foot-printing was performed using a protocol adapted for the use of fluorescently labeled DNA probes as previously described.<sup>18,19</sup> However, no detectable protected regions were identified in comparison to DNA samples in the absence of either BpeT or BpeS (data not shown).

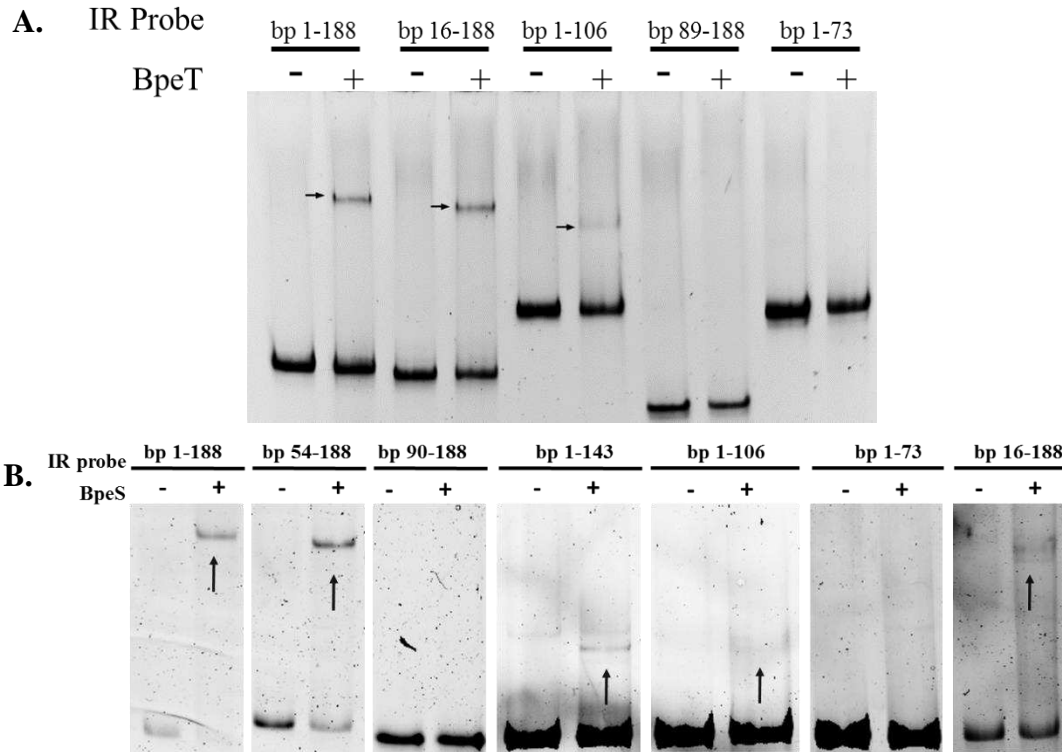


**Figure 3.2.8. BpeT and BpeS utilize the same or closely associated binding sites within the IR.** Recombinant BpeT (A.) and BpeS (B.) at final concentrations of approximately 2  $\mu$ M were incubated with different regions of the IR sequence to locate a potential binding site. Arrows indicate a detectable shift. No shift was detected in probes spanning base pairs 89-188, and 1-73 but was present in 1-106. This corresponds to a binding site located from base pair 74-88 of the *bpeT-llpE* intergenic sequence (Fig. 3.2.9).

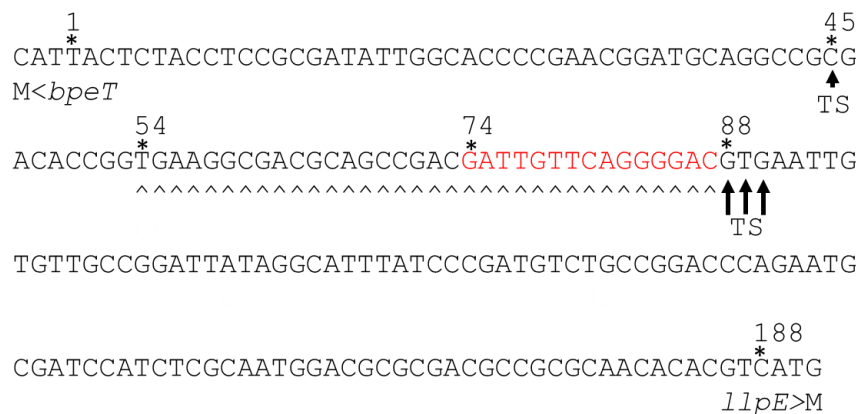


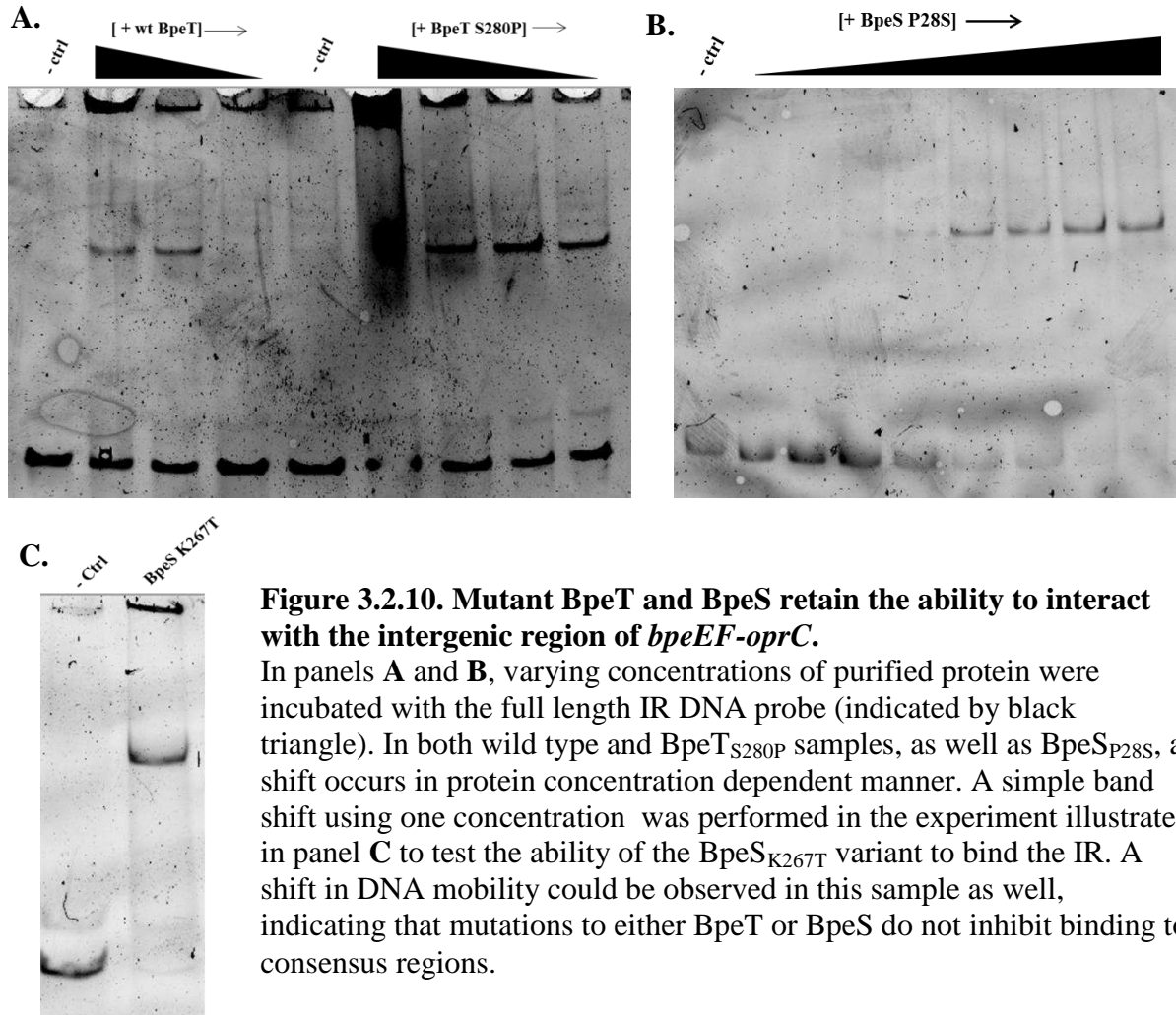
**Figure. 3.2.9 BpeT and BpeS share binding sequence located within the promoter regions of the intergenic sequence.** The binding region for BpeT and BpeS is located from nucleotide 75-89 (red letters), overlapping both the 5' transcript start sites of *bpeT* (black arrows at position 88-90), and the essential sequence for *llpE-bpeEF-oprC* transcription (open arrow heads). The *bpeT* transcript end identified by primer extension is marked by a black arrow at position 45. Numbers indicate IR position at black asterisks. The start codons of *bpeT* and *llpE* are indicated with a methionine (M).

The observation that this regulatory region may act as a shared promoter necessary for the auto-regulatory control of BpeT and inducible expression of *bpeEF-oprC* also poses questions of BpeS-BpeT interaction. LysR regulatory family proteins often interact with their binding regions by forming large complexes that may be either homomultimeric or heteromultimeric in response to environmental stimuli, and to alter the expression of their target operon.<sup>20</sup> To determine if either protein could still interact with its binding site in the absence of the other, lysates were extracted from Bp82 strains lacking either *bpeS*, *bpeT* or *bpeT* and *bpeS* and the shift assay was repeated using a full length IR probe generated with a 5'6-FAM linked oligo. After incubation and electrophoresis, the gel was imaged on a Typhoon Trio (GE Lifesciences, Little Chalfont, UK) to detect any changes in probe mobility, but the results remain inconclusive as no shift could be seen for any strains, not just those lacking either regulatory protein.

### **3.2.7 Mutations to BpeS and BpeT do not impede their ability to interact with the intergenic region.**

Our own observations have shown that mutations to the N or C terminus of both regulatory proteins cause constitutive overexpression of the BpeEF-OprC efflux pump, thereby causing elevated resistance to pump substrates. It was hypothesized that these mutations may affect the ability of the proteins to interact with their binding sites within the *bpeT-llpE* intergenic region, directly leading to altered pump expression and decreased susceptibility to antimicrobials. To assess if mutations altered the ability of the proteins to bind to the IR, gel shift assays were performed using purified recombinant BpeT<sub>S280P</sub>, BpeS<sub>P28S</sub> increasing from 17 nM to 40  $\mu$ M or 40  $\mu$ M BpeS<sub>K267T</sub> alone. All mutant forms of the protein retained their ability to bind the IR. Additionally, the addition of varying concentrations of protein produced a dose

dependent response for the two mutant forms tested. (Fig. 3.2.10). However, further study utilizing finer measurements of both probe and protein concentration is required to determine if the mutation causes an increase or decrease in the affinity of these interactions.



### 3.3 Conclusions

The 188 bp *bpeT-llpE* intergenic region located between *bpeT* and *llpE-bpeEF-oprC* contains the regulatory sequences necessary for control of BpeEF-OprC efflux pump expression. Based on a combination of EMSA, 5' successive deletion, and fluorescent primer extension and S1 nuclease protection assays, *cis* regulatory regions necessary for the control the operon were

identified. Interestingly, these regulatory sequences appear to be concentrated within an approximately 40 base pair region from bp 54-90 of the intergenic region, immediately upstream of a relatively AT rich sequence region. Both the *bpeT* predicted transcriptional start site identified through S1 nuclease assay, and the essential sequence identified for *llpE-bpeEF-oprC* transcription, overlap the 14 base pair sequence needed for both BpeS and BpeT binding (**Fig. 3.2.11**). The sequence fits the canonical T<sub>N11</sub>A composition identified as the LTTR box in studies of LysR proteins, and the high AT content of this particular IR region may promote the DNA bending function conserved by the LysR regulatory protein family.<sup>21,22</sup> However, BpeT or BpeS protein binding at this site may constitute only an auto-regulatory event. We were only able to identify a single binding region within the IR, as our attempts at DNaseI footprinting were

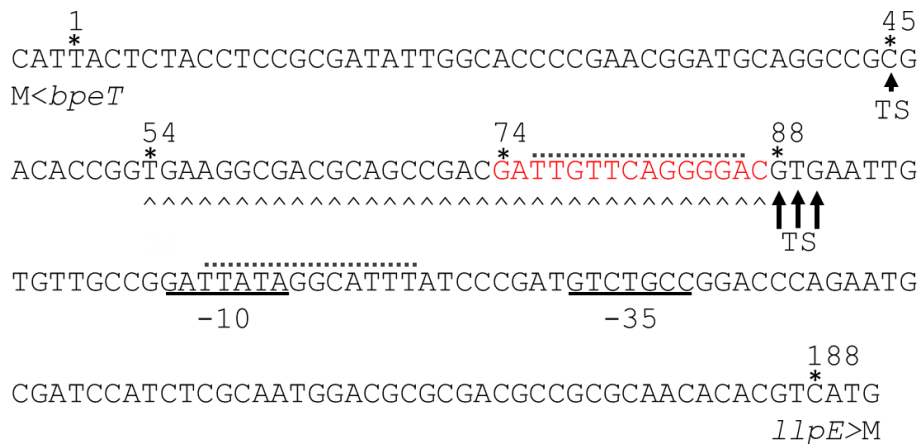


**Figure 3.2.11. Final summary of *cis* regulatory elements located within the *bpeT-llpE-bpeEF-oprC* intergenic sequence.** Numbers indicate IR position at black asterisks. Start codons of *bpeT* and *llpE* are indicated with a methionine (M). The binding region for BpeT and BpeS is located from nucleotide 75-89 (red letters), overlapping both the 5' transcript start sites of *bpeT* (black arrows at position 88-90), and the essential sequence for *llpE-bpeEF-oprC* transcription (open arrows). The *bpeT* transcript end identified by primer extension is marked by a black arrow at position 45. Based on the position of the S1 5' transcript end, binding sites and essential sequences, putative -10 and -35 regions were identified (black lines). A putative T<sub>N11</sub>A LTTR box (stippled black line) is marked within the BpeS and BpeT binding site. A second LTTR box motif be located within the putative -10 region and extend into the next ATTTA sequence immediately upstream.

unsuccessful. Proteins in this family typically protect large regions of DNA and have multiple binding sites within a promoter region. Based on interaction with the co-inducer molecule, these regulators show different affinities for either the auto-regulatory site needed to repress their own transcription, or the activation site needed to induce transcription of their target operon.<sup>21,22</sup> The identification of a single binding region could be caused by use of only the apo form of BpeT and BpeS, possibly incapable of interacting with any other site. This would correspond to the close association of the identified binding site to cis regulatory elements of *bpeT* regulation.

That being said, the IR region contains an additional T<sub>N11</sub>A sequence upstream of the identified binding site and within a putative *bpeT* -10 region. Under co-inducer binding conditions, this region may interact with either BpeS or BpeT. It is also interesting to note the overlap of the *llpE-bpeEF-oprC* essential sequence identified through 5' deletion studies and the binding sites of BpeS and BpeT. This sequence may contain a putative -35 region for transcription of *llpE-bpeEF-oprC* and as such, would explain both the overlap of BpeT-BpeS binding sites, and loss of transcriptional activity caused by its absence.

This study represents the initial identification regulatory sequences needed for transcription of *bpeEF-oprC* in response to yet unknown external stimuli, a process catalyzed by interaction with the LysR-type regulatory proteins BpeS and BpeT. The identification of these regions allows us a better understanding of the mechanisms in play during the generation of multi-drug resistant phenotype. It is interesting to note that both BpeT and BpeS utilize the same or overlapping binding regions, most likely due to their high degree of amino acid identity at the N-terminus. It is tempting to suggest that one gene or the other is a product of duplication or rearrangement through self-recombination or a transposition event. As a result, the fact that two different regulatory genes are capable of controlling the same gene and operon may point to the

efflux pump's ability to respond to stimuli other than only antimicrobial compounds.<sup>23,24</sup>

Hypothetically, different substrate specificities between the two proteins may allow greater transcriptional plasticity in response to altered environmental conditions. This in turn suggests that control of the operon is much more complex than previously believed and may be part of a larger network of systems necessary for maintaining cell homeostasis. Further study is needed to characterize the entire regulatory cascade in control of the efflux pump, in addition to identifying external stimuli that trigger its expression.

### Chapter 3 References

1. Podnecky, N. L., Rhodes, K. A. & Schweizer, H. P. Efflux pump-mediated drug resistance in *Burkholderia*. *Front. Microbiol.* **06**, 305 (2015).
2. Dance, D. Treatment and prophylaxis of melioidosis. *Int. J. Antimicrob. Agents* **43**, 310–318 (2014).
3. Chaowagul, W. *et al.* Open-label randomized trial of oral trimethoprim-sulfamethoxazole, doxycycline, and chloramphenicol compared with trimethoprim-sulfamethoxazole and doxycycline for maintenance therapy of melioidosis. *Antimicrob. Agents Chemother.* **49**, 4020–4025 (2005).
4. Dance, D. A., Wuthiekanun, V., Chaowagul, W. & White, N. J. The antimicrobial susceptibility of *Pseudomonas pseudomallei*. Emergence of resistance in vitro and during treatment. *J. Antimicrob. Chemother.* **24**, 295–309 (1989).
5. Podnecky, N. L., Wuthiekanun, V., Peacock, S. J. & Schweizer, H. P. The BpeEF-OprC efflux pump is responsible for widespread trimethoprim resistance in clinical and environmental *Burkholderia pseudomallei* isolates. *Antimicrob. Agents Chemother.* **57** 4381-4386 (2013).  
doi:10.1128/AAC.00660-13
6. Biot, F. V. *et al.* involvement of the efflux pumps in chloramphenicol selected strains of *burkholderia thailandensis*: proteomic and mechanistic evidence. *PLoS ONE* **6**, e16892 (2011).
7. Biot, F. V. *et al.* Interplay between three RND efflux pumps in doxycycline-selected strains of *Burkholderia thailandensis*. *PLoS ONE* **8**, e84068 (2013).
8. Choi, K.-H. *et al.* Genetic tools for Select-Agent-compliant manipulation of *Burkholderia pseudomallei*. *Appl. Environ. Microbiol.* **74**, 1064–1075 (2008).

9. Lopez, C. M., Rholl, D. A., Trunck, L. A. & Schweizer, H. P. Versatile dual-technology system for markerless allele replacement in *Burkholderia pseudomallei*. *Appl. Environ. Microbiol.* **75**, 6496–6503 (2009).
10. Chuanchuen, R. & Schweizer, H. P. Small broad-host-range lacZ operon fusion vector with low background activity. *BioTechniques* **31**, 1258–1262 (2001).
11. Choi, K.-H. *et al.* A Tn7-based broad-range bacterial cloning and expression system. *Nat. Methods* **2**, 443–448 (2005).
12. Liss, L. New M13 host: DH5F' competent cells. *Focus* **9**, (1987).
13. Casadaban, M.J., Chou, J. & Cohen, S. N. In vitro gene fusions that join an enzymatically active beta-galactosidase segment to amino-terminal fragments of exogenous proteins: *Escherichia coli* plasmid cloning of translational initiation signals. *J. Bacteriol.* **143**, 971–980 (1980).
14. Miller, J. H. *Experiments in Molecular Genetics*. (Cold Spring Harbor Laboratory Press, 1972).
15. Hirakawa, H., Schaefer, A. L., Greenberg, E. P. & Harwood, C. S. Anaerobic p-coumarate degradation by *Rhodopseudomonas palustris* and identification of CouR, a MarR Repressor protein that binds p-coumaroyl coenzyme A. *J. Bacteriol.* **194**, 1960–1967 (2012).
16. Hirakawa, H. *et al.* Activity of the *Rhodopseudomonas palustris* p-coumaroyl-homoserine lactone-responsive transcription factor RpaR. *J. Bacteriol.* **193**, 2598–2607 (2011).
17. Schlager, B., Straessle, A. & Hafen, E. Use of anionic denaturing detergents to purify insoluble proteins after overexpression. *BMC Biotechnol.* **12**, 95 (2012).
18. Wilson, D. O., Johnson, P. & McCord, B. R. Nonradiochemical DNase I footprinting by capillary electrophoresis. *Electrophoresis* **22**, 1979–1986 (2001).

19. Zianni, M., Tessanne, K., Merighi, M., Laguna, R. & Tabita, F. Identification of the DNA bases of a DNaseI Footprint by the use of dye primer sequencing on an automated capillary DNA analysis instrument. *J. Biomol. Tech.* **17**, 103–113 (April).
20. Knapp, G. S. & Hu, J. C. Specificity of the *E. coli* LysR-Type transcriptional Regulators. *PLoS ONE* **5**, e15189 (2010).
21. Maddocks, S. E. & Oyston, P. C. F. Structure and function of the LysR-type transcriptional regulator (LTTR) family proteins. *Microbiology* **154**, 3609–3623 (2008).
22. Schell, M. A. Molecular biology of the LysR family of transcriptional regulators. *Annu. Rev. Microbiol.* **47**, 597–626 (1993).
23. Blair, J. M. & Piddock, L. J. Structure, function and inhibition of RND efflux pumps in Gram-negative bacteria: an update. *Curr. Opin. Microbiol.* **12**, 512–519 (2009).
24. Piddock, L. J. V. Multidrug-resistance efflux pumps - not just for resistance. *Nat. Rev. Microbiol.* **4**, 629–636 (2006).
25. Mima, T. & Schweizer, H. P. The BpeAB-OprB efflux pump of *Burkholderia pseudomallei* 1026b does not play a role in quorum sensing, virulence factor production, or extrusion of aminoglycosides but is a broad-spectrum drug efflux system. *Antimicrob. Agents Chemother.* **54**, 3113–3120 (2010).

## Chapter 4: Regulatory functions of BpeS and BpeT

### Summary

The goal of Aim II part I is to address the contributions of both BpeS and BpeT to control of BpeEF-oprC at a local level by characterization of the regulators themselves. Part II interrogates the effects of BpeS and BpeT on the transcriptional landscape of *Bp* as a whole. The purpose of these investigations was to increase understanding of the relationship between RND mediated efflux and cell adaptation in an effort to better predict the potential clinical outcomes caused by mutations to these regulatory genes. We hypothesized that increased BpeEF-OprC expression was the result of changes to the structure of BpeS and BpeT, affecting both DNA binding capability and co-inducer dependence, and that BpeS is a global regulatory factor capable of influencing operons other than *bpeEF-oprC*. Through a variety of molecular and bioinformatic analyses, we established the possibility of an additional regulatory factor in control of BpeEF-OprC expression, the global regulatory function of BpeS, and investigated the effect of mutations on the structure and function of both BpeT and BpeS.

### Introduction

The BpeEF-OprC efflux system is the most significant RND family pump expressed by *Bp* based on its ability to cause decreased susceptibility to first line eradication phase therapy of melioidosis.<sup>1</sup> Two LysR-type proteins, BpeT and BpeS, are known to be involved in regulation of the pump, but little is understood of the exact mechanism by which this occurs.<sup>2</sup> A survey of co-trimoxazole resistant *Bp* clinical isolates identified mutations in a gene encoding a BpeT ortholog, BpeS, as a potential cause of elevated efflux pump expression. These mutations were similar to those found in BSL-2 laboratory selected, co-trimoxazole resistant Bp82 mutant

derivatives, and were confirmed in both instances to cause elevated expression of the BpeEF-OprC efflux pump, and decreased susceptibility to co-trimoxazole. Similarly, mutations affecting the carboxy-terminal amino acid sequences of BpeT cause increased expression of BpeEF-OprC, but only result in decreased susceptibility to trimethoprim.<sup>1</sup> While this evidence shows that a direct correlation exists between LysR regulatory mutations and overproduction of the efflux pump, the function of these proteins, and how the structure-function relationship disrupted by mutations results in altered antimicrobial susceptibility phenotypes, remains unknown.

Additionally, no investigations into any global effects of dysregulated expression of BpeEF-OprC have yet been conducted. The fact that BpeS is encoded on a chromosome 1, while its *bpeEF-oprC* target operon is encoded on chromosome 2, suggests that BpeS may have an additional role, potentially acting on multiple operons or in concert with many factors. While the identification of *cis* regulatory elements governing expression of the BpeEF-OprC described in the previous chapter allows for better understanding of the genetic context of the efflux operon, it is necessary to assess the contributions of BpeS and BpeT themselves. To that end, both molecular protein methods and Next-generation sequencing techniques were employed.

## **4.1 Materials and methods**

### **4.1.1 General DNA methodology**

Standard methods for DNA extraction and manipulation were utilized for all studies.<sup>1,3,4</sup> Genomic DNA was isolated using a Qiagen core Kit A (Germantown, MD) following the protocol for Gram-negative bacteria and re-suspended in TE buffer. Plasmid DNA was extracted from *E. coli* using a GeneJet Mini-prep (ThermoFisher, Waltham, MA) kit as directed by the manufacturer. All plasmids were re-suspended in either TE buffer or water and stored at -20 °C. Primers for general PCR were used at 10-30 µM concentrations, and at 10 µM for qRT-PCR.

**Table 4.1.A Cloning primers**

Number	Name	Sequence (5' > 3')
2536	NdeI <i>bpeT</i> _pet21bbpeT	CGGAGGTAGAc <u>at</u> ATGGACCGGCTGCAAGC
2537	HindIII_pet21bbpeT	CTGCGCGACTAA <u>aagctt</u> ATACGCCACCCACTC
2693	kpn1_ <i>bpeS</i> rev	<u>GGTACCTACGCGGCCACCTGC</u>
2694	<i>bpeS</i> _SOE	GCATGGACCGCATTTCAGGCAAT
2696	p1_ <i>bpeS</i> SOE	GCGGTCCATGCCATCAATCCTTCTTGTGAATC
2702	p12_hindII for	<u>AAGCTTTT</u> GACATAAGCCTGTTCCGGTTCG
2754	<i>bpeS</i> _p1SOE_for	GATTGATGGCATGGACCGCATTTCAGGCAAT
2849	pET21b_ <i>bpeS</i> _EcoR1	<u>GAA</u> TcCGCGCCACCTGCC
2850	pET21b_ <i>bpeS</i> _NdeI	<u>cat</u> ATGGACCGCATTTCAGGCAATGG
2871	<i>bpeS</i> for	ATGGACCGCATTTCAGGCAATGGAAGTCTTC

<sup>†</sup>Newly introduced restriction enzyme cleavage sites are underlined. Mutagenized bases are lowercased.

**Table 4.1.B Primers for gene deletion and mini-Tn7 insertion identification**

Target	Name	Sequence (5' > 3')
479	TN7L	ATTAGCTTACGACGCTACACCC
1509	BPGLMS1	GAGGAGTGGGCGTCGATCAAC
1510	BPGLMS2	ACACGACGCAAGAGCGGAATC
1511	BPGLMS3	CGGACAGGTTTCGCGCCATGC
2213	FK.chk.rev	AGCGCTCTGAAGTTCCTATACTTTCT
536	oriT-UP	TCCGCTGCATAACCCTGCTTC
537	oriT-DN	CAGCCTCGCAGAGCAGGATTC
1726	<i>oprB</i> -Rev	CTCTGGATCGCCTTCTCGTA
1729	<i>bpeA</i> -For	GTACGAGCGCCTATCTGGTC
1791	<i>dbpeT</i>	CGACGCATCGCGATGGAAAC
1790	<i>dbpeT</i>	ATGGACCGGCTGCAAGCCAT

**Table 4.1.C Primers utilized for qRT-PCR**

Number	Name	Sequence (5' > 3')
1516	Bp23S_F	GTAGACCCGAAACCAGGTGA
1517	Bp23S_R	CACCCCTATCCACAGCTCAT
1524	<i>bpeF</i> -F1_RT	TCCGAGTATCCGGAAGTCGT
1525	<i>bpeF</i> -R1_RT	GTCCTCGACACCGTTGATCT
1815	<i>bpeT</i> RT Rev	GTGAGTGGAAATTCGCAGAG
1816	<i>bpeF</i> RT For	TCACGAGCTACCAGATCAAC
2779	<i>bpeS</i> _RT_3_for	AAGCGCTCAGGTAATCGGG
2780	<i>bpeS</i> _RT_3_rev	GGTCGAAGAGGGGATCGATTG
2877	<i>dnaK</i>	CGCAGATCGAAGTGACCTT
2878	<i>dnakr</i>	ATCTTCTCGATCTCGGCTTC
2887	<i>bopA</i>	TCGGCGATCGACACCATGT

2888	bopAr	AAGCGATATGGCCCGGAAGG
2891	bapA	CAGCGAGACGTCGTTGAG
2892	bapAr	ACGAATCTCGTCGACATGG
2897	bipB	GCCTGATACTCGTCGGACTT
2898	bipBr	TCGAAGCAGAAGCTCTTCAC
2899	bicA	ATAGATGCCGTCCATCAGGT
2900	bicAr	CGACGTGAACATAGACGACA
2901	bsaQ	CAGCGGCACGATCAGCATC
2902	bsaQr	GAATCTCCTGATCAAGGCCCAAG
2915	fliC	CAGCAGATCTCGGAAGTGAA
2916	flicR	AGGATGTTCTTGCCGTTGTA

#### 4.1.2 Plasmids and bacterial strains

All *E. coli* strains were cultured in LB Lennox broth (Hardy Diagnostics, Santa Maria, CA) supplemented with the appropriate antibiotic for plasmid maintenance at 37 °C with shaking at 250 RPM, or on LB-Lennox agar (MoBio, Carlsbad, CA) incubated at 37 °C. RHO-3 strains were cultivated by supplementing the growth media with diaminopimelic acid (DAP) to a final concentration of 400 µg/ml. All *Bp* Bp82 strains were grown similarly to *E. coli*, but growth media was supplemented with adenine to a final concentration of 80 µg/ml. *E. coli* strains carrying plasmids were selected with 100 µg/ml ampicillin, 35 µg/ml kanamycin, 15 µg/ml gentamicin or 25 µg/ml zeocin. For *Bp*, *AmrA*<sup>+</sup>*B*<sup>+</sup>-*OprA*<sup>+</sup> strains were grown in media containing 1000 µg/ml kanamycin, 500 µg/ml gentamicin or 2000 µg/ml zeocin. Strains lacking *amrAB-oprA* were cultivated in 35 µg/ml kanamycin, 50 µg/ml gentamicin, or 35 µg/ml zeocin. Experiments with select agent excluded strain Bp82 and its derivatives were performed at BSL-2 with Institutional Biosafety Committee approval.

**Table 4.1.D Plasmids**

Name	Relevant properties	Source
pPS2594	pEXGm5B, dual counter-selectable allelic exchange suicide vector, Gm <sup>r</sup>	B. Kvitko
pGEM-TEasy	Ap <sup>r</sup> , TA cloning vector	Promega, Madison, WI

pET-21b	C-Terminal Hexahistidine fusion vector, IPTG inducible T7 promoter system,	Millipore, Billerica, MA
pPS2539	pEX-Km5 dual counter-selectable allelic exchange suicide vector, Km <sup>r</sup>	4
pPS2833	pEXKm5-Δ( <i>amrAB-oprA</i> ), pPS2539 containing Δ( <i>amrAB-oprA</i> ) SOEing product, Km <sup>r</sup>	6
pPS2234	pTNS3, transposition helper plasmid expressing <i>tnsABCD</i> from <i>P<sub>I</sub></i> and <i>P<sub>lac</sub></i> Ap <sup>r</sup>	6
pFLPe3	<i>P<sub>rhaB-rhaS-rhaR</sub></i> -FLPe-Km-rep(Ts)- <i>oriT</i> , plasmid encoding Flp recombinase, temperature sensitive replicon, Km <sup>r</sup>	6
pFLPe2	<i>P<sub>rhaB-rhaS-rhaR</sub></i> -FLPe-Km-rep(Ts)- <i>oriT</i> , plasmid encoding <i>flp</i> recombinase, temperature sensitive, Zeo <sup>r</sup> ;	6
pPS2280	pUC18T-mini-Tn7T-Km:: <i>FRT</i> , mini-Tn7 transposon, Km <sup>r</sup>	5
pPS2463	pUC18T-mini-Tn7T-Gm- <i>P<sub>I</sub>-bpeT</i> Gm <sup>r</sup>	T. Mima, unpublished
pPS2899	pEXGen5B-Δ( <i>bpeAB-oprB</i> ), Km <sup>r</sup>	This study
pPS2571	pEXKm5:Δ <i>bpeT</i> :: <i>FRT-ble-FRT</i> ,	T.Mima, unpublished
pPS3069	pET-21b- <i>bpeT</i> ,	This study
pPS3189	pEXKm5 <i>bpeS</i> <sub>P28S</sub> ,	N.Podnecky, unpublished
pPS3190	pEXKm5 <i>bpeS</i> <sub>K267T</sub>	N.Podnecky, unpublished
pPS3196	pGEM-TEasy <i>P<sub>I</sub>-bpeS</i> , pGEM-TEasy with <i>P<sub>I</sub></i> <sub>pTNS3</sub> - <i>bpeS</i> SOEing product amplified with primers 2702, 2693, 2694 and 2696. Ap <sup>r</sup>	This study
pPS3198	pUC18T-mini-Tn7T-Km- <i>FRT-P<sub>I</sub>-bpeS</i> , pPS2280 with <i>KpnI</i> + <i>HindIII</i> fragment from pPS3196. Km <sup>r</sup>	This Study
pPS3253	pET-21b <i>bpeT</i> <sub>S280P</sub> , pET-21b with <i>bpeT</i> amplified from Bp82.270 using primers 2536 and 2537,	This Study
pPS3258	pGEM-TEasy with <i>bpeS</i> <sub>P28S</sub> amplified from pPS3189 with primers 2849 and 2850,	This Study
pPS3259	pGEM-TEasy with <i>bpeS</i> amplified with primers 2849 and 2850,	This Study
pPS3260	pGEM-TEasy with <i>bpeS</i> <sub>K267T</sub> amplified from pPS3190 with primers 2849 and 2850.	This Study
pPS3262	pGEM-TEasy with <i>bpeS</i> <sub>K267T</sub> amplified from pPS3190 using primers 2693 and 2871,	This Study
pPS3263	pGEM-TEasy with <i>bpeS</i> <sub>P28S</sub> amplified from pPS3189 using primers 2693 and 2871,	This Study
pPS3265	pET-21b with <i>NdeI</i> + <i>EcoRI</i> wild-type <i>bpeS</i> fragment from pPS3259.	This study
pPS3266	pET-21b with <i>NdeI</i> + <i>EcoRI</i> <i>bpeS</i> <sub>K267T</sub> fragment from pPS3260.	This Study
pPS3269	pUC18T-miniTn7T-Km- <i>P<sub>I</sub>-bpeS</i> <sub>P28S</sub> , pPS3198 with <i>AleI</i> + <i>KpnI</i> fragment exchanged with that of pPS3263 to introduce <i>bpeS</i> . P28S	This Study

pPS3276	pET-21b with <i>NdeI</i> + <i>EcoRI</i> P28S <i>bpeS</i> fragment from pPS3258.	This Study
pPS3280	pUC18T-mini-Tn7T- <i>P1 bpeS</i> <sub>K267T</sub> , pPS3198 with the <i>AleI</i> + <i>KpnI</i> fragment exchanged with that of pPS3262 to introduce the <i>bpeS</i> <sub>K267</sub>	This Study

**Table 4.1.E *E. coli* strains utilized in this study**

Strain	Description	Source
DH5 $\alpha$	Subcloning strain, genotype: F <sup>-</sup> $\Phi$ 80 <i>lacZ</i> $\Delta$ M15 $\Delta$ ( <i>lacZYA-argF</i> ) U169 <i>recA1 endA1 hsdR17</i> (r <sub>k</sub> <sup>-</sup> , m <sub>k</sub> <sup>+</sup> ) <i>phoAsupE44 thi-1 gyrA96 relA1 <math>\lambda</math></i> <sup>-</sup>	7
NEB5 $\alpha$	Subcloning strain, K12 derivative, genotype: <i>fhuA2</i> $\Delta$ ( <i>argF-lacZ</i> )U169 <i>phoA glnV44 <math>\Phi</math>80 <math>\Delta</math>(lacZ)M15 gyrA96 recA1 relA1 endA1 thi-1 hsdR17</i>	New England Biolabs. Ipswich MA
BL21(DE3)	<i>E. coli</i> T7 lysogen lacking Lon and Omp proteases, protein expression strain. Genotype: <i>fhuA2 [lon] ompT gal (<math>\lambda</math> DE3) [dcm] <math>\Delta</math>hsdS<math>\lambda</math> DE3 = <math>\lambda</math> sBamHIo <math>\Delta</math>EcoRI-B int: lacI::PlacUV5::T7 gene1) i21 <math>\Delta</math>nin5</i>	New England Biolabs
BL21(DE3)-RP (codonplus)	BL21-(DE3) harboring Cm <sup>r</sup> tRNA codon plasmids for <i>argU</i> (AGA AGG) and <i>proC</i> (CCC)	Agilent, Santa Clara, CA.
RHO3	Mobilizer strain, SM10( <i><math>\lambda</math>pir</i> ) $\Delta$ <i>asd</i> :: <i>FRT</i> $\Delta$ <i>aphA</i> :: <i>FRT</i> diaminopimelic acid auxotroph, Km <sup>s</sup>	4

**Table 4.1.F *B. pseudomallei* strains utilized in this study**

Parent Strains		
Strain Number	Description	Source
Bp82	1026b $\Delta$ <i>purM</i> select agent excluded strain	4
Bp82.27	Bp82 $\Delta$ ( <i>amrAB-oprA</i> )	B. Kvitko, unpublished
Bp82.57	Bp82.27 $\Delta$ ( <i>bpeAB-oprB</i> )	This study
<i>bpeS</i> , <i>bpeT</i> mutant strain backgrounds		
Bp82.87	Bp82.57 $\Delta$ <i>bpeT</i>	This study
Bp82.253	Bp82 $\Delta$ <i>bpeT</i>	N. Podnecky, unpublished
Bp82.264	Bp82 $\Delta$ <i>bpeS</i>	N. Podnecky, unpublished
Bp82.270	Bp82 <i>bpeT</i> <sub>S280P</sub>	N. Podnecky, unpublished

Bp82.284	Bp82 <i>bpeS</i> <sub>P28S</sub>	N. Podnecky, unpublished
Bp82.285	Bp82 <i>bpeS</i> <sub>K267T</sub>	N. Podnecky, unpublished
Bp82.286	Bp82.264 $\Delta$ <i>bpeT</i>	This study
Bp82.292	Bp82.284 $\Delta$ <i>bpeT</i>	This Study
Bp82.317	Bp82.285 $\Delta$ <i>bpeT</i>	This Study
<b><i>bpeS bpeT</i> Expression Strains</b>		
Bp82.187	Bp82.87::pPS2463(mini-Tn7-Gm- <i>P1-bpeT</i> )	This study
Bp82.189	Bp82::87 pPS1399( mini-Tn7-Gm)	This Study
Bp82.323	Bp82.264::pPS2280 (mini-Tn7T-Km)	This Study
Bp82.324	Bp82.286::pPS2280(mini-Tn7T-Km)	This Study
Bp82.288	Bp82.286::pPS3198 (mini-Tn7T-Km- <i>P1-bpeS</i> )	This Study
Bp82.289	Bp82.264::pPS3198 (mini-Tn7T-Km- <i>P1-bpeS</i> )	This Study
Bp82.310	Bp82.264::pPS3269 (mini-Tn7T-Km- <i>P1-bpeS</i> <sub>P28S</sub> )	This Study
Bp82.311	Bp82.286::pPS3269 (mini-Tn7T-Km- <i>P1-bpeS</i> <sub>P28S</sub> )	This Study
Bp82.320	Bp82.264::pPS3280 (mini-Tn7T-Km- <i>P1-bpeS</i> <sub>K267T</sub> )	This Study
Bp82.321	Bp82.286::pPS3280 (mini-Tn7T-Km- <i>P1.bpeS</i> <sub>K267T</sub> )	This Study

#### 4.1.3 Construction of Bp82 strains

*Bp.* strains utilized in this study are listed in **Table 4.1.F**, with plasmids used to create those strains listed in **Table 4.1.D**. Chromosomal gene deletions were performed using the pEX allelic exchange system designed by previous members of the Schweizer laboratory and as described in Chapter 3 section 1.3.<sup>4</sup> In instances where the deletion was more difficult to obtain, the I-Sce homing endonuclease functions of the pEX system were utilized as described in the previous chapter. Flp recombinase target (*FRT*) flanked antibiotic resistance genes were removed

from the chromosome using the pFLP system developed by previous members of the Schweizer lab.<sup>6</sup> Strain Bp82.57 was constructed using this method with suicide vector pPS2899 to delete the *bpeAB-oprB* operon and confirmed with primers 2213, 1729 and 1726. Deletion of *bpeT* in strains Bp82.87, Bp82.286, Bp82.292 and Bp82.317 was achieved similarly, using pPS2571 and confirmed with primers 1789 and 1790. All isolates were later used in the experiments described in this chapter.

#### **4.1.4 Gene complementation and single copy insertions using the mini-Tn7 system**

The mini-Tn7 system is a useful tool for the introduction of a gene or construct of interest at a neutral site in the chromosome for further analysis. The system utilizes a helper plasmid pTNS3 encoding the transposase homing, excision and recombinase Tn7 subunits ABCD.<sup>5</sup> The Tn7 element inserts at an *attTn7* site downstream of one of the three copies of the *glmS* gene encoded by *Bp*. To introduce these insertions, the mini-Tn7 delivery vector carrying the gene of interest, and pTNS3, were co-electroporated into the host cell following the procedure outlined in Chapter 3. Transformants were isolated on LB + 80 µg/ml adenine with either kanamycin, gentamicin or zeocin, and allowed to grow for 24 h at 37°C. Resistant colonies were patched and screened for *glmS* insertions by PCR (primers 1509, 1510, 1511 and 479, **Table 4.1.B**). *GlmS* insertion positive clones produced bands from 200 to 400 bp depending on the insertion site. When possible, only isolates with insertions at *glmS2* were retained for further study.

#### **4.1.5 Construction of strains expressing *bpeS* and *bpeT* from the P1 promoter**

The *P1* integron promoter has previously been used to drive recombinant gene expression.<sup>41,42</sup> To construct a *P1-bpeT* strain, pPS2463 and the corresponding empty pUC18T-mini-Tn7T-Gm control vector (**Table 4.1.D**) were transposed into the  $\Delta bpeT$  background strain (Bp82.87, **Table 4.1.F**) using the pTNS3 helper plasmid system as described above.

Transposition of the mini-Tn7-*P1-bpeT* element downstream of one of three neutral *glmS* sites within the chromosome was assessed by PCR. Clones with confirmed single *glmS1* insertions were stored for further study as strains Bp82.187 and Bp82.189 yielded no single *glmS2* insertions (**Table 4.1.F**).

To create a *P1-bpeS* construct, primers 2702, 2693, 2694, and 2696 (**Table 4.1.A**) were utilized to PCR amplify the wild-type *bpeS* gene from Bp82 genomic DNA as well as engineer sequence homologous to the strong *P1* promoter fragment of plasmid pTNS3. The *P1* promoter region and *bpeS* amplicons were gel purified and SOEing PCR was performed to amplify a 1.5 kb amplicon with the *P1* promoter fused to the *bpeS* gene using the outermost 5' and 3' primers (2693 and 2702). This amplicon was subcloned into pGEM-TEasy to create pPS3196 and confirmed by sequencing. The 1.5 kb fragment was excised from pPS3196 using *KpnI* + *HindIII* and ligated into the same sites of linearized pUC18T-mini-Tn7T-KM to create pPS3198. The plasmid was confirmed using *KpnI*+*EcoRI* digest and sequencing. pPS3198 or pUC18T-mini-Tn7T-Km were electroporated into Bp82.264 and Bp82.286 and single *glmS* insertions were identified as outlined in the previous section. Confirmed insertion strains were *glmS3* insertions, and designated Bp82.288, Bp82.289, Bp82.323 and Bp82.324 (**Table 4.1.F**).

To introduce either a P28S mutation or K267T mutation into the wild type *P1-bpeS* construct, PCR amplification of mutant *BpeS* was performed using primers 2693 and 2871 (**Table 4.1.1A**) from pPS3189 (contains *bpeS*<sub>P28S</sub>) and pPS3190 (contains *bpeS*<sub>K267T</sub>) (**Table 4.1.D**). The one kb PCR amplicons were gel purified, and TA cloned into pGEM-TEasy to create pPS3262 and pPS3263 (**Table 4.1.D**) before inserts were confirmed through *EcoRI* and *KpnI* digests and sequencing using T7 and SP6 primers. pPS3262 or pPS3263 clones harboring the correct mutations were digested with *AleI* and *KpnI* to release a 900 bp fragment containing

either BpeS<sub>P28S</sub> or BpeS<sub>K267T</sub>. This was ligated into the dephosphorylated *AleI-KpnI* fragment of pPS3198, effectively swapping the wild type region of *bpeS* contained on this plasmid for the mutant versions carried on the pGEM-TEasy vectors to create pPS3269 and pPS3280 (**Table 4.1.D**). The wild type *PI-bpeS* construct, *PI-bpeS<sub>P28S</sub>*, *PI-bpeS<sub>K267T</sub>* mutant constructs, and an empty mini-Tn7-Km vector control were electroporated into Bp82.264 and Bp82.286 along with helper plasmid pTNS3. Single transposition clones were identified through *glmS* specific PCR as described previously, and insertions at *glmS2* or *glmS3* were utilized for further study. All final expression strains are listed in **Table 4.1.F**.

#### 4.1.6 Antibiotic susceptibility assays

Antibiotic susceptibility of each constructed mutant was assessed by determining the minimal inhibitory concentration (MIC) utilizing the E-test method following the manufacturers guideline (bioMerieux, Marcy-l'Etoile, France). Antimicrobial susceptibilities were assigned according to guidelines set by the Clinical Laboratory Standards Institute (CLSI).<sup>8</sup> Briefly, overnight cultures of interest were sub-cultured 1:100 into cation adjusted Mueller-Hinton broth (BD, Sparks, MD) containing 40 µg/ml adenine and incubated with shaking at 37 °C until they reached an OD<sub>600nm</sub> of 0.6-0.8. A 0.5 McFarland was created using the sub-cultured cells in sterile 85% saline and confirmed by visual comparison to a McFarland standard, or measurement of OD<sub>625nm</sub> to be between 0.08 and 0.1. Using a cotton swab, the McFarland sample was then struck onto cation-adjusted Mueller-Hinton agar (BD, Sparks, MD) plates supplemented with 40 µg/ml adenine and allowed to dry in the hood. E-test strips were allowed to warm to room temperature and placed in the center of the dry plate. Samples were incubated at 37°C for 18-20 h before the zone of 80% inhibition was measured on the strip, and recorded as the MIC.

#### 4.1.7 RNA extraction

Overnight cultures of the strain of interest grown in LB Lennox medium were used to subculture fresh media at a ratio of 1:100. Cultures were incubated at 37°C with shaking at 250 RPM until they reached an OD<sub>600nm</sub> of 0.6-0.8. RNA extraction was carried out using the RNeasy mini protect kit (Qiagen, Germantown,MD), following manufacturers guidelines with the addition of a RT incubation with 3 mg/ml lysozyme and vortexing every two minutes to ensure complete cell lysis. Samples were recovered in 30 µl of sterile, RNase-free water and stored at -80°C until further use.

#### 4.1.8 qRT-PCR

Total RNA isolated as described above was quantified, and 1 µg per sample was treated with DNase I (Invitrogen, Carlsbad, CA) in a total volume of 10 µl with supplied buffer. Reactions were incubated at 37°C for 20 min, and stopped with the addition of 25 mM EDTA followed by heating at 65°C. Four µl of each DNase I treated sample was then used to create cDNA with the Invitrogen Superscript III first strand synthesis kit, following the manufacturers protocol. Reverse transcription negative controls (-RT) were also generated at this time using 4 µl of DNase treated RNA and 16 µl of water in the place of active kit components. Quantitative reverse-transcriptase PCR was performed with 2 µl of cDNA or -RT template per 20 µl sample using Invitrogen SYBR-GreenER supermix (Carlsbad, CA) or Syber-select master mix for CFX (ABI, Foster City, CA), and oligos at 1.25-1.5 µM final concentration using primers listed in **Table 4.1.C**. qRT-PCR was carried out on a Bio-Rad Q5 or CFX 1000 (Hercules, CA). All expression levels were calibrated using basal expression of the 23S ribosomal RNA gene. Target gene expression was measured and fold changes were calculated using the  $\Delta\Delta C_t$  method, taking into account previously calculated efficiencies obtained via a standard curve. Samples with

corresponding –RT controls with a Ct value less than 30 cycles were excluded from analysis and the procedure was repeated for these samples. All experiments were conducted in at least biological duplicate before final analysis of expression using GraphPad Prism (La Jolla, CA).

#### **4.1.9 Drug dose dependent induction of *bpeEF-oprC***

Bp82 and Bp82 derivatives lacking *bpeT*, *bpeS* or both *bpeT* and *bpeS* (**Table 4.1.F**), were inoculated in LB Lennox + 80 µg/ml adenine broth and incubated overnight at 37°C. All strains were diluted into fresh media at a 1:50 subculture and incubated to an OD<sub>600</sub> nm of 0.4-0.5 at 37°C. At this point, the cultures were split into 5 aliquots and dosed with either trimethoprim (TMP), doxycycline (DOX), or chloramphenicol (CHL) ranging from 0-16 µg/ml in 2 fold increments. Cells were allowed to incubate for an additional hour, and were harvested for RNA extraction when they reached mid-log phase as described in section 4.1.7. cDNA was generated and samples were analyzed by qRT-PCR and relative gene fold expression was determined using the  $\Delta\Delta C_t$  method described in the previous section. Expression values were pooled between biological replicates, and final analysis was performed using GraphPad Prism. One-way ANOVA of fold expression was performed with Dunnet's multiple comparison test using all LB samples as control comparators.

#### **4.1.10 RNA sequencing and analysis**

RNA sequencing was performed at the University of Florida ICBR next-generation sequencing core. Bp82, Bp82 *bpeT*<sub>S80P</sub>, Bp82 *bpeS*<sub>P28S</sub> and Bp82 *bpeS*<sub>K267T</sub> were inoculated in LB-Lennox +80 µg/ml adenine and incubated overnight at 37°C with shaking. Overnight growth was sub-cultured 1:50 into fresh media, and the cultures were grown to mid-log phase. Total RNA was extracted as described earlier, and samples were stored at -80°C. This procedure was repeated to create two biological replicates. The samples were assessed for purity and integrity

with a fluorimeter. Samples with an  $A_{260/230}$  ratio of 1.9-2.0 were sent to the core for further analysis. There, RNA quality was confirmed on an TapeStation Bio-analyzer (Agilent, Santa Clara, CA), and ribosomal rRNA depletion was performed using RiboZero (Illumina, San Diego, CA). A sequencing library was created using an Illumina TruSeq paired end library prep kit for 150 bp fragments and the samples were analyzed on an Illumina HiSeq 2000 run at medium capacity.

A total of 155 million reads were returned for further analysis, averaging 20 million reads per sample. Quality control and analysis of reads was performed using NCBI Galaxy.<sup>9-11</sup> For each sample replicate, all reads were trimmed to an average phred score of 20 or above using QC filter.<sup>12</sup> Highly repetitive sequences were removed from the data set, and adaptors were trimmed from reads above the quality index cut. Cleaned sequences were then aligned to the *Bp* 1026b genome using Bowtie2 constrained for paired-end reads, where the resultant alignments were annotated against the 1026b genome.<sup>13</sup> The .bam output files were then merged and input to Cufflinks to calculate fragments per kilobase per million mapped reads (FPKM) with a false discovery rate of 0.5 and to determine transcripts present within those mapped reads.<sup>14</sup> These files were used as input in Cuffdiff in comparison to either the wild-type control replicate to determine relative fold differences between identified transcripts.<sup>15,16</sup> The tool was run using a classic-FPKM library normalization method, for pooled samples with a multi-read correction to improve the accuracy of the expression estimations and a false discover rate of 5%. Log base 2 of expression values from these comparisons were subjected to statistical testing within Cuffdiff based on the presence of both replicate fragments within the identified transcript. A list of all genes with significantly altered expression was compiled. Overall expression distributions were plotted using CummeRbund.<sup>15</sup>

#### 4.1.11 Protein purification

The *bpeT* or *bpeS* genes were PCR amplified from genomic DNA from Bp82, Bp82.270 (*bpeT*<sub>S280P</sub>) or plasmids pPS3189 (*bpeS*<sub>P28S</sub>) or 3190 (*bpeS*<sub>K267T</sub>) using primer pairs 2536 and 2537 or 2849 and 2850 listed in **Table 4.1.A**. 3' primers were designed to remove the stop codon of each gene and to facilitate an in-frame hexahistidine fusion when subcloned into pET-21b to obtain pPS3265, pPS3266 and pPS3272 (**Table 4.1.D**). All cloning procedures to create these vectors and initial testing methods used to confirm protein expression in BL21(DE3) or BL21(DE3)RP are described in Chapter 3 section 1.11. Protein was expressed by induction with 1 mM to 5 mM IPTG starting at OD<sub>600nm</sub>=0.8-1.0 for up to 4 h or an OD of 1.5-2.0 depending on expression strain, target protein and expression clone. Cells were pelleted and proteins were extracted using an adapted protocol first developed elsewhere and described in Chapter 3.<sup>17</sup> Proteins were dialyzed overnight as described in Chapter 3 and concentrations of protein samples were measured using a BCA assay Kit (ThermoPierce, Rockford, IL) and averaged concentrations of 1-2 mg/ml. Glycerol was added to samples to a final concentration of 20% and samples were stored at -80°C until further use.

#### 4.1.12 Native gel electrophoresis

Five hundred ng to 1 µg of protein per sample was mixed 1:2 with native sample buffer containing 62.5 mM Tris-HCl pH 6.8, 0.01% bromophenol blue, and 40% glycerol. All samples and 5 µl of Native Mark Standard (Lifetech, Carlsbad, CA) diluted 1:20 in sample buffer were loaded onto a 4-15% mini-protean TGX gel (Bio-Rad, Hercules, CA) and electrophoresed in buffer containing 25 mM Tris-Hcl 250 mM glycine without SDS. Gels were run at 130 V for approximately 1 h before being removed from the electrophoresis chamber and fixed in a solution containing 30% ethanol and 10 % acetic acid for 30 min. The gels were later washed

with ultrapure water , and stained with silver stain (ThermoPierce, Rockford, IL) according to the manufacturer's protocol for native polyacrylamide gel visualization.

#### **4.1.13 Size exclusion chromatography**

To estimate the native sizes of purified His-tagged BpeT and BpeS, low-pressure size exclusion chromatography analysis was conducted as adapted from Chuanchuen, 2006.<sup>22</sup> Briefly, a 50 cm column was filled with a 50% slurry of de-gassed Bio-Rad Sephadex G-200 swelled in water for 24 h prior to packing. The column was connected to a Bio-Rad peristaltic pump system leading to a UV monitor. The column was packed at a flow rate of 7.2 ml/hour until compressed by 2/3 with degassed buffer (20 mM TRIS-HCl pH7.5, 1 mM EDTA, 0.1 mM DTT and 15% glycerol) and fitted with a flow adaptor. Sigma gel filtration standards for 12kD to 200 kD proteins were resuspended in chromatography buffer according to the manufacturers recommendations. Blue Dextran, ATP and pUC18 DNA were used to measure void and retention peaks.

One aliquot per sample was injected into the flow adaptor with care to avoid bubble introduction and allowed to enter the column at the packing flow rate. Injection times were recorded as time zero. Peaks detected at 280 nm by the UV monitor were recorded for each sample and the injections were repeated two additional times to generate a standard curve. 500  $\mu$ l aliquots of either BpeT or BpeS at approximately 1 mg/ml were injected into the flow adaptor at constant rate. Peaks were recorded following the same time measurement procedure as the standards, and peak distance from the start time was measured. Each sample was analyzed in triplicate and generated peaks were compared to the standard curve. The partition coefficient was calculated using the formula  $(V_e - V_0)/(V_t - V_0)$  and used to determine for identification of the native size of each protein.

## 4.2 Results and discussion

### 4.2.1 BpeT is a transcriptional activator of the *bpeEF-oprC* efflux pump operon.

To determine the function of BpeT, transcript levels of *bpeT* and *bpeF* were determined by qRT-PCR using gene specific primers and 23S ribosomal RNA as a control comparator. Total RNA from Bp82, strains harboring a mini-Tn7-*P1 bpeT* construct, or an empty vector control, was used as template.

As expected, no *bpeT* transcripts could be detected in un-complemented strains lacking endogenous *bpeT* (**Fig. 4.2.1**). The *bpeF* transcript levels in these strains were less than that of Bp82. In the strain harboring a single copy of *bpeT* under the control of the strong P1 promoter, *bpeT* mRNA levels were 30-40 fold higher than in wild type Bp82. The *bpeF* transcript levels in this isolate increased 10 fold in comparison to wild type Bp82. This suggests that *bpeT* may act as a transcriptional activator of the operon, as overexpression of *bpeT* directly correlates to transcriptional upregulation of pump gene expression.

The presence of functional BpeEF-OprC protein was confirmed through MIC assays for BpeEF-OprC substrates using the E-test method (**Table 4.2.1**). Overexpression of BpeEF-OprC was confirmed by phenotypic decreases in the antimicrobial susceptibility of strains containing the *P1-bpeT* construct. Compared to wild type Bp82, the Bp82 $\Delta$ *bpeT*::mini-Tn7 strain did not show an increase in MICs for trimethoprim (TMP), sulfamethoxazole (SMX), or co-trimoxazole (SXT). In the strain containing the *P1-bpeT* construct, MIC levels for TMP are increased from 0.094 to 16  $\mu$ g/ml, classifying them as TMP resistant. There is a modest increase in the MIC levels of SMX, but not SXT in this strains. SMX is not known to be a substrate of the pump at wild type expression levels less than those seen in the *P1-bpeT* construct strains. This fact may explain the slightly elevated SMX MIC value and lack of significant increases in SXT resistance

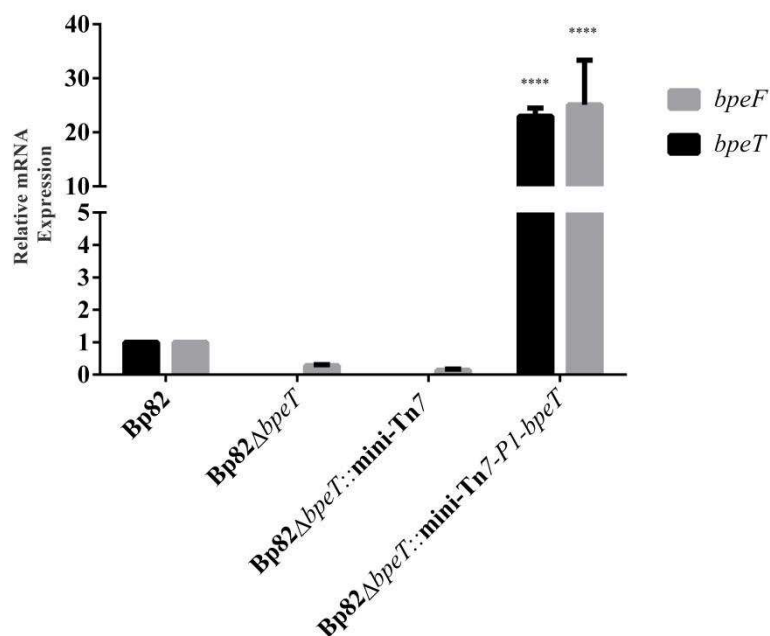


**Figure 4.2.1. BpeT is a transcriptional activator of the *bpeEF-oprC* operon.**

Either an empty vector control or pPS2463 containing a copy of *bpeT* driven by the strong P1 promoter was integrated into the chromosome of Bp82Δ*bpeT* using the miniTn7 system. RT-qPCR analysis of both *bpeT* and *bpeF* of these strains, in addition to the parent strain Bp82 and background strain lacking *bpeT* was performed in biological duplicate. Bars represent mean expression of two biological replicates one with standard deviation. Statistical analysis was performed by Two-way ANOVA with Tukey's multiple comparison post test using GraphPad Prism V6 to determine inter-strain differences.  $P \leq 0.0001 = ****$ .

**Table 4.2.1 MIC testing in Bp82 *bpeT* overexpression strains**

Minimal Inhibitory Concentration (μg/ml)			
Strain	TMP	SMX	SXT
Bp82	0.75	4	.094
Bp82Δ <i>bpeT</i> :: mini-Tn7	1	8	0.094
Bp82Δ <i>bpeT</i> :: mini-Tn7-P1- <i>bpeT</i>	16	128	1-1.5

MICs for the indicated antibiotics were determined using the E-test method in technical triplicate, in at least biological duplicate. MIC values represent the mode of all measurements. Detection limits for TMP, SMX and SXT are 32, 1024 and 32 μg/ml, respectively. CLSI break points for a resistant classification in *Bp* are TMP > 8 μg/ml, SMX >256 μg/ml SXT > 2/38 μg/ml at a 1:19 ratio of TMP to SMX.

in the *P1-bpeT* overexpression. As SXT is a combination of both sulfamethoxazole and trimethoprim, efflux activity insufficient to remove both TMP and SMX from the cell would leave one component of the drug combo active within the cell. This would result in a MIC that is still classified as susceptible according to CLSI guidelines.<sup>8</sup>

#### **4.2.2 BpeS is not a transcriptional activator of the *bpeEF-oprC* operon under wild-type *in-vitro* conditions.**

To repeat the analysis conducted with *bpeT* for determination of BpeS function, a similar approach was utilized. To assess phenotypic changes caused by overexpression of *bpeS*, E-test MIC analyses were conducted as in the *bpeT* overexpression experiments to assess a possible role of BpeS in activation of *bpeEF-oprC* operon expression. (**Table 4.2.2**). qRT-PCR was employed to assess *bpeS* transcript levels in Bp82, Bp82  $\Delta bpeS$ , Bp82  $\Delta bpeS\Delta bpeT$  isolates harboring a chromosomally integrated mini-Tn7 isolate expressing *bpeS* from the strong P1 promoter (**Fig. 4.2.2**).

Despite overexpression of *bpeS* in both *P1-bpeS* strains when compared to Bp82, this did not result in any changes in MIC levels in either Bp82 $\Delta bpeS$  or Bp82 $\Delta bpeS\Delta bpeT$  strains containing *P1-bpeS*. This could implicate *bpeS* as a transcriptional repressor except for the fact that strain controls lacking *bpeS* but retaining *bpeT* showed no increase in *bpeF* expression. Decreased drug susceptibility would be expected after loss of such a repressor protein but was not observed in isolates lacking *bpeS*. Later data will show that both BpeS and BpeT are dispensable for drug-dependent induction of BpeEF-oprC, and in light of this fact it may be possible that BpeS is necessary for activation of the operon only under specific environmental settings. This may suggest it is unable to perform an activatory function under currently identified laboratory conditions.

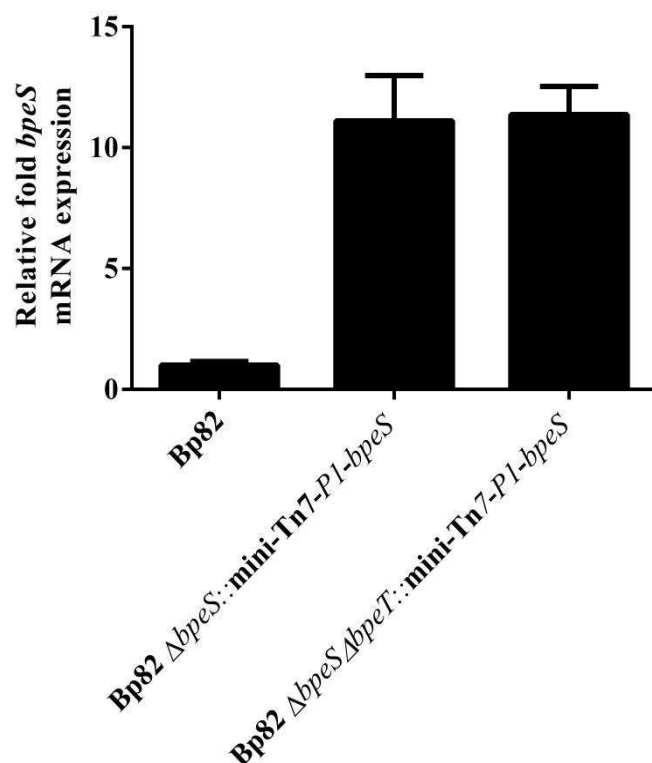


**Figure 4.2.2. Transcription from the *P1* promoter causes overexpression of wild-type *bpeS*.** qRT-PCR analysis was performed using total RNA isolated from strains lacking *bpeS* or both *bpeS* and *bpeT*, but harboring a mini-Tn7 construct on which *bpeS* is expressed by the strong *P1* promoter. *bpeS* expression is highly elevated in comparison to Bp82.

**Table 4.2.2. BpeS is not a direct transcriptional regulator of *bpeEF-opC*.**

Minimal Inhibitory Concentration ( $\mu\text{g/ml}$ )		
Strain	TMP	SXT
Bp82	0.75	.094
Bp82 $\Delta bpeS::mini-Tn7-P1-bpeS$	0.75	0.094
Bp82 $\Delta bpeS\Delta bpeT::mini-Tn7-P1-bpeS$	0.75	0.125

MICs were determined using the E-test method. *bpeS* overexpression is not accompanied by increased resistance to Trimethoprim (TMP) or co-trimoxazole (SXT) indicating that *bpeEF-oprC* expression was unaffected by overexpression of BpeS. Clinical Laboratory Standards Institute break points for a resistant classification in *Bp* are TMP > 8  $\mu\text{g/ml}$ , and SXT > 2/38  $\mu\text{g/ml}$  at a 1:19 ratio of TMP to SMX.

### 4.2.3 *bpeS* mutations, not changes to *bpeS* expression level, cause BpeEF-OprC dependent resistance to co-trimoxazole.

Based on the lack of *bpeEF-oprC* over-expression in strains containing *PI-bpeS*, the effect of the mutations themselves may give insight into the function of *bpeS*. Mini-Tn7 constructs expressing either *bpeS*<sub>P28S</sub> (located on pPS3269) or *bpeS*<sub>K267T</sub> (located on pPS3280) (**Table 4.1.D**) were introduced into Bp82 lacking *bpeS* or both *bpeS* and *bpeT*. Resistance to SMX, SXT and TMP was measured by the E-test method, and expression levels of *bpeT*, *bpeF* and *bpeS* were measured by qRT-PCR.

The presence of functional BpeS<sub>P28S</sub> protein was confirmed through MIC analysis (**Table 4.2.3**). This showed decreases in the susceptibility of the BpeS<sub>P28S</sub> mutants to both TMP and SMX, confirming previous data by Podnecky et al (unpublished observations), that high level BpeEF-OprC overexpression also causes SMX extrusion. This in turn is confirmed by the increase of SXT MIC in these strains to 6 µg/ml, while the MIC levels in Bp82 and *PI-bpeS* strains described in **Table 4.2.2** remained indistinguishable from one another at 0.094 µg/ml. This suggests that the mutation, not the increased presence of the regulator, is responsible for changes in expression levels of the target operon. A similar trend was observed when the *PI-bpeS*<sub>K267T</sub> variants were analyzed. MIC analysis displayed a similar trend to that of strains expressing the *PI-bpeS*<sub>P28S</sub> variant with both TMP and SMX MIC levels measured to the limit of detection for the assay (**Table 4.2.3**).

Analysis of gene expression by qRT-PCR analysis confirmed observations made by E-Test MIC analysis. Mini-Tn7 vector controls showed no increase in gene expression attributable to the vector. For strains possessing the *PI-bpeS*<sub>P28S</sub> construct, *bpeF* expression levels in all strain backgrounds were 2 to 3 times higher than those of *bpeS* and were from 40 to 60 fold

**Table 4.2.3. Antibiotic susceptibility of strains expressing BpeS<sub>P28S</sub> or BpeS<sub>K267T</sub> variants lacking native *bpeS* or *bpeS* and *bpeT*.**

Minimal Inhibitory Concentration in (µg/ml)			
Strain	TMP	SMX	SXT
Bp82	1	4	.094
Bp82Δ <i>bpeS</i> :: <i>PI-bpeS</i> <sub>P28S</sub>	>32	>1024	6
Bp82Δ <i>bpeS</i> Δ <i>bpeT</i> :: <i>PI-bpeS</i> <sub>P28S</sub>	>32	>1024	6
Bp82Δ <i>bpeS</i> :: <i>PI-bpeS</i> <sub>K267T</sub>	>32	>1024	6
Bp82Δ <i>bpeS</i> Δ <i>bpeT</i> :: <i>PI-bpeS</i> <sub>K267T</sub>	>32	>1024	6

All isolates were analyzed using the E-test method. Loss of *bpeT* appeared to have no effect on MIC. Detection limit for both TMP and SXT is 32 µg/ml, and >1024 µg/ml for sulfamethoxazole. CLSI break points for a resistant classification in *B. pseudomallei* are TMP > 8 µg/ml, SMX > 256 and SXT > 2/38 µg/ml at a 1:19 ratio of TMP to SMX.

increased from wild type and empty control samples (**Fig. 4.2.3**). Statistical analysis showed that both *bpeS* and *bpeF* levels in *PI-bpeS*<sub>P28S</sub> samples were significantly different from both Bp82 samples and empty vector control strains. These data also indicate that *bpeS* is not a direct regulatory activator of *bpeT*, as *bpeT* expression levels in *bpeT*<sup>+</sup> strains remained unaffected by the presence of the overexpressed *bpeS* mutant and were not statistically different from wild type samples.

When the analysis was repeated in isolates harboring the *PI-bpeS*<sub>K267T</sub> constructs, a similar trend could be observed. Transcript levels of *bpeF* in these strains were elevated more than 100 fold when compared to wild type or vector control strains and statistically significant in comparison to these isolates (**Fig. 4.2.4**). The *bpeS* transcript levels were not found to be statistically different from wild type in either the *bpeT*<sup>+</sup> or *bpeT* strain backgrounds, although their expression was increased approximately 5 fold compared to wild type or vector controls.

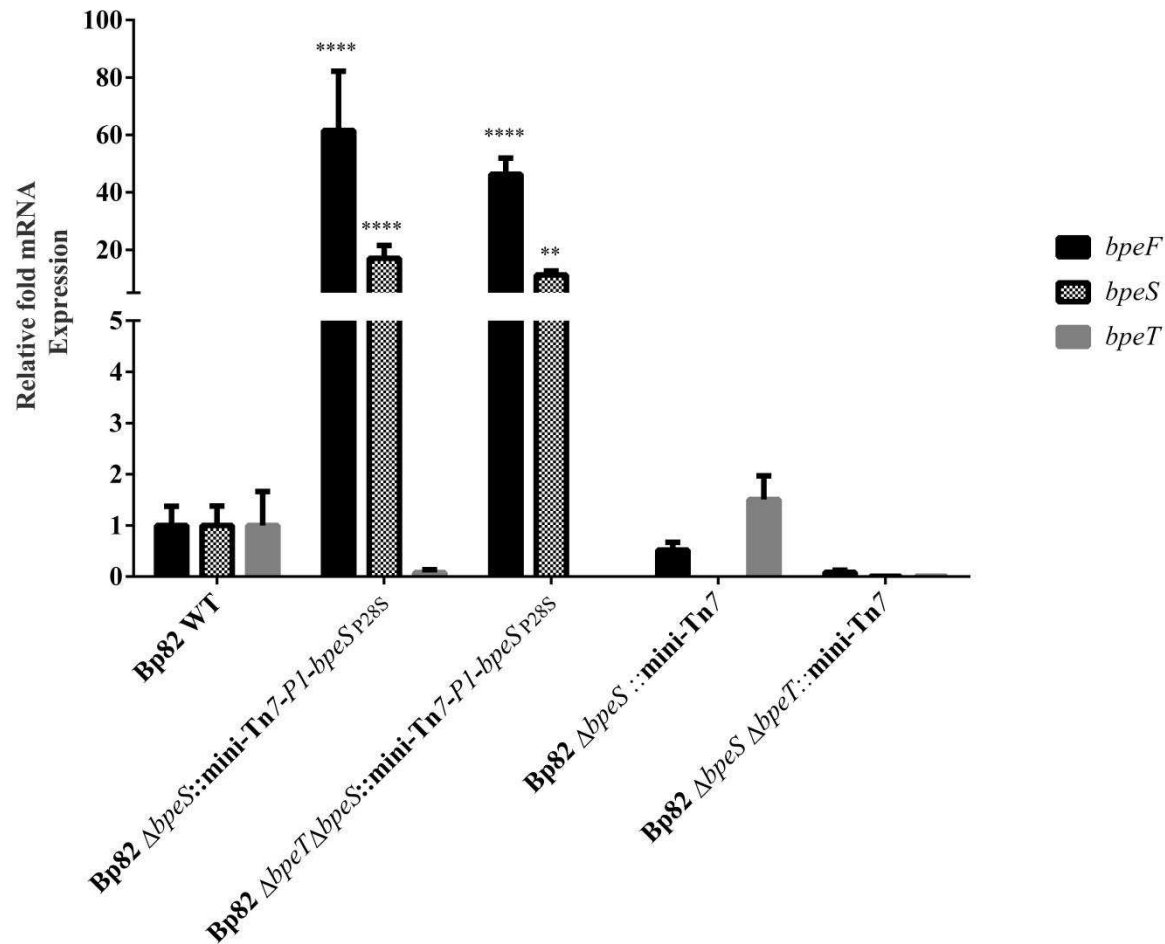


**Figure 4.2.3. The *bpeS*<sub>P28S</sub> mutation causes high level expression of *bpeF*.** Mini-Tn7 construct expressing *bpeS*<sub>P28S</sub> from the P1 promoter was introduced into Bp82 variants lacking *bpeS*, or *bpeS* and *bpeT* (Table 4.1.D. and 4.1.F.). The expression of *bpeS*, *bpeT* and *bpeF* in the resulting strains was measured by qRT-PCR and two-way ANOVA was performed with Dunnet's post test to determine significance compared to the wild type control. Bars represent mean expression of two biological replicates with one standard deviation. Strains with *P1.bpeS*<sub>P28S</sub> displayed elevated expression of *bpeS* and *bpeF* but not *bpeT* when still present at the native locus. \*\*\*\* =  $p < 0.0001$ , \*\*\* =  $p < 0.001$ , \*\* =  $p < 0.01$ .

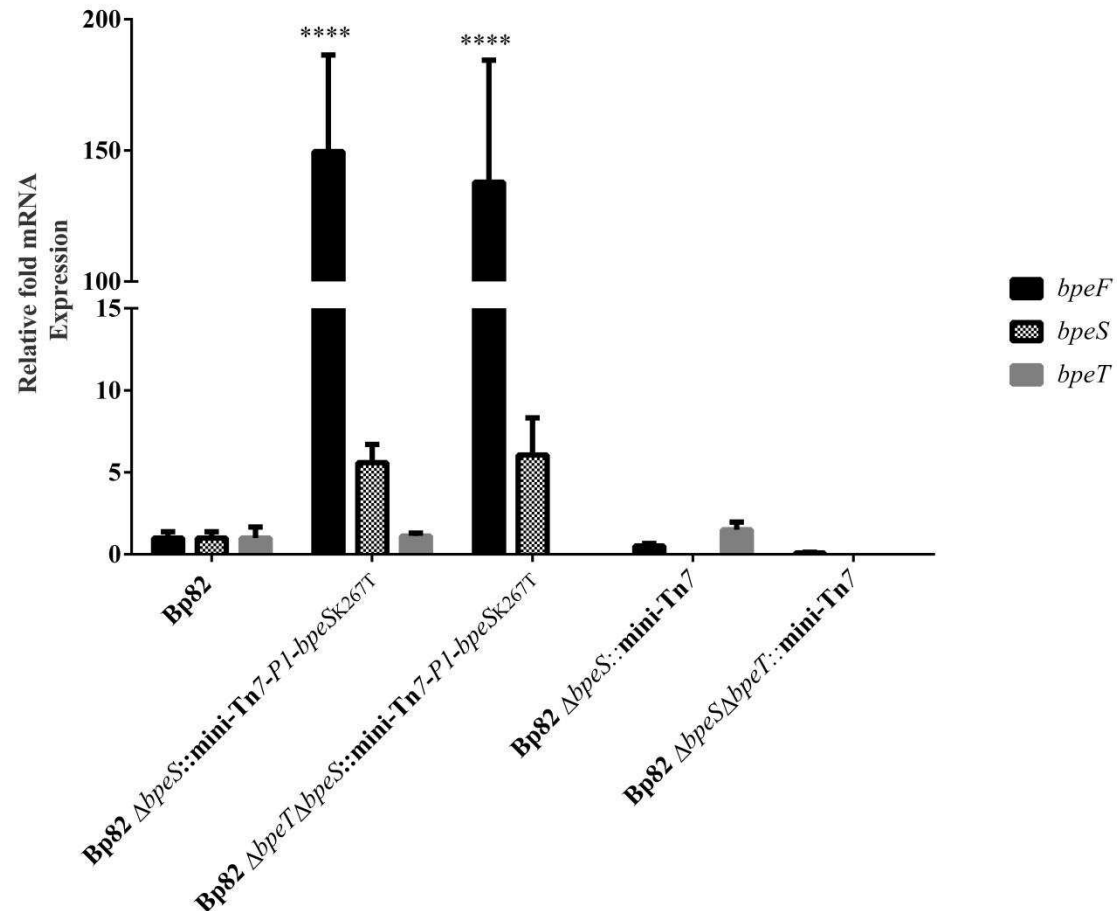


**Figure 4.2.4. The *bpeS*<sub>K267T</sub> mutation causes high level expression of *bpeF*.**

A mini-Tn7 construct expressing *P1-bpeS*<sub>K267T</sub> was introduced into Bp82 variants lacking *bpeS*, or *bpeS* and *bpeT* (Table 4.1.D and 4.1.F). The expression of *bpeS*, *bpeT* and *bpeF* in the resulting strains was measured by qRT-PCR and Two-way ANOVA with Dunnet's post test was used to determine significance compared to the wild type control. Bars represent mean expression of two biological replicates with one standard deviation. *bpeF* levels in strains with *P1.bpeS*<sub>K267T</sub> constructs were significantly elevated regardless of the presence or absence of *bpeT*. Although *bpeS* expression was increased in these isolates, it was not statistically different from the wild type control despite a minimum 5 fold increase. *bpeT* levels were not affected by the presence of mutant *bpeS*. \*\*\*\* =  $p < 0.0001$ , \*\*\* =  $p < 0.001$ , \*\* =  $p < 0.01$ .

#### 4.2.4 Mutation position in BpeS alters expression phenotypes of BpeF.

Comparisons of changes that may arise from lack of *bpeT* in strains overexpressing mutant BpeS were performed using two way ANOVA with Tukey's multiple comparison to assess inter-strain effects. No significant difference could be detected in expression levels of *bpeF* based on presence or absence of *bpeT* (data not shown). This would suggest that *bpeS* is the dominant force driving expression of the pump. However, a significant difference in *bpeF* transcript levels did exist in comparisons of strains expressing BpeS<sub>P28S</sub> vs BpeS<sub>K267T</sub> independent of strain background (**Fig. 4.2.5**). Strains encoding the BpeS<sub>K267T</sub> variant displayed significantly higher levels of *bpeF* mRNA than those with BpeS<sub>P28S</sub> variant despite there being no statistically significant difference between their *bpeS* expression levels. This may speak to the position of the respective mutations in the context of protein function. The P28S amino acid substitution is found within the N-Terminal DNA binding region of BpeS.<sup>8</sup> Alterations within the helix-turn-helix motif at this region may cause enhanced specificity to the binding region associated with *bpeEF-oprC* thereby promoting transcription in a manner not seen by simple overexpression of the protein in previous studies. The K267T substitution is located in the C-terminal domain necessary for putative protein-protein interaction and co-inducer binding in LysR-type regulatory proteins.<sup>8</sup> We previously hypothesized that in mutants encoding an S280P amino acid substitution in BpeT, a co-inducer independent state occurs because of changes to the C-terminus of the protein. This subsequently results in constitutive pump expression. It may be possible that the K267T mutation affects BpeS in a similar manner. Changes to the different domains of the BpeS protein may in turn lead to subtle variations in resistance and expression phenotypes observed, and may contribute to observed changes in resistance profiles through perturbations of the same regulatory mechanism in different ways.

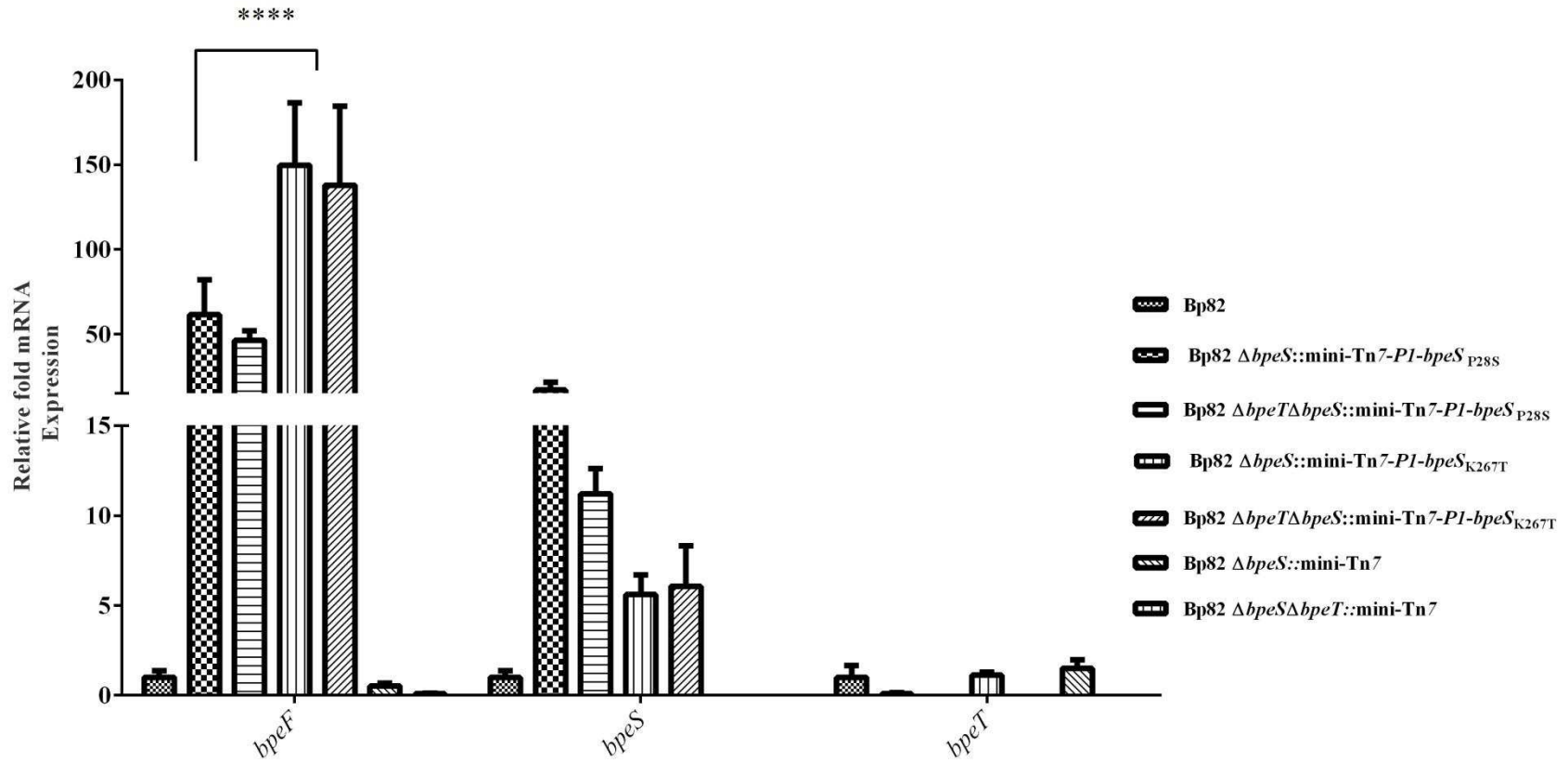


**Figure 4.2.5. Position of mutations in *bpeS* has an effect on expression of *bpeF*.**

Expression of *bpeF*, *bpeS*, and *bpeT* in Bp82 strains overexpressing either BpeS<sub>P28S</sub>, BpeS<sub>K267T</sub>, or carrying the empty mini-Tn7 was re-analyzed by Two-way ANOVA and Tukey's multiple comparison to assess the contribution of each mutation on expression of each gene. Bars represent mean expression fold change over Bp82 controls with one standard deviation in two biological replicates. Expression of *bpeF* is significantly different between P28S and K267T variants, while *bpeS* and *bpeT* expression are unaffected. \*\*\*\* =  $p < 0.0001$ , \*\*\* =  $p < 0.001$ , \*\* =  $p < 0.01$ .

#### 4.2.5 BpeT and BpeS are not required for pump substrate induction of *bpeEF-oprC* expression.

Wild-type Bp82 or Bp82 mutants lacking *bpeT*, *bpeS* or *bpeT* and *bpeS* (**Table 4.1.F**) were exposed to increasing concentrations of either trimethoprim, doxycycline or chloramphenicol and allowed to incubate for one hour before total RNA was extracted. The expression of *bpeF* mRNA was quantified through qRT-PCR in at least biological duplicate, and evaluated in GraphPad Prism V.6 by One-Way ANOVA and Dunnet's multiple comparisons

In the wild type strain, a dose dependent response to the presence of either chloramphenicol or doxycycline can be seen in *bpeF* levels that are significantly different to the control sample (**Fig. 4.2.6, panel A**). However, with 1h trimethoprim exposure, this trend is not observed. Only the highest dose of TMP produces a significant increase in *bpeF* expression. In strains lacking only *bpeT*, a similar response can be seen, with one hour exposure to either doxycycline or chloramphenicol causing significant increases in expression of *bpeF* in a concentration dependent manner (**Fig. 4.2.6, panel B**). Exposure to trimethoprim produces decreased levels of *bpeF* expression in these isolates.

In strains lacking only *bpeS*, a dose dependent trend similar to that of Bp82 is observed, while trimethoprim produces no significant response (**Fig. 4.2.7, panel A**). In the absence of both *bpeS* and *bpeT*, expression levels of *bpeF* in response to doxycycline or chloramphenicol were significantly increased as in wild type, *bpeT*, and *bpeS* deletion strains (**Fig. 4.2.7, panel B**). Two conclusions can be drawn from these results; an additional regulatory factor is responsible chloramphenicol and doxycycline related pump induction, and *bpeT* may specifically interact with trimethoprim to activate *bpeEF-oprC* expression. Neither protein appears to be responsible for expression of *bpeEF-oprC*, as induction occurs in the absence of both genes.

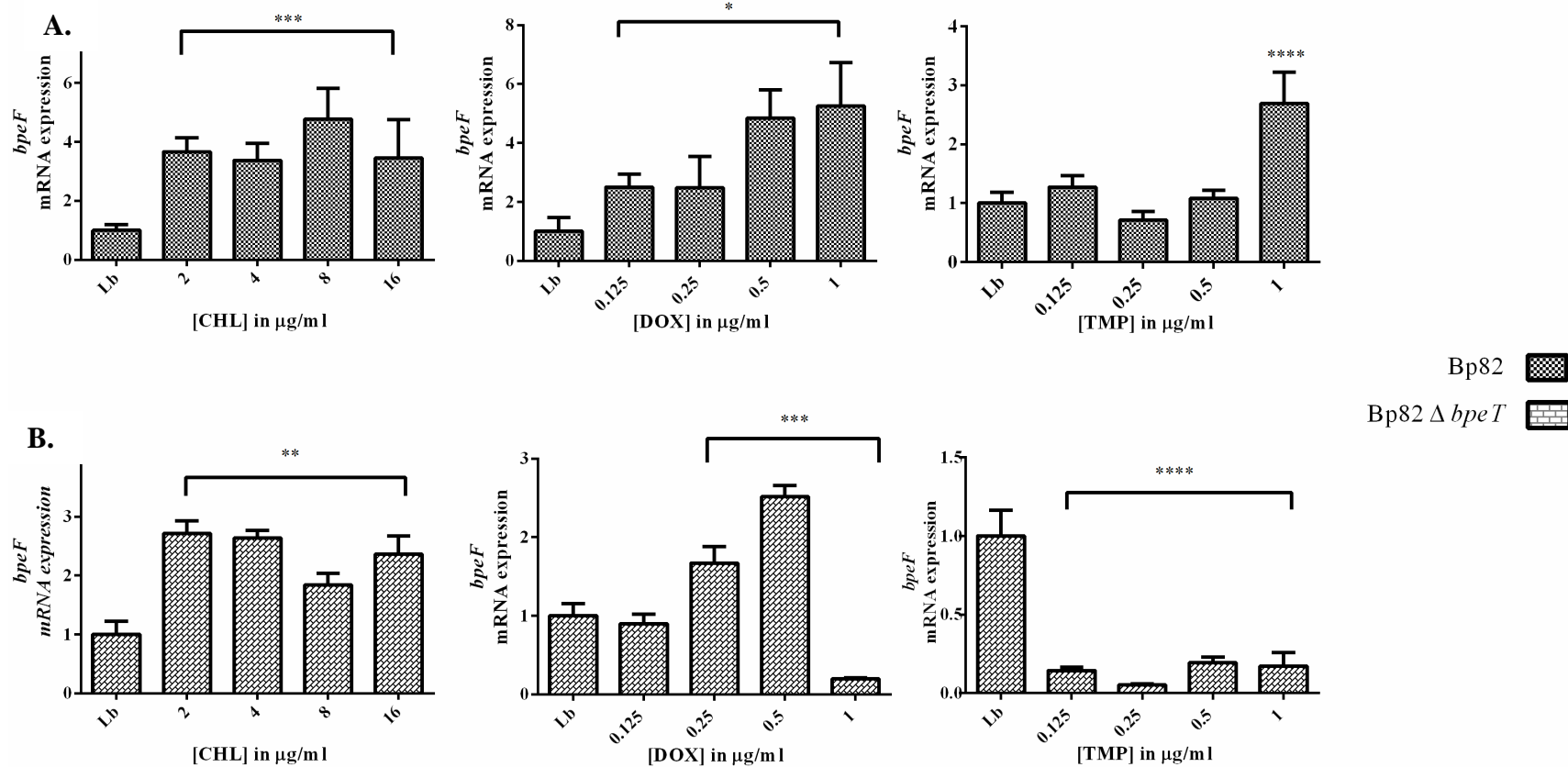


**Figure 4.2.6. *bpeT* is dispensable for efflux pump substrate mediated induction of *bpeF* expression.**

(A, crosshatched bars) Wild type or (B, brick pattern bars) Bp82 $\Delta$ *bpeT* was exposed to sub inhibitory concentrations of CHL, DOX or TMP for 1 h prior to RNA extraction. qRT-PCR analysis was performed to determine *bpeF* expression at each drug concentration. Bars depict mean fold change and one standard deviation of *bpeF* expression in comparison to the LB growth medium only control in a representative experiment. One-way ANOVA and Dunnet's multiple comparison were performed to determine significant differences from the LB only control. In every test except TMP, significantly elevated *bpeF* induction was observed in the absence of *bpeT*. \*\*\*\* =  $p < 0.0001$ , \*\*\* =  $p < 0.001$ , \*\* =  $p < 0.01$ , \* =  $p < 0.05$ . Abbreviations: CHL, chloramphenicol, DOX, doxycycline, TMP, trimethoprim.

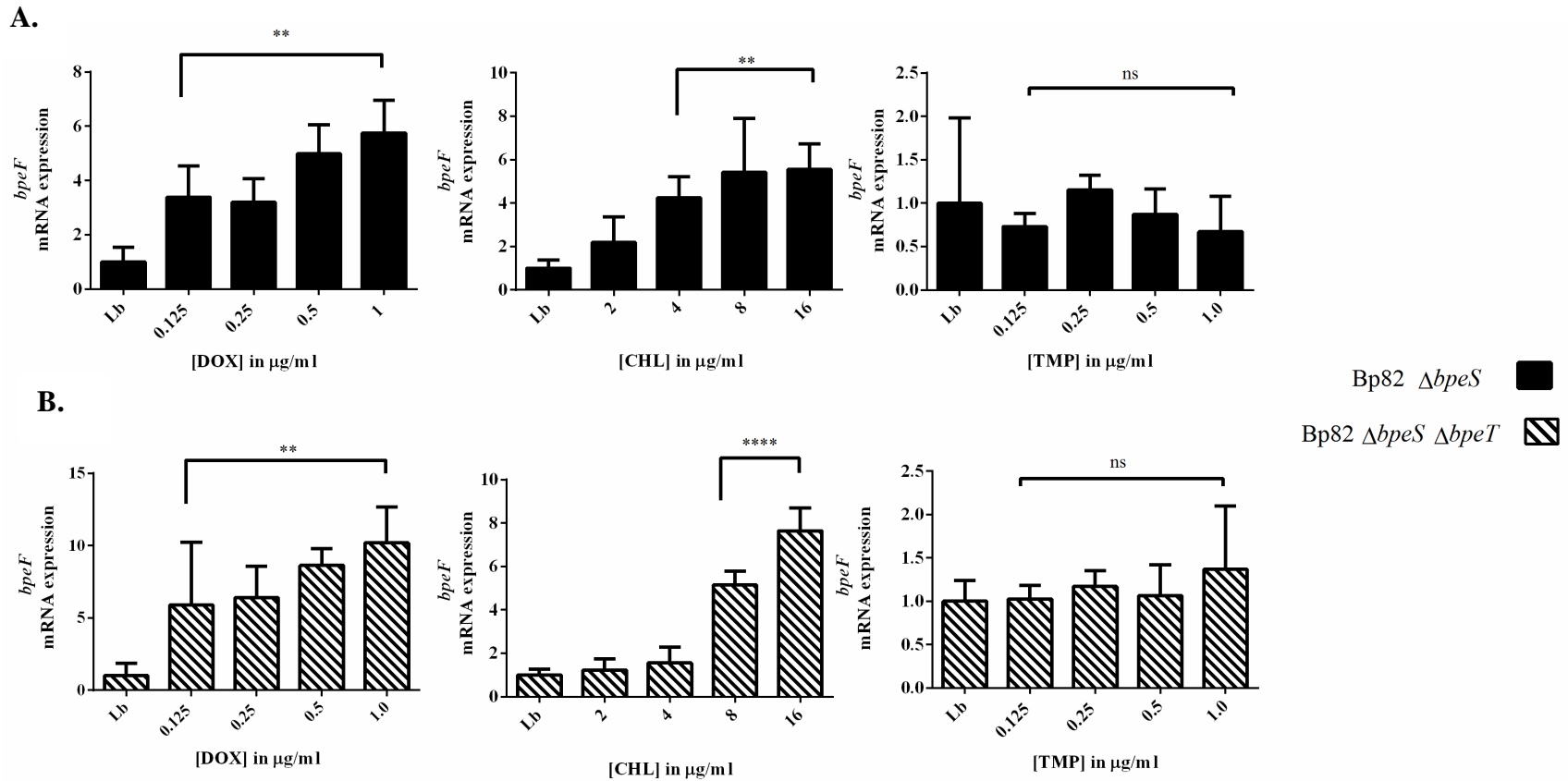


**Figure 4.2.7. *bpeS* is dispensable for efflux pump substrate mediated induction of *bpeF* expression.**

**A.** Bp82  $\Delta bpeS$ (solid bars), or **B.** Bp82  $\Delta bpeS \Delta bpeT$ (striped bars), was exposed to sub inhibitory concentrations of CHL, DOX or TMP for 1 h prior to RNA extraction. qRT-PCR analysis was performed to determine *bpeF* expression at each drug concentration. Bars depict mean fold change and one standard deviation of *bpeF* expression in comparison to the growth medium only control in two biological replicates. One-way ANOVA and Dunnet's multiple comparison were performed to determine significant differences from the LB only control. With the exception of TMP tests, significant *bpeF* expression occurred independent of both *bpeS* and *bpeT*. \*\*\*\* =  $p < 0.0001$ , \*\* =  $p < 0.01$ , Abbreviations: CHL, chloramphenicol, DOX, doxycycline, TMP, trimethoprim.

These data suggest that there is an additional mechanism in play controlling the expression of the efflux pump. If either BpeT or BpeS was the sole activator of pump transcription, loss of one or both regulators would result in abrogated pump expression, even in the presence of inducing pump substrates. While overexpression and mutation studies show that both BpeT and BpeS are important for the expression of the pump, the continued activation of pump expression in response to antibiotic exposure confirms that there is an additional regulatory factor able to manipulate BpeEF-OprC.

Attempts were made to identify the unknown regulatory mechanism by stepwise selection of a Bp82  $\Delta bpeS \Delta bpeT$  strain with co-trimoxazole, to isolate mutants with decreased susceptibility attributable to increased expression of BpeEF-OprC. The idea was that once these isolates were identified, BpeEF-OprC expression would be assessed, and those isolates displaying high levels of efflux pump expression would be sent for whole genome sequencing to identify mutations within novel regulatory genes. However, only two resistant isolates were obtained, and of these, none displayed increased expression of the *bpeEF-oprC* operon (data not shown).

It is most likely that mutations to the genes encoding proteins FoaA or FolP, the folate pathway targets of trimethoprim and sulfamethoxazole, are responsible for decreased susceptibility in this particular pool of mutants and that much higher throughput is necessary to isolate an efflux-related resistant isolate. The thought that such an isolate exists, and that we can identify the missing regulatory gene, also relies on the assumption that this network is solely based on DNA-protein interactions. This completely disregards the possibilities that regulation of BpeEF-OprC could also be rooted in post-transcriptional or post-translational modifications, and if so would not be detected by the methods currently employed.

#### 4.2.6 BpeS and BpeT form multimers.

It was hypothesized that changes in expression to *bpeEF-oprC* in the presence of mutations in *bpeS* or *bpeT* may be promoted by alterations in the ability of these proteins to form oligomeric structures. Members of the LysR-type regulatory protein family typically interact with their binding target by assembling into multimeric protein complexes, consisting of two to eight copies of a single protein.<sup>18–20</sup> Structural analysis of the LysR protein family suggests the presence of a protein oligomerization domain in the C-terminal region as well as a co-inducer binding domain.<sup>20,21</sup>

To assess how mutations in this region may alter protein-protein interaction, the native sizes of both wild type and mutant BpeT or BpeS were determined by both size exclusion chromatography (SEC) and native polyacrylamide gel electrophoresis. Low pressure SEC analysis was performed on purified recombinant BpeT and BpeS using plasmid DNA, ATP, and blue dextran to determine void and partition values for the column (**Fig. 4.2.8**).<sup>22</sup> A standard curve was generated using calculated partition coefficients for bovine serum albumin, yeast alcohol dehydrogenase, sweet potato  $\beta$ -amylase, horse heart cytochrome C oxidase, and bovine erythrocyte carbonic anhydrase, ranging from 12.4 kDa to 200,000 kDa in size. All standards and samples were filtered under identical conditions, and time-on-column was monitored by UV peak detection at 280 nm.

For BpeT samples, two peaks were detected, one with a calculated partition coefficient correlating to a molecular weight of 66 kDa, consistent with the formation of a dimer. The second peak had a calculated molecular weight of under 15 kDa, and may be indicative of a contaminant protein in the BpeT sample, or of protein degradation. Three peaks were detected in BpeS samples, with molecular weights estimated at approximately 12, 34 and 202 kDa. The

presence of a peak below the estimated weight of 35-37 kDa is most likely again the result of either protein degradation or a contaminating protein carried over from the purification process. It is interesting to note the absence of the monomeric form of BpeT. With SDS-PAGE analysis, this protein displays a single band at approximately 37 kDa, which is consistent with the size predicted by the amino acid sequence. However, this peak was not detected in our initial attempts at gel chromatography. This could be caused by a high affinity for the protein to aggregate into a dimeric form, or improper chromatography conditions that prevented dissociation of the native monomer while in solution.

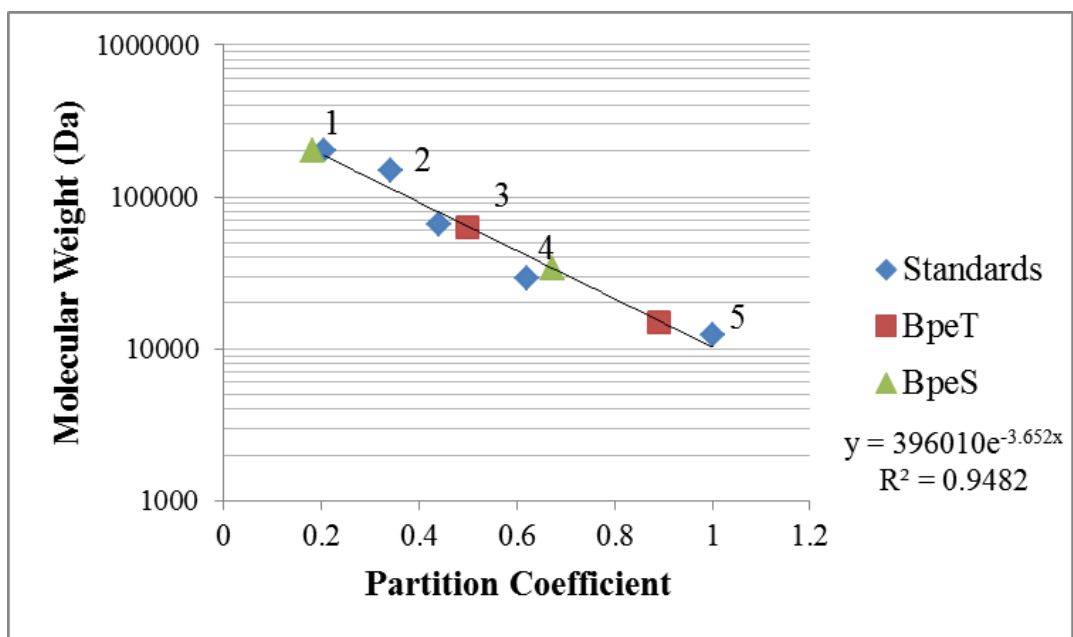


**Figure 4.2.8. Molecular weight characterization of BpeS and BpeT by size exclusion chromatography shows both proteins form multimers.**

Low pressure SEC analysis of recombinant standards (1-5) was conducted under native conditions. The average partition coefficient of each standard was calculated and used to generate a standard curve relating partition coefficient to molecular weight. Two replicate samples of purified 6x histidine tagged BpeS or BpeT were filtered on the same column and their molecular weight was calculated using the standard curve. BpeS was detected in both monomer and hexamer forms at 34 kDa and ~202 kDa, while BpeT was detected in dimer form at ~ 66 kDa. The predicted molecular weight of BpeT-6xHis is 38 kDa, while BpeS-6xHis is 36.3 kDa. **Standards:** 1.  $\beta$ -amylase, 200 kDa, 2. Alcohol dehydrogenase, 150 kDa, 3. Bovine serum albumin, 66 kDa 4. Carbonic anhydrase, 29 kDa 5. Cytochrome C oxidase, 12.4 kDa

#### 4.2.7 Mutations causing elevated pump expression do not influence multimer formation of BpeT or BpeS.

To assess possible changes in multimer formation caused by BpeS and BpeT mutations, these samples were analyzed by native gel electrophoresis and silver staining (Figs. 4.2.9 and 4.2.10). In BpeT samples, strong bands at approximately 110 kDa, 420 kDa and 500 kDa are visible, possibly correlating to the formation of a protein trimer and 12-mer using the calculated 38 kDa weight of BpeT-6xHis. While the 110 kDa band is most likely a naturally forming complex, it is possible that the larger forms are the products of non-specific interactions caused by aggregation. However, these bands lack the laddering stain pattern typically associated with

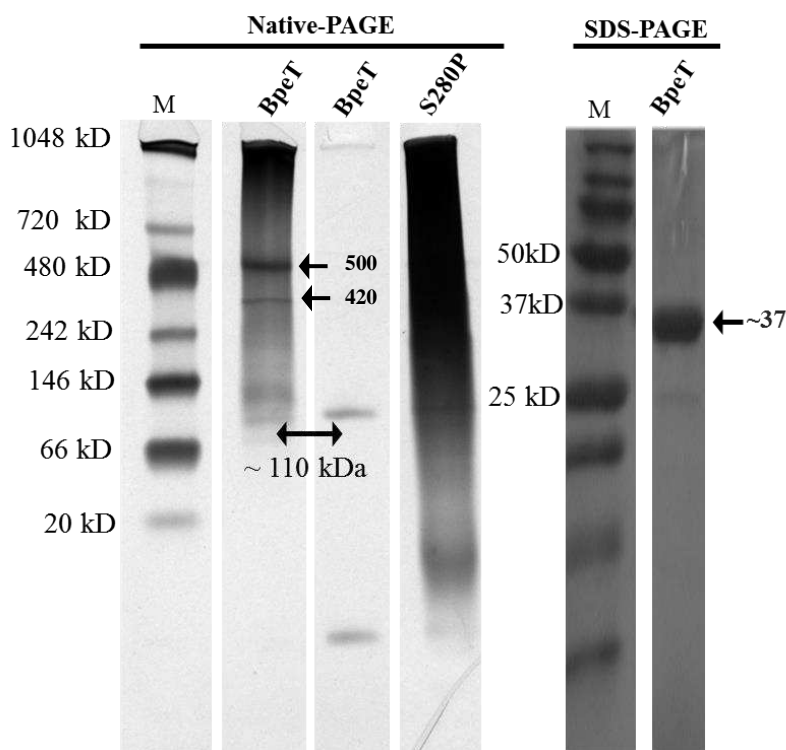


**Figure 4.2.9. BpeT forms high molecular weight complexes under native conditions.** **Left panel:** 500 ng of BpeT or BpeT<sub>S280P</sub> recombinant protein was loaded on to a 4-20% TGX native gel and detected with silver stain. Size was determined by comparison to a Native Mark standard. Large complexes are visible at 110, 420 and 500 kDa. **Right panel:** 1 µg of purified the same BpeT batch was heat-denatured, analyzed on a 12% SDS polyacrylamide gel and stained with Coomassie blue. Although the monomer is close to the predicted size of 38 kDa under denaturing conditions, it is not detected during native PAGE

detection of non-functional protein aggregates that form as a result of heat. It is also important to note that these high-order bands also appear at sizes that could be comprised of a dimer or trimer of trimers, as opposed to individual monomers combining in a range of sizes. The formation of these large complexes has been cited as a cause of insolubility at high concentrations in other LysR family proteins, and may be responsible for the bands we detected above 300 kDa.<sup>43</sup> No free monomer is detectable although a clear ~37-38 kDa band is detectable by SDS-PAGE analysis shown in the right panel of Figs. 4.2.9 and 4.2.10. This correlates to the inability to detect a peak at this same size through SEC analysis, despite the slightly different distribution of detectable protein sizes.

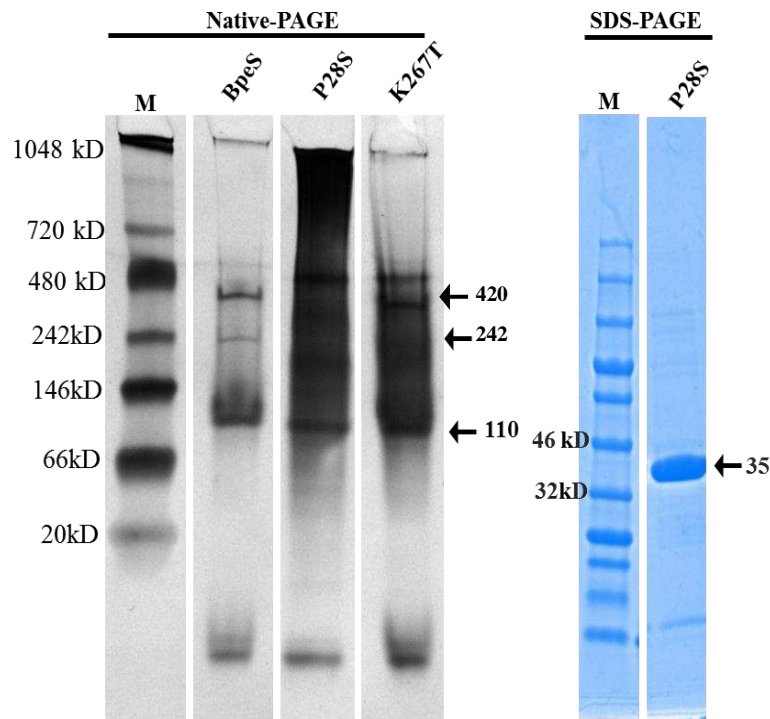


**Figure 4.2.10. BpeS and BpeS mutants form high molecular weight complexes under native conditions.** **Left panel:** 500 ng of BpeS or BpeS<sub>P28S</sub>, or BpeS<sub>K267T</sub> recombinant protein were loaded on to a 4-20% TGX native gel and proteins and their complexes were detected with silver stain. Sizes were determined by comparison to a Native Mark standard. Large complexes are present at 110, 242 and 420 kDa **Right panel:** 10  $\mu$ l of the same BpeS<sub>P28S</sub> purification batch was heat-denatured and subjected to SDS-PAGE on a 4-20% TGX gel before staining with Coomassie blue. Although the monomer is close to the predicted size of 36 kDa under denaturing conditions, it is not detected during native PAGE.

In wild type BpeS samples, a band is detected at 110, 242 kDa and 420 kDa. These oligomers would correspond to protein formations containing 3, 6 and 12 copies of the 36 kDa hexa-histidine tagged monomer. In both BpeS<sub>P28S</sub> and BpeS<sub>K267T</sub> samples a distinct 110 kDa band is detectable, but larger forms are less clear due to heavy staining from 110 kDa to ~ 500 kDa resulting in a partial smear, thus suggesting our initial hypothesis was incorrect. These samples were concentrated 10-fold prior to loading on the native gel, as their purified concentrations were low. It is possible that this manipulation caused aggregates to form, or that the concentration estimates of samples extrapolated from initial BCA protein quantities was inaccurate, leading to overloading. Repeated SEC analysis may be necessary for confirmation.

#### **4.2.8 Mutations to BpeT and BpeS alter global gene expression of *B. pseudomallei***

It was hypothesized that BpeS may act to alter transcriptional network phenotypes. However, it was unknown if this would be due to metabolic changes brought on by over-expression of the pump, or if BpeS and BpeT are capable of targeting multiple operons in a fashion similar to the MexT-MexS regulatory scheme of *Pseudomonas aeruginosa*<sup>23</sup>. To determine if either BpeS or BpeT exhibit a global regulatory affect, Next-generation RNA sequencing and analysis was used. Differential expression analysis revealed that in both mutant BpeS and BpeT samples, the expression of a large number of genes was altered in comparison to wild-type (**Fig. 4.2.11**). Alterations in expression of the *bpeEF-oprC* operon were observed in all samples but Bp82 and were used as an internal control to confirm the accuracy of the analysis across two biological replicates. However, while each gene of this operon was upregulated in each mutant sample, not all the expression levels were deemed significant in all samples. This was probably based on sequence quality of one mate pair precluding some transcripts from statistical analysis, or their false-discovery rate (FDR) adjusted P value.

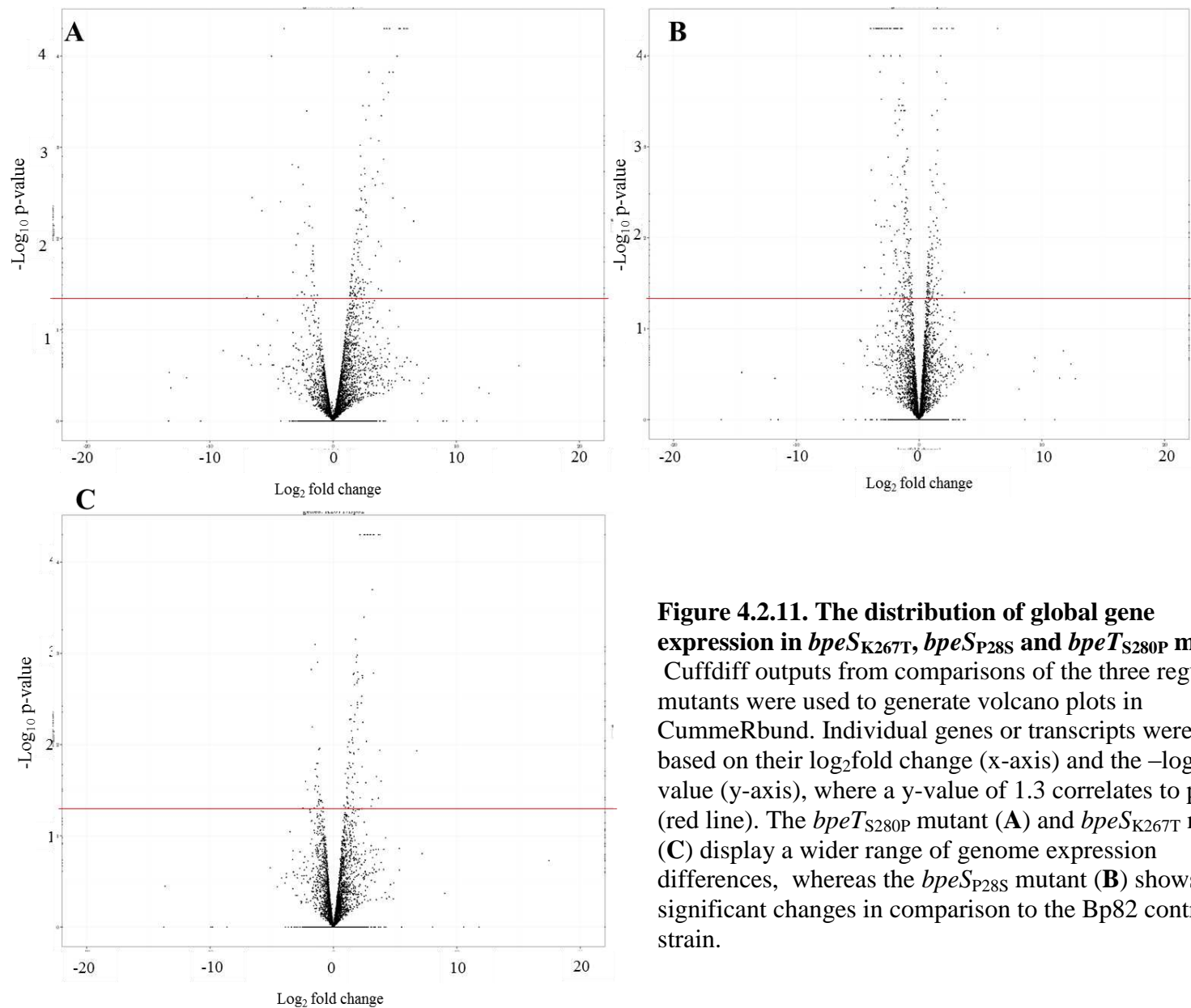


**Figure 4.2.11. The distribution of global gene expression in *bpeS*<sub>K267T</sub>, *bpeS*<sub>P28S</sub> and *bpeT*<sub>S280P</sub> mutants.** Cuffdiff outputs from comparisons of the three regulatory mutants were used to generate volcano plots in CummeRbund. Individual genes or transcripts were plotted based on their  $\text{log}_2$ fold change (x-axis) and the  $-\text{log}_{10}$ p-value (y-axis), where a y-value of 1.3 correlates to  $p=0.05$  (red line). The *bpeT*<sub>S280P</sub> mutant (A) and *bpeS*<sub>K267T</sub> mutant (C) display a wider range of genome expression differences, whereas the *bpeS*<sub>P28S</sub> mutant (B) shows more significant changes in comparison to the Bp82 control strain.

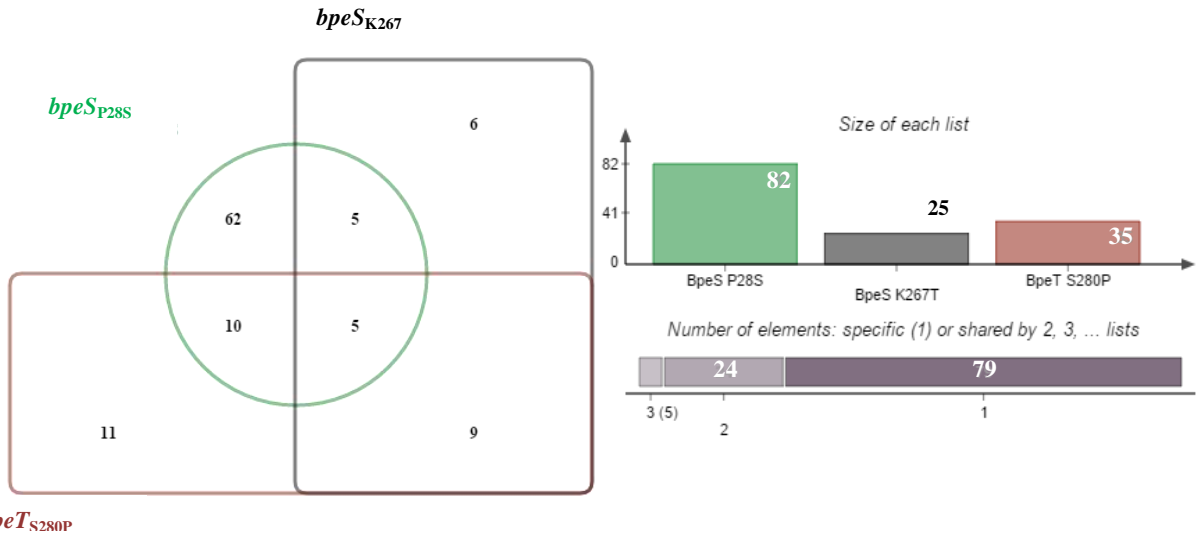


**Figure 4.2.12. *bpeT* and *bpeS* mutants show significantly altered global gene expression.**

A list of significantly altered genes was compiled from the large Cuffdiff gene expression output. Only 5 genes were significantly upregulated in all samples, including *bpeF*.

A much reduced list of significantly altered genes was generated, and submitted for Kegg pathway analysis and gene function annotation (**Appendix, Tables A2-5**). Perhaps most interestingly, significantly altered expression levels were detected in genes associated with the Type 3 secretion system cluster 3 (T3SS-3 or *Burkholderia* secretion apparatus, *bsa*) known to be required for cell invasion, intracellular persistence and virulence. Also commonly upregulated were genes associated with cell stress, including several chaperone proteins that could be indicative of the effects of dysregulated transcriptional and translational responses triggered by upregulated BpeEF-OprC expression. Overall, there were a relatively small number of genes shared among the mutants (**Fig. 4.2.12**), while the *bpeS*<sub>P28S</sub> mutation seemed to elicit the largest significant change across the genome. The majority of shared genes were involved in cell metabolism and the stress response. A full listing of the genes displaying altered expression, and their annotation, is provided in the Appendix. To confirm the results of RNA seq analysis, a subset of these genes were analyzed by qRT-PCR using primers adapted from a study on the *Bsa* T3SS, *fliC*, and *dnaK*, using 23S rRNA as a control calibrator.<sup>24</sup>

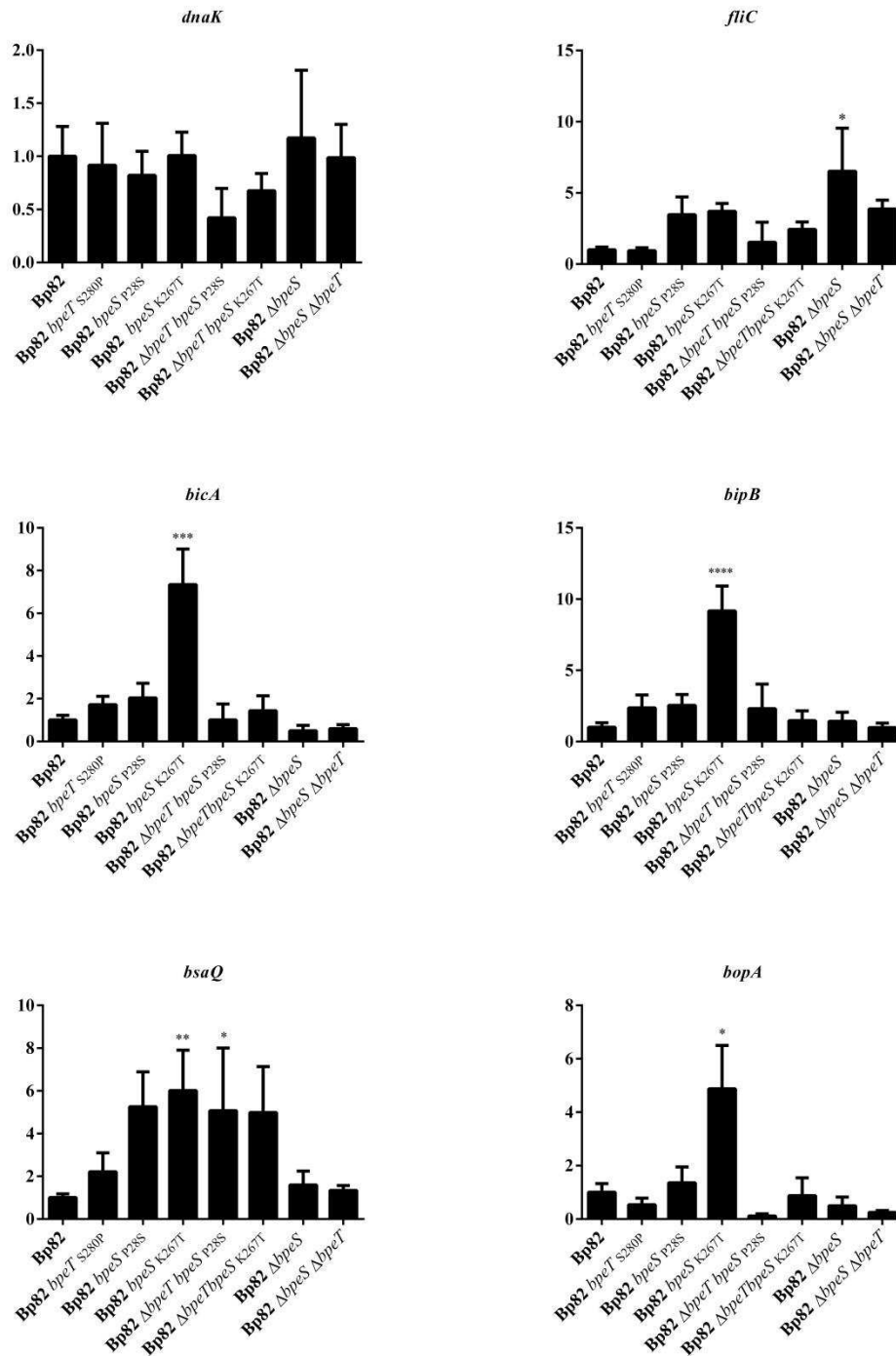


**Figure 4.2.13. *bpeS* mutations cause upregulation of the *Bsa* Type III secretion system of *Bp*.** To confirm the results of RNA-Seq analysis, qRT-PCR was performed on a subset of significantly altered T3SS-3 genes using *dnaK* as an additional internal control for constant expression. Bars represent mean expression with standard error of at least two biological replicates in technical triplicate. Two-way ANOVA with Dunnet's post test was utilized to determine statistical differences from the Bp82 control. In all T3SS-3 targets, mutations to *bpeS* resulted in significant upregulation compared to Bp82. \*\*\*\*= $p < 0.0001$ , \*\*\*= $p < 0.001$ , \*\*= $p < 0.01$ , \*= $p < 0.05$ .

Strains with amino acid substitutions to BpeS or BpeT were re-analyzed, as were *bpeS<sub>P28S</sub>ΔbpeT* and *bpeS<sub>K267T</sub>ΔbpeT*, and *ΔbpeTΔbpeS* Bp82 mutants. In all BpeS<sub>K267T</sub> strains, including those lacking *bpeT*, significantly increased expression of genes associated with T3SS-3 was observed, while *dnaK* and *fliC* remained unchanged from wild type Bp82 (**Fig. 4.2.13**). BpeS<sub>P28S</sub> strains with or without *bpeT* also displayed increased expression of genes associated with structural and secreted elements of the T3SS-3. However, these levels were not high enough to be considered statistically different from the Bp82 control. A strain-to-strain analysis followed by Tukey's post test showed that with the exception of *fliC* in Bp82 *ΔbpeS*, only strains with mutations to *bpeS* and intact *bpeT* produced T3SS-3 expression levels that were truly different from those measured in other backgrounds (**Fig. 4.2.15**). This is most noticeable in *bpeS<sub>K267</sub>* isolates; in the absence of *bpeT*, transcript levels of *bicA*, *bipB*, and *bopA* all decrease to at least half their expression in the *bpeT<sup>+</sup>* isolate. Despite this observation, there is a noticeable trend towards increased transcript of *bsaQ* in all BpeS mutants. The *bsaQ* gene encodes an exporter protein essential for the extrusion of the effector protein BopA through translocon BipB, allowing it to be modified by chaperone BicA.<sup>24-27</sup>

The increased expression of these genes in response to *bpeS*, but not *bpeT*, mutations suggests that the altered transcriptional response is due directly to BpeS interaction with T3SS-3 regulatory cascade. Transcriptional control by BpeS<sub>K267T</sub> could aberrantly prompt utilization of a different set of adaptation mechanisms e.g. those needed for host persistence, regardless of environmental cues caused by co-inducer independence. It is important to note that these observations deal only with expression of virulence factors *in vitro* and may not correlate to alterations in the ability of *Bp* to infect the host. Further testing is essential to determine if such transcriptional modulations have any effect on fitness during host or environmental persistence.

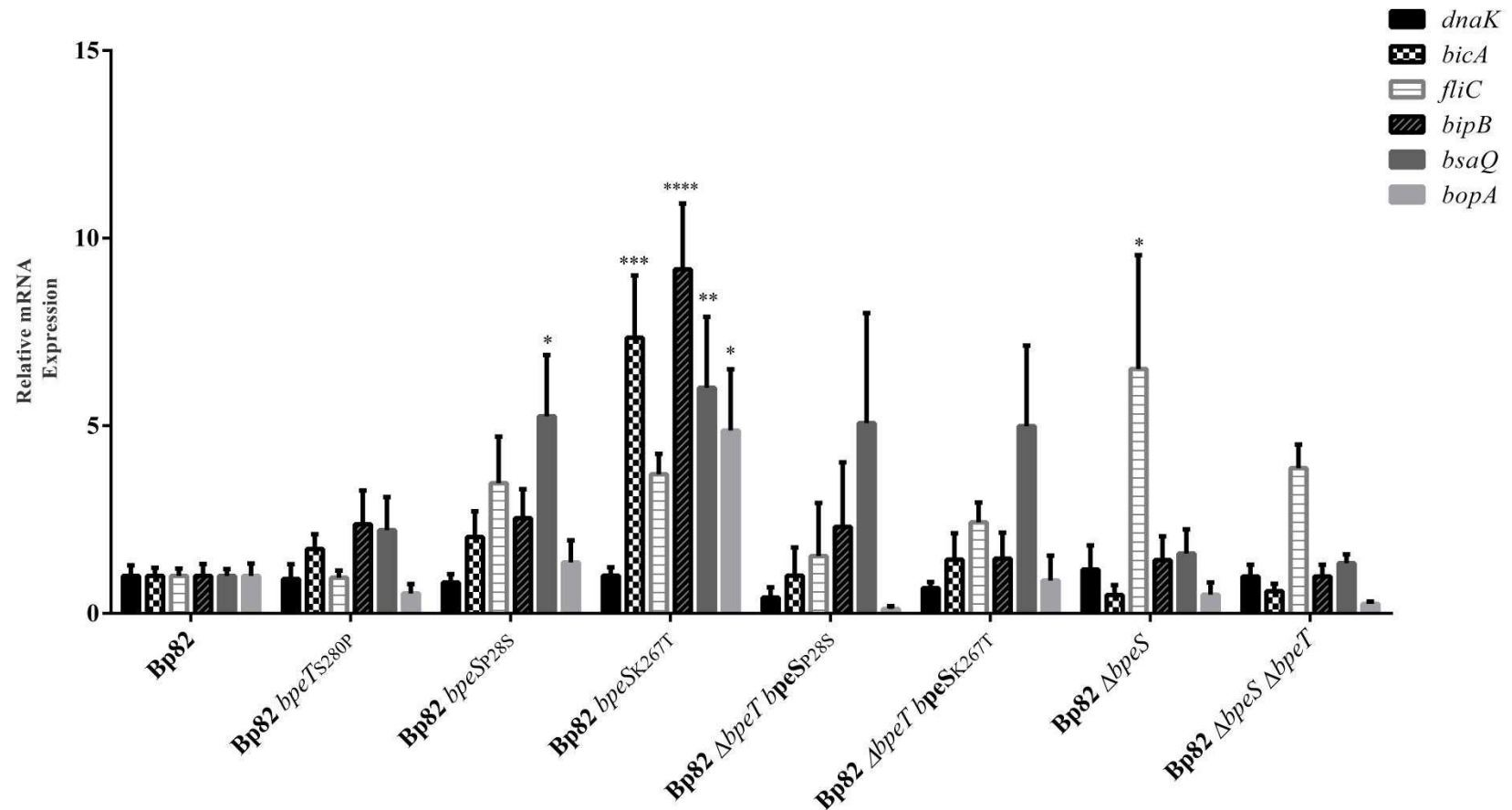


**Figure 4.2.14. Virulence related gene expression depends on the presence of BpeS.** The gene expression results of T3SS-3 in Bp82 isolates with mutations to *bpeS* or *bpeT* were reanalyzed by Two-Way ANOVA and Tukey's multiple comparison test to assess dependency on strain background. *bpe*<sub>SK267T</sub> displayed markedly higher expression of all genes except control target *dnaK*. Increases in the relative quantity of *bsaQ* are tied to the presence of *bpeS*. \*\*\*=  $p < 0.001$ , \*\* =  $p < 0.01$ , \* =  $p < 0.05$ .

### 4.3 Conclusions

Alterations to the amino acid sequence of BpeS and BpeT appear to play a major role not only in changing expression of the genes encoding the BpeEF-OprC efflux pump, but highlight the ability of BpeS to interact with other genes and operons on a global scale. What remains unclear is the mechanism by which these mutations cause transcriptional changes to occur, and what the complete role of the proteins might be in their native state. Our investigations into native size and oligomer formation showed no discernable difference between wild type or mutant forms of either protein (**Figs. 4.2.8 to 4.2.10**). As the LysR-type regulatory protein family is known to interact with a co-inducer at the C-terminus of the protein, it may be possible that the sequence divergence of BpeT and BpeS may alter their substrate specificity.<sup>20,28</sup> The loss of rapid TMP inducibility in strains lacking *bpeT* combined with the constitutive activation of the pump in BpeT<sub>S280P</sub> mutants may point to a direct interaction between BpeT and trimethoprim.

The differences in substrate specificity may also explain the seemingly redundant nature of BpeT and BpeS, demonstrated by their shared role in hyper-expression of *bpeEF-oprC* and continued induction of pump gene expression after their deletion (**Figs. 4.2.6 to 4.2.7**). It is possible that BpeS and BpeT promote homeostasis by interacting with specific environmental compounds to activate the pump at different times and conditions. This is supported by the broad specificity of the pump itself, as well as the continued induction of pump gene expression even after loss of both currently identified regulatory genes. The inability of BpeS to act as a direct activator solely by overexpression (**Fig 4.2.2**), and apparent existence of an additional regulatory factor reinforce this mechanism.

Mutations to *bpeT* and *bpeS* alter not only the expression of the BpeEF-OprC pump, but play a larger role in manipulating the global transcriptional response of *Bp*. Previous studies into

the effects of antimicrobial resistance on cell fitness in other species had noted changes on global transcriptional networks both promoting, and in response to, highly upregulated efflux operon expression. In *P. aeruginosa*, the MexEF-OprN RND family efflux pump follows such a scheme, in which the efflux pump is controlled in part by MexT and MexS.<sup>29–32</sup> The gene encoding the LysR regulatory MexT is immediately upstream of the *mexEF-oprN* operon, and is flanked by oxido-reductase MexS. Both proteins are involved in control of efflux pump operon expression as disruption of either gene results in hyper-expression of MexEF-oprN, though it remains unclear if this can occur independent of MexT.<sup>30,31</sup> This is similar to overexpression of *bpeEF-oprC* we observed as the result *bpeS* and *bpeT* mutations, although the proteins share more functional than sequence homology with their *P.aeruginosa* counter-parts.

Perhaps most relevant to our latest findings is that MexT is also known to repress virulence and host colonization genes, specifically *P. aeruginosa*'s lone T3SS, pyocyanin production, and early host cell attachment factors.<sup>23,33,34</sup> This may be reminiscent of the mutant BpeS dependent de-repression of T3SS genes we observed through RNA-seq and qRT-PCR analysis (**Fig 4.2.11 to 4.2.14**). However, in *Bp*, this may be linked to co-inducer independence leading to constitutive activation as opposed to direct repression. In *P.aeruginosa*, these processes are linked to the redox state of the cell, and may be a product of a global regulatory shift necessary to switch between host and environmental lifestyles.<sup>23,29,35</sup> This is evidenced by the complexity of currently known factors controlling expression of MexEF-OprN, ranging from direct repression by H-NS family protein MvaT known to control many other virulence genes, to indirect activation by two component regulatory system ParRS needed for lifestyle adaptation and direct activation by biofilm linked MerR family protein BrlR.<sup>34,36–40</sup>

This study represents a preliminary investigation into the connection between BpeEF-OprC efflux and virulence factors in *B.pseudomallei*. While it is tempting to suggest that BpeS and BpeT could act in a fashion similar to that of MexS and MexT in *P. aeruginosa*, only one target operon other than *bpeEF-oprC* has been confirmed. Additionally, no examination of the cell stress response or redox state under conditions where BpeEF-OprC is overexpressed has taken place, although changes in expression of nitrogen metabolism genes and genes encoding chaperone protein were noted in RNA-seq results (**Appendix, Tables A.2 to A.5**). As no increases in TSS-3 genes were observed in strains lacking *bpeS* via qRT-PCR, it is probable that there are many additional factors at play, and that *bpeS* only contributes to regulation of TSS-3 under very specific circumstances.

Also, while transcriptional changes to some genes may theoretically enhance virulence, e.g. increased BopA secretion and autophagy evasion, it remains unknown if any associated fitness cost would prevent this from occurring in-vivo.<sup>26</sup> Cell infection, invasion and cytotoxicity studies, as well as qRT-PCR analysis of other altered genes need to be conducted. In order to understand the biological significance of these observations it is necessary to examine the expression of more operons identified by RNA-seq analysis, as well as the effects of mutations to BpeS and BpeT on *Bp*'s ability to infect a host cell.

## Chapter 4 References

1. Podnecky, N. L., Wuthiekanun, V., Peacock, S. J. & Schweizer, H. P. The BpeEF-OprC efflux pump is responsible for widespread trimethoprim resistance in clinical and environmental *Burkholderia pseudomallei* isolates. *Antimicrob. Agents Chemother.* **57**, 4381-4386 (2013). doi:10.1128/AAC.00660-13
2. Podnecky, N. L., Rhodes, K. A. & Schweizer, H. P. Efflux pump-mediated drug resistance in *Burkholderia*. *Front. Microbiol.* **06**, (2015).
3. Randall, L. B., Dobos, K., Papp-Wallace, K. M., Bonomo, R. A. & Schweizer, H. P. Membrane bound PenA  $\beta$ -lactamase of *Burkholderia pseudomallei*. *Antimicrob. Agents Chemother.* **60**, 1509-1514 (2015). doi:10.1128/AAC.02444-15
4. Lopez, C. M., Rholl, D. A., Trunck, L. A. & Schweizer, H. P. Versatile dual-technology system for markerless allele replacement in *Burkholderia pseudomallei*. *Appl. Environ. Microbiol.* **75**, 6496–6503 (2009).
5. Choi, K.-H. *et al.* A Tn7-based broad-range bacterial cloning and expression system. *Nat. Methods* **2**, 443–448 (2005).
6. Choi, K.-H. *et al.* Genetic tools for select-agent-compliant manipulation of *Burkholderia pseudomallei*. *Appl. Environ. Microbiol.* **74**, 1064–1075 (2008).
7. Liss, L. New M13 host: DH5F' competent cells. *Focus* **9**, (1987).
8. Clinical and Laboratory Standards Institute. 2015. Performance standards for antimicrobial susceptibility testing: twenty-fifth informational supplement M100-S25., Wayne, PA.
9. Blankenberg, D. *et al.* Galaxy: a web-based genome analysis tool for experimentalists. *Curr. Protoc. Mol. Biol. Ed. Frederick M Ausubel Al Chapter 19, Unit 19.10.1–21 (2010).*

10. Goecks, J., Nekrutenko, A., Taylor, J. & Galaxy Team. Galaxy: a comprehensive approach for supporting accessible, reproducible, and transparent computational research in the life sciences. *Genome Biol.* **11**, R86 (2010).
11. Giardine, B. *et al.* Galaxy: a platform for interactive large-scale genome analysis. *Genome Res.* **15**, 1451–1455 (2005).
12. Patel, R. K. & Jain, M. NGS QC Toolkit: a toolkit for quality control of next generation sequencing data. *PLoS ONE* **7**, e30619 (2012).
13. Langmead, B., Trapnell, C., Pop, M. & Salzberg, S. L. Ultrafast and memory-efficient alignment of short DNA sequences to the human genome. *Genome Biol.* **10**, R25 (2009).
14. Trapnell, C. *et al.* Transcript assembly and quantification by RNA-Seq reveals unannotated transcripts and isoform switching during cell differentiation. *Nat. Biotechnol.* **28**, 511–515 (2010).
15. Trapnell, C. *et al.* Differential gene and transcript expression analysis of RNA-seq experiments with TopHat and Cufflinks. *Nat. Protoc.* **7**, 562–578 (2012).
16. Trapnell, C. *et al.* Differential analysis of gene regulation at transcript resolution with RNA-seq. *Nat. Biotechnol.* **31**, 46–53 (2012).
17. Schlager, B., Straessle, A. & Hafen, E. Use of anionic denaturing detergents to purify insoluble proteins after overexpression. *BMC Biotechnol.* **12**, 95 (2012).
18. Ruangprasert, A., Craven, S. H., Neidle, E. L. & Momany, C. Full-length structures of BenM and two variants reveal different oligomerization schemes for LysR-type transcriptional Regulators. *J. Mol. Biol.* **404**, 568–586 (2010).
19. Gong, W., Xiong, G. & Maser, E. Oligomerization and negative autoregulation of the LysR-type transcriptional regulator HsdR from *Comamonas testosteroni*. *J. Steroid Biochem. Mol.*

*Biol.* **132**, 203–211 (2012).

20. Maddocks, S. E. & Oyston, P. C. F. Structure and function of the LysR-type transcriptional regulator (LTTR) family proteins. *Microbiology* **154**, 3609–3623 (2008).
21. Deghmane, A.-E. & Taha, M.-K. The *Neisseria meningitidis* adhesion regulatory protein CrgA acts through oligomerization and interaction with RNA polymerase: Functional organization of *N. meningitidis* CrgA. *Mol. Microbiol.* **47**, 135–143 (2002).
22. Chuanchuen, R., Gaynor, J. B., Karkhoff-Schweizer, R. & Schweizer, H. P. Molecular characterization of MexL, the transcriptional repressor of the *mexJK* multidrug efflux operon in *Pseudomonas aeruginosa*. *Antimicrob. Agents Chemother.* **49**, 1844–1851 (2005).
23. Jin, Y., Yang, H., Qiao, M. & Jin, S. MexT regulates the Type III Secretion System through MexS and PtrC in *Pseudomonas aeruginosa*. *J. Bacteriol.* **193**, 399–410 (2010).
24. Sun, G. W. *et al.* Identification of a regulatory cascade controlling Type III Secretion System 3 gene expression in *Burkholderia pseudomallei*. *Mol. Microbiol.* **76**, 677–689 (2010).
25. Muangsombut, V. *et al.* Inactivation of *Burkholderia pseudomallei* *bsaQ* results in decreased invasion efficiency and delayed escape of bacteria from endocytic vesicles. *Arch. Microbiol.* **190**, 623–631 (2008).
26. Gong, L. *et al.* The *Burkholderia pseudomallei* Type III Secretion System and BopA Are required for evasion of LC3-associated phagocytosis. *PLoS ONE* **6**, e17852 (2011).
27. Galyov, E. E., Brett, P. J. & DeShazer, D. Molecular insights into *Burkholderia pseudomallei* and *Burkholderia mallei* pathogenesis. *Annu. Rev. Microbiol.* **64**, 495–517 (2010).
28. Schell, M. A. Molecular biology of the LysR family of transcriptional regulators. *Annu. Rev. Microbiol.* **47**, 597–626 (1993).
29. Fetar, H. *et al.* *mexEF-oprN* multidrug efflux operon of *Pseudomonas aeruginosa*: regulation

- by the MexT activator in response to nitrosative stress and chloramphenicol. *Antimicrob. Agents Chemother.* **55**, 508–514 (2011).
30. Uwate, M. *et al.* Two routes of MexS-MexT-mediated regulation of MexEF-OprN and MexAB-OprM efflux pump expression in *Pseudomonas aeruginosa*: Two routes of *mexEF-oprN* regulation. *Microbiol. Immunol.* **57**, 263–272 (2013).
31. Sobel, M. L., Neshat, S. & Poole, K. Mutations in PA2491 (*mexS*) promote MexT-dependent *mexEF-oprN* expression and multidrug resistance in a clinical strain of *Pseudomonas aeruginosa*. *J. Bacteriol.* **187**, 1246–1253 (2005).
32. Maseda, H., Uwate, M., & Nakae, T. Transcriptional regulation of the *mexEF-oprN* multidrug efflux pump operon by MexT and an unidentified repressor in *nfxc*-type mutant of *Pseudomonas aeruginosa*. *FEMS Microbiol. Lett.* **311**, 36–43 (2010).
33. Tian, Z.-X. *et al.* MexT modulates virulence determinants in *Pseudomonas aeruginosa* independent of the MexEF-OprN efflux pump. *Microb. Pathog.* **47**, 237–241 (2009).
34. Zaoui, C. *et al.* An orphan sensor kinase controls quinolone signal production via MexT in *Pseudomonas aeruginosa*. *Mol. Microbiol.* **83**, 536–547 (2012).
35. Fargier, E. *et al.* MexT functions as a redox-responsive regulator modulating disulfide stress resistance in *Pseudomonas aeruginosa*. *J. Bacteriol.* **194**, 3502–3511 (2012).
36. Westfall, L. W. *et al.* *mvaT* mutation modifies the expression of the *Pseudomonas aeruginosa* multidrug efflux operon *mexEF-oprN*. *FEMS Microbiol. Lett.* **255**, 247–254 (2006).
37. Li, X.-Z., Plésiat, P. & Nikaido, H. The challenge of efflux-mediated antibiotic resistance in Gram-negative bacteria. *Clin. Microbiol. Rev.* **28**, 337–418 (2015).
38. Liao, J., Schurr, M. J. & Sauer, K. The MerR-Like regulator BrIR confers biofilm tolerance by activating multidrug efflux pumps in *Pseudomonas aeruginosa* biofilms. *J. Bacteriol.* **195**,

3352–3363 (2013).

39. Wang, D., Seeve, C., Pierson, L. S. & Pierson, E. A. Transcriptome profiling reveals links between ParS/ParR, MexEF-OprN, and quorum sensing in the regulation of adaptation and virulence in *Pseudomonas aeruginosa*. *BMC Genomics* **14**, 618 (2013).

40. Balasubramanian, D. *et al.* Deep sequencing analyses expands the *Pseudomonas aeruginosa* AmpR regulon to include small RNA-mediated regulation of iron acquisition, heat shock and oxidative stress response. *Nucleic Acids Res.* (2013). doi:10.1093/nar/gkt942

41. DeShazer, D. & Woods, D. E. Broad-host-range cloning and cassette vectors based on the R388 trimethoprim resistance gene. *BioTechniques* **20**, 762–764 (1996).

42. Damron, F. H. *et al.* Construction of mobilizable mini-Tn7 vectors for bioluminescent detection of Gram-negative bacteria and single-copy promoter lux reporter analysis. *Appl. Environ. Microbiol.* **79**, 4149–4153 (2013).

43. Ezezika, O. C., Haddad, S., Neidle, E. L. & Momany, C. Oligomerization of BenM, a LysR-type transcriptional regulator: structural basis for the aggregation of proteins in this family. *Acta Crystal.* **63**, 361–368 (2007).

## Chapter 5

### Conclusions and future directions

The results of our study into the regulation of BpeEF-OprC driven efflux may have posed more questions than it answered. Without continued investigation of the complex network linking BpeEF-oprC to both drug resistance and virulence, the answers to these questions will remain unclear.

Aim I in Chapter 3 dealt with the identification of *cis* regulatory elements necessary for activation of the *bpeEF-oprC* operon. To do this, we used a combination of fluorescently linked oligomer extension and S1 nuclease protection assays to identify the transcriptional start site of *bpeT*. Unfortunately, these methods were unable to determine the location of the 5' transcript end of *llpE-bpeEF-oprC*. While we were able to locate a putative promoter region in control of this section of the operon through 5' deletion assays, the function of *llpE* and its role in control of *bpeEF-oprC* transcription remains unclear. This method provided no answers to the putative essential sequences necessary for *bpeT* transcription in the constitutive BpeT<sub>S280P</sub> background used for the first  $\beta$ -galactosidase tests.

The fact that no real change in expression could be detected for deletions 5' of *bpeT* may be the result of the LysR family's auto-regulatory function.<sup>1-3</sup> Repeating the assay in a strain background possessing the BpeS<sub>K267T</sub> variant produced similarly muddled results, that we later attributed to the fact that BpeS may play no role in the activation of BpeT. We would see that overexpression of either wild-type or mutant forms of the secondary regulator caused no increase in *bpeT* mRNA (observed later in Chapter 4). Additionally, while we were able to demonstrate that both BpeT and BpeS interact with the intergenic region at a defined sequence through

EMSA, it is not definite how mutations to these proteins might alter their ability to perform this function. The BpeT<sub>S280P</sub>, BpeS<sub>K267T</sub> or BpeS<sub>P28S</sub> mutations were unable to inhibit DNA-protein interactions similar to those we detected in EMSAs with wild type BpeS or BpeT proteins.

Aim II of Chapter 4 focused on the function of these proteins on the expression of BpeEF-OprC in part I, and the global transcriptional response in part II. Though we were able to determine the molecular weight of both proteins through a combination of native gel electrophoresis and low-pressure gel filtration chromatography, no changes in molecular weight between mutant and wild type forms were detected under native conditions. This disproves our hypothesis that the mutations may interrupt the formation of the high-order protein complexes demonstrated to be necessary for proper LysR protein function.<sup>1-6</sup> More complex molecular analysis may be necessary to determine how these mutations alter the structure-function relationship of these proteins. To this end, methods such as Surface-Plasmon resonance may be capable of detecting changes in protein conformation in the presence of a co-inducer.<sup>7</sup> This may prove a valuable tool for both confirming and identifying co-inducer substrates through compound library screens, as well as assessing the ability of mutant versions of those proteins to interact with such compounds.

Over expression of wild type BpeT demonstrated very clearly that the protein is capable of transcriptional activation of the efflux operon, but when this was repeated with BpeS, a completely different result was obtained. In its wild type form, this BpeS is incapable of activating the BpeEF-OprC pump; it was not until the introduction of two mutations known to cause co-trimoxazole resistance (BpeS<sub>P28S</sub> and BpeS<sub>K267T</sub>) to the overexpressed gene that a change in expression could be detected. While this could suggest that BpeS is a repressor, in control strains lacking *bpeS* no de-repression of *bpeF* transcription could be observed, either by

qRT-PCR or antibiotic susceptibility assays. This may be attributed to experimental conditions; most LysR proteins require a co-inducer binding event to cause a conformational change allowing them to carry out a physiological function.<sup>1,2,4</sup> If we have yet to identify the necessary physiological conditions for BpeS activation in its native state, it could be possible that we would see no concomitant increase in *bpeEF-oprC* expression in response. As such, BpeS may act as a transcriptional activator, but is only necessary during a strict set of environmental or physiological conditions, and mutations to the co-inducer binding region of this protein would remove the dependency on these conditions. This would explain the constitutive *bpeEF-oprC* overexpression observed in *bpeS* mutant strains.

Additionally, it may be possible that an additional regulatory factor exists that is essential for wild-type BpeS control of the efflux operon. This theory is supported by our observations that neither BpeS nor BpeT is essential for activation of *bpeEF-oprC*. When both of the genes encoding these proteins are deleted, there is no simultaneous decrease in expression of *bpeF* transcript in response to either chloramphenicol, or doxycycline, suggesting that neither BpeT nor BpeS acts as the primary regulatory factor for triggering pump expression under these conditions. Identification of this element may be a vital step in complete characterization of the pump, and may occur through more high-throughput methods utilizing transposon mutagenesis of co-trimoxazole resistant  $\Delta bpeS \Delta bpeT$  isolates, or isolates bearing a *bpeE*<sub>promoter</sub>-*lacZ* reporter, and/or co-immunoprecipitation and pull down experiments using the IR sequence. However, these methods have limitations as they rely on the assumption that another protein drives the BpeT/BpeS independent induction of BpeEF-OprC.

When these investigations were expanded to examine the role of BpeT and BpeS on a global scale, again, more questions are raised. Through RNAseq analysis, we observed that in

strains carrying mutations to *bpeS*, significant changes to accessory gene expression occurred, confirming our initial hypothesis that the protein could target a wider range of operons. While all strains showed alterations in metabolic function in comparison to a Bp82 control, we are unable to determine if this is an artifact of growth conditions or analysis at this time or if these operons respond directly to overexpression of *bpeEF-oprC*.

Perhaps most interesting was the identification of a putative link between BpeS and the Bsa T3SS of *Bp*. When a selection of genes from this operon were tested by qRT-PCR it was found that their expression was significantly altered from Bp82 samples and between different BpeS mutations. This was not observed in all strains overexpressing BpeEF-oprC, leading us to

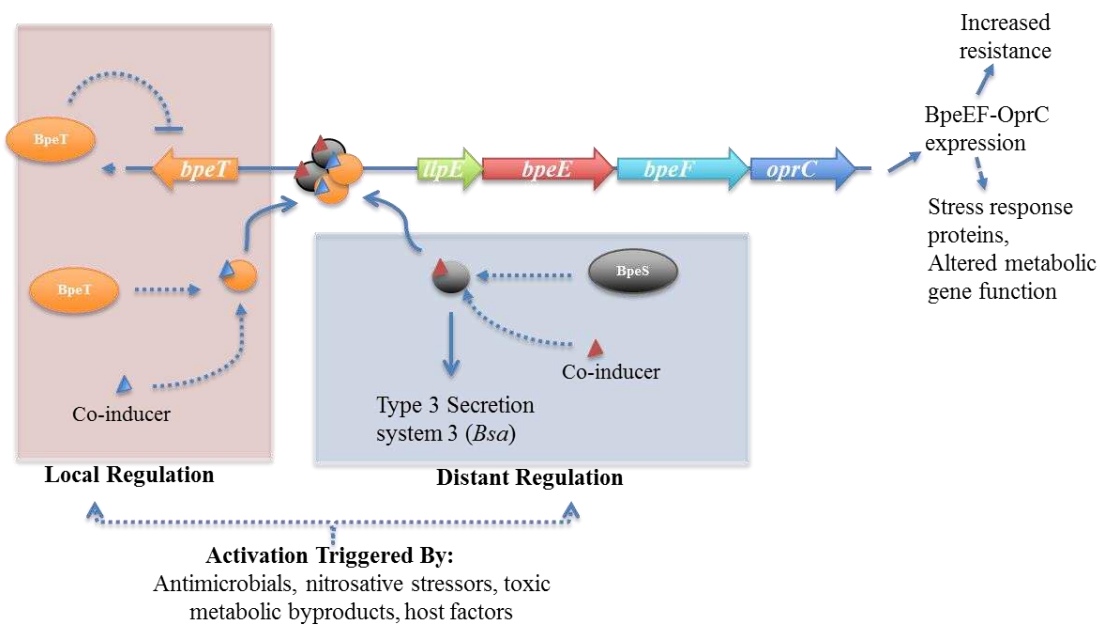


**Figure 5.1. The BpeT BpeS regulatory cascade.** The *bpeEF-oprC* operon is depicted by block arrows. Local regulation (red box) is driven by expression of BpeT protein (orange ovals), thought to repress expression of *bpeT*. Distant regulatory networks (blue box) are affected by BpeS (black oval). Co-inducer (triangles) binding to either BpeT or BpeS is suspected to promote a conformational change to these proteins and binding to a consensus site located in the *bpeT-llpE* intergenic region. This promotes expression of the BpeEF-OprC efflux pump, and subsequent increases in resistance to efflux pump-substrates. Hyper-expression of BpeEF-OprC may prompt expression of proteins associated with the cell stress response. Functional BpeS acts as a conditional activator of Type 3 Secretion System-3, or Bsa, gene expression.

suggest that it is not caused by transcript alterations in response to cell stress driven by overexpression of the efflux pump.<sup>8</sup> We believe BpeS may be part of a global regulon and capable of activating the Bsa T3SS directly, as genes from multiple operons within the 11 transcriptional unit Bsa locus displayed altered expression. A summary of the currently known regulatory cascade associated with BpeEF-OprC is shown in **Fig. 5.1**.

It remains unknown if these in-vitro expression levels cause changes in the in-vivo infection phenotype of bacteria with the BpeS<sub>K267T</sub> mutation. Further studies investigating the effect of these mutations on cellular invasion, persistence and spread need to be conducted to confirm the connection identified by RNAseq and qRT-PCR analysis, and identify any in-vivo relevance that this phenotype may bestow. While this is the first putative link in regulation between BpeEF-OprC efflux and virulence reported in *Bp* 1026b, a complex network of regulatory proteins is known to control BpeEF-OprC functional homologue MexEF-OprN of *Pseudomonas aeruginosa* (*Pa*). In this organism, the expression of virulence and efflux seem to alternate based on control by many factors, and highlights the apparent necessity of efflux expression in cell homeostasis, not just antibiotic resistance.<sup>9-17</sup>

If a similar trend is true in *Bp*, it may be possible that the changes we observe as resistance phenotypes indicate vastly altered cell function. Whether this results in a decrease or increase in cell viability and virulence remains unknown, but could have an impact on the way that such isolates are handled in a clinical setting. If there is a correlation between disrupted BpeS and decreased cell fitness, these mutations pose less of a risk to patients and may not necessitate changes to the way the infection is treated. If T3SS activation dependent on mutant BpeS causes an increase in cell fitness *in-vivo*, it could result more serious disease. This could mean that more stringent therapy is vital for clearance of the infection either through use of an

efflux pump inhibitor to potentiate antibiotic use, or a switch from eradication phase therapy to imipenem or meropenem for the duration of treatment.

While this work examines this process in the context of resistance to antimicrobials, it is important to remember that these efflux pumps can be triggered by a variety of stressors regularly encountered in both host and environmental settings. This could include anything from the byproducts of metabolism, to reactive oxygen or nitrogen species produced by host cells. In both *Bp* and *Pa*, it is likely that the induction of efflux systems such as MexEF-OprN and BpeEF-OprC is promoted in a similar fashion, thereby necessitating activation of these RND systems in an effort to regain homeostasis. This observation is strengthened by the fact that BpeEF-OprC exhibits no basal expression and only becomes active in the presence of inducing substrates e.g. doxycycline, and chloramphenicol, and is confirmed by the apparent dependence on another regulatory element in the absence of both BpeT and BpeS. In a study examining the MexT regulatory system in *Pa*, it was discovered that pump induction occurred in the absence of antibiotic compounds and independent of functional MexT.<sup>21</sup> Other investigations linked expression of MexEF-OprN to nitrosative and disulfide stress, biofilm formation and quorum sensing, in both MexT dependent and independent fashions.<sup>9,10,13-15,21,22</sup> These observations highlight the potentially expansive repertoire of regulatory factors capable of controlling the expression of the efflux pump under a wide range of environmental conditions.

It is possible that in *Bp*, BpeS and BpeT are only a small part of a similarly adaptable regulatory cascade. While these proteins may be essential under certain forms of environmental stress, and activated by co-inducers produced by that environmental condition, a much wider regulatory network most likely exists that allows activation of the efflux pump to maintain homeostasis in response to many adverse conditions.

Understanding the interplay of these factors in promotion of cell homeostasis, efflux, and virulence may both increase our understanding of the biology of *Bp*, and improve the way we treat melioidosis. Furthermore, these observations may prove applicable to a larger group of infections; though *Bp* causes devastating disease in endemic regions, its increasing impact on a global scale is still less than that of other more commonly encountered Gram negative bacteria.

The RND efflux pump family is highly conserved, and many representatives can be found in Gram-negative community acquired pathogens including *P. aeruginosa* and *Acinetobacter baumannii*.<sup>12,14,18,19</sup> These infections, now part of the ESKAPE designation including *Enterococcus faecalis*, *Staphylococcus aureus*, *Klebsiella pneumoniae* and *Enterobacter* spp., are a serious problem in hospitals world-wide based on their increasing antibiotic resistance levels.<sup>20</sup> In many instances, this is caused by possession of wide range of resistance mechanisms including efflux pumps which may be functionally similar to BpeEF-OprC. In the absence of effective antimicrobials, these infections represent a global threat to our current standard of medical care. Even incremental increases in the body of knowledge surrounding RND efflux through investigations of its function and regulation in many species, including *Bp*, could provide us with a better understanding of this mechanism in all species, and translate to improved management of antibiotic resistant infections on a global scale.

## Chapter 5 References

1. Maddocks, S. E. & Oyston, P. C. F. Structure and function of the LysR-type transcriptional regulator (LTTR) family proteins. *Microbiology* **154**, 3609–3623 (2008).
2. Schell, M. A. Molecular biology of the LysR Family of transcriptional regulators. *Annu. Rev. Microbiol.* **47**, 597–626 (1993).
3. Deghmane, A.-E. & Taha, M.-K. The *Neisseria meningitidis* adhesion regulatory protein CrgA acts through oligomerization and interaction with RNA polymerase: Functional organization of *N. meningitidis* CrgA. *Mol. Microbiol.* **47**, 135–143 (2002).
4. Knapp, G. S. & Hu, J. C. The oligomerization of CynR in *Escherichia coli*. *Protein Sci.* **18**, 2307–2315 (2009).
5. Ruangprasert, A., Craven, S. H., Neidle, E. L. & Momany, C. Full-length Structures of BenM and two variants reveal different oligomerization schemes for LysR-Type transcriptional regulators. *J. Mol. Biol.* **404**, 568–586 (2010).
6. Gong, W., Xiong, G. & Maser, E. Oligomerization and negative autoregulation of the LysR-type transcriptional regulator HsdR from *Comamonas testosteroni*. *J. Steroid Biochem. Mol. Biol.* **132**, 203–211 (2012).
7. Joshi, G. S., Zianni, M., Bobst, C. E. & Tabita, F. R. Further unraveling the regulatory twist by elucidating metabolic coinducer-mediated CbbR-cbbI promoter interactions in *Rhodopseudomonas palustris* CGA010. *J. Bacteriol.* **194**, 1350–1360 (2012).
8. Olivares, J., Alvarez-Ortega, C. & Martinez, J. L. Metabolic compensation of fitness costs associated with overexpression of the multidrug efflux pump MexEF-OprN in *Pseudomonas aeruginosa*. *Antimicrob. Agents Chemother.* **58**, 3904–3913 (2014).

9. Liao, J., Schurr, M. J. & Sauer, K. The MerR-Like regulator BrIR confers biofilm tolerance by activating multidrug efflux pumps in *Pseudomonas aeruginosa* biofilms. *J. Bacteriol.* **195**, 3352–3363 (2013).
10. Westfall, L. W. *et al.* *mvaT* mutation modifies the expression of the *Pseudomonas aeruginosa* multidrug efflux operon *mexEF-oprN*. *FEMS Microbiol. Lett.* **255**, 247–254 (2006).
11. Jin, Y., Yang, H., Qiao, M. & Jin, S. MexT regulates the Type III Secretion System through MexS and PtrC in *Pseudomonas aeruginosa*. *J. Bacteriol.* **193**, 399–410 (2010).
12. Beaudoin, T., Zhang, L., Hinz, A. J., Parr, C. J. & Mah, T.-F. The biofilm-specific antibiotic resistance gene *ndvB* is important for expression of ethanol oxidation genes in *Pseudomonas aeruginosa* biofilms. *J. Bacteriol.* **194**, 3128–3136 (2012).
13. Fargier, E. *et al.* MexT functions as a redox-responsive regulator modulating disulfide stress resistance in *Pseudomonas aeruginosa*. *J. Bacteriol.* **194**, 3502–3511 (2012).
14. Fetar, H. *et al.* *mexEF-oprN* multidrug efflux operon of *Pseudomonas aeruginosa*: regulation by the MexT activator in response to nitrosative stress and chloramphenicol. *Antimicrob. Agents Chemother.* **55**, 508–514 (2011).
15. Maseda, H., Uwate, U., & Nakae, T. Transcriptional regulation of the *mexEF-oprN* multidrug efflux pump operon by MexT and an unidentified repressor in *nfxc*-type mutant of *Pseudomonas aeruginosa*. *FEMS Microbiol. Lett.* **311**, 36–43 (2010).
16. Tian, Z.-X. *et al.* MexT modulates virulence determinants in *Pseudomonas aeruginosa* independent of the MexEF-OprN efflux pump. *Microb. Pathog.* **47**, 237–241 (2009).
17. Zaoui, C. *et al.* An orphan sensor kinase controls quinolone signal production via MexT in *Pseudomonas aeruginosa*. *Mol. Microbiol.* **83**, 536–547 (2012).

18. Lin, M.-F., Lin, Y.-Y., Tu, C.-C. & Lan, C.-Y. Distribution of different efflux pump genes in clinical isolates of multidrug-resistant *Acinetobacter baumannii* and their correlation with antimicrobial resistance. *J. Microbiol. Immunol. Infect.* (2015). doi:10.1016/j.jmii.2015.04.004
19. Li, X.-Z., Plésiat, P. & Nikaido, H. The challenge of efflux-mediated antibiotic resistance in Gram-negative bacteria. *Clin. Microbiol. Rev.* **28**, 337–418 (2015).
20. Boucher, H. W. *et al.* Bad Bugs, No Drugs: No ESKAPE! An update from the Infectious Diseases Society of America. *Clin. Infect. Dis.* **48**, 1–12 (2009).
21. Kumar, A. and Schweizer, H.P. Evidence of MexT-independent overexpression of the MexEF-OprN efflux pump of *Pseudomonas aeruginosa* in presence of metabolic stress. *PLoS ONE*. **6**, e26520 (2011) doi: 10.1371/journal.pone.0026520
22. Dongping, W. *et al.* Transcriptome profiling reveals links between ParS/ParR, MexEF-OprN, and quorum sensing in the regulation of adaptation and virulence in *Pseudomonas aeruginosa*. *BMC Genomics*. **14**, 618 (2013).

## APPENDIX

**Table A 1. Mapping statistics of RNAseq analysis**

	Bp82				Bp82 <i>bpeS</i> <sub>P28S</sub>			
Replicate	1		2		1		2	
Total raw reads	19920358		19810732		18079264		19654454	
Total reads passing QC <sup>1</sup>	10287908		12131448		11953310		12676310	
Chromosome	1	2	1	2	1	2	1	2
Mapped reads	8704324	1457437	10382071	1630019	10358880	1461309	11086352	1512484
Paired but unmapped (Placed)	75271	12538	69999	10961	79049	11044	65250	8782
Unmapped and unpaired	38338		38398		43028		3442	
Total mapped per replicate	10161761		12012090		11820189		12598836	
Percent mapped per replicate	98.8%		99.0%		98.9%		99.4%	
Total placed per replicate	10249570		12093050		11910282		12672868	
Percent placed per replicate	99.6%		99.7%		99.6%		99.97%	
Total passable reads per isolate	22419356				24629620			
Total mapped per isolate	22173851				24419025			
Total placed per isolate	22342620				24583150			
Percent mapped per isolate	98.9%				99.1%			
Percent placed per isolate	99.7%				99.8%			
Total raw reads per isolate	39731090				37733718			
Percent mapped of raw total	55.8%				64.7%			
Percent placed of raw total	56.2%				65.1%			

<sup>1</sup>Only reads passing QC were mapped to the chromosome, therefore all mapping percentages are calculated out of the total reads passing QC unless otherwise stated.

**Table A 1. continued**

	Bp82 <i>bpeS</i> <sub>K267T</sub>				Bp82 <i>bpeT</i> <sub>S280P</sub>			
Replicate	1		2		1		2	
Total raw reads	20793180		17026780		19825430		20431704	
Total reads passing QC <sup>1</sup>	11916948		3036514		8567630		11099501	
Chromosome	1	2	1	2	1	2	1	2
Mapped reads	1E+07	1661644	1031807	1899803	4023941	846047	9612747	1385977
Paired but unmapped (Placed)	68290	11286	60266	11120	1193855	251277	57478	8355
Unmapped and unpaired	40728		33518		2252510		34944	
Total mapped per replicate	11796644		2931610		4869988		10998724	
Percent mapped per replicate	99.0%		96.5%		56.8%		99.1%	
Total placed per replicate	11876220		3002996		6315120		11064557	
Percent placed per replicate	99.7%		98.9%		73.7%		99.7%	
Total passable reads per isolate	14953462				19667131			
Total mapped per isolate	14728254				15868712			
Total placed per isolate	14879216				17379677			
Percent mapped per isolate	98.5%				80.7%			
Percent placed per isolate	99.5%				88.4%			
Total raw reads per isolate	37819960				40257134			
Percent mapped of raw total	38.9%				39.4%			
Percent placed of raw total	39.3%				43.2%			

<sup>1</sup>Only reads passing QC were mapped to the chromosome, therefore all mapping percentages are calculated out of the total reads passing QC unless otherwise stated.

**Table A2. RNAseq gene expression in Bp82 *bpeS*<sub>K267T</sub> vs. Bp82**

<b>Gene</b>	<b>Bp82 <i>bpeS</i><sub>K267T</sub> Rep. 1</b>	<b>Bp82 <i>bpeS</i><sub>K267T</sub> Rep. 2</b>	<b>Gene Annotation</b>
BP1026B_I0948	2.38796	2.39059	cation-binding hemerythrin HHE family protein
BP1026B_I0961	3.26142	3.23776	cyclic nucleotide-binding domain-containing protein
BP1026B_I0964	2.50678	2.60219	hypothetical protein
BP1026B_I0965	3.37783	3.39893	U32 family peptidase
BP1026B_I0966	2.94796	2.87414	hypothetical protein
BP1026B_I1039	1.89048	1.89588	low molecular weight protein-tyrosine-phosphatase
BP1026B_I1490	2.37286	2.25289	outer membrane protein W precursor
<i>arcA</i>	2.70957	2.72954	arginine deiminase
<i>arcB</i>	3.87568	3.83995	ornithine carbamoyltransferase
<i>arcC</i>	3.6681	3.75125	carbamate kinase
<i>cydA</i>	2.20997	2.16932	cytochrome d ubiquinol oxidase subunit I
<i>fliC</i>	1.99358	2.00754	flagellin
BP1026B_I0099	2.9893	3.07257	hypothetical protein
BP1026B_I0205	2.40126	2.40374	hypothetical protein
<i>narH</i>	4.04032	4.22773	nitrate reductase, beta subunit
BP1026B_I1338	2.56118	2.59853	LysR family transcriptional regulator
<i>motA</i>	1.85548	1.89919	flagellar motor protein MotA
<i>bpeF</i>	7.2299	nd	RND transporter protein
BP1026B_II2095	3.12535	4.48518	poly-beta-hydroxybutyrate polymerase

Gene	Bp82 <i>bpeS</i> <sub>K267T</sub> Rep. 1	Bp82 <i>bpeS</i> <sub>K267T</sub> Rep. 2	Gene Annotation
BP1026B_II2055	2.8626	nd	acetoacetyl-CoA reductase
BP1026B_II2100	nd	3.33302	OsmY domain-containing protein
BP1026B_II0164	nd	1.86669	amylase
BP1026B_II0548	nd	-2.10899	chitin binding domain-containing protein
<i>adhA</i>	nd	3.90545	alcohol dehydrogenase, zinc-containing
BP1026B_II2466	4.28849	4.0463	HSP20/alpha crystallin family protein

<sup>1</sup>Data listed in Rep. 1 and Rep. 2 columns represents FPKM gene expression in comparison to Bp82 control expression. Only genes with a false-discovery rate adjusted P value <0.05 were included. Nd indicates no mapped or placed fragments passing QC were identified in that particular replicate for a given gene.

**Table A3. RNA-seq gene expression in *bpeS*<sub>P28S</sub> vs. Bp82**

Gene	Bp82 <i>bpeS</i> <sub>P28S</sub> Rep. 1	Bp82 <i>bpeS</i> <sub>P28S</sub> Rep. 2	Gene annotation
<i>aer</i>	-2.65096	-2.36602	aerotaxis protein
<i>arcA</i>	-1.80081	nd	arginine deiminase
<i>arcD</i>	-2.0431	-1.94323	arginine/ornithine antiporter
<i>argD</i>	1.65042	2.24639	acetylornithine transaminase protein
<i>aroG</i>	-1.53639	-1.51772	phospho-2-dehydro-3-deoxyheptonate aldolase
<i>bapB</i>	-3.08902	-3.25575	acyl carrier protein
<i>bicA</i>	nd	-2.68158	type III secretion low calcium response chaperone LcrH/SycD
<i>bipB</i>	nd	-3.11008	BipB protein

<b>Gene</b>	<b>Bp82 <i>bpeS</i><sub>P28S</sub> Rep. 1</b>	<b>Bp82 <i>bpeS</i><sub>P28S</sub> Rep. 2</b>	<b>Gene annotation</b>
<i>bipC</i>	nd	-3.07753	cell invasion protein
BP1026B_I0091	-1.21425	-1.29493	hypothetical protein
BP1026B_I0157	-1.97865	-1.99614	hypothetical protein
BP1026B_I0205	2.38309	2.42599	hypothetical protein
BP1026B_I0267	0.984171	0.99637	23S ribosomal RNA
BP1026B_I0531	nd	1.62922	undecaprenyl-phosphate galactosephosphotransferase
BP1026B_I0534	1.97577	1.97876	Tyrosine-protein kinase Wzc
BP1026B_I0537	1.54382	nd	serine O-acetyltransferase
BP1026B_I0538	2.3717	2.34708	Glycosyltransferase
BP1026B_I0711	1.3277	1.3263	ABC transporter, membrane permease
BP1026B_I0713	1.14294	1.13129	ABC transporter, ATP-binding component
BP1026B_I0714	1.48191	nd	hypothetical protein
BP1026B_I0723	-1.0918	nd	hypothetical protein
BP1026B_I0948	-2.21467	-2.22455	cation-binding hemerythrin HHE family protein
BP1026B_I0949	-3.0457	-3.04405	Rrf2 family protein
BP1026B_I0963	-2.05623	-2.08451	2-nitropropane dioxygenase
BP1026B_I0964	-2.01628	-2.02317	hypothetical protein
BP1026B_I1020	-2.4879	-2.49477	nitrate/nitrite transporter
BP1026B_I1283	-1.87523	-1.82689	polysaccharide deacetylase family protein
BP1026B_I1284	-1.99526	-1.94863	allantoicase
BP1026B_I1286	-1.65174	-1.62218	hypothetical protein

<b>Gene</b>	<b>Bp82 <i>bpeS</i><sub>P28S</sub> Rep. 1</b>	<b>Bp82 <i>bpeS</i><sub>P28S</sub> Rep. 2</b>	<b>Gene annotation</b>
BP1026B_I1287	-2.06306	-1.98523	Transthyretin family protein
BP1026B_I1321	-2.23908	-2.24282	hypothetical protein
BP1026B_I1490	-1.53128	-1.5202	outer membrane protein W precursor
BP1026B_I1518	-1.45287	nd	LacI family transcription regulator
BP1026B_I1564	-3.43757	-3.4902	hypothetical protein
BP1026B_I1565	-3.08544	-2.96906	polyhydroxyalkanoate depolymerase domain-containing protein
BP1026B_I1664	-1.7479	-1.71691	carbamoyl transferase
BP1026B_I1665	-1.31439	-1.26417	hypothetical protein
BP1026B_I1672	-1.31902	nd	kinase
BP1026B_I1674	-1.71262	nd	Arginine succinate synthase
BP1026B_I1675	-1.71761	nd	Non-ribosomal peptide synthetase
BP1026B_I1676	-1.17454	nd	hypothetical protein
BP1026B_I1697	-1.73891	nd	hypothetical protein
BP1026B_I2216	-1.21843	-1.23999	putative exported protein
BP1026B_I2218	-1.47969	-1.44678	hypothetical protein
BP1026B_I2302	1.03547	1.04811	23S rRNA
BP1026B_I2615	1.48586	1.48648	hypothetical protein
BP1026B_I2723	-2.20103	nd	tagatose 6-phosphate kinase protein
BP1026B_I2915	2.07545	1.78669	acyl carrier protein
BP1026B_I2917	nd	2.21558	hypothetical protein
BP1026B_I2921	1.22037	nd	sigma-54 dependent transcriptional regulator

<b>Gene</b>	<b>Bp82 <i>bpeS</i><sub>P28S</sub> Rep. 1</b>	<b>Bp82 <i>bpeS</i><sub>P28S</sub> Rep. 2</b>	<b>Gene annotation</b>
BP1026B_I2923	nd	1.77155	glycosyl transferase, group 1 family protein
BP1026B_I3039	-1.15945	-1.13933	D-methionine ABC transporter, periplasmic D-methionine-binding protein
BP1026B_I3465	1.02162	1.03408	23S ribosomal RNA
BP1026B_II0548	nd	-3.52545	chitin binding domain-containing protein
BP1026B_III1185	1.6027	1.54437	GTP cyclohydrolase II
BP1026B_III1232	-2.65785	nd	TauD/TfdA family dioxygenase
BP1026B_III1232	-2.55682	nd	TauD/TfdA family dioxygenase
BP1026B_III1241	nd	-4.38642	non-ribosomal peptide/polyketide synthase
BP1026B_III1250	-2.7975	-2.79257	nonribosomal peptide synthetase
BP1026B_III1256	-1.72862	-1.69779	hypothetical protein
BP1026B_III1266	-2.00923	-1.99759	hypothetical protein
BP1026B_III1610	-2.12661	-2.00777	hypothetical protein
BP1026B_III1643	-3.23871	-3.20854	type III secretion system protein PrgH/EprH
BP1026B_III1644	-3.54283	-3.65142	MxiH protein
BP1026B_III1794	-1.80232	-1.85181	outer membrane porin
BP1026B_II2095	-2.73961	-2.7555	poly-beta-hydroxybutyrate polymerase
BP1026B_II2146	2.11812	2.1122	hypothetical protein
BP1026B_II2466	-2.10643	-2.70532	HSP20/alpha crystallin family protein
<i>bpeF</i>	6.86283	nd	RND efflux transporter protein
<i>bpeF</i>	5.69087	nd	
<i>bsaO</i>	-3.21953	-3.27295	YscC/HrcC family type III secretion outer membrane protein

<b>Gene</b>	<b>Bp82 <i>bpe</i><sub>SP28S</sub> Rep. 1</b>	<b>Bp82 <i>bpe</i><sub>SP28S</sub> Rep. 2</b>	<b>Gene annotation</b>
<i>bsaQ</i>	-2.45621	-2.48254	type III secretion system protein BsaQ
<i>bsaR</i>	nd	-3.43555	surface presentation of antigens protein
<i>cspD</i>	1.39336	1.39566	cold shock transcription regulator protein
<i>flgK</i>	-1.24803	-1.25689	flagellar hook-associated protein FlgK
<i>glpD</i>	nd	1.72983	glycerol-3-phosphate dehydrogenase
<i>hmpA</i>	-1.69811	-1.69953	Flavo-hemoprotein
<i>ipk</i>	0.963744	nd	4-diphosphocytidyl-2-C-methyl-D-erythritol kinase
<i>narG</i>	-3.15097	-3.191	nitrate reductase, alpha subunit
<i>narH</i>	-2.06898	-2.17402	nitrate reductase, beta subunit
<i>narK</i>	-3.56095	-3.55651	nitrate/nitrite transporter NarK
<i>potF</i>	-1.18096	-1.15257	putrescine-binding periplasmic protein precursor
<i>spaP</i>	-2.86041	-2.85832	surface presentation of antigens protein SpaP
<i>xdhB</i>	-1.53458	nd	xanthine dehydrogenase, subunit B

<sup>†</sup>Data listed in Rep. 1 and Rep. 2 columns represents FPKM gene expression in comparison to Bp82 control expression. Only genes with a false-discovery rate adjusted P value <0.05 were included. Nd indicates no mapped or placed fragments passing QC were identified in that particular replicate for a given gene.

**Table A4. RNAseq gene expression in Bp82 *bpeT*<sub>S280P</sub> vs. Bp82**

<b>Gene</b>	<b>Bp82 <i>bpeT</i><sub>S280P</sub> Rep. 1</b>	<b>Bp82 <i>bpeT</i><sub>S280P</sub> Rep. 2</b>	<b>Gene Annotation</b>
<i>adhA</i>	4.51641	nd	alcohol dehydrogenase, zinc-containing
<i>arcB</i>	4.44324	4.47742	ornithine carbamoyltransferase
<i>arcC</i>	3.71689	4.01325	carbamate kinase
BP1026B_I0099	4.28698	4.56119	hypothetical protein
BP1026B_I0263	3.51776	3.48071	16s ribosomal RNA
BP1026B_I0267	3.25448	nd	23S ribosomal RNA
BP1026B_I0948	3.51355	3.63566	cation-binding hemerythrin HHE family protein
BP1026B_I0963	3.30071	nd	2-nitropropane dioxygenase
BP1026B_I0964	4.13105	4.33206	hypothetical protein
BP1026B_I0965	4.97345	5.23078	U32 family peptidase
BP1026B_I0966	5.34037	5.12838	hypothetical protein
BP1026B_I0969	3.98981	4.21551	hypothetical protein
BP1026B_I0970	4.41938	4.50606	anaerobic ribonucleoside triphosphate reductase
BP1026B_I1039	2.42559	2.37946	low molecular weight protein-tyrosine-phosphatase
BP1026B_I1321	-4.05941	-3.97679	hypothetical protein
BP1026B_I1564	nd	-3.39953	hypothetical protein
BP1026B_I1565	nd	-4.12986	polyhydroxyalkanoate depolymerase domain-containing protein
BP1026B_I2302	3.27218	nd	23S ribosomal RNA
BP1026B_I2833	nd	3.43612	hypothetical protein
BP1026B_I3469	nd	3.71401	16S ribosomal RNA

Gene	Bp82 <i>bpeT</i> <sub>S280P</sub> Rep. 1	Bp82 <i>bpeT</i> <sub>S280P</sub> Rep. 2	Gene Annotation
BP1026B_II0292	nd	3.43972	outer membrane porin
BP1026B_III1185	nd	4.85605	GTP cyclohydrolase II
BP1026B_III1186	4.6855	nd	WD domain-containing protein
BP1026B_II1232	-4.25168	-4.49045	TauD/TfdA family dioxygenase
BP1026B_III1241	-6.22629	nd	non-ribosomal peptide/polyketide synthase
BP1026B_II1250	-5.87298	-6.11703	Non-ribosomal peptide synthetase
BP1026B_III1251	nd	- 5.26036	<i>N</i> -acylhomoserine lactone synthase
BP1026B_III1979	3.20696	nd	lipoprotein
BP1026B_II2055	3.38014	3.62167	acetoacetyl-CoA reductase
BP1026B_II2095	nd	3.64642	poly- $\beta$ -hydroxybutyrate polymerase
BP1026B_II2466	5.61381	5.16004	HSP20/ $\alpha$ -crystallin family protein
<i>bpeF</i>	nd	7.17971	multidrug-efflux transporter protein
<i>bpeF</i>	nd	6.0139	
<i>cydA</i>	3.84688	4.23419	cytochrome d ubiquinol oxidase subunit I
<i>cydB</i>	nd	3.18341	cytochrome d ubiquinol oxidase, subunit II
<i>nosZ</i>	nd	4.64764	nitrous-oxide reductase

<sup>1</sup>Data listed in Rep. 1 and Rep. 2 columns represents FPKM gene expression in comparison to Bp82 control expression. Only genes with a false-discovery rate adjusted P value <0.05 were included. Nd indicates no mapped or placed fragments passing QC were identified in that particular replicate for a given gene.

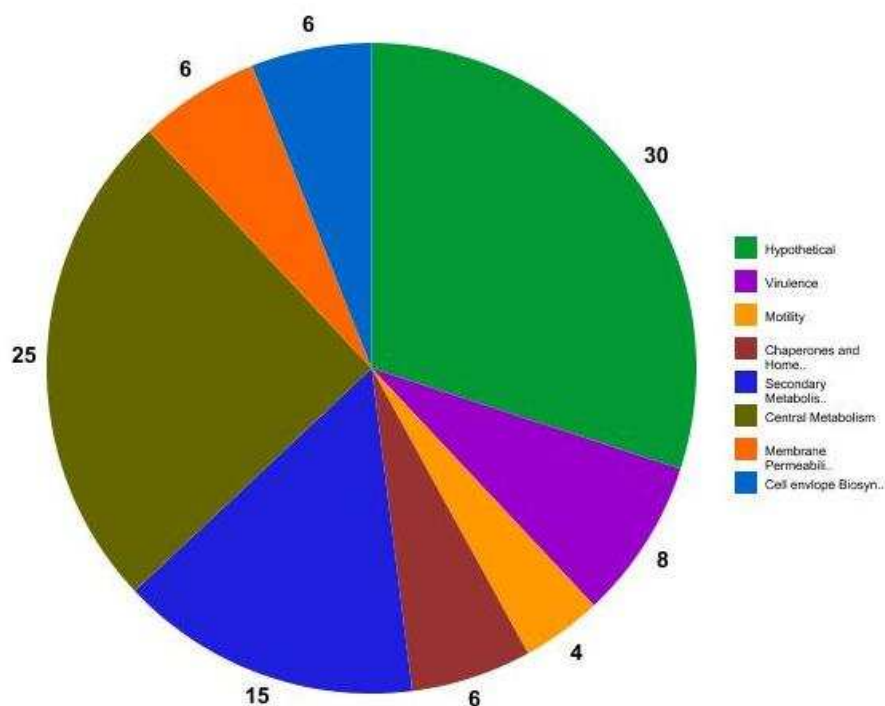


**Figure A.1. Kyoto encyclopedia of genes and genomes (KEGG) functional pathway associations of transcriptionally altered genes identified by RNAseq.**

The pool of 103 significantly upregulated genes from Bp82 *bpeT*<sub>S280P</sub>, *bpeS*<sub>P28S</sub>, and *bpeS*<sub>K267T</sub> were analyzed using the KEGG pathway search tool to identify putative metabolic or functional pathway associations. Genes were grouped into hypothetical, virulence, motility, chaperone and homeostasis, secondary metabolism, central metabolism, membrane permeability and transport, and cell envelope biogenesis categories. Data is represented as percentages of the total number of genes. A full listing of pathway associations can be seen in **Table A.5**.

**Table A.5 RNAseq KEGG pathway analysis**

**metabolic pathways bpz01100**

bpz:BP1026B_I0970	anaerobic ribonucleoside triphosphate reductase
bpz:BP1026B_I1284	allantoicase
bpz:BP1026B_I1287	transthyretin family protein
bpz:BP1026B_I1674	argininosuccinate synthase
bpz:BP1026B_I2723	tagatose 6-phosphate kinase protein
bpz:BP1026B_II0164	amylase
bpz:BP1026B_III1185	GTP cyclohydrolase II
bpz:BP1026B_II2084	<i>adhA</i> ; alcohol dehydrogenase, zinc-containing
bpz:BP1026B_I1699	<i>arcA</i> ; arginine deiminase
bpz:BP1026B_I1700	<i>arcB</i> ; ornithine carbamoyltransferase
bpz:BP1026B_I1701	<i>arcC</i> ; carbamate kinase
bpz:BP1026B_I2613	<i>argD</i> ; acetylornithine transaminase protein
bpz:BP1026B_I0472	<i>aroG</i> ; phospho-2-dehydro-3-deoxyheptonate aldolase
bpz:BP1026B_I2997	<i>cydA</i> ; cytochrome d ubiquinol oxidase subunit I
bpz:BP1026B_I2998	<i>cydB</i> ; cytochrome d ubiquinol oxidase, subunit II
bpz:BP1026B_I2973	<i>ipk</i> ; 4-diphosphocytidyl-2-C-methyl-D-erythritol kinase
bpz:BP1026B_I0588	<i>xdhB</i> ; xanthine dehydrogenase, subunit B
bpz:arcD	arginine/ornithine antiporter
bpz:BP1026B_I1283	uridylate kinase, putative urate catabolism protein

**bpz01110 Biosynthesis of secondary metabolites**

bpz:BP1026B_I1674	argininosuccinate synthase
bpz:BP1026B_III1185	GTP cyclohydrolase II
bpz:BP1026B_II2084	<i>adhA</i> ; alcohol dehydrogenase, zinc-containing
bpz:BP1026B_I1699	<i>arcA</i> ; arginine deiminase
bpz:BP1026B_I1700	<i>arcB</i> ; ornithine carbamoyltransferase
bpz:BP1026B_I2613	<i>rgD</i> ; acetylornithine transaminase protein
bpz:BP1026B_I0472	<i>aroG</i> ; phospho-2-dehydro-3-deoxyheptonate aldolase
bpz:BP1026B_I2835	<i>glpD</i> ; glycerol-3-phosphate dehydrogenase
bpz:BP1026B_I2973	<i>ipk</i> ; 4-diphosphocytidyl-2-C-methyl-D-erythritol kinase
bpz:arcD	arginine/ornithine antiporter
bpz:BP1026B_I1672	Kinase Protein involved in propanediol utilization,

**bpz01120 Microbial metabolism in diverse environments**

bpz:BP1026B_I1284	allantoicase
bpz:BP1026B_I1287	transthyretin family protein
bpz:BP1026B_II2055	acetoacetyl-CoA reductase
bpz:BP1026B_II2084	<i>adhA</i> ; alcohol dehydrogenase, zinc-containing

bpz:BP1026B\_I1701 *arcC*; carbamate kinase  
bpz:BP1026B\_I2613 *argD*; acetylornithine transaminase protein  
bpz:BP1026B\_I1018 *narG*; nitrate reductase, alpha subunit  
bpz:BP1026B\_I1017 *narH*; nitrate reductase, beta subunit  
bpz:BP1026B\_I1546 *nosZ*; nitrous-oxide reductase  
bpz:BP1026B\_I0588 *xdhB*; xanthine dehydrogenase, subunit B

#### **bpz01130 Biosynthesis of antibiotics**

bpz:BP1026B\_I1674 argininosuccinate synthase  
bpz:BP1026B\_II2084 *adhA*; alcohol dehydrogenase, zinc-containing  
bpz:BP1026B\_I1699 *arcA*; arginine deiminase  
bpz:BP1026B\_I1700 *arcB*; ornithine carbamoyltransferase  
bpz:BP1026B\_I2613 *argD*; acetylornithine transaminase protein  
bpz:BP1026B\_I0472 *aroG*; phospho-2-dehydro-3-deoxyheptonate aldolase  
bpz:BP1026B\_I2973 *ipk*; 4-diphosphocytidyl-2-C-methyl-D-erythritol kinase

#### **bpz01200 Carbon metabolism**

bpz:BP1026B\_II2055 acetoacetyl-CoA reductase  
bpz:BP1026B\_I1701 *arcC*; carbamate kinase

#### **bpz01210 2-Oxocarboxylic acid metabolism**

bpz:BP1026B\_I2613 *argD*; acetylornithine transaminase protein

#### **bpz01230 Biosynthesis of amino acids**

bpz:BP1026B\_I0537 serine O-acetyltransferase  
bpz:BP1026B\_I1674 argininosuccinate synthase  
bpz:BP1026B\_I1700 *arcB*; ornithine carbamoyltransferase  
bpz:BP1026B\_I2613 *argD*; acetylornithine transaminase protein  
bpz:BP1026B\_I0472 *aroG*; phospho-2-dehydro-3-deoxyheptonate aldolase  
bpz:*arcD* arginine/ornithine antiporter

#### **bpz01220 Degradation of aromatic compounds**

bpz:BP1026B\_II2084 *adhA*; alcohol dehydrogenase, zinc-containing

#### **bpz00010 Glycolysis / Gluconeogenesis**

bpz:BP1026B\_II2084 *adhA*; alcohol dehydrogenase, zinc-containing

#### **bpz00052 Galactose metabolism**

bpz:BP1026B\_I2723 tagatose 6-phosphate kinase protein

**bpz00500 Starch and sucrose metabolism**

bpz:BP1026B\_II0164 amylase

**bpz00630 Glyoxylate and dicarboxylate metabolism**

bpz:BP1026B\_II2055 acetoacetyl-CoA reductase

**bpz00650 Butanoate metabolism**

bpz:BP1026B\_II2055 acetoacetyl-CoA reductase

bpz:BP1026B\_II2095 poly-beta-hydroxybutyrate polymerase

**bpz00190 Oxidative phosphorylation**

bpz:BP1026B\_I2997 *cydA*; cytochrome d ubiquinol oxidase subunit I

bpz:BP1026B\_I2998 *cydB*; cytochrome d ubiquinol oxidase, subunit II

**bpz00910 Nitrogen metabolism**

bpz:BP1026B\_I0963 2-nitropropane dioxygenase

bpz:BP1026B\_I1020 nitrate/nitrite transporter

bpz:BP1026B\_I1701 *arcC*; carbamate kinase

bpz:BP1026B\_I1018 *narG*; nitrate reductase, alpha subunit

bpz:BP1026B\_I1017 *narH*; nitrate reductase, beta subunit

bpz:BP1026B\_I1019 *narK*; nitrate/nitrite transporter NarK

bpz:BP1026B\_I1546 *nosZ*; nitrous-oxide reductase

bpz:BP1026B\_I1283 uridylate kinase, putative urate catabolism protein

**bpz00920 Sulfur metabolism**

bpz:BP1026B\_II1232 TauD/TfdA family dioxygenase

**bpz00071 Fatty acid degradation**

bpz:BP1026B\_II2084 *adhA*; alcohol dehydrogenase, zinc-containing

**bpz00564 Glycerophospholipid metabolism**

bpz:BP1026B\_I2835 *glpD*; glycerol-3-phosphate dehydrogenase

**bpz00230 Purine metabolism**

bpz:BP1026B\_I0970 anaerobic ribonucleoside triphosphate reductase

bpz:BP1026B\_I1284 allantoicase

bpz:BP1026B\_I1287 transthyretin family protein

bpz:BP1026B\_I1701 *arcC*; carbamate kinase

bpz:BP1026B\_I0588 *xdhB*; xanthine dehydrogenase, subunit B

**bpz00240 Pyrimidine metabolism**

bpz:BP1026B\_I0970 anaerobic ribonucleoside triphosphate reductase

**bpz00250 Alanine, aspartate and glutamate metabolism**

bpz:BP1026B\_I1674 argininosuccinate synthase

**bpz00300 Lysine biosynthesis**

bpz:BP1026B\_I2613 *argD*; acetylornithine transaminase protein

**bpz00220 Arginine biosynthesis**

bpz:arcD arginine/ornithine antiporter  
bpz:BP1026B\_I1674 argininosuccinate synthase  
bpz:BP1026B\_I1699 *arcA*; arginine deiminase  
bpz:BP1026B\_I1700 *arcB*; ornithine carbamoyltransferase  
bpz:BP1026B\_I1701 *arcC*; carbamate kinase  
bpz:BP1026B\_I2613 *argD*; acetylornithine transaminase protein

**bpz00350 Tyrosine metabolism**

bpz:BP1026B\_II2084 *adhA*; alcohol dehydrogenase, zinc-containing

**bpz00400 Phenylalanine, tyrosine and tryptophan biosynthesis**

bpz:BP1026B\_I0472 *aroG*; phospho-2-dehydro-3-deoxyheptonate aldolase

**bpz00430 Taurine and hypotaurine metabolism**

bpz:BP1026B\_II1232 TauD/TfdA family dioxygenase

**bpz00740 Riboflavin metabolism**

bpz:BP1026B\_III1185 GTP cyclohydrolase II

**bpz00900 Terpenoid backbone biosynthesis -**

bpz:BP1026B\_I2973 *ipk*; 4-diphosphocytidyl-2-C-methyl-D-erythritol kinase

**bpz00625 Chloroalkane and chloroalkene degradation**

bpz:BP1026B\_II2084 *adhA*; alcohol dehydrogenase, zinc-containing

**bpz00626 Naphthalene degradation**

bpz:BP1026B\_II2084 *adhA*; alcohol dehydrogenase, zinc-containing

**bpz03010 Ribosome**

bpz:BP1026B\_I0263 16S ribosomal RNA  
bpz:BP1026B\_I0267 23S ribosomal RNA

bpz:BP1026B\_I2302 23S ribosomal RNA  
bpz:BP1026B\_I3465 23S ribosomal RNA  
bpz:BP1026B\_I3469 16S ribosomal RNA

#### **bpz02010 ABC transporters**

bpz:BP1026B\_I0711 ABC transporter, membrane permease  
bpz:BP1026B\_I0713 ABC transporter, ATP-binding component  
bpz:BP1026B\_I3039 D-methionine ABC transporter, periplasmic D-methionine-binding protein  
bpz:BP1026B\_I1493 *potF*; putrescine-binding periplasmic protein precursor

#### **bpz03070 Bacterial secretion system**

bpz:BP1026B\_II1644 MxiH protein  
bpz:BP1026B\_II1641 *bsaO*; YscC/HrcC family type III secretion outer membrane protein  
bpz:BP1026B\_II1639 *bsaQ*; type III secretion system protein BsaQ  
bpz:BP1026B\_II1633 *spaP*; surface presentation of antigens protein SpaP  
bpz:bapB acyl carrier protein  
bpz:bicA type III secretion low calcium response chaperone LcrH/SycD  
bpz:bipB translocator protein  
bpz:bipC cell invasion protein  
bpz:bsaR surface presentation of antigens protein  
bpz:BP1026B\_II1643 type III secretion system protein PrgH/EprH

#### **bpz02020 Two-component systems**

bpz:BP1026B\_II0303 *aer*; aerotaxis receptor  
bpz:BP1026B\_I2997 *cydA*; cytochrome d ubiquinol oxidase subunit I  
bpz:BP1026B\_I2998 *cydB*; cytochrome d ubiquinol oxidase, subunit II  
bpz:BP1026B\_I3555 *fliC*; flagellin  
bpz:BP1026B\_I3544 *motA*; flagellar motor protein MotA  
bpz:BP1026B\_I1018 *narG*; nitrate reductase, alpha subunit  
bpz:BP1026B\_I1017 *narH*; nitrate reductase, beta subunit

#### **bpz02030 Bacterial chemotaxis**

bpz:BP1026B\_II0303 *aer*; aerotaxis receptor  
bpz:BP1026B\_I3544 *motA*; flagellar motor protein MotA

#### **bpz02040 Flagellar assembly**

bpz:BP1026B\_I3232 *flgK*; flagellar hook-associated protein FlgK  
bpz:BP1026B\_I3555 *fliC*; flagellin  
bpz:BP1026B\_I3544 *motA*; flagellar motor protein MotA

### **Membrane permeability and transport**

bpz:bpeF , RND efflux exporter protein  
bpz:BP1026B\_II0292 outer membrane porin  
bpz:BP1026B\_III1794 outer membrane porin  
bpz:BP1026B\_II490 outer membrane protein W precursor

### **Cell envelope and EPS biogenesis**

bpz:BP1026B\_I2915 acyl carrier protein  
bpz:BP1026B\_I2923 glycosyl transferase, group 1 family protein  
bpz:BP1026B\_I0538 Glycosyltransferase, Involved in the biosynthetic pathways of fatty acids, phospholipids, lipopolysaccharides, and oligosaccharides  
bpz:BP1026B\_I0948 cation-binding hemerythrin HHE family protein, Inorganic ion transport and metabolism, cell envelope biogenesis  
bpz:BP1026B\_II0548 chitin binding domain-containing protein, cell envelope biogenesis  
bpz:BP1026B\_I0534 Tyrosine-protein kinase Wzc, EPS biosynthesis  
undecaprenyl-phosphate galactosephosphotransferase, exopolysaccharide biosynthesis polyprenyl  
bpz:BP1026B\_I0531 glycosylphosphotransferase

### **Hypothetical proteins or proteins with unknown pathway association**

bpz:BP1026B\_I0964 hypothetical protein  
bpz:BP1026B\_I0966 hypothetical protein  
bpz:BP1026B\_II286 hypothetical protein  
bpz:BP1026B\_II697 hypothetical protein  
bpz:BP1026B\_I2917 hypothetical protein  
bpz:BP1026B\_I0091 hypothetical protein  
bpz:BP1026B\_I0099 hypothetical protein  
bpz:BP1026B\_I0157 hypothetical protein  
bpz:BP1026B\_I0205 hypothetical protein  
bpz:BP1026B\_I0714 hypothetical protein  
bpz:BP1026B\_I0723 hypothetical protein  
bpz:BP1026B\_I0961 hypothetical protein  
bpz:BP1026B\_I0969 hypothetical protein  
bpz:BP1026B\_II321 hypothetical protein  
bpz:BP1026B\_II564 hypothetical protein  
bpz:BP1026B\_II665 hypothetical protein  
bpz:BP1026B\_II676 hypothetical protein  
bpz:BP1026B\_I2615 hypothetical protein  
bpz:BP1026B\_I2833 hypothetical protein  
bpz:BP1026B\_III256 hypothetical protein  
bpz:BP1026B\_III266 hypothetical protein  
bpz:BP1026B\_III610 hypothetical protein

bpz:BP1026B\_II2146 hypothetical protein  
 bpz:BP1026B\_II1979 lipoprotein  
 bpz:BP1026B\_I1039 low molecular weight protein-tyrosine-phosphatase  
 bpz:BP1026B\_II2100 OsmY domain-containing protein  
 bpz:BP1026B\_I1565 polyhydroxyalkanoate depolymerase domain-containing protein  
 bpz:BP1026B\_I2921 sigma-54 dependent transcriptional regulator  
 bpz:BP1026B\_I0965 U32 family peptidase  
 bpz:BP1026B\_II1186 WD domain-containing protein  
 bpz:BP1026B\_I1518 LacI family transcription regulator, similar to purR needed for purine biosynthesis  
 bpz:BP1026B\_I0949 Rrf2 family protein, Icsa transcriptional regulator

### **Non-ribosomal peptide synthesis**

bpz:BP1026B\_I1675 nonribosomal peptide synthetase  
 bpz:BP1026B\_II1250 nonribosomal peptide synthetase  
 bpz:BP1026B\_II1241 non-ribosomal peptide/polyketide synthase  
 bpz:BP1026B\_I1664 carbamoyl transferase  
 bpz:BP1026B\_II1251 N-acylhomoserine lactone synthase

### **Maintenance of homeostasis**

bpz:cspD cold shock transcription regulator protein  
 bpz:BP1026B\_I2218 heat shock protein  
 bpz:BP1026B\_I2216 HSP20 family protein, stress induced  
 bpz:BP1026B\_II2466 HSP20/alpha crystallin family protein, similar to molecular chaperone IbpA , stress induced  
 bpz:hmpA flavohemoprotein nitric oxide dioxygenase, protects from nitrosative stress  
 bpz:BP1026B\_I1338 Sigma 54 modulation protein YhbH

---

<sup>1</sup> KEGG pathway analysis places genes in functional groupings based on annotation and/or empirical data identified through literature meta-analysis. All groups lacking a bpz designation were unable to be placed by KEGG pathway searches, and were grouped according to predicted functions assigned by the NCBI-Conserved Domain Database (CDD).

## ABBREVIATIONS AND DEFINITIONS

A	Absorbance
ade	adenine
ANOVA	analysis of variance
Amp	ampicillin
ATP	adenosine triphosphate
<i>B.</i>	<i>Burkholderia</i>
BCA	Bicinchoninic acid assay
Bm	<i>Burkholderia mallei</i>
bp	base pair
<i>Bp</i> or <i>Bp</i>	<i>Burkholderia pseudomallei</i>
BSA	bovine serum albumin
BSL	Biosafety level
°C	degrees Celsius
CDC	Centers for Disease Control and Prevention
CHL	chloramphenicol
CNS	central nervous system
Ct	cycle threshold
Da	dalton
DNA	deoxyribonucleic acid
DOX	doxycycline
FDA	Federal Drug Administration
Gm	gentamicin
h	hour
HIV	human immunodeficiency virus
HPLC	high pressure liquid chromatography
IR	intergenic region
K	lysine
kb	kilobase
kDa	kilodalton
Km	kanamycin
LB	Luria Bertani
LPS	lipopolysaccharide
MDR	multi-drug resistant
μl	microliter
μM	micromolar
mg	milligram
min	minute
ml	milliliter
mM	millimolar
mRNA	messenger RNA
nm	nanometers
nM	nanomolar

OD	optical density
P	proline
P.O.W.	prisoner of war
PBP3	penicilin binding protein 3
PCR	polymerase chain reaction
pg	picograms
RNA	ribonucleic acid
RPM	rotations per minute
rRNA	ribosomal RNA
RT	room temperature
qRT-PCR	real-time quantitative reverse transcription PCR
s	seconds
S	serine
SA	Select Agent
SMX	sulfamethoxazole
SXT	co-trimoxazole
T	threonine
TAT	twin arginine transport
TB	tuberculosis
TMP	trimethoprim
UV	ultra-violet
V	volts
WHO	World Health Organization
WWI	World War I
WWII	World War II
zeo	zeocin